

https://dspace.org/

An Investigation into the dynamic perfomance of a two wavelength skin reflectance oximeter

Revow, Michael David

2015
http://hdl.handle.net/10539/19200

Downloaded from a DSpace repository. https://dspace.org/

AN INVESTIGATION INTO THE DYNAMIC PERFORMANCE OF A TWO WAVELENGTH SKIN REFLECTANCE OXIMETER

Michael David Revow

A Dissertation submitted to the Faculty of Engineering, University of the Witwatersrand, Johannesburg, in part fulfilment of the requirements for the degree of Master of Science.

Johannesburg 1980

ABSTRACT

The feasability of a two wavelength skin reflectance oximeter is investigated with the view as an aid to non invasive patient monitoring. The approach emphasises the need to observe time responses, as opposed to simply measuring steady state values. It is suggested that the human body may be "observed" (i.e.information concerning the state of the system may be extracted) from the oximeter's outputs via an integrated model structure incorporating measurement and physiological subsystems.

An in-depth study is made into the underlying physiology and physical properties of light propogation through an inhomogeneous medium with a view to constructing an integrated model. Various measurement models are compared, and it was found that the three dimensional geometrical structure cannot be approximated by a single dimensional theory. A series of controlled experiments were performed to assess the repeatability of the instrument. The results obtained were repeatable and indicate that the instrument is sensitive enough to detect small changes in peripheral blood volume and oxygen saturation. This in turn is encouraging for the long term goal of patient monitoring.

Preliminary investigation into a measurement model indicates that the model is very sensitive to parameter choice. Published parameters give predictions which are qualitatively contradictory to experimental results. It is thought that the general model structure is valid, but that the values of the parameters have to be investigated via carefully controlled experiments.

The project is not complete in itself, but is considered to be the first iteration in an area of ongoing research. Many suggestions for further work are presented.

DECLARATION

I declare that this dissertation is my own, unaided work. It is submitted for the degree of Master of Science to the faculty of Engineering in the University of the Witwatersrand, Johannesburg. It has not been submitted before for any degree or examination in any other University, nor has it been prepared under the aegis or with the assistance of any other body or organisation or person outside the University of the Witwatersrand, Johannesburg.

_____

22 day of OCTOBER, 1980

To my parents

Το περιεχόμενο

ACKNOWLEDGEMENTS

The author wishes to acknowledge the immensely valuable encouragement and assistance obtained from his supervisor, Dr Ken Garner. The field of biomedical engineering was completely new to the author and Dr Garner's experience and enthusiasm was essential in stimulating interest in the project.

Financial assistance, received during the period 1979-1980 from the following sources is appreciated:

The Henry Bradlow Scholarship. The author thanks the patron and administrators for the honour of receiving this award.

The University Senior Bursary.

The Council for Scientific and Industrial Research Bursary.

Help and advice from the staff and students of the Department of Electrical Engineering is also acknowledged. In particular, Chris Moreton, whose suite of graphic routines provided the basis for producing many of the graphical results which play a central role in the work.

Finally, the much needed and appreciated assistance of Ms Wendy Tobais in completing this dissertation is acknowledged.

TABLE OF CONTENTS

	PAGE
ABSTRACT	ii
ACKNOWLEDGEMENTS	v
GLOSSARY OF SYMBOLS	ix
LIST OF FIGURES AND TABLES	x
CHAPTER 1 INTRODUCTION	1
1.1 BACKGROUND	1
1.2 AIMS	3
1.3 OUTLINE OF THE DISSERTATION	5
1.4 REVIEW OF THE LITERATURE	6
CHAPTER 2 BACKGROUND PHYSIOLOGY	7
2.1 OVERVIEW OF CARDIOVASCULAR SYSTEM	7
2.1.1 Layout of Vessels	7
2.1.2 Structure of the Vessels	8
2.1.3 Arteriovenous Anastomosis	9
2.2 BLOOD VESSELS OF THE ARM AND HAND	11
2.3 THE SKIN	15
2.3.1 Anatomy	15
2.3.2 Skin Colour	19
2.4 VASCULATURE OF THE SKIN	20
2.5 A SIMPLE MODEL OF THE SKIN VASCULATURE ..	24
2.6 CONTROL OF BLOOD FLOW	26
2.6.1 Local Control	26
2.6.2 Central Control	28
2.7 THE EFFECT OF VARIOUS STIMULI ON THE BLOOD FLOW	31
2.7.1 Response to changes in temperature ..	31
2.7.2 Emotional Response	37
2.7.3 Response to a deep inspiration	37
2.7.4 Response to arterial occlusion	38
2.7.5 Response to changes in transmural pressure	39
2.8 BLOOD FLOW MEASUREMENTS	40
2.8.1 Range of Blood Flows	40

2.8.2 Methods of measuring peripheral blood flow 41
2.9 TRANSPORT OF GASES IN THE BLOOD 42
2.9.1 Oxygen 42
2.9.2 Carbon Dioxide 45
2.9.3 Blood-Tissue Gas Exchange 45
2. 10 CLINICAL SIGNIFICANCE OF PERIPHERAL BLOOD FLOW 46

CHAPTER 3 PROPOGATION OF LIGHT IN BLOOD AND TISSUE .. 48
3.1 INTRODUCTION 48
3.2 PHOTOMETRIC DETERMINATION OF OXYGEN SATURATION.. 50
3.2.1 Lambert-Beer Law 50
3.2.2 The Extinction Coefficient 52
3.2.3 The Calculation of Oxygen Saturation .. 52
3.3 FACTORS WHICH DETERMINE THE PROPOGATION OF LIGHT 55
3.3.1 Absorption and Scattering 55
3.3.2 Whole Blood 57
3.3.3 Tissue 58
3.3.4 Transmission and Reflection Oximetry .. 61
3.3.5 Physiological factors 62
3.4 THEORIES OF LIGHT PROPOGATION IN BLOOD .. 63
3.4.1 Multi-scattering theory 63
3.4.2 A Phenomenological Approach 66
3.4.3 The Diffusion Equation 69
3.5 COMPARISON OF THEORIES 75
3.5.1 Complexity 75
3.5.2 Applicability and Accuracy 76
3.5.3 Practical Application 77
3.5.4 Predicted Outputs 78
3.6 ABSOLUTE AND TREND ANALYSIS 81
3.7 DISCUSSION AND CONCLUSIONS 83

CHAPTER 4 HARDWARE DESCRIPTION 89
4.1 INTRODUCTION 89
4.1.1 The Need for Acquiring and Storing Data .. 89
4.1.2 The Instrumentation 89
4.2 THE PULSE MONITOR 91
4.2.1 The Transducer 91
4.2.2 The Electronic Signal Processing .. 93
4.3 THE OXIMETER 96
4.3.1 An overview 96

4.3.2 Modifications 98
4.3.3 Transducer Design 104
4.4 COMPUTER BASED DATA CAPTURE AND STORAGE .. 111

CHAPTER 5 RESULTS AND MODELLING 115
5.1 INTRODUCTION 115
5.2 ARTERIAL OCCLUSION 117
5.3 BREATH HOLDING TESTS 122
5.4 THE EFFECTS OF LOCAL TEMPERATURE CHANGE .. 124
5.5 SPECTRAL STUDIES 127
5.6 PULSATILE FLOW 140

CHAPTER 6 CONCLUSIONS AND SUGGESTIONS FOR FURTHER WORK 144
6.1 INTRODUCTION 144
6.2 CONCLUSIONS 145
6.3 SUGGESTIONS FOR FURTHER WORK 147
6.3.1 Short Term 148
6.3.2 Long Term 149

LIST OF REFERENCES 150

APPENDIX 1 BLOOD VESSELS OF THE HAND 161

APPENDIX 2 VASCULATURE OF THE FINGER 163

APPENDIX 3 ABSORPTION AND SCATTERING FACTORS .. 166
A.3.1 ABSORPTION FACTOR 166
A.3.2 SCATTERING FACTOR 169
A.3.3 CONCLUSION 170

APPENDIX 4 DETAILED DESCRIPTION OF DATA HANDLING ROUTINES 171
A.4.1 Introduction 171
A.4.2 MicroNova Routine 172
A.4.3 The Task Manager and Utilities 176
A.4.4 IBM Routines 180

APPENDIX 5 SAMPLE SESSION 184

APPENDIX 6 LED DATA 186

APPENDIX 7 RESULTS 194

APPENDIX 8 PROGRAM LISTINGS 213

GLOSSARY OF SYMBOLS.

a	Absorption coefficient
b	Fraction of backscattered light
C	Concentration of absorbing pigment
c	Speed of light propogation in the medium
D	Diffusion constant
d	Sample depth
e	Extinction coefficient
$\vec{F}_0$	Diffuse flux
$\vec{F}_1$	Incident flux
H	Hematocrit
Hb	Haemoglobin
HbO_2	Oxygen saturated haemoglobin
I	Intensity of illumination after scattering or absorption
I_0	Incident illumination
O.D.	Optical density
P_0	Diffuse photon density
P_1	Incident photon density
p	$\frac{a}{b\ s} - 1$
q	$\sqrt{a(a+2s)}$
R	Reflectance
S	Oxygen saturation of Haemoglobin
s	Scattering coefficient
T	Transmission
$\tilde{u}$	Unit vector in a given direction
β	Total effective scattering cross section
β_1	Effective absorption cross section
β_2	Effective coherant scattering cross section
β_3	Effective incoherant scattering cross section
γ	Refractive index of the medium
ξ	Fraction of light scattered in direction of the detector
τ	Photon lifetime
λ	Wavelength

LIST OF FIGURES AND TABLES

		Page
1.1	Breath Holding Test	2
2.1	Deep Arteries of the Arm and Hand	12
2.2	Superficial Arteries of the Arm and Hand	13
2.3	Posterior Arteries of the Arm and Hand	14
2.4	Schematic Layout of Vasculature in the Skin ..	16
2.5	Schematic Representation of the Digital Circulation	22
2.6	A Simple Peripheral Blood Flow Model	25
2.7	Oxygen Dissociation curve	44
3.1	Absorption Spectrum of Hb and HbO_2	49
3.2	Illustration of the Roles Played by Scattering and Absorption	59
3.3	Geometry for Diffusion Equation	72
3.4	Boundary Conditions for Two Layer Model	73
3.5	Comparison of the Three Dimensional Diffusion, Kubelka and One Dimensional Models	79
3.6	Comparison of the Three Dimensional Diffusion, Kubelka and One Dimensional Models	80
3.7	Heuristic Model of Three Dimensional Geometry ..	84
3.8	Comparison of the Three Dimensional Line Model to the Heuristic Model	86
3.9	Reflectance vs Fractional Blood Volume for the Line Source Model	88
3.10	Reflectance vs Fractional Blood Volume for the Line Source Model with Modified Parameters ..	88b
4.1	Strain Gauge Pulse Monitor	92
4.2	Gramophone Pickup Pulse Monitor	92
4.3	Circuit Diagram of Pulse Monitor	94
4.4	Step Response of Pulse Monitor	95
4.5	Block Diagram of the Oximeter	97
4.6	Response of Phototransitor	99
4.7	Circuit Diagram of Oximeter	100

..8 Oscillator 103

..9 FET Drivers 103

..10 Transducer using an Annulus of Detectors 105

..11 Schematic of Transducer using OPB 253A Reflective Sensor 105

4.12 Finger Cap in Position 107

4.13 Experimental Setup for Checking Transducer Linearity 108

4.14 Response of Transducer in the Infra Red Region .. 109

4.15 Transducer Response in the Red Region 110

4.16 Information Flow in Data Capture Region 112

5.1 Experimental Setup for Arterial Occlusion 118

5.2 Arterial Occlusion Experiment 120

5.3 Breath Holding Test 123

.4 Local Heating of Finger 126

5.5 Spectrum from I.R. Channel When Sitting 129

5.6 Spectrum from I.R. Channel When Breathing at 0,1Hz 130

5.7 Spectrum from I.R. Channel When Breathing at 0,2Hz 131

5.8 Spectrum from I.R. Channel When Breathing at 0,5Hz 132

5.9 Spectrum from Red Channel When Sitting Still .. 134

5.10 Spectrum from Red Channel When Breathing at 0,2Hz 135

5.11 Spectrum from Heat Rate Monitor When Sitting Still 137

5.12 Spectrum from Heat Rate Monitor When Breathing at 0,1Hz 138

5.13 Spectrum from Heat Rate Monitor When Breathing at 0,2Hz 139

5.14 I.R. Channel and Pulse Monitor Showing Pulsatile Blood Flow 142

5.15 Inverted I.R. Channel and Pulse Monitor Showing Phase Relationships 143

A2.1 Blood Vessels of the Skin 165

A3.1 Normalised Absorption Coefficients of Blood (Table) 168

A3.2 Comparison of Blood Scattering Factors (Table) .. 170

A4.1 The Data Handling Process .. .. 1..

A4.2	The Sampling Process	174
A4.3	Conversion and Transmission	175
A4.4	Data Record Format	179
A7.1	Arterial Occlusion Test	195
A7.2	Arterial Occlusion Test	196
A7.3	Arterial Occlusion Test	197
A7.4	Arterial Occlusion Test	198
A7.5	Breath Holding Test	199
A7.6	Breath Holding Test	200
A7.7	Breath Holding Test	201
A7.8	Effects of Local Heating	202
A7.9	Effects of Local Heating	203
A7.10	Effects of Local Heating	204
A7.11	Effects of Local Heating	205
A7.12	Spectrum When Sitting Still	206
A7.13	Spectrum When Breathing at 0,2Hz	207
A7.14	Spectrum When Breathing at 0,1Hz	208
A7.15	Spectrum After Vigorous Exercise	209
A7.16	Spectrum Half an Hour after Exercising	210
A7.17	Output from I.R. Channel and Pulse Monitor, Showing Phase Relationships	211
A7.18	Output from I.R. Channel and Pulse Monitor, Showing Phase Relationships	212

CHAPTER 1 INTRODUCTION

1.1 BACKGROUND

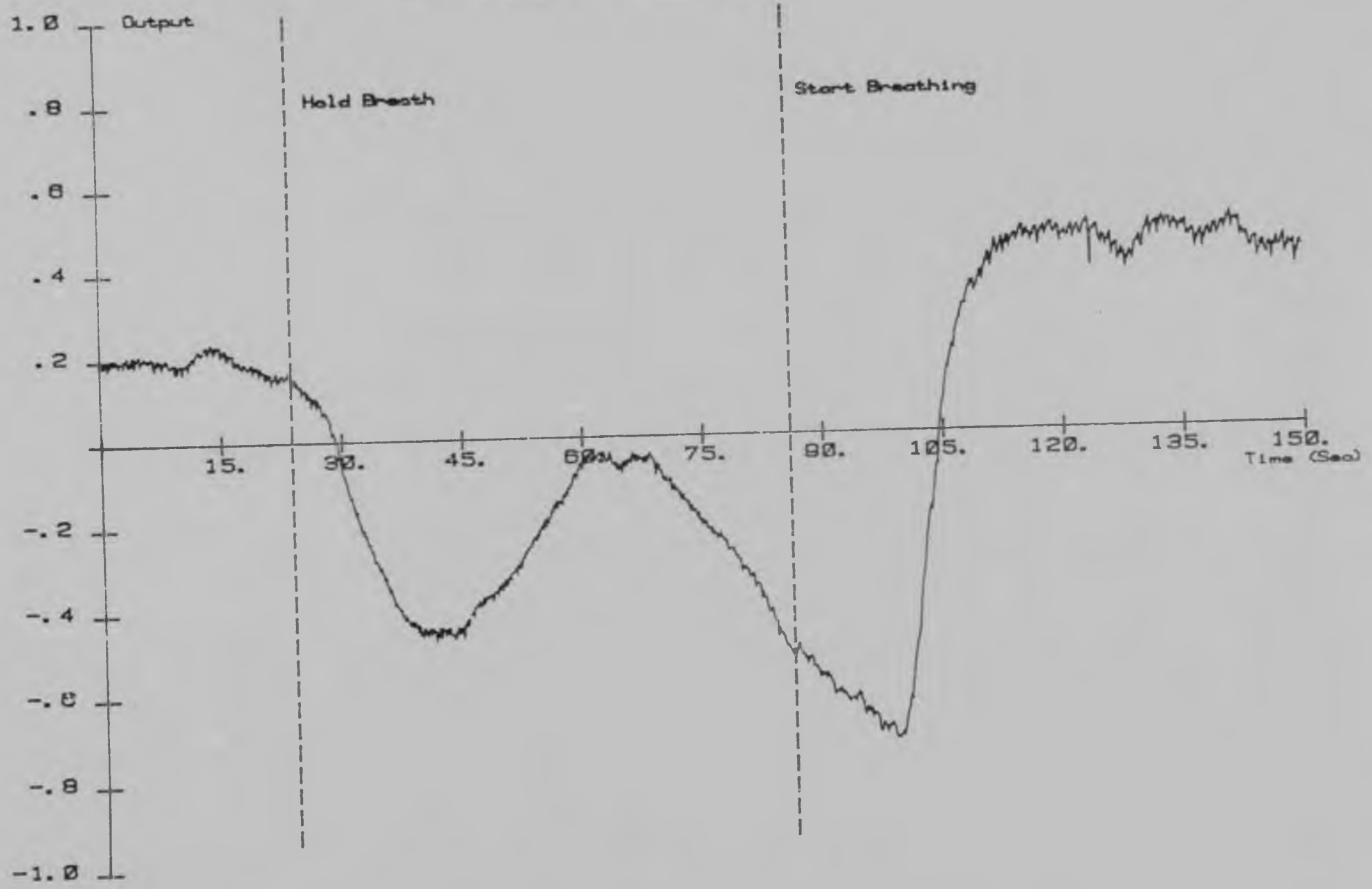
In 1978 Dr Garner proposed the development of a two wavelength oximeter as a fourth year laboratory project for electrical engineers. Initially, the main aim for such a device was to aid in the measurement of blood gas transport delay times to be used in a model of the respiratory system. A reflectance type oximeter was developed mainly because it can be applied to most parts of the body.

During initial testing by Turner and Wigdorowitz [99] it appeared that the output from the instrument might contain much valuable information concerning the respiratory and vascular systems. Breath-holding tests (figure 1.1) showed a peculiar initial rapid response followed by a recovery and then a larger response as the deoxygenated blood reached the site of measurement. The subsequent spectral work of Dr Garner suggested that the instrument might be useful in a "black box" approach, whereby correlations and spectra are computed from the responses to several manoeuvres.

The above results were interesting but were not understood. It was also questionable as to what exactly the instrument was measuring. There is a large body of literature which addresses itself to light reflection and transmission in blood, however, the much more complicated case of blood plus tissue in unknown proportions, has not recieved much attention.

Many explanations and theories were suggested, but all were mainly speculative, without a sound backing. It was therefore proposed that this mini-thesis should "further investigate" the potentials of the instrument.

Figure 1.1 Breath Holding Test.



1.2 AIMS

Although at the start of the project, there were a number of speculative ideas based on some preliminary tests, as to the potentials of the instrument, the exact aim and direction were not explicit. It was broadly defined as to investigate the quantitative ramifications of the instrument and to develope the speculative ideas as to the possibility of using the instument to aid in the measurement of the state of the "Controlled Human Body". This forms part of the general philosophy of patient monitoring which advocates that the human body may be viewed as a controlled plant, and hence it would be more valuable to deal with the dynamic state of the plant as a whole, rather than only with the controlled variables. This approach, while not ignoring the importance of the steady state, emphasises the need to consider the dynamic behaviour. From a control engineer's point of view, this is the classical problem of system observability. It is suggested that ultimately the system (i.e. the human body) may be "observed" via instruments such as a reflectance oximeter. This would be a valuable aid in both a laboratory modelling of the cardiovascular and respiratory systems context as well as in a clinical enviroment.

It is suggested that because oxygen is an essential ingredient of life and that the peripheral tissue represents a comparatively "disposable" tissue mass, it may be possible to monitor, in a clinical environment, the state of a patient much more closely than is possible by measurement of the controlled variables; temperature, heart rate, etc. It is argued that because these are controlled variables, no system degradation can be detected until the situation has degraded to such an extent that the control systems cannot cope. This philosophy is the underlying motivation for this type of research.

At the outset it was felt that the many unknowns and complications involved, demanded that an integrated systems approach be adopted. The system should comprise both a physiological model and a measurement model. This approach set the theme for the investigation. To this end, three stages of developement evolved:

(i) Obtaining and recording results from controlled experiments in order to judge repeatability.

(ii) Investigation and development of a transducer model.

(iii) Investigation and development of a physiological model.

Stage (i) may be viewed as a feasibility study and is a pre-requisite for the following two iterative stages. Should the instrument be capable of detecting, in a repeatable fashion, physiological changes, then these changes may be used via a model structure to obtain information which would be valuable in a patient monitoring enviroment.

The full realisation of the above aims will demand much research. The present project is thus aimed at providing a foundation for this work. Its aims are twofold:

(i) Investigation of the feasability of the instrument.

(ii) To provide a framework upon which models may be constructed.

The first aim was tackled via a series of controlled experiments. The results of approximately fifty experiments (mainly using a single subject, although the results were checked using other subjects) were recorded. The viability of the instrument was

confirmed by these tests. Commonly accepted physiological phenomina were detectable in a repeatable fashion. An encouraging aspect of these results is the sensitivity of the instrument. It is thought that fluctuating quantities, such as the peripheral pulsatile flow and cyclic oxygen tension changes in the blood, corresponding to the respiratory rhythm, are detectable.

The second aim was approached by providing an in depth literary survey on the physiological and physical problems. As this work is inherantly inter-disciplinary, various data obtained from previously unrelated work have been brought together to provide firm foundation and direction for further work. In this connection, it is hoped that the manner in which the work is presented will not have too many gaps for the researcher who is entering a new field, while at the same time not insulting the expert.

Time limitations resulted in only a brief examination and qualitative interpretation of the results in terms of a model structure. It was found that the models and parameters in the literature predict contradictory results to the experimental results.

1.3 OUTLINE OF THE DISSERTATION

Chapter 2 provides a background to the underlying physiology. The emphasis is mainly on the fingers, as this is the site at which it is proposed that measurements be taken because, of (1) the sites's accessibility, (2) high degree of vasculature and (3) relatively low skin absorption. A description of its structure and functional aspects is presented. The known responses of the vascular system to different stimuli is discussed and the nature of the peripheral controllers is outlined.

Chapter 3 deals with the physical properties of the oximeter. The historical development is given. This began with the measurement of the degree of oxygenation of haemolysed blood. The situation

confirmed by these tests. Commonly accepted physiological phenomina were detectable in a repeatable fashion. An encouraging aspect of these results is the sensitivity of the instrument. It is thought that fluctuating quantities, such as the peripheral pulsatile flow and cyclic oxygen tension changes in the blood, corresponding to the respiratory rhythm, are detectable.

The second aim was approached by providing an in depth literary survey on the physiological and physical problems. As this work is inherantly inter-disciplinary, various data obtained from previously unrelated work have been brought together to provide firm foundation and direction for further work. In this connection, it is hoped that the manner in which the work is presented will not have too many gaps for the researcher who is entering a new field, while at the same time not insulting the expert.

Time limitations resulted in only a brief examination and qualitative interpretation of the results in terms of a model structure. It was found that the models and parameters in the literature predict contradictory results to the experimental results.

1.3 OUTLINE OF THE DISSERTATION

Chapter 2 provides a background to the underlying physiology. The emphasis is mainly on the fingers, as this is the site at which it is proposed that measurements be taken because, of (1) the sites's accessibility, (2) high degree of vasculature and (3) relatively low skin absorption. A description of its structure and functional aspects is presented. The known responses of the vascular system to different stimuli is discussed and the nature of the peripheral controllers is outlined.

Chapter 3 deals with the physical properties of the oximeter. The historical development is given. This began with the measurement of the degree of oxygenation of haemolysed blood. The situation

became more complicated as the requirements to measure whole blood, tissue and blood and finally an inhomogeneous structure of tissue plus blood were introduced. It is important that the instrument model be carefully considered. The different theories concerning the propogation of light in a medium such as human flesh are presented and discussed. Simple models are compared to more complicated ones. It is concluded that a one dimensional structure cannot be used to approximate the three dimensinal geometry of the problem.

Chapter 4 deals with the hardware that was used to perform some preliminary experiments. The results are presented and discussed in chapter 5.

Finally, chapter 6 concludes the dissertation and suggests a probable path for future research.

1.4 REVIEW OF THE LITERATURE

Usually a section on the review of the literature concerning a project would be included at this point. However, because the major portion of this project could be regarded as a literature review, this convention will be dispensed with at this point. Chapters 2 and 3 present and discuss previous work in related fields.

A note on the references is pertinant. These may be divided up into those concerning the physiological aspects of the dissertation (references 1-70) and those concerning the physical properties of the oximeter (references 71-100). The remaining references refer to the hardware used for the experimental work. Many secondary references (particulary those concerning the physiological aspects) are not quoted. Review texts such as Johnson [43], Greenfield [18] and Shepherd [62] provide useful sources.

CHAPTER 2 BACKGROUND PHYSIOLOGY

2.1 OVERVIEW OF CARDIOVASCULAR SYSTEM

2.1.1 Layout of Vessels [35, 43]

The arteries exiting from the heart (pulmonary and systemic) undergo repeated division and simultaneously diminish in size. Repeated division of the arteries give rise to arterioles which in turn supply the capillaries (exchange vessels.). The capillaries drain into the venules which in turn join up to form veins. Eventually all the veins return to the heart via the Superior Vena Cava (neck, head and upper limbs) and the Inferior Vena Cava (lower limbs and trunk). Blood leaves the heart via the innominate artery which divides to supply the head, neck and upper limbs, and the descending thoracic aorta which supplies the abdomen and lower limbs.

As the blood vessels divide, the cross-sectional area of the vascular bed increases. It has been estimated [35] that the cross sectional area of the total capillary bed is about 800 times that of the main artery (aorta). This means that the blood flow is much slower in the capillaries [43] than in the arteries. In the resting aldult, the cardiovascular system circulates 4 - 6 l/min of blood. [43]

2.1.2 Structure of the Vessels

As the vessels divide and become smaller, so do the walls become thinner. All blood vessels have an inner coat of endothelium. This layer prevents clotting of the blood and promotes a smooth flow. The larger arteries have varying thicknesses of elastic layers. These aid in maintaining blood flow and pressure throughout the whole cardiac cycle. As the arteries approach the capillaries, so the elastic coating becomes thinner and eventually disappears in the capillary bed. The calibre of the vessels diminishes from approximately 10mm in the aorta to 3,7µm in the capillaries. In the minute exchange vessels the diameter of the vessels is comparable with the diameter of the red blood cell and thus one cannot refer to a "blood flow" in these vessels, but must rather consider the movement of individual cells.

The elastic nature of the larger arteries aids in smoothing out the large pulsations associated with the cardiac cycle. [87] In the capillaries, the endothelium layer is capable of varying degrees of active and passive contraction/dilation. The degree to which individual capillaries can contract varies from region to region and is partly governed by the local requirements of the region. For example, the coronary and cerebral circulations have large oxygen requirements and so the flow to these regions is governed by local metabolic requirements. The skin, on the other hand, has a low metabolic requirement and so the flow to this region is governed more by central effects. Thus the capillaries in the skin are richly endowed with nerve endings.

Since the primary function of the capillaries is to exchange nutrients and waste products between tissue cells and the blood, the walls of these vessels are generally very thin and semi-porous. An important result of this exchange property of the vessels, is that fluid can move from the blood into the interstitial tissue spaces, thereby increasing the tissue pres-

sure and constricting th capillaries. This has important consequences in the regulation of the blood flow.

2.1.3 Arteriovenous Anastomosis [34, 63, 43, 35]

Arterioles and venules are not only connected together via the capillary networks, but there are also relatively large channels which connect the artery and venous systems together. These vessels are found in many locations and vary in complexity ranging from simple direct links between arteries (which are capable of shunting relatively large amounts of blood away from or to metabolising tissue), to complex interconnecting organs which are usually termed glomus organs. In order to be able to differentiate between capillaries and complex anastomoses, one may define an arteriovenous anastomosis as a "connection between arterial and venous sides of the circulation, through which nutrient materials, metabolic product and gases are not normally exchanged with tissue fluids." [63]

Arteriovenous Anastomoses (AVA's) are most numerous in the fingers, toes and nose. The relative abundance of these shunts and blood vessels (see also appendix 1), make the finger a good site for measuring changes in the shunt perfusion ratio. The average diameter of the AVA's in the fingers is 50µm, although larger ones are found. The length of the vessels range from a few micrometers to 2 - 4 mm in length.

Opening and closing of the AVA's significantly affect the blood flow through the associated capillary bed. The AVA's thus act as a fine and rapid controller for the partitioning of the local circulation.

The arteriovenous anastomoses of the finger are richly innervated. They can thus be centrally controlled. Under normal conditions they are seen to rhythmically dilate and contract at a faster rate than the arterioles from which they arise. They tend to act independently from neighbouring AVA's and arterioles. In

addition they are also affected by local conditions such as humoral substance, local oxygen tension, PH and trauma.

When the AVA opens there is a rise in local venous pressure which spreads to the capillary bed which diminishes and in some cases might even reverse the capillary flow. The irregularity of flow observed in the capillaries is a result of the lack of correlation between the random fluctuations in the contractions of the AVA'S and the arteriols supplying the region. This results in an irregular pattern of filling and emptying of regional vessels. It should be noted that most authors [7, 35, 55, 63] agree that the anastomoses of the skin are not fixed, permanent features but grow as a response to local conditions. Observations [55] made on new born, normal babies show that at birth, the AVA'S of the skin are not present, but rather develope, into their various forms of complexity during the baby's first few months.

An interesting type of anastomosis occurs when an artery supplying a given tissue mass becomes occluded. Connecting vessels can develop between the occluded artery and adjacent arteries so as to eventually supply the tissue mass with as much blood as before the vessel became occluded (collateral circulation). If this type of connection was not possible, then such an occlusion would result in a cessation of flow to the vascular territory, the tissue mass would die and gangrene would set in. Full collateral circulation developes better in young patients. In some cases, such a circulation might become effective immediately after an obstruction. In older subjects, the anastomes might be so poor that the tissue mass dies.

The precise function on circulatory dynamics of the AVA's is not known. The simple shunt function of the AVA's is accepted. This function has its main importance in temperature regulation, as the AVA's would allow a relatively large volume of blood to be shunted from the arterial to venous circulations. However, the structure of the more complex and specialised glomus organs suggests that their function is not simply that of a shunt. Some type of secretory function [34] has been suggested.

The variation in the shunt perfusion ratio, in the tissue, as a response to various stimuli (see section 2.7) helps maintain hemostasis. Therefore, this ratio, and the manner in which the ratio can change may be able to provide a measure of the state of the body as a whole. In other words, this ratio may represent one of the less controlled variables mentioned in section 1.2.

A secondary function of the AVA is to regulate vascular pressure. As has been mentioned previously, opening up the AVA raises the venous pressure. The role of the arteriovenous anastomosis in disease is not clear. It has, however, been noted that when the AVA's become permanantly dilated then the flow to the vascular region diminishes.

2.2 BLOOD VESSELS OF THE ARM AND HAND [24]

The arteries supplying the forearm and hand (figures 2.1 - 2.3) arise from the Brachial artery (also see appendix 1). The Brachial artery divides up into two main arteries, the radial and ulna arteries, which run down either side of the forearm. They join up in the hand via three arches (superficial pulmer arch, deep pulmer arch and posterior carpal arch). The digital arteries which arise from these arches supply the fingers. The digital arteries give rise to a fairly complicated capillary structure which becomes very dense at the finger tips. Taken as a whole, the blood supply consists of numerous interconnecting vessels, which form a grid over the hand.

Most workers, when determining blood flow to the hand, do not distinguish between the whole hand, and the digits. Greenfield determined the proportion of the total hand flow which flows in the digits. It was found that this proportion varied with individuals and with temperature.

The greatest proportion (59%) flowed through the digits in

FIG. 21 DEEP ARTERIES OF THE ARM AND HAND

(HAND COPIED FROM [60], FIG. 743)

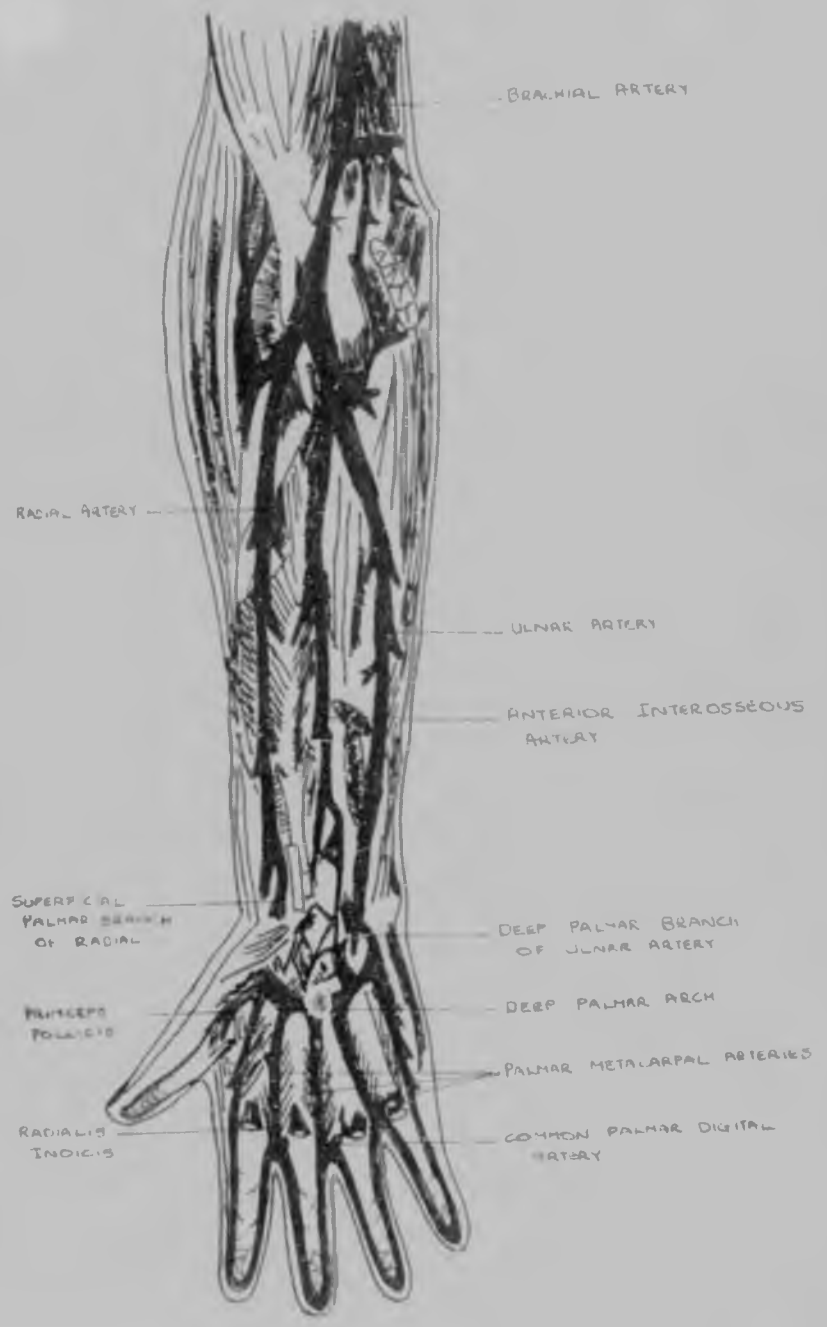


FIG. 22 SUPERFICIAL ARTERIES OF THE ARM AND HAND

(HAND COPIED FROM [WO], FIG. 744)

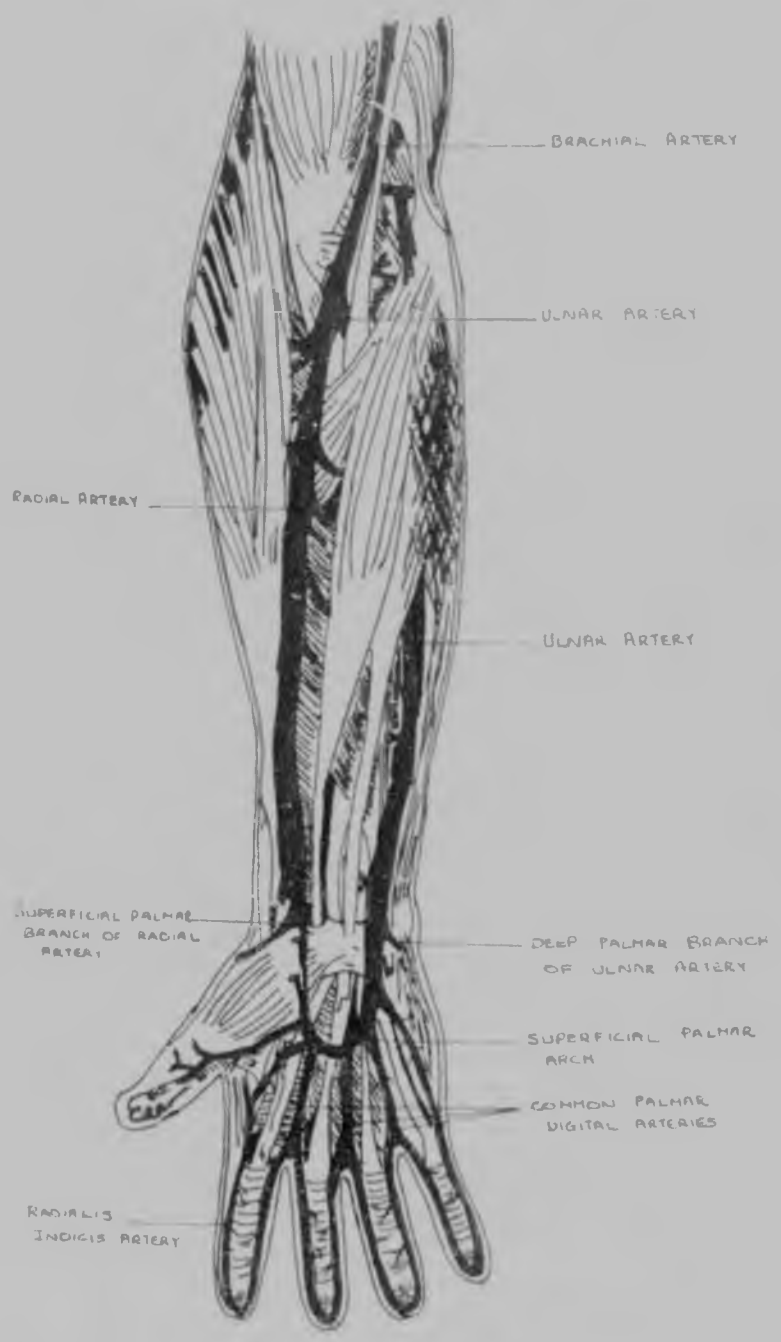
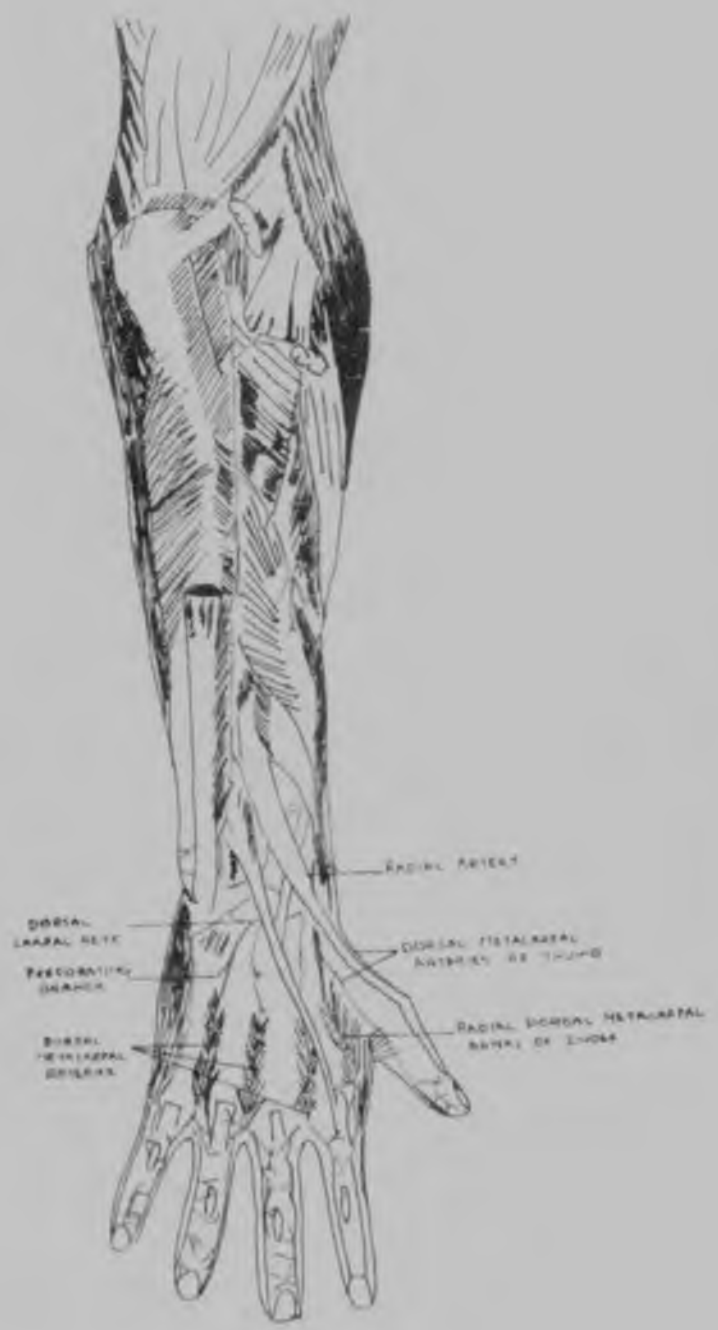


FIG. 2.3 POSTERIOR ARTERIES OF THE ARM AND HAND

(HAND COPIED FROM [60], FIG. 744)



comfortable range of temperatures. At either extreme the digital flow dropped to 44% of the total hand flow. Thus, the vessels of the digits dilate at a different temperature to that of the rest of the hand, whose blood vessels are similar to those of the forearm (section 2.6.2).

It is also interesting to note that 30% of the hand is skin and 15,5% muscle (by mass), while the corresponding quantities of the forearm are 13% and 58,6%. Thus again, the finger is a likely choice because of the large variations which can take place in skin blood flow.

2.3 THE SKIN

2.3.1 Anatomy

The total mass of the skin is approximately 16% of the body mass and has a specific gravity of 1,25. [70] The thickness of the skin varies from about 0,1 mm on the lips to 4 mm on the palms and soles. It is continuous over the whole healthy body and serves many functions, such as protective coating, waterproofing, temperature regulation etc. Infra-red radiation will only penetrate " a few millimetres" and the penetration depth of sunlight is also not large. [35]

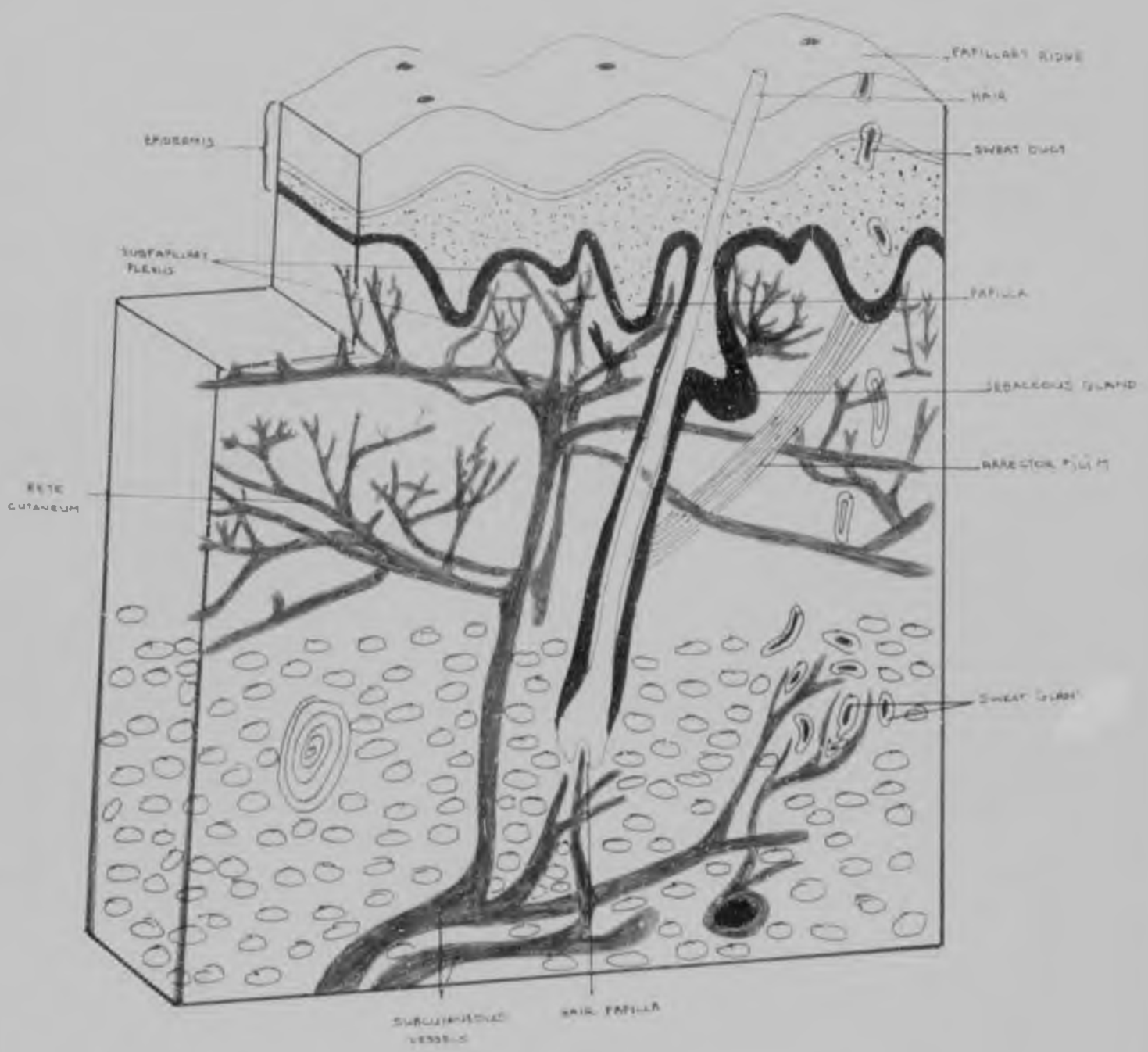
The skin is usually considered to be composed of three major parts (see figure 2.4)

(i) The EPIDERMIS (cuticle) is the extreme outer covering of the body.

(ii) The CORIUM (cutis vera) constitutes the greater part of the skin thickness.

FIG 24 SCHEMATIC LAYOUT OF VASCULATURE IN SKIN

(HAND COPIED FROM [35]; FIG 79A)



(iii) Subcutaneous fat provides insulation between the inner body and outer skir surface. It also allows relative movement between the two.

The thickness of the Epiderris layer varies at different parts of the body from about 0,3 mm to 1 mm. It is thickest on the palms and soles. Five sublayers are identified in the Epidermis, from the outermost layer inwards they are;

(i) Stratum Corneum

(ii) Stratum Lucidum

(iii) Stratum Granulosum

(iv) Stratum Mucosum

(v) Stratum Germinativum

The different layers are classified according to the type of cells from which they are composed. Most of the cells of the outer layers of the epidermis are dead and are continuously being rubbed off with the outermost layers being replaced by the lower layers. The cells are hard, hence the term "horny layer" is frequently used.

The epidermis is characterized by the absence of blood vessels. It does contain nerve endings which are usually sensitive to touch. Skin pigmentation is produced by the substance melanim which is produced from melanocyte cells. These cells are formed in the deeper layers of the epidermis (principally the stratum mucosum, see section 2.3.2.) The density of melanim varies from location to location on the body. The density of the melonocytes diminishes as the lower layers migrate towards the surface.

The Corium is a flexible, elastic layer. It has numerous blood vessels, lymphatic channel and nerves. The tissue layer is usually divided up into the deeper (reticular) and superficial

(papillary) layers. The reticular layer is fibrous and gradually merges with the subcutaneous fat. This region contains the roots of the hair and the sweat glands, which are richly supplied with blood vessels.

The papillary layers are vascular eminences (papillae) which rise perpendicular to the skin surface. They are received into pits on the underside of the epidermis. In the hands, fingers and toes, there are large numbers of papillae. They are closely spaced together in parallel curved lines. On the finger tips, these parallel ridges are seen as the lines which make up ones "finger prints'. In each papilla there is a single capillary loop.

The oxygen permeability of the skin, under resting conditions, is low. The stratum corneum provides a barrier to oxygen perfusion. The oxygen tension at the skin surface is approximately 7 mm Hg, while in the basal layer it increases to 20 mm. [64] Therefore, the oxygen in the corium is supplied almost entirely from the capillary bed, and the blood is mainly venous.
In addition the average oxygen tension increases with an increase in temperature. Both these observations are in accordance with the vascular structure of the skin (section 2.4).

The Corium layer does have a considerable oxygen uptake. Experiments [64] have shown that 1-1,5 min after complete cessation in the circulation, the oxygen tension in the basal layer dropped to almost zero, while the oxygen in the epidermis was lost much more slowly.

The role of oxygen tension and oxygen gradients in the skin have been investigated. It is widely accepted that oxygen plays a major role in cutaneous repair processes. Not only is the skin permeability changed, but normal oxygen gradients may be reversed, especially where the dermal capillaries are not dilated. It might be reasonable to postulate that the control of epidermal growth and replacement could depend to some extent on the direction and magnitudes of the oxygen gradients within the epidermis. If this is the case, then it would clearly be

clinically advantageous to have some measure of these quantities. In the case of a wound where the blood vessels are damaged (e.g. severe burns), repair might be delayed as a result of the unavailability of oxygen.

2.3.2 Skin Colour

The colour of the skin has long been used as a diagnostic aid in assessing the amount of peripheral blood flow. Although, the skin colour is mainly determined by the fractional blood volume, there are other factors which contribute to skin colour [21]. Light incident on the skin surface will penetrate 3-5mm into the skin and hence the colour (or spectral reflectance) will be governed by the optical properties of the epidermis, corium and upper layers of the subcutaneous fat.

The first factor which determines skin colour is the amount of melanin present. The variation of skin colour between races is attributable to the different amounts of melanin found in light and dark skinned people. Two origins of melanin have been identified. The primary origin is hereditary, while the secondary source is a response to the exposure of sunlight. The susceptibility to secondary pigmentation depends on the ease of light penetration into the skin and the manner in which the skin reacts. Hence, secondary pigmentation is less important in both extremely fair and dark skinned people.

Absorption by melanin [21] increases from the red to the ultra violet regions of the spectrum. The distribution of melanin varies from location to location [21].
Thus when observing the r al properties of the skin, a site of low melanin concentratic s ld be selected. The palms and fingers provide such a site.) ensity of melanin is highest in the deep layers of the epidermis and decreases towards the surface. A derivative of melanin, melanoid was identified by Edwards and Duntley [21] to account for skin absorption in the ultra violet region. The details of melanoid are of no concern in

this investigation as the ultra violet region of the spectrum is not used.

The substance Carotene which is found mainly in the Corium and subcutaneous fat has an absorption band around 450-480nm (blue region). Above 500nm its transmission is near to 100% and hence is not important at the wavelengths used in this work.

Haemoglobin (a main constituent of blood) has an absorption spectrum which depends upon whether it is in the oxidised or reduced state. A fuller discussion is presented in section 3.1. However, it should be noted that factors which can mask the absorption bands of haemoglobin are:

(i) The relative area of subpapillary plexus which is venous.

(ii) The distribution of melanin.

(iii) The scattering properties of the stratum mucoseum.

The transparent upper layers of the epidermis do not exhibit much scattering, whereas the opaque deeper layers (e.g. mucoseum) scatter light to a greater extent, because reflection from these layers is larger (see figure 9, page 13 and figure 19, page 23 in [21]).

2.4 VASCULATURE OF THE SKIN [34,60]

Research into the vascular structure of the skin (cutaneous) circulation was started early in the nineteenth centuary. Although extensive work has subsequently been done, this topic is still not fully understood.

Near the finger tip, the primary digital arteries divide into two branches. The Periosteal branch (P) (see figure 2.5) turns up towards the nail bed, while the Terminal branch (T) runs parallel to the skin surface at about one third of the finger thickness from the bottom skin surface. It curves near the finger tip to form the nail artery.

The terminal artery (appendix 2) has branches which continue towards the skin surface. The following vascular layers are recognized.

1. A deep arterial arcade is formed in the lower layers of the Corium (vessel diameter approximately 100 um. [42])

2. Ascending vessels through the mid corium which have branches supplying sweat glands and the hair follicles.

3. A horizontal arterial plexus (subpapillary plexus) located just below the epidermis.

4. Hairpin loops supplying the papillae. These are the most superficial vascular structure and can often be seen through the upper layers of the epidermis. [42]. The papillary loops are about 0,2 - 0,4 mm in length.

5. The papillary loops drain into the subpapillary venous plexus which freely intermingles with the subpapillary arterio plexus.

6. Venules descend from the venous plexus in a candelabra fashion to the deep venous drainage plexus.

The concentration of superficial capillaries have been estimated at 16-65 per square mm. [70] Each papillary vessel has a diameter of approximately 0,015 mm.[42] As these rise perpendicular to the surface, the relative blood to tissue volume may be estimated to be approximately 0,04. The combined volume of the superficial,

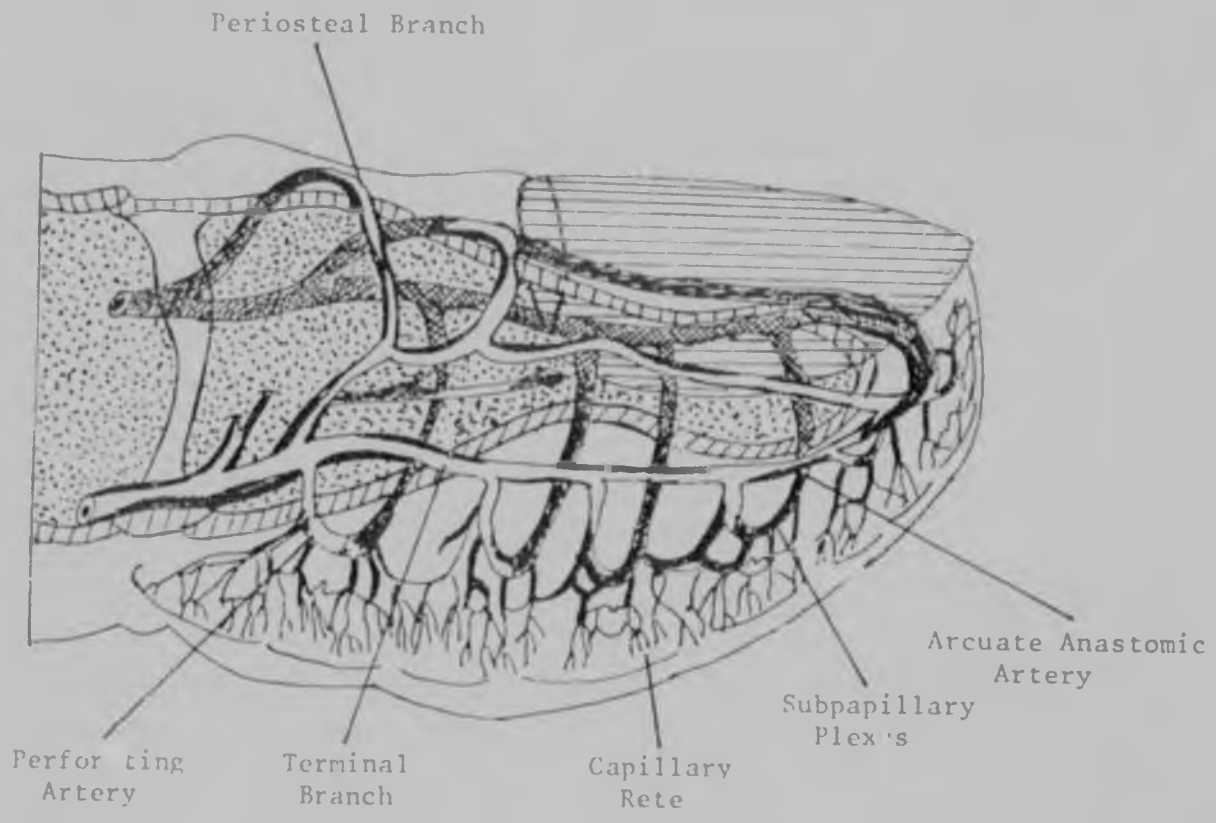


Figure 2.5 Schematic Representation of the Digital Circulation.
(Hand copied from [34], fig 12, page 209)

intermediate and deep plexus layers are about fifteen times that of the arterial supply. The venules and capillaries do not have the same contractile ability as the arterioles. However, some investigators have shown that the endothelium cells of the capillaries can change shape, which results in a change in the capillary diameter. [35]

Arteriovenous anastomoses occur at all levels of the cutaneous vascular structure. These vary in complexity fr[illegible]mple channels which simply connect together the arterioles and venules through varying stages of muscular wall complexity to the highly developed glomus organs. The average diameter of the vessels vary from 20 - 70 µm. In the finger tips there are about 236 arteriovenous anastomosis. [62]

The arteriovenous anastomoses a[illegible] usually richly innervated and hence can play a major role in temperature control. When they open up, the blood flow to the skin can be increased tenfold so as to enable an increased heat exchange function with the environment. Under normal, comfortable temperature conditions, the AVA's will dilate and contract rhythmically with a period of 0,5-2 minutes. This accounts for the periodic blood flow which has been observed in the comfortable temperature range. [6,28] The AVA's can be viewed as prefferential channels. The capillaries provide more circuitous channels between arteriols and venules. The muscle at the point of exit from th[illegible] preferential channel, is capable of contracting and hence diverting the flow into the papillary loops. In the deeper layers of the skin, the arteries and veins are in close proximity to one another. This allows for heat exchange between the venous and arterial circulations. This type of heat exchange is important when the body has to conserve heat.

During steady state (i.e. subject sitting still), periodicity in the output of the oximeter has been observed. The spectral work (see section 5.5) shows that oscillations are present at low frequencies.

2.5 A SIMPLE MODEL OF THE SKIN VASCULATURE

The previous sections have described the structure of the skin and blood vessels in the extremeties, with special reference to the finger. Based on this physiology, an extremely simple, "lumped parameter" model may be formulated. It should be emphasized, that no rigour or high degree accuracy is alluded to.

Figure 2.6 shows a two compartment model. This model would represent the state of blood supply in the superficial layers of the skin (i.e. in epidermis and corium). The two compartments represent arterial and venous blood respectively. In other words, the model assumes that the blood in the skin can be categorised either as venous (i.e. low oxygen saturation) or arterial blood (high oxygen blood). The combined volume as well as the individual volumes of each compartment, as a fraction of the total tissue volume, is variable. The exact manner in which blood is transferred between compartments is not clear. The following two sections suggest that physiological controllers will adjust these volumes in response to various stimuli. This is suggested by the valves 1-3 which regulate the flow into and out of the compartments.

As blood is shunted away from the surface by the deep arteriovenous anastomosis, so the combined inflow through valve 1 will decrease. Should the requirement for increased arterial blood increase (or alternatively if the incoming supply is decreased) then there could be an exchange between the compartments through valve 2.

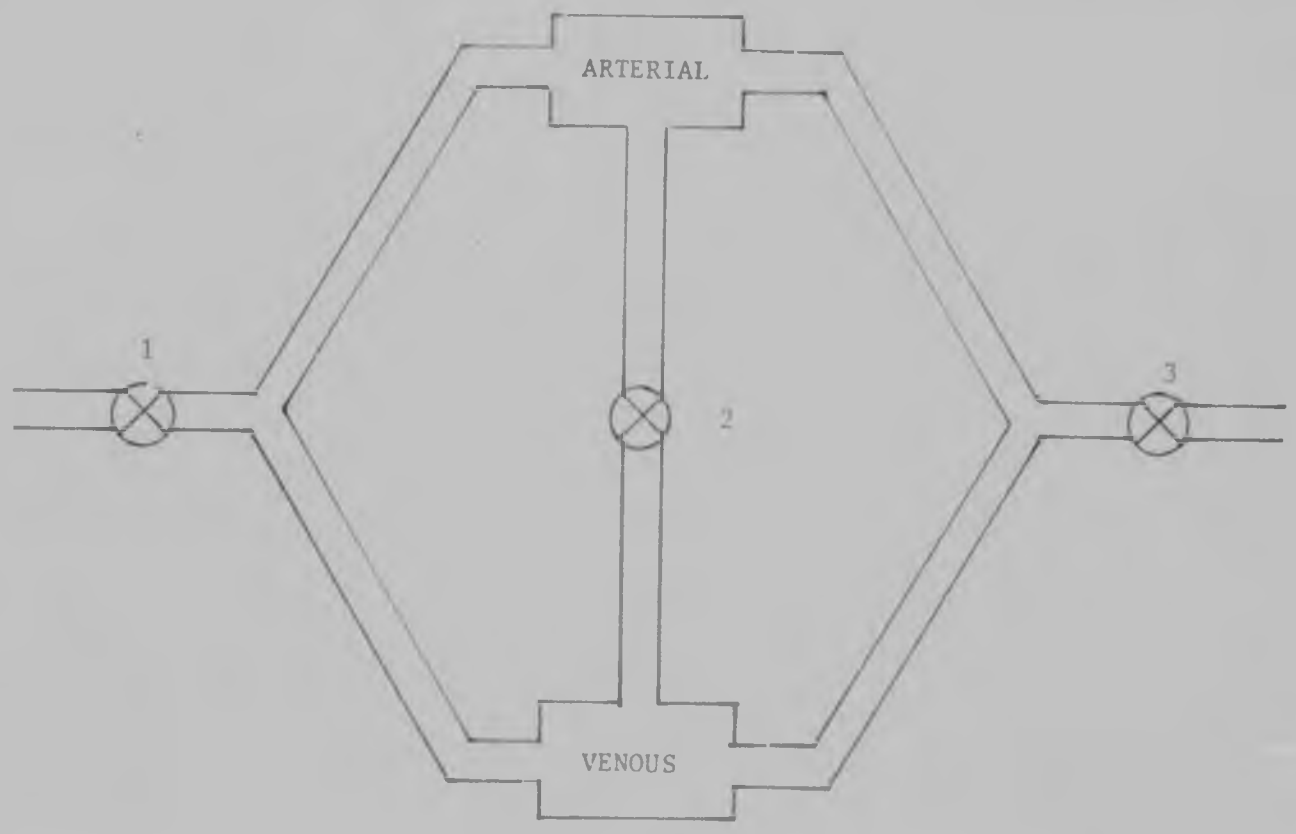


Figure 2.6 A Simple Peripheral Blood Flow Model

The model may be extended by including a metabolically active tissue mass. Gas tension gradients between the blood and tissue would ensure a transfer of carbon dioxide and oxygen between the two (see references [32] and [65]) In steady state, the partial gas pressures in the skin and venous compartments are equal. Oxygen stores in the tissues may also be included. As a first approximation these features may be dispensed with in a tissue mass such as the skin.

2.6 CONTROL OF BLOOD FLOW

The cutaneous blood flow responds to a number of stimuli. These might be local or central responses. The most important of these responses is that, due to the requirement for thermal regulation. Other responses are a result of emotional stresses, changes in blood pressure (both local and central), occlusion to blood flow, shock, diabetes and Raynauds disease.

2.6.1 Local Control

The blood flow through organs and tissue is partly regulated by local requirements. Amongst the factors involved are:

(i) The satisfaction of metabolic requirements. This means that nutrients (mainly oxygen) must be delivered and waste products removed.

(ii) Mairtenance of approximately constant blood pressure in the face of changing arterial and hydrostatic pressures.

(iii) Temperature regulation, especially the protection of the local tissues from extremes in temperature. This factor is strongly related to the central temperature regulation.

(iv) Injury or wound.

The amount of priority afforded tc each of the above factors varies from location to location in the body and also according to the general state of the body. For example, the satisfaction of nutrient requirements in the brain takes precedence over any of the other factors, while it is a relatively minor factor in the peripheral tissue.

There are, at present, three major theories as to the mechanism of local blood flow regulation.[44] The metabolic model hypothesises that the objective of the blood flow is to maintain the correct supply of materials. If the blood flow is not sufficient to supply the metabolic requirement then there is a local buildup of metabolites. These metabolites then act as vasodilators (cause the blood vessels to dilate), thereby allowing an increased flow, which would in turn reduce the amount of metabolites present, i.e. a negative feedback system. Carbon dioxide, a major product of metabolism, is a potent vasodilator. Other metabolites also have a dilator effect on blood vessels. An example of this model is provided by the phenomenon of "reactive hyperaemia". Restoring the blood flow to a limb in which the flow had previously been occluded results in the limb becoming warm and flushed. This is explained by an increased blood flow above the resting value as a result of dilation of the blood vessels. This dilation is owing to the accumulation of metabolites during the period of occlusion. This explanation is often referred to as "debt and repayment model". [62] However, the validity of the model is still questionable. (see sections 2.7.4 and 5.2)

Bayliss [4] showed that the arterial wall responds to an increase of internal pressure by contracting. This type of response is known as the "Bayliss response" and is found to a greater or lesser extent in most blood vessels. The mechanism that detects changes in transmural pressure has not been explained, although it has been suggested that the endothelium cells have some pressure receptor properties. "Reactive hyperaemia" can also be explained in terms of this hypothesis (see section 2.7.4) Regulation of the vessel calibre in response to the internal pressure would tend to smooth out pulsatile blood flow and might even lead to a reversal in the phase relationship between the volume and pressure pulsations. To the writer's knowledge, there is no reference to this type of effect in the literature. Section 5.6 indicates that such a phenomenon might take place. A possible objection to the Bayliss response is that it is positive feedback

type control. Thus one should expect that this type of regulation should act in conjunction with other mechanisms.

The third major theory of autoregulation is the tissue pressure hypothesis. This model does not require an active response from the blood vessels. Basically, this theory relies on an increase in intravascular pressure causing an increase in fluid filtration through the permeable capillary walls. This in turn increases the tissue pressure which, because the tissue is relatively incompressible, causes a decrease in the vessel calibre.

Other theories on the local regulation of blood flow are the local reflex and the cell separation hypotheses. In certain organs and limbs, local axon (nervous) reflexes play a major role in autoregulation. These nervous reflexes must be distinguished from central nervous reflexes.

The cell separation model relies on a change in viscosity of the blood in response to the separation of the blood cells. Blood is a non-newtonian fluid, made up of a plasma and a cell suspension. The orientation and degree of aggregation of the cells can greatly influence the viscosity of the blood. [43]

At any one site, the regulation of the actual blood flow is most probably determined by a combination of all the above factors, as well as by other central regulatory requirements (see section 5.2)

2.6.2 Central Control

The central control is governed by emotion, mental activity, physical exercise and temperature regulation. The central reflex mechanisms are initiated by impulses along the afferent nerves, which stimulate the relevant regulating centre and by the release of hormones into the blood. These centres in turn send out integrated responses to the different parts of the body. [43] In control of the blood vessels, the afferent signals arise from the

baro-receptors and chemo-receptors in the aortic arch and carotid sinus, stretch receptors in the lung, themo-receptors in skin and internal organs. In addition the temperature of the circulating blood, directly affects the thermo regulating centre (see section 2.7.1)

An important point about central control is that any one stimulus can affect more than one site. Furthermore, a given stimulus may result in completely opposite effects in different tissue. For example, constriction of the vascular vessels in the muscles of the forearm, is often accompanied by dilation of the cutaneous vessels. [37] This indicates an overall control strategy which attempts to distribute resources according to some priority structure, while optimising some performance criteria.

An increase in the calibre of the blood vessels may be achieved by either actively dilating the vessels or reducing the amount by which they are presently being constricted [50, 59] (i.e. reducing the amount of constrictor tone). Experiments [30, 37, 62] show that increased blood flow in the hand and fingers is almost exclusively a result of a reduction in constrictor tone. In the skin of the forearm, both constrictor and dilator nerve fibres play a role in changing the blood flow. If the dilator nerves in the forearm are blocked, then upon heating a subject, the blood flow will increase to 2-4ml per 100ml tissue per min. However, under normal conditions, the flow would increase to approximately 10ml per 100ml tissue per min.

It has been suggested [23] that sweating plays a major role in dilator activity. The sweat glands are stimulated via the somatic nerve fibres. Sweating in turn releases a bradykinin forming enzyme. Bradykinin is a powerful vasodilator. This is an example of the interaction between local and central effects.

Central control via the release of constrictor tone in the fingers can vary the blood flow from 1ml per 100 ml tissue per min to about 90ml per 100ml tissue per min. [7] This large range of flows is achievable mainly as a result of the numerous

arteriovenous anastomoses (see section 2.1.3) in the fingers. The control of this tone is almost completely mediated by the temperature regulator. The effect of this controller is apparent in the comfortable temperature range (20-25°C). This would be represented in the model (figure 2.6) by adjusting the total volume of the two compartments.

The blood flow in the fingers is a fluctuating quantity. [28, 7] The amplitude and frequency of the fluctuations depends on the ambient temperature. The greatest amplitude is found in the mid range temperature. Burton [6] has identified two frequencies:

(1) A small amplitude fluctuation which is closely related to the respiratory rhythm.

(2) A larger amplitude component of period 15-120 sec. This component is characterised by a steep constriction followed by a slower recovery.

There is a gradual decrease in the frequency of fluctuations as the ambient temperature increases. It has been shown that following a brief stimulus of the sympathetic nerves to the blood vessels of the frog, relaxation may not be complete for two minutes. The sluggishness of the response helps maintain constrictor tone between sympathetic bursts. With more rapid bursts (e.g. cold conditions), the vessels would be maintained in a constricted state, hence the amplitude of fluctuations would be less, and the frequency higher.

In summary, central control is mediated by central regulating systems, which receive and integrate signals from all parts of the body. The peripheral blood vessels are then controlled either directly or indirectly by signals passed along the sympathetic nerve fibres, which can cause contraction in some tissue, while at the same time dilating others. Changes in the calibre of the vessels can take place either as a result of the reduction in the

amount of resting (basal) constrictor tone, or by actively causing dilation. In the hand and fingers, changes are mainly a result of release of constrictor tone.

The main objective of the central control is to ensure that sufficient nutrients are supplied and waste removed from all sites so as to provide a "comfortable enviroment" for life of the whole body. The definition of a "comfortable enviroment" would differ from location to location as indicated above. At a local level, (e.g. in the hand), local controls attempt to optimise the resources allocated to it by the central control. The possibility then arises of an interaction between the local and central controls during crisis situations, when the local controller cannot manage with its currently available resources. The manner in which such a contention is resolved must be investigated. A measure of how close local and central are from instabilities (i.e. crisis situations) would be clinically very valuable.

2.7 THE EFFECT OF VARIOUS STIMULI ON THE BLOOD FLOW

The cardiovascular system responds to many stimuli so as to retain a general level of homostasis. Some of the stimuli arise in normal everyday activity such as postural changes and changes in environmental conditions. Other responses may be caused by pathological conditions, such as fever, hypertension etc. Examining the response of a subject to various stimuli might provide information of clinical importance (see section 2.10 and 3.5.2)

2.7.1 Response to changes in temperature

The skin provides a comparatively large surface area to the environment and hence is capable of large amounts of heat dissipation. The skin dissipates heat by radiation, convection and evaporation. Conduction through the skin is not a significant factor as the fatty layers provide an insulating function. Under

normal conditions approximately 60% [35] of the body heat loss is via Infra-red radiation. Convection losses are enhanced when the environment allows circulating air currents close to the skin. Heat loss via evaporation is facilitated by the sweat glands. [11] The dilation and constriction of the cutaneous blood vessels is closely linked to the operation of the sweat glands. The temperature of the skin depends partly on the rate of blood flow through it. [3] When the blood flow to the fingers is arrested, the fingers cool until their temperature settles near to that of the surrounding air. However at maximum blood flow, the temperature of the fingers may come within 1^0C of the core temperature (approximately 36^0C). Between these two extremes the relationship between blood flow and temperature is non linear. [28] Heat is mainly generated within the body (At rest the brain produces 20%, internal organs (viscera) 53%, skin and muscle 27%. Under conditions of exercise the muscles may provide 75% of the total heat) [73]

Therefore, the physical regulation of overall body temperature depends largely on the peripheral circulation. The temperature regulating centre is under the influence of different afferent stimuli. The relationships between the various stimuli is not fully understood. The setting of the peripheral circulation is made by a modification of the underlying sympathetic tone, which itself is complicated by local effects (see section 2.6.1). Peripheral blood flow to serve the needs of heat elimination must proceed simultaneously with other requirements such as the local metabolic and homostasis of blood pressure. The blood flow in the fingers provides an indication of the factors involved in temperature regulation because: [7]

(i) They are richly supplied with arteriovenous anastomosis (which can shunt relatively large quantities of blood).

(ii) They are relatively free from muscular tissue which often experience different vascular changes to those found in the skin.

The body responds in both a local and central manner to temperature.

(a) Local Response

Changes in local peripheral tissue results in a predominantly local effect. [28] The effect on the rest of the body is slight. The object of the local control is to provide optimum conditions for life. This is achieved by attempting to maintain correct nutritional flow and to protect against deleterious effects. It should be borne in mind that local responses (especially in the peripheral tissue) are affected by the environmental conditions.

The blood flow through the hand is lowest at about 15^0C [28] Changing the temperature from 15^0C results in a modest increase in flow. Above 29^0C to body temperature (approximately 36^0C), there is a faster increase. Raising the local temperature above body temperature until the maximum temperature, that the body can be subjected to without feeling pain, (about 45^0C) results in an even larger increase in flow. Above body temperature the high blood flow is required to protect against possible thermal damage to tissue below the surface. (At these high temperatures, the blood flow cannot be arrested without the occurence of pain.) The high local blood flow is maintained for about 2 hours after immersion of the limb in water at 41^0C. [28] This local response to heating is thought to be a direct response of the vessels, but also involving local nervous pathways.

The reaction to cold was first investigated by Lewis. [48] The response to cold is immediate and dramatic. After immersing the fingers in water at 0^0C-6^0C, [48, 28, 31, 62] there is an initial, rapid vasoconstriction which lasts for 5-10 minutes. Following this initial constriction, the vessels begin to dilate. Lewis called this reaction "Cold Vasodilation". Thereafter there is an irregular pattern of vasoconstrictions and vasodilations. The

period between constrictions is about 20-25 minutes. This oscillatory behaviour is termed the "Hunting Reaction".

Measurement of flow rates is difficult, but it is suggested that during the vasoconstriction there is complete cessation of blood flow owing to the co-ordinated activity of all the arteriovenous anastomosis. Peak pain is experienced during the periods of vasoconstriction. [43, 31]

During the periods of vasodilation, the pain sensation subsides and the blood flow reaches orders of magnitude comparable to maximal flows through the vasculative. [62] Again, it should be recalled that the general thermal state of the body will affect the response. The cold vasodilation is reduced when the body is cold and is enhanced when hot.

The factors involved in the reduction of blood flow are:

(i) Local reflex action of vasoconstrictor fibres.

(ii) Direct constriction of smooth muscle surrounding the blood vessels.

(iii) Change in viscosity (changing the temperature of blood from $20^{0}C$ to $4,7^{0}C$ increases the viscosity by 50%. [62]

(iv) Local change in metabolism.

The reason for the cold vasodilation is not known. One theory, hypothesizes that following vasoconstriction, the local temperature drops until a temperature is reached at which the smooth vascular muscles can no longer constrict. They therefore relax, the blood flow increases, local temperature rises and constriction can once again take place. Another theory surmises that the oscillatory behaviour is the result of oscillatory sympathetic activity. [70]

The effects of severe and/or prolonged exposure to cold, can cause weeks of hyperaemia (enhanced blood flow). [28] In extreme cases, the vessels may become blocked (frostbite) and gangrene will set in.

(b) Central Response

The local response to changes in temperature can be largely overcome by "body heating". This is usually achieved by observing the changes in flow of the hand and forearm after immersing the legs and trunk in a bath of water whose temperature can be adjusted.

There are two mechanisms whereby the overall body temperature is regulated by adjusting the heat loss from the periphery. [58] The first mechanism is a reflex axon effect which is stimulated from the thermoreceptors. These govern the initial response when there is a sudden change in body temperature.

The second mechanism is a slower acting component, in which the central temperature receptor centre reacts to changes in temperature of the returning mixed venous blood. A side effect is that changes in temperature are distributed to all tissues as the arterial blood traverses the systemic capillaries.

A stimulus of cold gives rise to an immediate, cutaneous vasoconstriction which passes off. Should the stimulus persist then the central mechanism is activated by the cool returning blood. This is then the defence mechanism for prolonged effects of cold (and excessive heat). Pickering [58] shows that there is a change in peripheral vasculature when the rectal (i.e. core) temperature changes by $0,025^{0}C$ to $0,05^{0}C$

Body heat is further conserved as a result of the efficient heat exchange arrangement between arteries and veins in the deeper layers of the skin. (see section 2.4). By shunting more blood

through the deeper anastomosis, more heat is returned to the body core. (The temperature of the blood at the skin may be 30^{0}C below that of the core). The trunk and head have poor defences against heat loss, and therefore are dependant on clothing and insulation. (The heat loss from the uncovered head may account for half the resting heat production when the ambient temperature is below freezing point. [24])

Heating the body results in an increased flow in the peripheral tissue. In the hand vasodilation takes place by reducing the amount of constrictor tone, while in the forearm it is the result of both a reduction in constrictor tone and active dilation. (section 2.6.2) The blood flow increases first in the hand, and at higher temperatures in the forearm. High blood flows in the forearm are usually coincident with the onset of sweating. [62]

In summary, the regulation of body temperature is a complex interaction between local and central responses. These responses can either work in the same direction or oppose each other. Both mechanisms working together result in a higher blood flow than could be obtained by either procedure acting alone. This either means that neither mechanism can realize full dilation/contraction, or that the two mechanisms act on different vessels. [62] At extremes of temperature, the temperature controller takes precedence over other functions. Fainting, while standing in the sun is an example of stimuli from the baro- and chemo-receptors being largely overridden.

The complexity of the temperature controller is summed up by Burton [7] "The accurate adjustment of the average value of so fluctuating a flow in the peripheral vessels to a level, which ensures the measure of constancy of body temperature achieved by the homotherm, is one of the most highly developed integrated mechanisms of the nervous system."

2.7.2 Emotional Response [28]

The circulation in the periphery is particularly sensitive to emotional stimuli in the middle range of flows. An emotional stimulus such as pain, apprehension, uneasiness or mental arithmetic [1,2] causes a transient vasoconstriction. Prolonged emotional stress will cause an increase in flow. Emotional sweating, especially on the palms, accompanies the increased flow.

A problem arises when attempting to judge the effect of drugs on the vascular system. The pain introduced while administering will cause a vasoconstriction. Even anticipation of the pain can cause a change in the vasculature.

The effects of emotional stimuli are only apparent when the more powerful controllers (e.g. temperature) are not changing.

2.7.3 Response to a deep inspiration

Following a deep inspiration there is a transient decrease in blood flow. [5,28,53] The response is a neural effect since it is lost after a nerve block. The response is independant of the composition of the inhaled gas. All the evidence points to the origin of the stimulus being stretch receptors in the chest, since if the volume of the chest is constrained (by for example, straps), the effect is reduced. The precise functional importance of this type of response is, at present, not clear. Breath-holding experiments (section 5.3) using the oximeter exhibit this phenomenon.

2.7.4 Response to arterial occlusion (Reactive Hyperaemia).

The circulation through the skin is often arrested by local pressure, for example, in the hand when holding a heavy object. Arresting the arterial blood supply to a limb will obviously result in hypoxia (Reduced amount of oxygen available). The response to this type of stimulus is a reflex dilation in the skin, with a simultaneous constriction on the muscle. This manoeuvre will direct blood away from the higher metabolic muscle tissue, to the low oxygen consuming, cutaneous circulation without a significant change in arterial pressure.

The skin is better able than most other tissues to withstand an arrest of its blood flow. Frequently, when the blood flow is restored, the flow is higher than the resting level. This increased flow is termed "reactive hyperaemia". The theory of "debt and repayment" hypothesises that the amount of extra blood flowing during this period is equal to the quantity that would have flowed through the tissue had the flow not been arrested. However, this is frequently not the case [28,62] since (a) the resting skin flow is usually in excess of the metabolic requirements and (b) the tissues are able to extract a greater amount of oxygen from the blood during the period following restoration of the circulation.

Reactive Hyperaemia occurs after denervation and thus must be a local effect. There are two possible mechanisms whereby the vessels may be dilated. During the period of zero blood flow, metabolites accumulate which cause vasodilation. An objection to this explanation is that the peak values of reactive hyperaemia are not greatly increased by prolonging the period of arrest, nor is the period of reactive hyperaemia infinitely extendable.

The second possible explanation is that during the period of arrest, the blood pressure drops and so vascular tone decreases (Bayliss response, see section 2.6). Continuation of this dec-

2.7.4 Response to arterial occlusion (Reactive Hyperaemia).

The circulation through the skin is often arrested by local pressure, for example, in the hand when holding a heavy object. Arresting the arterial blood supply to a limb will obviously result in hypoxia (Reduced amount of oxygen available). The response to this type of stimulus is a reflex dilation in the skin, with a simultaneous constriction on the muscle. This manoeuvre will direct blood away from the higher metabolic muscle tissue, to the low oxygen consuming, cutaneous circulation without a significant change in arterial pressure.

The skin is better able than most other tissues to withstand an arrest of its blood flow. Frequently, when the blood flow is restored, the flow is higher than the resting level. This increased flow is termed "reactive hyperaemia". The theory of "debt and repayment" hypothesises that the amount of extra blood flowing during this period is equal to the quantity that would have flowed through the tissue had the flow not been arrested. However, this is frequently not the case [28,62] since (a) the resting skin flow is usually in excess of the metabolic requirements and (b) the tissues are able to extract a greater amount of oxygen from the blood during the period following restoration of the circulation.

Reactive Hyperaemia occurs after denervation and thus must be a local effect. There are two possible mechanisms whereby the vessels may be dilated. During the period of zero blood flow, metabolites accumulate which cause vasodilation. An objection to this explanation is that the peak values of reactive hyperaemia are not greatly increased by prolonging the period of arrest, nor is the period of reactive hyperaemia infinitely extendable.

The second possible explanation is that during the period of arrest, the blood pressure drops and so vascular tone decreases (Bayliss response, see section 2.6). Continuation of this dec-

reased tone is responsible for the hyperaemia. There is evidence supporting both theories [62] and so the response is most probably a result of a combination of the two.

2.7.5 Response to changes in transmural pressure

Vessel wall tension has three components:

(i) Elastic tension mainly from elastic fibres which maintain wall tension without any energy expenditure.

(ii) Active tension which is the result of constrictor tone in the muscular fibres. This component requires a continuous energy expenditure and may be modified by nervous, humoral and local factors.

(iii) Interfacial tension between fluid in vessel and vessel wall.

If the transmural pressure is reduced below a certain minimum value, ("critical closing pressure") then vessel closure takes place. From Laplaces pressure law, (transmural pressure inversely proportional to the vessel radius), critical closure will most probably take place in the small diameter arterioles.

Transmural pressure can be decreased by raising the limb or increasing the external tissue pressure. In both cases, the perfusion pressure will also decrease. Venous occlusion will increase the transmural pressure but decrease the perfusion pressure. By noting the response to the above three manoeuvres, the response to a reduction in transmural pressure may be deduced. Critical closure has been observed in the superficial vessels of the nail fold when the transmural is reduced below the critical closing pressure. [62]

If the vessels behaved passively, then increasing the transmural pressure would simply distend the vessels. Observations show that there are three ranges of responses. [62]

Small increases in pressure (i.e. < 50mm Hg) tend to distend the blood vessels and so lead to an increased blood flow. It should be noted that conclusions of this kind are not conclusive as it is not possible to compare observed responses with a purely passive response. Moderate increases (50mm Hg - 150mm Hg) do not significantly alter the flow. This tends to indicate that as the pressure increases, so does the resistance to flow. Thus a Bayliss type response (see section 2.5.1) must occur. Large increases (>150mmHg) cause a vasodilation [12]. Perhaps these higher pressures overcome the action contractile response of the vessels.

2.8 BLOOD FLOW MEASUREMENTS

2.8.1 Range of Blood Flows

The blood flow through the hand and fingers has been measured during a variety of manoeuvres. [6, 28, 30, 39, 42] The minimum blood flow to support skin life is about 1ml per 100ml tissue per min. In full vasodilation, the flow rate increses up to 90ml per 100ml tissue per min. Burton [7] quotes the average flow under comfortable environmental conditions to be 15-40ml per 100ml tissue per min at 28^{0}C. The proportion of the total blood flowing through arteriovenous anastomosis increases as the temperature increases. At 28^{0}C the finger tip arteriovenous flow is estimated to be 49,8 ml per 100ml tissue per min. [43]

2.8.2 Methods of measuring peripheral blood flow

There are currently many methods [29] of estimating blood flow rates in peripheral tissue. Some methods are invasive and as such may disturb the conditions for blood flow. Others measure total limb flow (i.e. both deep muscle and superficial skin flow) while others give only an estimate of regional flow.

Classically, two techniques are used to measure blood flow rate. The change in limb volume following occlusion of the venous return is measured (venous occlusion plethysmography). This method gives total blood flow and is invasive since it requires arresting the venous flow. However, the meth assumes that, initially, this has no effect on the flow rate, since the initial rate of change of limb volume is taken as the blood flow rate. The disadvantages of this method are that it is fairly difficult to apply and that it is not robust. Furthermore, it cannot separate deep tissue flow from superficial flow.

The second technique is to measure the rate of heat dissapation from a limb. It is assumed that heat conduction through the deep tissue layers is negligible and that heat is transported from the core to the tissue via the blood flow. The accuracy of this method is not as good as volume plethymography because the temperature of the arterial and venous bloods can only be estimated from core and skin temperature respectively. [29] A further disadvantage is that the method does not give instantaneous values for flow, because of the lag time involved in calorimetry. Also this method, generally estimates the total limb flow, although it can be adapted to give local flows (but this usually involves inserting needle tip thermo-junctions into the tissue)

A more recent technique is to measure the clearance of a radioactive trace from tissue. This method will usually give a measurement of local blood flow. A problem arises in adminis-

tering the traces as this involves disturbing the local conditions.

A possible, promising technique is to use the different spectral reflectance and transmission properties of blood and tissue. [41] An added feature of this method is that it is also sensitive to the oxygen saturation of the blood. Hertzman [38] originally showed that the method could be used for estimating blood flow. Hocherman [39] did not obtain a good correlation between this method and that using volume plethysmography. However, his attempt to keep a constant finger volume might not be valid. In addition, he showed that the photoelectric output depends on the local spatial vasculature, whereas the volume plethysmograph gives an integrated volume change. The results of Weinman [68] and Davis [16] show that the method is promising. Davis concludes that there is a good correlation betwen this method and other established methods, when all methods observe the same vascular bed

All the above investigators ignored the effects of oxygen saturation and mainly used transmission measurements. Weinman is the only one to quote a theoretical justification for the method, and in doing so, he used the simple Lambert-Beer equation (section 3.2.1) and thus obtained a linear model. As this method forms the major part of this dissertation, chapter 3 discusses this method more fully.

2.9 TRANSPORT OF GASES IN THE BLOOD

2.9.1 Oxygen

There is no chemical reaction between oxygen and blood plasma. Therefore, the amount of oxygen dissolved in governed by Henry's law (amount of dissolved gas is proportioned to the partial pressure of the gas). Normal arterial blood has an oxygen partial

pressure of 100 mm Hg. At this pressure, plasma will dissolve 0,3 ml oxygen/100 ml plasma. Resting tissue, on average, requires 250 ml oxygen/min. Thus, to satisfy this requirement with plasma alone, would require circulation of 83 l/min of plasma.

The haemoglobin (Hb) present in the red blood cells can combine chemically with oxygen in an unique manner. The amount of Hb combined with oxygen (oxy-haemoglobin) depends, in a non linear fashion, on the partial pressure of oxygen (see figure 2.7). The oxygen capacity of Hb is 1,34m oxygen/gm Hb. Normal blood has a concentration of 15gm Hb/100ml blood and thus the oxygen capacity of haaemoglobin is 20,6 ml oxygen/100ml blood [13]. The absorption spectrum of the haemoglobin molecule (molecular mass 16 700) changes when it combines with oxygen (figure 3.1)

The dissociation curve [65] (figure 2.7) shows the following points:

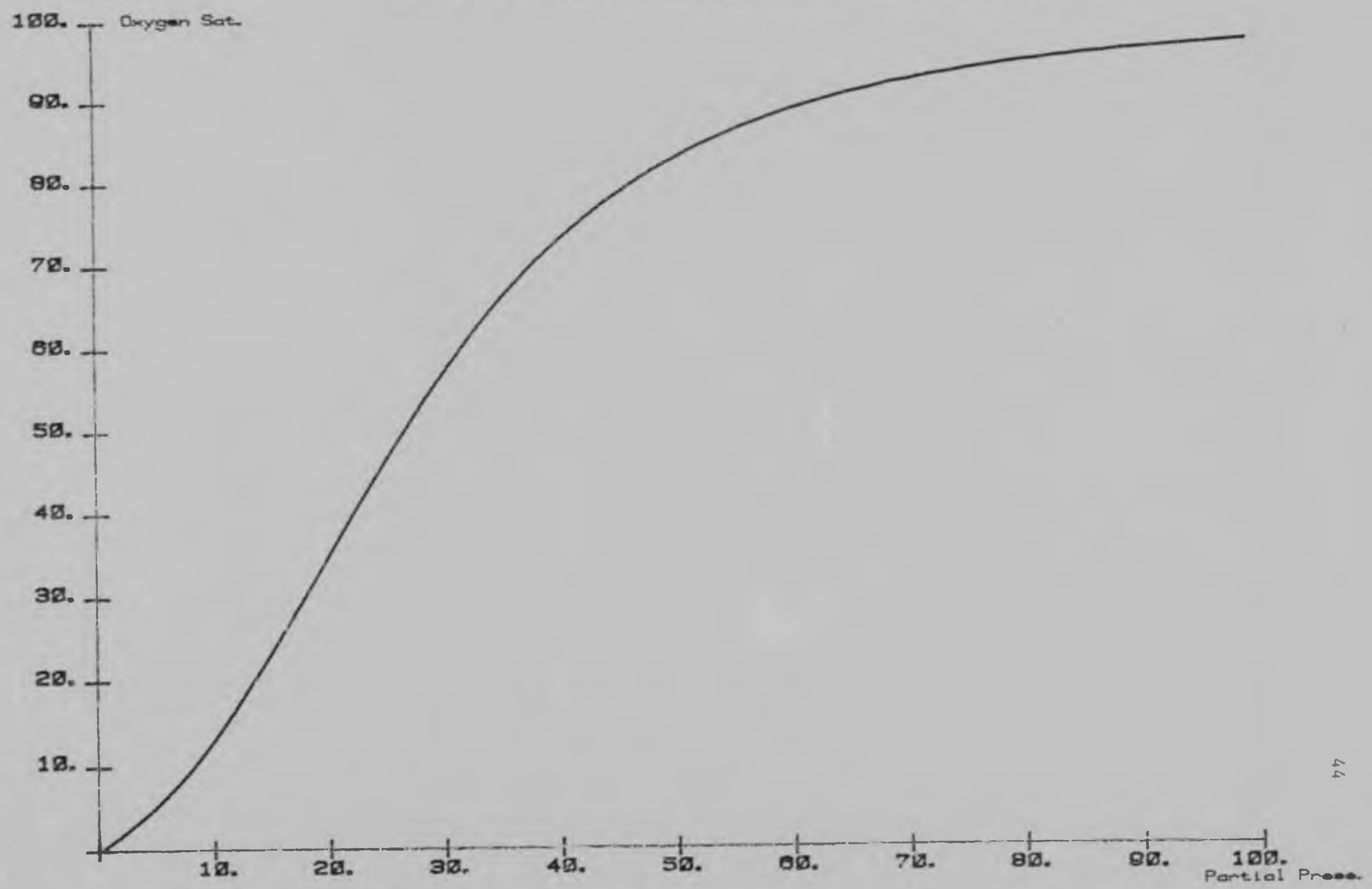
1. The oxygen content is not significantly changed when the partial pressure of oxygen is increased above 100mm Hg.

2. Changing the pressure from 70 - 100 mm Hg only changes the oxygen content by about 5%.

3. In the range 10-40mm Hg, the curve is very steep, thus in this pressure range the blood can unload large quantities of oxygen.

4. The dissociation curve is affected by blood pH (the Bohr effect) and temperature. Increasing the acidity or temperature of blood shifts the curve to the right. Thus more oxygen can be unloaded in tissue having a higher metabolic rate.

Figure 2.7 Oxygen Dissociation Curve (PH=7.4)



2.9.2 Carbon Dioxide

Carbon dioxide is also carried in two major forms. A small proportion is physically dissolved in the plasma and fluid of the erythrocytes. Carbon dioxide can hydrate into carbonic acid which in turn dissociates into protons and bicarbonate ions. The hydration reaction is catalysed in the red blood cells, hence the major portion of carbon dioxide is carried in the form of bicarbonate ions. The blood pH is closely linked to the amount of carbon dioxide in the blood (because of the dissociation of the carbonic acid.)

2.9.3 Blood-Tissue Gas Exchange

Oxygen diffuses from the capillaries into the extracellular fluid and hence to the mitochondria of the tissue. Only the blood flow through the thin walled capillary vessels contribute to the gas exchange. Flow through the arteriovenous anastomosis (see section 2.1.3) do not contribute significantly to the tissue gas tension. The movement of oxygen in the tissue (and carbon dioxide) is a diffusion process and so depends on a concentration gradient. The oxygen pressure at a point depends on the distance from the point to the nearest capillary with flowing blood, intercapillary distance, rate of oxygen consumption, magnitude of the oxygen gradient and rate of blood flow through the capillaries. It should be noted that gas tension gradients are an intrinsic property of the tissue. Therefore, it is not strictly true to refer to a "mean tissue tension". [54]. Local gas tension gradients are most efficiently changed by the opening and closing down of local capillaries. Increasing the blood flow has a reduced effect on the gradients. Tissue edema (increased tissue fluid) will increase the distance to open capillaries as well as causing the closure of local capillaries. Both effects reduce the amount of tissue oxygen.

The partial pressure of oxygen in the lungs is 100-105 mm Hg. Figure 2.7 therefore indicates that the haemoglobin is almost fully saturated. The oxygen tension drops to approximately 20 - 40 mm Hg in metabolising tissue (section 2.3.1). Therefore, there can exist a substantial arterio-venous oxygen difference. Increased oxygen requirements can be supplied either by increased blood flow or increased oxygen extraction. Sometimes both mechanisms operate.

2.10 CLINICAL SIGNIFICANCE OF PERIPHERAL BLOOD FLOW

All forms of life are critically dependant on a sufficient supply of oxygen. In the human body, the chief supply of oxygen is via the blood circulation. (see section 2.9). It thus seems reasonable to assume that knowing the state of the cardiovascular system will provide insight into the general state of the body as a whole. (In a simplistic way, this argument may be seen as an extension to the classical subjective assesment of skin colour as a tool in clinical diagnosis. A white, "pale" appearance identifies a paucity of blood supply, while a "flushed" appearance indicates a rich supply.)

The significance of oxygen and blood supply during wound healing has already been discussed (see section 2.3.1). The level of tissue perfusion is important in post operative, plastic surgery care. The effects of various pathological conditions on the cardiovascular system have been reviewed by Heistad [37].

During shock there is an initial vasoconstriction of muscle and cutaneous vessels. The constriction is more severe in the skin. After prolonged shock there is a loss of constriction (possibly as a result of the accumulation of metabolites) in the arterioles, while the constriction on the venous side remains. The combined affect of arteriole dilation and venous constriction is an increase in perfusion pressure which in turn raises the capillary filtration coefficient. This results in an accumulation

of intra vascular fluid which can contribute to shock by the pooling of venous blood in the periphery with a resulting decrease in blood P.H. [7]

In hypertension (high blood pressure) there is an initial dilation in the muscles and constriction in the skin. In later hypertension, both the skin and muscle resistance increase. In arteriosclerosis (hardening of the arteries), the resting blood flow may not significantly change, but high flow requirements may not be fully satisfied. Heart failure has similar symptoms. During exercise, the patient would have exaggerated vasoconstriction in the skin, (which is a compromise on thermoregulation).

Diabetes can result in autonomic neuropathy (degradation in nerval activity) which would result in abnormalities in the reflex control of cutaneous vessels, with impaired neurogenic sweating and thermoregulation. Raynauds disease (spasm of the arteries in the finger) results in a sharp decrease in blood flow with cooling. The capillary "nutritional" flow is significantly depressed in patients suffering from Raynauds disease.

It therefore appears that a knowledge of tissue flow, particularly skin flow can provide valuable information in a curative as well as a patient monitoring clinical enviroment.

CHAPTER 3 PROPOGATION OF LIGHT IN BLOOD AND TISSUE

3.1 INTRODUCTION

The study of the propogation of light through a medium may be approached from many different points of view. When the medium is homogeneous (i.e. the particle size of the medium is small compared to the wavelength used), then the familiar phenomina of reflection, refraction and diffraction can be identified. However, when the medium particle size becomes comparable with the wavelength, then it is not possible to differentiate between these three phenomina. A microscopic approach must be adopted which describes the interaction between the incident light and the medium in terms of scattering and absorption. The amount of scattering and absorption depends upon the properties of the medium and the wavelength of the incident light. Blood and tissue fall into the latter category

The spectral properties of blood, in the ultra-violet through infra-red range [80] are interesting. It is well known that arterial blood is red, while venous blood is bluer. Thus the absorption coefficient for haemoglobin changes strongly with wavelength and more important, there are differences between the coefficient for oxygenated and deoxygenated haemoglobin (see figure 3.1). The optical properties of haemoglobin have long been recognised as a potential method for determining the oxygen saturation of haemoglobin in blood samples. It should be remembered, when comparing photometric to manometric methods, that the former only gives an indication of oxygen combined with haemoglobin, while the latter usually gives total oxygen in the blood However the relationship between the two is readily and routinely available.

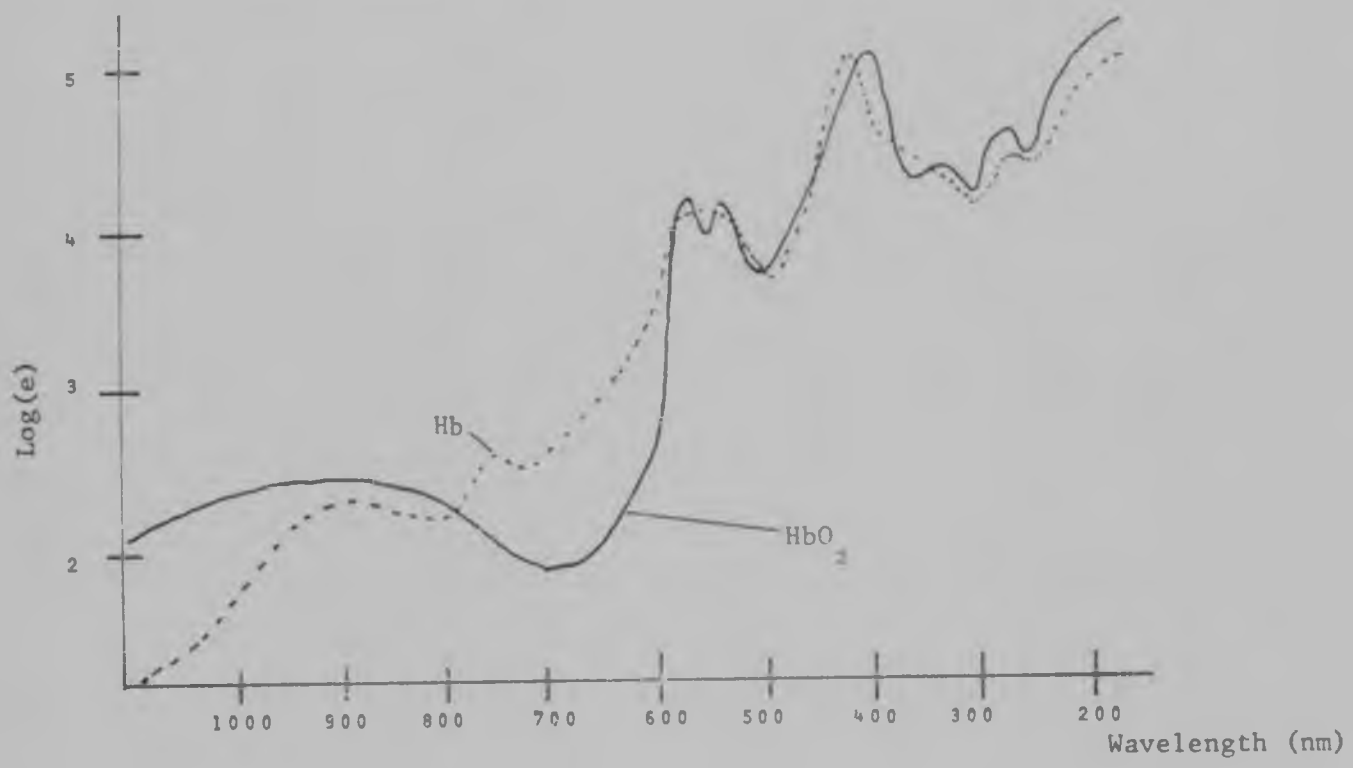


Figure 3.1 Absorption Spectrum of Hb and HbO_2

(Data from Gordy and Drabkin [80])

There have been four major theories in modelling the propogation of light in blood

(i) Lambert-Beer law

(ii) Kubelka-Munk equations

(iii) Twersky's multiple scattering theory

(iv) Diffusion equation

The first two theories are relatively simple and are essentially a one dimensional treatment. Twersky's theory is fundamental, but is mathematically complicated and difficult to apply in practice. The diffusion equation approach is borrowed from the work done on the diffusion of free carriers in semi-conductors.

3.2 PHOTOMETRIC DETERMINATION OF OXYGEN SATURATION

3.2.1 Lambert-Beer Law

The Lambert-Beer law governs the propogation of light through a solution. Since the solution is assumed to be homogeneous, only absorption is considered. This law states two important principles:

(i) The rate of change of intensity with distance is proportional to the absorption coefficient.

(ii) The absorption coefficient is linearly proportional to the concentration of absorbing substance.

Thus from property (i) [89];

$$\frac{dI}{dx} = e\,C \qquad (3.1)$$

where:

I - the intensity of the light

C - concentration of absorbing substance

The extinction coefficient (e) is a property of the absorbing substance and is a constant for a given wavelength. For convenience. the solution for the intensity of light is written from equation 3.1 in terms of base 10. The extinction coefficient is then defined as:

$$e = \log(T/Cd) \qquad (3.2)$$

T is the ratio of transmitted light to incident light. The logarithm of T (base 10) is called the optical density.

A consequence of property (ii) is that the resultant extinction coefficient of a mixture of absorbing substances (pigments) is given by:

$$e = \sum_{i=1}^{n} V_i\, e_i$$

where: V_i is the volumetric fraction of pigment i

e_i is the extinction coefficient of pigment i

3.2.2 The Extinction Coefficient

Extinction coefficients for oxy and reduced haemoglobin have been measured (figure 3.1). It is clear from figure 3.1 that there are several isobestic points (i.e. wavelengths for which the extinction coefficients of oxy and reduced haemoglobin are equal). These wavelengths are useful, since the absorption of blood at the isobestic wavelengths is independant of oxygen saturation and hence a measurement at this wavelength could be used to highlight variations in other factors which affect light propogation (see section 3.3). One isobestic point occurs at 805nm, thr are in the green part of the spectrum (500-600nm) and more are found in the ultra violet portion. In practice, the isobestic point at 805nm is used, because the absorption in the green and ultra-violet parts of the spectrum is about 100 times that in the infra-red, and thus one would have to deal with much lower level signals. However, it is also clear that the curves for oxygenated and reduced haemoglobin are much closer together in the green region whereas around 805nm they diverge quickly. Therefore, the isobestic points in the green region have the advatage that any shift or broadening in the spectrum of the illuminating light will have less of an effect than in the infra-red region.

A second useful wavelength lies in the range 650-700nm. It can be seen that there is a relatively large difference between the extinction coefficients of oxygenated and reduced haemoglobin in this region.

3.2.3 The Calculation of Oxygen Saturation

The most common method of obtaining the oxygen saturation of blood is based on the Lambert-Beer law. The optical density [i.e. log(T)] is measured at two wavelengths, where one of the wavelengths is an isobestic point (The other being in the range 650-700nm.). The concentration and depth of sample are assumed to

be the same for both measurments, and the blood is assumed to be made up of two components, viz. oxygenated and reduced haemoglobin. Then the resultant extinction coefficient is calculated from:

$$e = S\,eo + (1-S)\,er$$

where:

eo - extinction coefficient of oxygenated haemoglobin

er - extinction coefficient of reduced haemoglobin

S - Oxygen saturation of the sample

Taking the ratio of the two optical densities, we finally obtain that the oxygen saturation can be calculated from: [81,86]

$$S = \frac{O.D.^{660}}{O.D.^{805}} \cdot \frac{e^{805}}{er^{660} - eo^{660}} + \frac{er^{660}}{er^{660} - eo^{660}} \qquad (3.3)$$

where:

$O.D.^{660}$ is the optical density at a wavelength of 660nm

$O.D.^{805}$ is the optical density at a wavelength of 805nm

Experimental results at constant haemoglobin concentration and sample depth verify the linear relationship between saturation and optical density expressed in (3.3) [78,80,95], although (3.3) predicts that the relationship between the ratio of optical densities and the oxygen saturation should be the same for all

sample depths and haemoglobin concentrations, this is only true for haemolysed blood (blood in which the red blood cells have been destroyed and haemoglobin is in solution). For whole blood the slope and intercept in (3.3) change for different haemoglobin concentrations. In other words the extinction coefficient (as defined by equation (3.2)), is not independant of the haemoglobin concentration. Kramer [86] also showed that varying C and d (see equation 3.2), while keeping their product constant does not result in a linear relationship.

A further complicating factor is that the linear relationship found (at constant C and d) occurs when the optical system is essentially one dimensional (i.e. transmission type experiment). When a three dimensional arrangement is used, [62, 75, 90] as in reflection measurements, then the relationship between reflectance and oxygen saturation is non-linear and depends on the transducer geometry. Cohen and Longini [75] suggest that other "normalising functions" (besides that of the ratio of reflectances) be sought via the theoretical results of the diffusion equation.

Therefore, it would appear that the results of the Lambert-Beer law are only useful for a small class of problems, when the other variables affecting the measurement are either kept constant or are known.

3.3 FACTORS WHICH DETERMINE THE PROPOGATION OF LIGHT

3.3.1 Absorption and Scattering

When light traverses a medium its path is determined by absorption and scattering of the photons. In the previous section, (Lambert-Beer law), only absorption was considered. It was assumed that haemoglobin is the only absorbing substance in blood and that hemolysed blood is made up of a solution of haemoglobin and plasma.

The absorption factor depends upon the nature of the light. Janssen [83] showed that the absorption factor for diffuse light is twice that for collimated light. Therefore, this should be considered when calculating absorption factors for diffuse (i.e. scattered) light from extinction coefficients as extinction coefficients are normally measured using collimated light sources. Numerical values for absorption coefficients presented by some authors (see appendix 3) do not appear to take this into account.

When the medium consists of a suspension, there are other phenomina besides pure absorption which attenuate the incident wave. These phenomina are termed scattering. The degree of scattering also depends on the shape, dimension, orientation and space distribution of the particles in the medium. The red blood cells (RBC) act as scattering agents in whole blood.

The treatment of scattering can either be approached from the simple case of a single scatter, which means that the particles in the medium are only exposed to the incident beam. This will occur when the mean path length before scattering is large. However, when the density of scattering particles increases then

multiple scatters must be taken into account. By multiple scattering, it is meant that each particle is not only exposed to the incident wave but also to waves which originate from scattering by adjacent particles. Loewinger [88] suggests that if the measured attenuation of light in passing through a scattering medium is greater than exp(-0,1), then multiple scattering must be assumed.

Most authors, when working with the problem of both absorption and scattering in whole blood, assume that haemoglobin is the only absorbing agent in whole blood and that its absorption properties are independant of whether the haemoglobin is in solution or contained in the RBC. This means that the absorption coefficient of whole blood is taken to be equal to that of haemolysed blood. The observed optical density (or reflection) of whole blood is then used to calculate the scattering coefficients. It is generally agreed [73,75,78,82,83,88,98,100] that the scattering factor initially increases with increasing hematocrit, reaches a maximum around a hematocrit of 0,3-0,45 and then decreases again, i.e. a parabolic dependance on hematocrit. (Janssen [83] fitted an exponential dependance on haemoglobin concentration to the scattering factor.)

The dependance of the scattering coefficient on wavelength and oxygen saturation is not clear. Most workers have dismissed or ignored this dependance. Zdrojkowski and Pisharoty [100] considered the dependance but dispensed with it as follows: "We assume that scattering by erythrocytes is by far the most significant scattering mechanism and that this scattering is independant of oxygen saturation. Secondly, since the erythrocytes are large with respect to the optical wavelength involved, we assume that scattering is independant of wavelength over the range of interest." Janssen [83] uses a similar argument, nevertheless, he presents curves of scattering factors in which the scattering of oxyhaemoglobin at 633nm is approximately three times its value at 805nm at a haemoglobin concentration of ten millimole per litre! (typical for healthy human blood). Appendix 3 presents and discusses published values of absorption and

multiple scatters must be taken into account. By multiple scattering, it is meant that each particle is not only exposed to the incident wave but also to waves which originate from scattering by adjacent particles. Loewinger [88] suggests that if the measured attenuation of light in passing through a scattering medium is greater than exp(-0,1), then multiple scattering must be assumed.

Most authors, when working with the problem of both absorption and scattering in whole blood, assume that haemoglobin is the only absorbing agent in whole blood and that its absorption properties are independant of whether the haemoglobin is in solution or contained in the RBC. This means that the absorption coefficient of whole blood is taken to be equal to that of haemolysed blood. The observed optical density (or reflection) of whole blood is then used to calculate the scattering coefficients. It is generally agreed [73,75,78,82,83,88,98,100] that the scattering factor initially increases with increasing hematocrit, reaches a maximum around a hematocrit of 0,3-0,45 and then decreases again, i.e. a parabolic dependance on hematocrit. (Janssen [83] fitted an exponential dependance on haemoglobin concentration to the scattering factor.)

The dependance of the scattering coefficient on wavelength and oxygen saturation is not clear. Most workers have dismissed or ignored this dependance. Zdrojkowski and Pisharoty [100] considered the dependance but dispensed with it as follows: "We assume that scattering by erythrocytes is by far the most significant scattering mechanism and that this scattering is independant of oxygen saturation. Secondly, since the erythrocytes are large with respect to the optical wavelength involved, we assume that scattering is independant of wavelength over the range of interest." Janssen [83] uses a similar argument, nevertheless, he presents curves of scattering factors in which the scattering of oxyhaemoglobin at 633nm is approximately three times its value at 805nm at a haemoglobin concentration of ten millimole per litre! (typical for healthy human blood). Appendix 3 presents and discusses published values of absorption and

scattering coefficients. Sections 3.5 and 3.7 further consider the question of absorption and scattering coefficients.

3.3.2 Whole Blood

Whole blood (or non-haemolysed blood) consists of a suspension of red blood cells in plasma. Measurement of the attenuation of light through whole blood shows two important results: [86]

(i) The attenuation through whole blood samples is larger (up to 20 times) than through haemolysed blood.

(ii) While haemolysed blood follows Lambert-Beer's law, whole blood does not.

Thus early photometric determination of oxygen saturation for whole blood required a calibration in terms of the number of red blood cells. Although haemoglobin concentration in the circulating blood can change over a relatively short period of time, it will generally remain constant. However, the possibility of changes in optical properties as a result of a haemoglobin concentration change should be borne in mind.

In summary, the propogation of light through whole blood is affected by the two phenomina of absorption and scattering. Absorption takes place by the haemoglobin inside the red blood cells, while scattering is a result of one of the gross particle nature of the RBC. Absorption by the haemoglobin depends on whether the haemoglobin is oxygenated or reduced and on the wavelength of light used. The absorption is a property of the haemoglobin and is not influenced by the red blood cell concentration. Hence absorption may be determined from haemolysed blood samples and characterised by an extinction coefficient. On the other hand, scattering is influenced by the red blood cells, i.e. on the hematocrit of the blood.

Anderson and Sekelj [72] attempted, to use Twersky's multiple scattering theory to separate the absorbing and scattering phenomina in whole blood. Their results (figure 3.2) shows that the above assumption is approximately true. When the absorption factor is dominant, e.g. in the ultra violet portion of the spectrum, (figure 3.1) then the Lambert-Beer law is approximately satisfied, and optical density is a linear function of haemoglobin concentration, while in the red portion of the visible spectrum, absorption becomes negligible compared to scattering, and optical density becomes parabolic with haemoglobin concentration.

3.3.3 Tissue

Any "In Vivo" measurement on blood will mean that the effect of the surrounding tissue will have to be taken into account. A simple technique suggested by Longini and Zdrojkowski [90] is to take the resultant absorption and scattering factors as a weighted combination of the tissue and blood coefficients. Therefore we would introduce the idea of a "fractional blood volume" as the proportion of the total illumunated volume which is blood. The important tissue in peripheral oximetry is the upper layers of the skin. (see section 2.3.1). Obtaining reliable scattering and absorption coefficients for skin is more difficult than for blood because:

(i) The factors cannot be simply separated as in the case whole and hemolysed blood.

(ii) It is not simple to obtain 'in vivo' bloodless human skin. It has been suggested that bloodless skin may be approximated by pressing on the skin surface, and hence sqeezing out the blood. However, this manoeuvre changes the optical geometry.

(iii) Skin samples from cadavers are more turbid than "living skin". [21]

(iv) There is not much published data to work with.

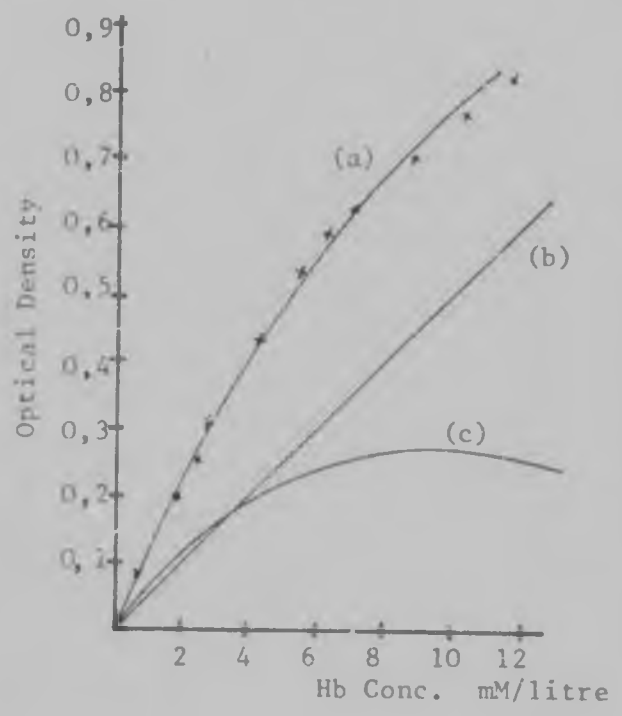


Figure 3.2 Illustration of the roles played by scattering and absorption. (a)Non linear relationship between O.D. and Hb concentration. (b)Linear relationship between O.D. and absorption. (c)Parabolic relationship between O.D. and scattering. Wavelength 550nm Sample depth 0,011cm (From Anderson and Sekelj [71], figure 6)

Care should be exercised when accepting "tissue" [75,98] values presented in the literature, as the present author does not believe that the optical properties of skin (i.e. mainly dead cells) are similar to those of internal tissue, which is mainly fluid. Appendix 3 further discusses this discrepancy.

A further difficulty, is that associated with homogeneity. Most authors have recognised that light propogation through an inhomogeneous medium is very much more complicated than that through a homogeneous medium. Thus the approach has always been to assume some average parameters (i.e. to neglect the inhomogeneity). However, tissue, and in particular, the skin is structurally inhomogeneous. The skin (see section 2.3.1) consists of an epidermis layer (which in itself consists of a number of layers of diffusing cells) and the Corium. Beneath the Corium is fatty tissue, however, as a first approximation, the lower layers may be neglected since it is unlikely that the penetration depth of light photons is greater than the thickness of the above two skin layers.

The apprcach of the Kubelka Munk theory (see section 3.4.2) attempts to approach the problem of inhomogeneity by considering the medium to be made up of a series of thin parallel sheets which are homogeneous in themselves. However, the problem geometry is essentially one dimensional. Takatani and Graham [98] have approached the problem of a two layer tissue model using the diffusion equation. This concept appears to be promising, but the present author was not able to obtain meaningful results from their equations.[1]

---

[1] In Takatani's dissertation (On the theory and development of a noninvasive tissue reflectance oximeter. Ph.D, Case Western University. 1978.), there is a dicrepancy between the equation presented for the reflectance from a two layer model (equation 2.17, page 52) and the final equation in the development of the model (equation G.40, page 268)

3.3.4 Transmission and Reflection Oximetry.

Most of the early work on the determination of oxygen saturation in the blood was done using transmitted light. This method has the advantage of having one dimensional geometry. Thus the clinical calibrations were performed using the Lambert-Beer law. [45, 80, 86] The blood was usually held in a glass curvette and hence the boundary affects could be neglected. "In Vivo", non invasive type oximeters have been developed [97]. However, the disadvantage of these types of oximeters is that there are only a few locations on the body where they can be used. The most commonly used location is the ear-lobe. It has also been suggested [93] that transmission oximetry might be clinically used in skin flaps during and after plastic surgery. The skin in the ear is thin and measurements are usually taken in a vasodilated condition (either by heating or by administering histamine). [77] Thus the effects of the tissue are neglected [97] and the Lambert-Beer law is applied.

Reflection oximetry has the advantage that it can be applied at almost any location in the body. The disadvantage of the method is that the source and receiver cannot be in the same straight line and hence the problem becomes two dimensional (polar cylindrical co-ordinates are used with cylindrical symmetry.) Thus a more sohisticated analysis is required. Rodrigo [95] attempted to surmount this problem by using a focussed beam. He argued that under these conditions of illumination, the reflection will be "mirror like". However, his treatment does not involve the deeper layers. His "normalising function" was the ratio of reflected light in fully saturated blood to the reflectance at the measured saturation. Extending this concept to a two wavelength measuring system (as is done with transmission oximetry) [72] is dubious since reflection is strongly a non linear function of wavelength. [82, 98]

An important geometric parameter in reflectance oximetry is the

sample depth. Reflectance will increase with sample depth up to approximately 3mm at which point it becomes asymptotic with depth. However, this asymptotic depth varies wih haemoglobin concentration and wavelength. As the attenuation of the incident wave change, (either as a result of changing oxygen saturation, haemoglobin concentration or wavelength) so the light will penetrate deeper and the reflected light will contain information about deeper layers. In locations such as the finger, the total depth of penetration is much less than the sample depth and hence the "infinitely thick" sample may be assumed.

3.3.5 Physiological factors

Chapter 2 gives a background to the physiology of the extremeties. For completeness, the physiological factors which would affect the optical behaviour of the tissue/blood system, will be briefly reviewed. In order to obtain meaningfull results, it has been suggested [93] that certain physiological conventions be adopted.

In Section 3.3.3 it was shown that owing to the different properties of tissue and blood, the fractional volume of blood present in the illuminated volume would be significant. Therefore the actual vasculature in the site would be important. Different vascular structures in different parts of the body, [16] would make it difficult to compare measurements taken at different sites. In addition the extent of vessel dilation must be taken into account. Thus temperature must be carefully controlled. When measuring oxygen saturation, it would be desirable to have a standard vessel dilation. Full vasodilation (e.g. by administering histamine) has been suggested [93]. The height of the peripheral tissue above the heart also affects the fractional blood volume.

Changes in haemoglobin concentration and skin pigmentation are known to affect the propogation of light. During short periods of measurements, it can be assumed that these factors remain

constant, however for long term or trend analysis, these changes might become significant.

Respiratory movements affect the vasculature. The tissue geometry is also important. A two layered model for skin is mentioned in section 3.5.

Finally, the transducer is not completely non-invasive. The pressure of the transducer will affect the blood flow through the thin papillae close to the skin. Thus the pressure should be kept as small as possible and not be allowed to vary. Further, local heating by the light sources should be considered.

3.4 THEORIES OF LIGHT PROPOGATION IN BLOOD

3.4.1 Multi-scattering theory [71,88]

The Lambert-Beer law (section 3.2.1) is the simplest type of optical attenuation law. It is only applicable to pure solutions, as it does not take into account the scattering by the particles of the medium. The Raleigh-scattering theory holds for the case when the particle sizes are small compared to the wavelength of light used and hence only considers a single scattering of an incident wave. However, blood does not fall into this category at the wavelengths used in oximetry. A fundamental approach to the case of random multi-scattering of a plain incident wave has been studied by Twersky.

The details of Twersky's theory will not be given here, but only the essentials, as they relate to the attenuation of light in blood will be presented. True absorption is assumed to take place in the red blood cells and that the characteristic length of the red blood cell is larger than the wavelength. Then the Lambert-Beer law will hold for the interior of the cell, giving:

$$\frac{I}{I_0} = \exp(-\beta_1 C d) \qquad (3.4)$$

where:

β_1 is the effective absorption cross-section.

I_0 is the incident intensity.

I is the intensity after absorption.

The scattering phenomina is divided up into coherant and incoherant scattering. The attenuation as a result of coherant scattering also follows an exponential law.

$$\frac{I}{I_0} = \exp(-\beta d)$$

The scattering cross-section, β, depends upon the index of refraction, characteristic lengths of scatters and the fractional volume of the scatters. (i.e. haematocrit (H) for blood). Hence the attenuation by coherant scattering is

$$\frac{I}{I_0} = \exp[-\beta_2 H(1-H)] \qquad (3.5)$$

where β_2 is a constant determined by the size of the RBC.

The light which is not coherantly scattered (i.e. incoherantly scattered), can be received by the detector. Only the fraction, ξ, of this intensity which is scattered into the angle of the cone which allows it to be detected must be added to (3.5). Its contribution will be:

$$\frac{I}{I_0} = \xi\{1 - \exp[-\beta_2 H(1-H)d]\} \qquad (3.6)$$

The combined effect of absorbing and scattering is given by the sum of their respective cross-sections. In general, the absorption cross-section for the incoherantly scattered portion (β_3) will be different to that for the coherantly scattered light.

Thus we finally obtain the Twersky formulation for multiply scattered waves from equation 3.4 - 3.6 as:

$$\frac{I}{I_0} = \exp[-\beta_2 H(1-H)d] \exp(-\beta_1 Cd) + \xi \{1 - \exp[-\beta_2 H(1-H)d]\} \exp(-\beta_3 Cd) \qquad (3.7)$$

if we assume $\beta_1 = \beta_3$ [71]

and write (3.7) in terms of optical densities (O.D.) (i.e. taking logs) then the O.D. consists of two terms viz.

$$O.D. = \beta_1 Cd + \log F(s) \qquad (3.8)$$

The first term in (3.8) is equivalent to the Lambert-Beer law and the second term depends only on scattering parameters. It is non-linear with respect to both haematocrit and optical depth. Anderson [71] gives experimental evidence to support equation 3.8 (figure 3.2).

The above theory is fundamental, but because most of the parameters involve quantities which are very difficult to measure (e.g. characteristic lengths), it does not present a practical theory. In addition, it is not obvious as to how the transducer geometry is to be incorporated.

3.4.2 A Phenomenological Approach

An attempt to overcome the difficulties associated with the fundamental approach of the previous section is to use a phenomenological approach (actually, chronologically, this was the first approach).

The Schuster radiation theory approaches the problem of scattering and absorption by dividing the propogation up into two fluxes which are directed in opposite directions, one of which is the direction of the incident wave. Attenuation of the light is assumed to take place in a thin layer which can be characterised by an absorption and scattering factor. According to this theory, the reflection from an "infinitely thick" sample is given by: [95]

$$R = p - \sqrt{p^2 - 1} \qquad (3.9)$$

where:

$$p = \frac{a}{bs} - 1$$

and b is the fraction of backscattered light and will depend on the size of the particles. Expanding (3.9) using a Taylor series, it can be shown that to a first approximation the reflection is inversely proportional to p.

Further development of the theory leads to the Kubelka-Munk equations. The assumptions involved in de iving these equations are:

(i) The medium is divided up into a series of layers. Each layer is thick enough to incorporate all absorption

and scattering phenomina. The intensity of absorbed and scattered light is proportional to layer thickness.

(ii) The sample is assumed to have one-dimensional geometry.

(iii) The incident illumination is diffuse (if the incident light is a collimated beam then the intensity distribution will gradually change to diffuse with increasing penetration into the medium. In this case no simple approach may be adopted.

Using the above three assumptions the differential equations for transmission and reflection from an elementary layer may be written as [83]

$$\frac{dT}{dx} = -(a+s)T + sR \qquad (3.10)$$

$$\frac{dR}{dx} = (a+s)R - sT \qquad (3.11)$$

where:

a - the absorption coefficient

s - scattering coefficient

The reversal of signs between 3.10 and 3.11 is because R and T are in opposite directions (i.e. T is in the direction of increasing x while R is in the direction of decreasing x)

The solutions to (3.10) and (3.11) are [83,90]:

$$k(d) = \frac{s}{\eta} T(d) \text{ Sinh}(qd) \qquad (3.12)$$

$$= \frac{1}{\text{Cosh}(qd) + \frac{a+\eta}{q} \text{Sinh}(qd)} \qquad (3.13)$$

$$q = \sqrt{a(a+2s)}$$

d = sample depth

limit of an "infinitely thick" sample (ie one for which sample thickness is much larger than the photon penetration , reflectance is:

$$= \frac{}{} \qquad (3.15)$$

practical. The absorption factor can be calculated from the extinction coefficient measured on haemolysed blood (section 3.3.1) and the scattering factors may be calculated from 3.12 - 3.15 The main objection to this theory is that it is only applicable to one dimensional problems. In fact, similarity between this solution and the solution for the one dimensional diffusion equation [100] (see next section) suggest that the Kubelka-Munk equation may be regarded as a special case of this more general approach. Hirko et al [82] suggest that the radial distance from a point source to detector may be app-

roximated by assuming a decrease in intensity inversely proportional to the square of the radius from source to detector.

Multi-layer models are simply treated using this theory. Longini and Zdrojkowski [90] briefly examined a three layer model.

3.4.3 The Diffusion Equation

Longini and Zdrojkowski [90] first suggested that the scattering and absorption factors given in equations 3.10 and 3.11 be related to the mean free path and diffusion constant which are employed in the diffusion equation. This equation was first used by Shockley to model the movement of free carriers in semiconductors. The partial differential diffusion equation degenerates into a simple second order, ordinary differential equation when a one dimensional model is assumed, (i.e. similar to the Kubelka Munk geometry). Zdrojkowski and Pisharoty [100] have solved this equation. The results for reflectance are similar to those obtained from the Kubelka-Munk equations (see section 3.5).

A sketch of the derivation of the diffusion equation will now be presented. The theory considers the diffusion of photons. Incident photons penetrate the medium and become scattered. The incident photons will be denoted by P_1, while once they become scattered they obey the diffusion equations and are designated P_0. The corresponding fluxes are $\bar{F}_1$ and $\bar{F}_0$.

The incident flux (i.e. rate of photons crossing a cross-sectional area per unit time in a given direction $\bar{u}$) is given simply by:

$$\bar{F}_1 = P_1 \, c \, \bar{u} \qquad (3.16)$$

where c is the velocity of photon propogation in the medium. The diffussed photon flux is:

$$\tilde{F}_2 = - D \nabla P_2 \qquad (3.17)$$

where D is the diffusion constant and ~ del) is the divergence operator. The mean photon lifetime assumed to be the same for both P_0 and P_1. The continuity equation for photons requires that the total flux into a given volume must be equa. to the rate at which photons are lost, i.e.

$$-\int_A \tilde{F}_2 \cdot d\tilde{A} = \frac{1}{T}\int_V (P_0 + P_1) \, dV \qquad (3.18)$$

Where A is the surface enclosing volume V. Applying the divergance theorem and using 3.17 yields:

$$D \nabla^2(P_2) - \frac{P_2}{T} = \frac{P_1}{T} \qquad (3.19)$$

The diffusion constant and lifetime are related to the scattering and absorption constants by [82,90]

$$D = \frac{c}{2s + a} \qquad (3.20)$$

$$T = \frac{1}{s\ c} \qquad (3.21)$$

The solution of 3.19 depends on how the incident photon density $P_1(x,y,z)$ is chosen. This is important since only randomly scattered photons (i.e. non-source) photons obey the diffusion equation. Because source photons penetrate some depth into the sample, a distributed source actually lying in the medium has been suggested [100]. Three models for the sources have been considered [76].

(i) An exponentially decaying line source lying along the the z axis (figure 3.3) would approximate a source whose penetration depth (equal to 1/(a+s), see equations 3.10-3.11) is much larger than the source diameter. A narrow collimated source would approximate to this model.

(ii) A uniform source whose diameter is much larger than its penetration depth. This would be represented by the boundary condition 3.22. This model will approximate a diffuse source.

(iii) A cylindrical source whose intensity decreases with penetration depth into the medium.

Model (iii) best approximates to a real source, but is the most complex to treat.

The next problem is to decide on the boundary conditions. Most authors assume that the medium is homogeneous and "infinitely thick" hence the photon density must tend to zero with increasing depth. The interface at the surface of the medium is assumed to be perfectly absorbing. Thus using cylindrical polar co-ordinates and recognising that for a cylindrical source density, P_1, will be zero everywhere on the surface except under the source, where it will have uniform density P.

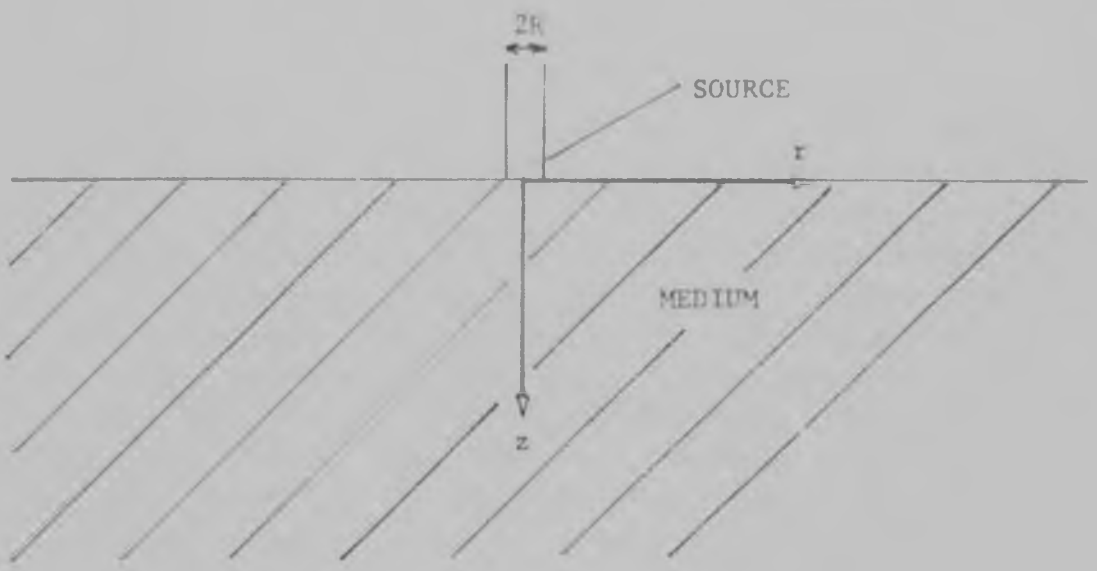


Figure 3.3 Geometry for Diffusion Equation

Referring to figure 3.3 we see that the boundary conditions require that:

(i) At the surface z=0

$$P_1 = 0 \qquad r>R \qquad (3.22)$$

$$P_1 = P \qquad r<R \qquad (3.23)$$

(ii) as z becomes large, P_1 tends to zero.

If we now recognise that the medium is structually inhomogeneous and model this as several layers (see figure 3.4) having different optical parameters, then the boundary conditions at the interfaces between the layers must be defined. At a boundary between two layers the photon flux must be continuous. Thus using equations 3.16 and 3.17 for the incident and diffused photon

fluxes we get for the boundary between layer 1 and layer 2 that: [75, 98]

$$\eta \frac{\partial P_1}{\partial z}\Big|_{\text{layer 1}} = D \frac{\partial P_1}{\partial z}\Big|_{\text{layer 2}} \qquad (3.24)$$

$$c\,P_1\Big|_{\text{layer 1}} = c\,P_1\Big|_{\text{layer 2}} \qquad (3.25)$$

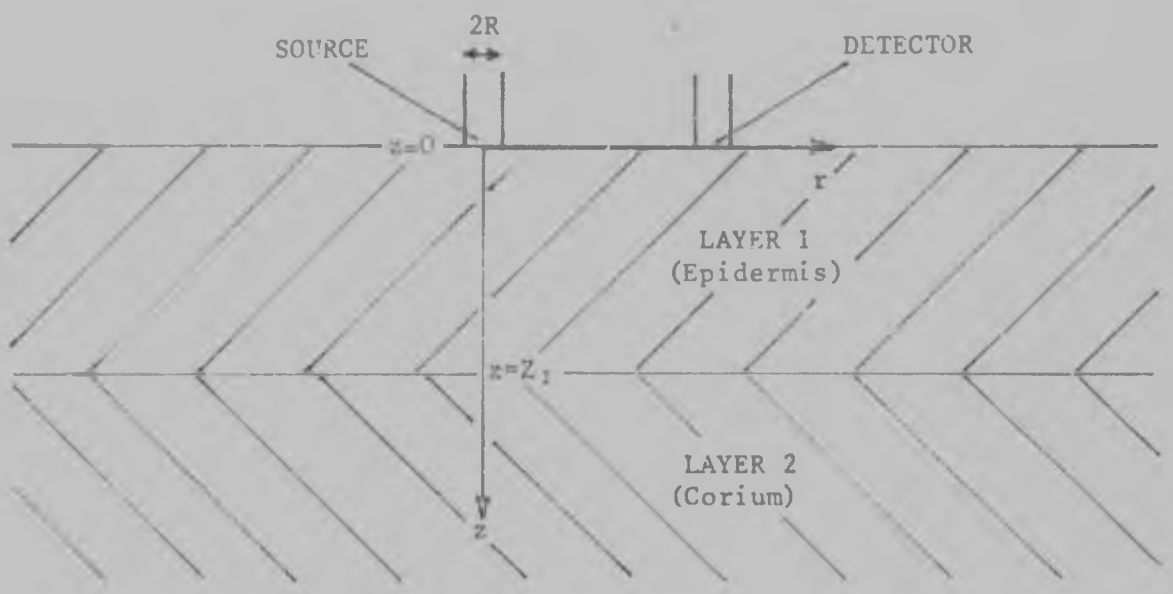


Figure 3.4 Boundary Conditions for 2 Layer Model

Furthermore, a second boundary condition requires that the ratio of the boundary photon densities bear the following relationship to the refractive indices of the two layers.

$$\frac{P\ (r,z=Z_1^-)}{P\ (r,z=Z_1^+)} = \frac{(\gamma_1)^2}{(\gamma_2)^2} \qquad (3.26)$$

Where Z is the depth of the interface γ_1 and γ_2 are the refractive indices of the two layers. Takatani and Graham [98] have found solutions for equation 3.19 subject to the boundary conditions (3.22 - 3.26). They however do not make it clear as to what source model they have used. Their results show that the significance of reflection from the second layer depends upon the following:

(i) Incident wavelength: The absorption constant is wavelength dependant, and hence the penetration depth of the photons will depend upon the choice of wavelength (figure 3.1). If the penetration depth (penetration depth = 1/[a+s]) is comparable to the thickness of the first layer, then reflectance from layer 2 will be significant.

(ii) Oxygen saturation: For wavelengths for which the absorption of oxy and reduced haemoglobin differ by a significant amount (e.g. near 650 nm), then the penetration depth will depend upon the degree of oxygen saturation.

(iii) Changes in the fractional blood volume: The scattering and absorption factors (see appendix 3) differ for blood and tissue. Thus the penetration depth will depend on how much of each is present.

(iv) Tissue and transducer geometry: The relative and absolute thickness of the two layers will influence the amount of reflectance from the second layer. For a layer thickness ratio of 1mm:3mm (a good approximation for a two layer skin model), the

second layer is significant. The separation (r) (figure 3.4) between source and collector is important. As the separation increases, so the reflection from the second layer will increase.

3.5 COMPARISON OF THEORIES

Three theories of light propogation through an absorbing and scattering medium were discussed in section 3.4. An inhomogenous medium such as the outer tissue layers of the human body makes an accurate description very complicated. In order to construct a working model for use with the oximeter a balance must be found between accuracy and complexity, where it must be remembered that measurement of human skin and blood parameters are often difficult to realise. It is therefore constructive to compare a relatively simple model, such as the phenomenological approach to a more complex model, such as the diffusion equation. The models are compared with respect to complexity, applicability, practical application and predicted results.

3.5.1 Complexity

The mathematical tractability of the models increase by a few orders of magnitude when moving from a single dimensional model to a three dimensional approach. The case where source and detector are in the same straight line and where scattering is only allowed in the line of incident radiation, have closed form solutions. The phenomenological, Twersky multiple scattering and one dimensional diffusion equation fall into this category. When the problem geometry is extended to three dimensions, the problem no longer has closed form solution. [76,98] Even although the geometry may be reduced to essentially two dimensions by an appropriate choice of co-ordinate system, the solutions must still be numerically sought. The complexity of these solutions

increase rapidly as the source model is changed from a line source to a cylindrical source. This occurs because a line integral becomes a volume integral, which significantly increases the complexity.

The numerical solutions, besides being tedious and time consuming, do not allow a physical understanding of the model. The roles of scattering and absorption are not explicit as they become merged into the "diffusion constant" and "photon life time" parameters of the diffusion equation which in turn appear in a fairly complex form in the solution.

3.5.2 Applicability and Accuracy

As the problem geometry is obviously three dimensional, a three dimensional model would be more accurate. The question then arises as to how well the single dimensional models approximate the situation. The important assumptions in the latter model are that scattering can only take place in the line of incident radiation. This implies that photons which are not scattered in this line must be completely absorbed as they cannot be again scattered into the region of interest. In other words, a cylindrical medium with perfectly absorbing walls. The fingertip tissue obviously does not fit into this description as can be easily verified by simply placing a light source at the skin surface; a broad region of illumination results.

Secondly, because the detector is not in the same line as the source, all the received light must have been scattered in three dimensions, i.e., this type of scattering is primary and not secondary to the model.

If it is accepted that scattering in three dimensions must be considered, then the question of the choice of source model arises. Three models were suggested in section 3.4.3. The best approximation is a cylindrical source which decays exponentially into the medium. However, if the source diameter is small

compared to the source collector separation and depth of penetration into the medium, then a line source may be used. The source collector separation used in the experiments (Chapter 5) is approximately 5mm, while the source radius is 1,5mm.

3.5.3 Practical Application.

As the model is required for prediction in a real situation, its practicality must be assessed. This problem is intimately associated with the question of parameter measurement. The multiple scattering theory requires parameters such as the effective absorption and scattering cross-sections. These are not readily measurable and hence the theory is of little practical value.

The remaining theories requires scattering and absorption parameters for tissue and blood. Only one of these four parameters, the absorption coefficient of blood, has been accurately measured. Values for the other parameters have appeared in the literature but these values show a large amount of scatter between different authors (see Appendix 3).

The measurement of human parameters is heavily constrained, thus the measurement problem is not simple because, firstly, the absorption and scattering phenomena must be separated and secondly, the tissue and blood must be separated. Blood is relatively easy to isolate, but tissue is not. Elimination of the blood component was attempted "in vivo" by compressing the tissue, hence forcing the blood out of the superficial capillaries. However, the results obtained are unreliable because optical geometry is changed when the tissue is compressed. It is suggested that parameter values will have to be obtained via an indirect method where the fractional blood volume is changed by a fixed amount in a controlled experimental environment. Correlation between the oximeter results and an independent method of measurement (Section 2.8.2) would allow values to be calculated.

3.5.4 Predicted Outputs.

Probably the most important point when comparing the models is to consider their outputs. The decision to adopt a simpler model lies mainly in its ability to closely represent a more complicated model. The predications of the Kubelka [90], one dimensional diffusion [100] and the three dimensional diffusion equation using a line source [76] are presented in figures 3.5 and 3.6. At present, the main interest is not to observe absolute values of reflection, but rather to study the manner in which reflection changes with variations in the optical properties of the medium (see section 3.6). Therefore, in order to facilitate comparison, the curves in figure 3.5 and 3.6 have been normalised to a scale of (0-1).

Figure 3.5 presents the variation of normalised reflectance with scattering factor. A "thick" layer has been assumed, the absorption coefficient has been arbitrarily set to 0,5 and source collector separation in the three dimensional model to 5,0. (Note that the unit chosen for absorption and scattering coefficients and the source detector separation are unimportant, so long as they are all measured in the same unit. The above values were chosen with the unit of length being the millimetre.) Figure 3.6 shows the variation of reflection with absorption coefficient. The scattering coefficient was chosen to be 1,0 and the source detector separation remained 5,0. Changing the absorption coefficient over a range of 0,05 to 1,0 and the scattering coefficient in figure 3.6 over a range of 0,1 to 1,0 does not significantly change the form of the curves. Variations in the source collector separation do affect the curves but for separations greater than 0,5 (same units as above), the forms of the curves are essentially the same. Also, accurate deductions cannot be obtained from the three dimensional model at small separations because the solutions are not "well behaved" for the separation tending to zero. [76]

Figure 3.5 Comparison of the Three dimensional Diffusion, Kubelka and One Dimensional Models. Absorption = 0.5; Source-Collector Sep = 5.0.

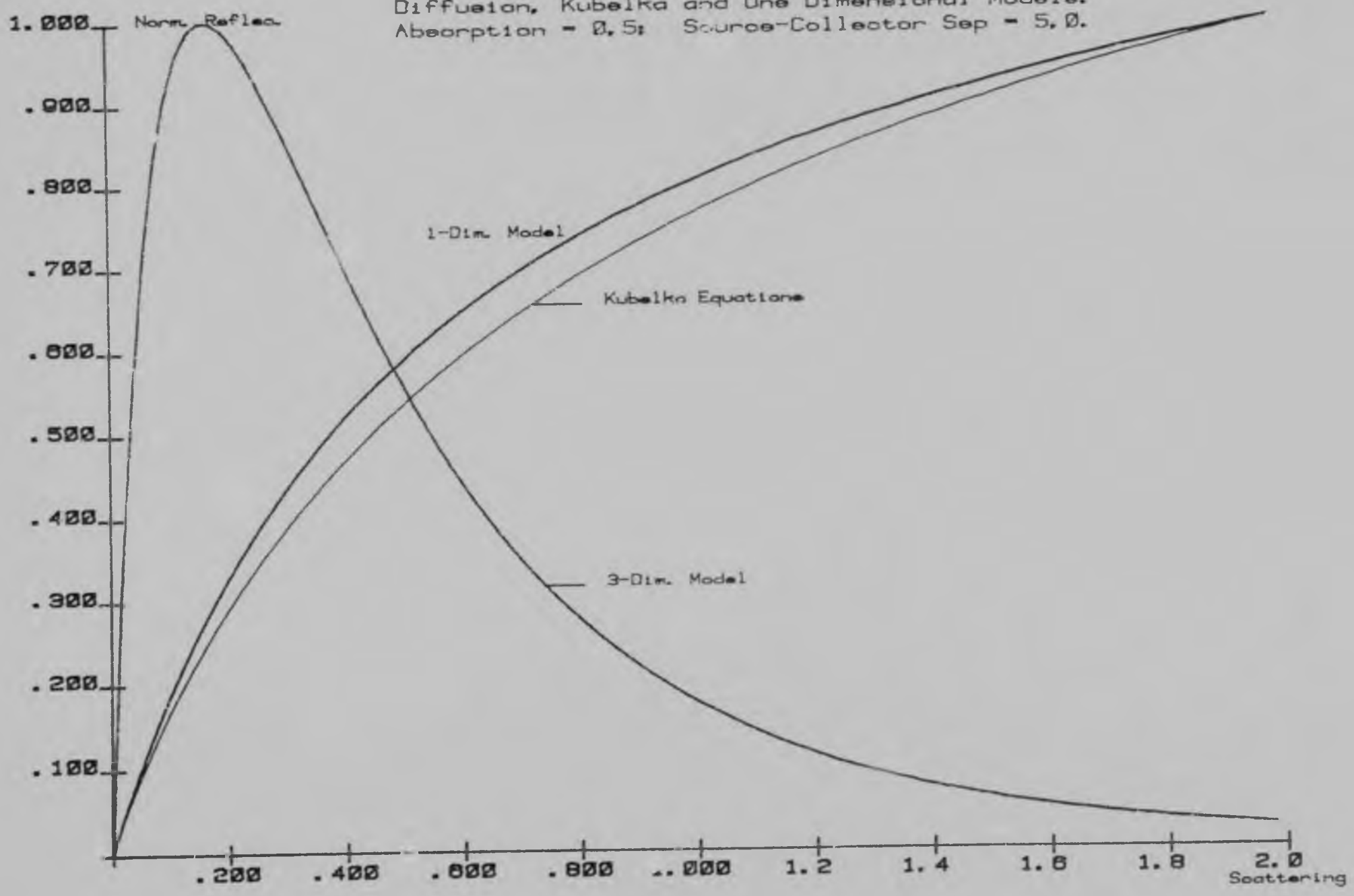


Figure 3.5 Comparison of the Three dimensional Diffusion, Kubelka and One Dimensional Models. Absorption = 0.5; Source-Collector Sep = 5.0.

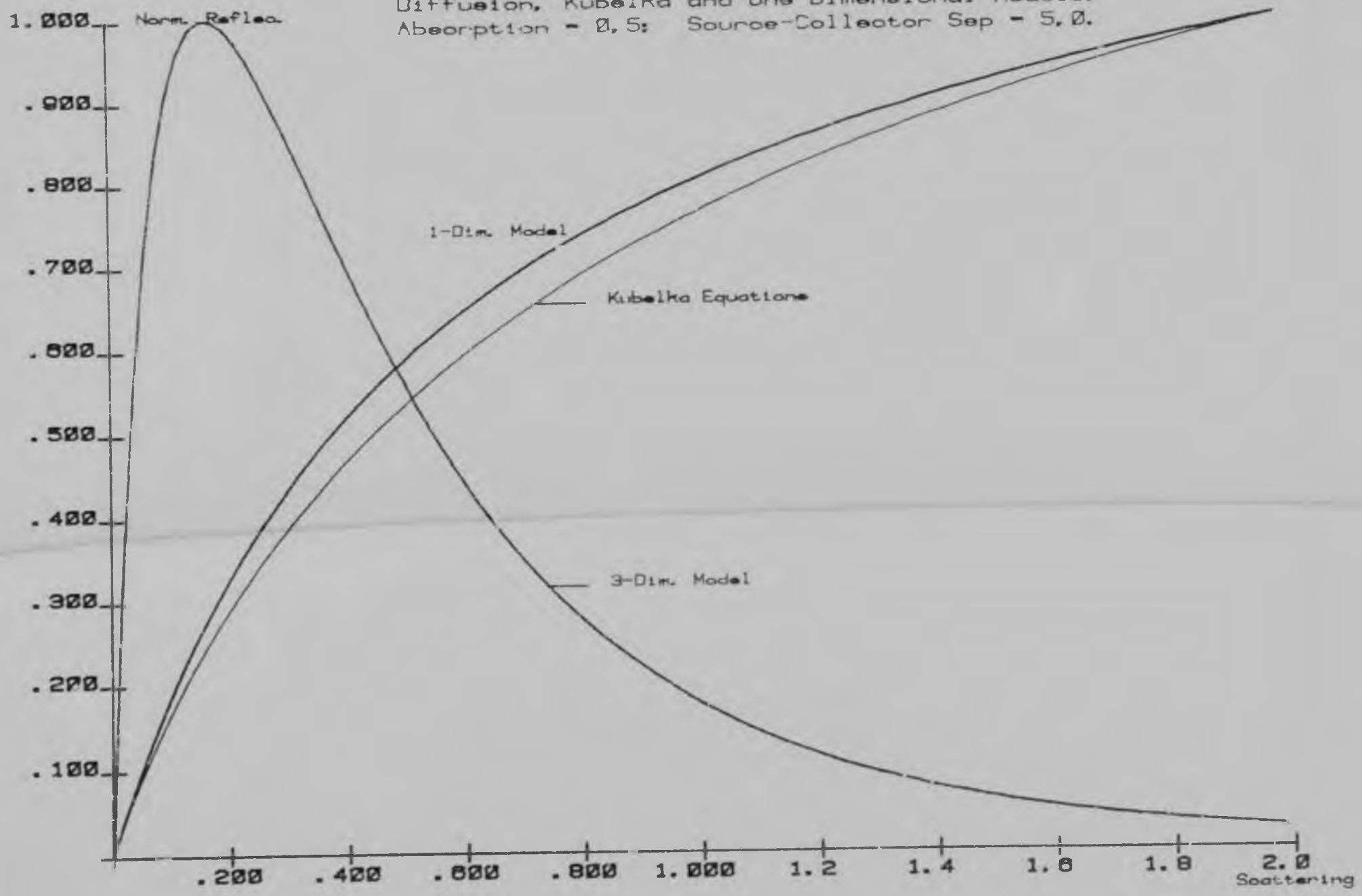
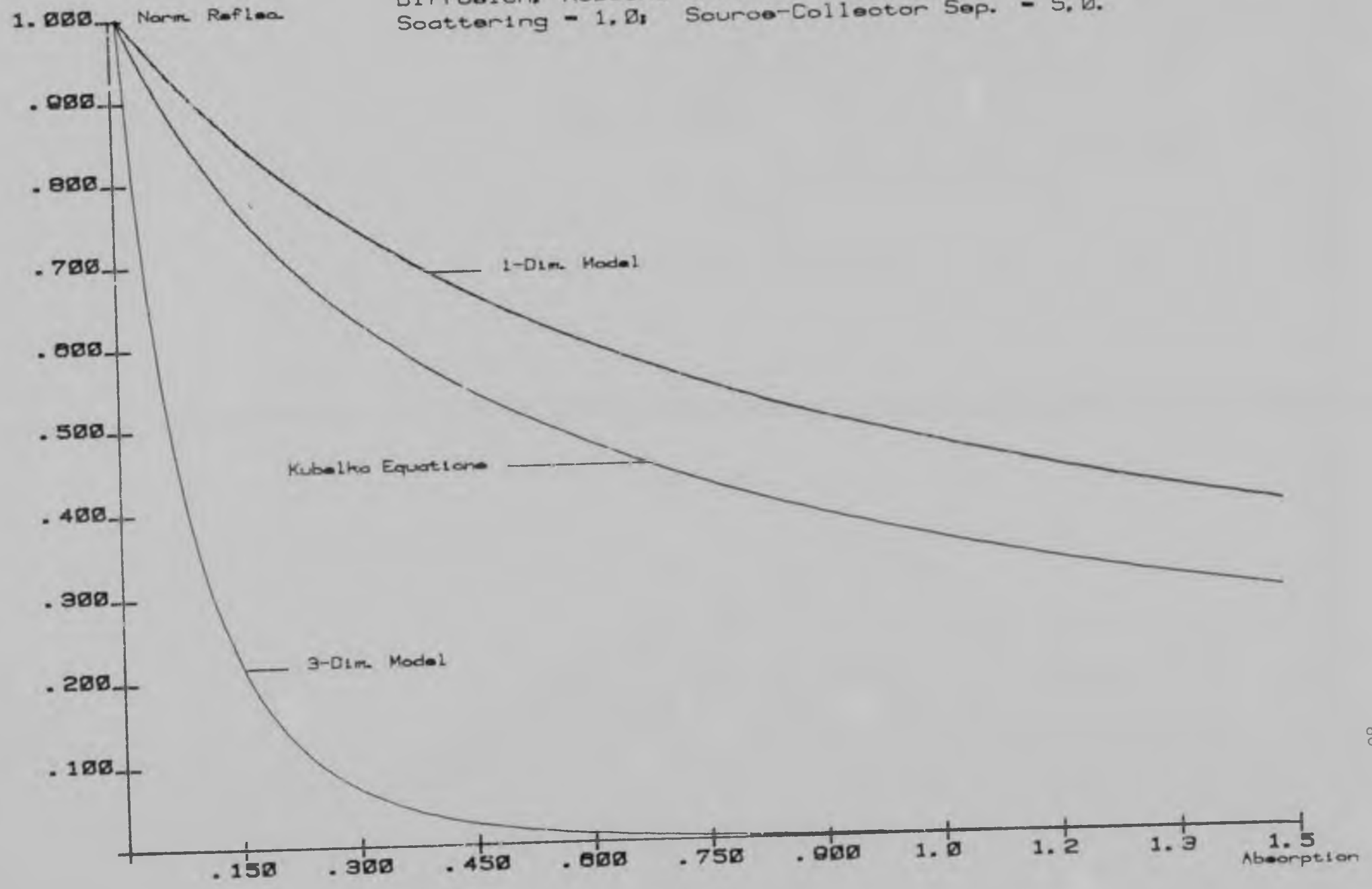


Figure 3.6 Comparison of the Three Dimensional Diffusion, Kubelka and One Dimensional Models. Scattering = 1.0; Source-Collector Sep. = 5.0.



The first observation to note is that the predictions of the three dimensional model differ considerably from the one dimensional theories, especially in figure 3.5 where a maximum exists in the former case but the latter are monotonically increasing with scattering factor. This difference is critical in a trend monitoring environment where the dynamic behaviour is examined, as an increase in optical parameters (e.g. fractional blood volume) in one model would be interpreted as a decrease in the other.

Secondly, the differences in rates of change of reflectance with the optical properties should be noted, together with the ranges of parameter values over which reflectance is significant. This point is important when parameter values derived from one theory are transported to another theory.

3.6 ABSOLUTE AND TREND ANALYSIS

Originally oximetry was investigated and developed [72, 80, 86] in order to be able to obtain absolute measurements of the oxygen saturation of blood samples. Empirical, non linear nomograms were developed which were able to determine the oxygen saturation of whole blood to within 2% [72]. By means of transducer design and analogue electronic circuits, [78, 84, 97] direct readings of oxygen saturation, haemoglobin concentration and dye dilution curves are obtainable via optic fibre catheter oximeters. The accuracy of the readings (2%) is perfectly acceptable for clinical applications.

It therefore appears that the photometry problem has been solved for the case of whole blood. What has not been investigated is the photometry problem in the presence of differing layers of tissue intermingled with capillaries; each capillary carrying blood of a different oxygen saturation. Absolute measurement in this case, are almost impossible because;

(i) The inhomogeneity present in the tissue structure can only be approximated.

(ii) Tissue scattering and absorption parameters are difficult to measure.

(iii) The structure and geometry of the blood vessels is not known and varies from individual to individual.

(iv) Physiological factors affect the state of dilation constriction of the vasculature. These factors are not fully understood.

(v) The oxygen saturation varies between capillaries and hence only a mean value can be hoped for. The dynamics of the change in saturation in response to changes in vasculature and metabolic requirements is not known.

(vi) The physical laws governing the optical behavior are much more complicated and no simple, valid theory is available.

As a result of the above, the best that can be expected from photometric measurements through skin is to be able to observe trends and the general form of response to various stimuli. It is postulated that by using a two layer reflectance model in conjunction with a lumped parameter physiological model, an understanding of the peripheral blood flow phenomina may be obtained.

It is hypothesised that as an adequate oxygen supply is essential for cell life and the cardiovascular and respiratory systems comprise an integrated system throughout the body, that any pathological (or other) changes in one part of the body will affect the rest of the body. Furthermore, one may argue that

since the peripheral tissue represents a comparatively "non essential" and hence potentially "disposable" tissue mass, any changes will first be reflected here.

Commonly measured variables for clinical use (e.g. temperature, blood pressure, heart rate) are controlled variables, and hence any adverse phenomina which affect these variables will only be detectable once they have degraded to such a degree that further compensation via their respective controllers is not possible. Therefore it may be possible by monitoring the peripheral vasculature to detect these phenomina at an early stage when treatment will be simpler. It should be emphasized at this point, that the above argument is a hypothesis. The peripheral changes have not been clearly identified. Time traces of the outputs exhibit periodic behaviour, for example the heart rate is clearly visible. Others such as temperature rhythm can be seen, but are not easily extracted from the raw data. The spectral work in section 5.5 examines this point further. It is thought that by examining large amounts of data from healthy and various pathological patients, that some correlation will be found. Such measurements may be obtained using a non invasive type reflection oximeter. Before such an attempt can be made, it is important that the output from such an instrument is better understood.

3.7 DISCUSSION AND CONCLUSIONS

The investigation presented in the preceding sections into existing models indicate many inadequacies. There are major qualitative and quantitative differences between the predictions of the simple and more complex models. Extreme care must be exercised when accepting a single dimensional model in place of a three dimensional model. This can only be justified when the source and detector are very close together. This may occur if a fibre optic transducer system is used in which the source and collector bundles are intermingled. However, in the present case where commerical LEDs are used, this approximation is not valid.

The major differences occur because of the manner in which light is received by the detector. In the one dimensional models, scattering is only permitted in the same line as the incident beam, whereas in the three dimensional model the detector receives reflected light as a result of scattering of photons off the line of incident radiation. It proves convenient to consider the heuristic model illustrated in figure 3.7.

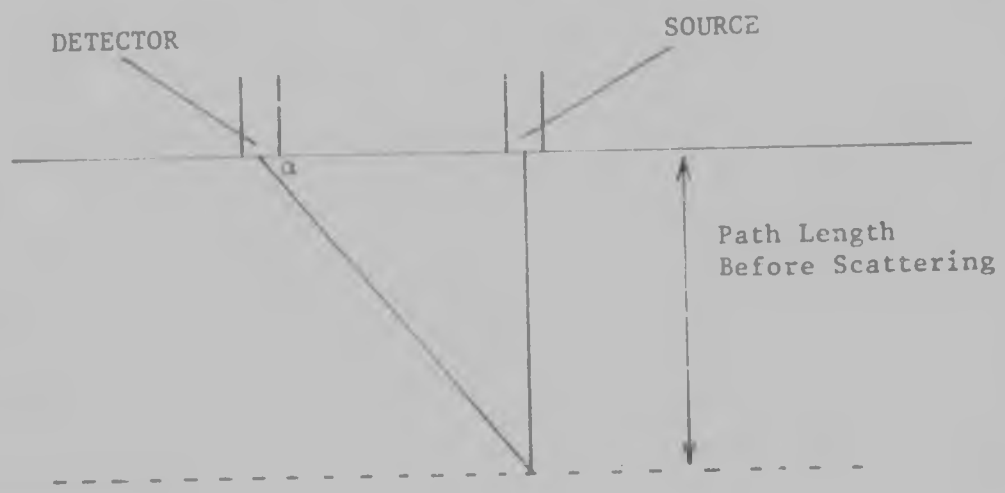


Figure 3.7 Heuristic Model of 3-Dimensional Geometry.

Only those photons scattered into the cone, angle α may be received by the detector. Therefore as the path length before scattering increases (i.e. the scattering coefficient decreases), so α will increase. However, for a fixed absorption coefficient, the photon density decreases exponentially with distance into the medium. Thus it is clear that as the scattering coefficient is decreased, the reflectance will initially increase, reach a maximum and then decrease. Mathematically this concept is represented by:

$$R = A \exp(B/Scat) \times \arctan(C/Scat)$$

where in figure 3.8,

$$A = 1,66; \quad B = -0,055; \quad C = 0,177$$

A comparison of this equation and the line source model is given in figure 3.8. In contrast to this explanation, the one dimensional model predicts that the shorter the path length to the first scatter (i.e. the greater the value of the scattering coefficient), the larger the reflectance. Hence the strict increase in reflectance in figure 3.5.

The second observation concerns the choice of parameter values. In the three dimensional model, reflectance drops off sharply with absorption coefficients resulting in an extremely small reflectance for an absorption coefficient greater than 0,5, whereas in the one dimensional case variations are easily detectable up to coefficient values of 2,0. This point is important when using published values, as these are usually obtained from a one dimensional model. Published blood absorption coefficients vary from approximately 0,3 (mm^{-1}) to above 2,0 (mm^{-1}). The prediction from the three dimensional model over this range is very different from the single dimensional model.

The differences are more poignant in the case of the scattering factor, as the slope in figure 3.5 changes at a relatively low value (compared to the published one). This means that in the "physiological range", an increase in scattering factor in the three dimensional model would result in a decrease in reflectance while the model from which the values were derived predict an increase.

In other words it is questionable as to whether the values obtained from a simple model may be used in a more complex model. Although accurate values are not required for trend monitoring

$$R = A \exp(B/Scat) \times \arctan(C/Scat)$$

where in figure 3.8,

$$A = 1,66; \quad B = -0,055; \quad C = 0,177$$

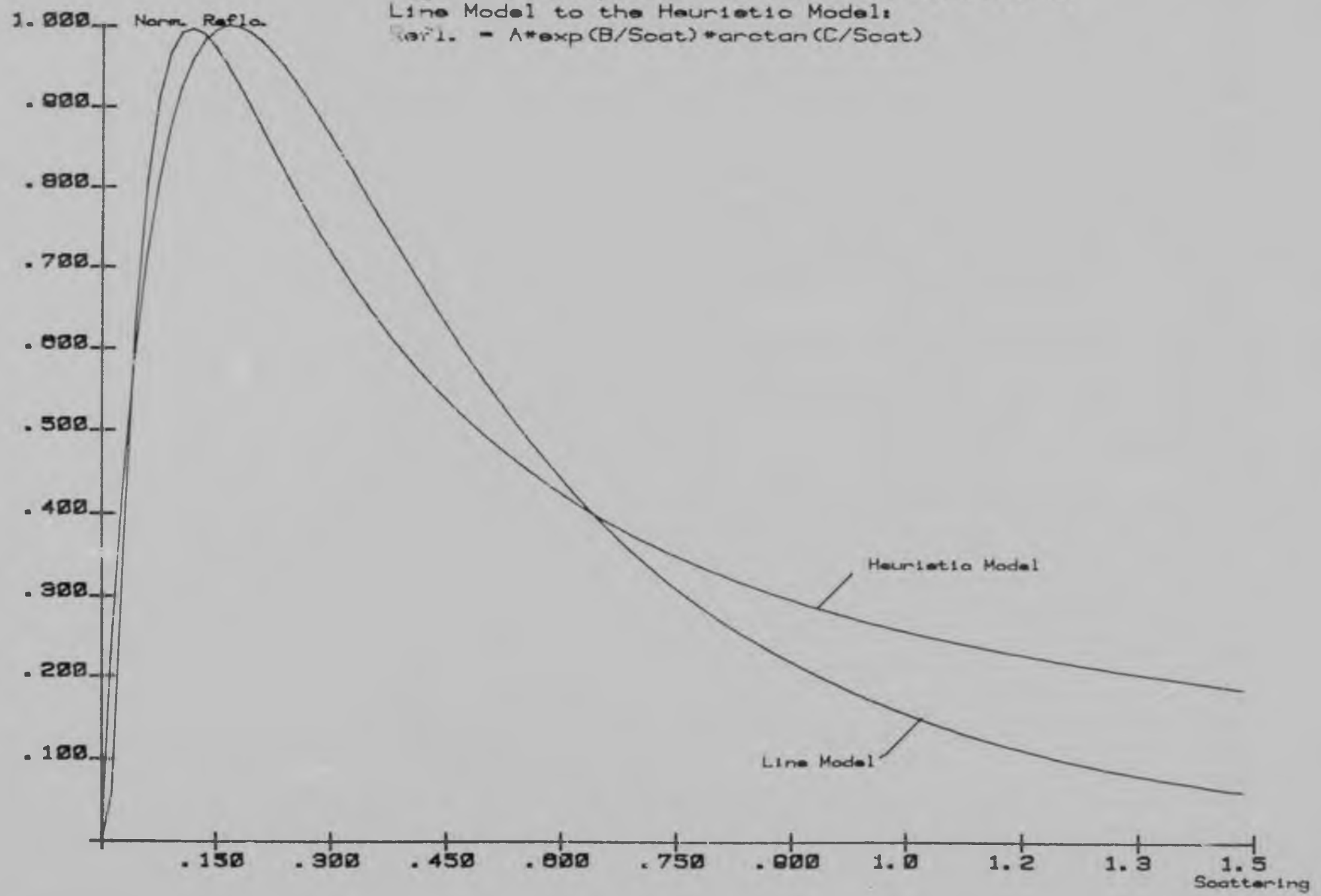
A comparison of this equation and the line source model is given in figure 3.8. In contrast to this explanation, the one dimensional model predicts that the shorter the path length to the first scatter (i.e. the greater the value of the scattering coefficient), the larger the reflectance. Hence the strict increase in reflectance in figure 3.5.

The second observation concerns the choice of parameter values. In the three dimensional model, reflectance drops off sharply with absorption coefficients resulting in an extremely small reflectance for an absorption coefficient greater than 0,5, whereas the one dimensional case variations are easily detectable up to coefficient values of 2,0. This point is important when using published values, as these are usually obtained from a one dimensional model. Published blood absorption coefficients vary from approximately 0,3 (mm^{-1}) to above 2,0 (mm^{-1}). The prediction from the three dimensional model over this range is very different from the single dimensional model.

The differences are more poignant in the case of the scattering factor, as the slope in figure 3.5 changes at a relatively low value (compared to the published one). This means that in the "physiological range", an increase in scattering factor in the three dimensional model would result in a decrease in reflectance while the model from which the values were derived predict an increase.

In other words it is questionable as to whether the values obtained from a simple model may be used in a more complex model. Although accurate values are not required for trend monitoring

Figure 3.8 Comparison of the Three Dimensional Line Model to the Heuristic Model:
Norl. = A*exp(B/Scat)*arctan(C/Scat)



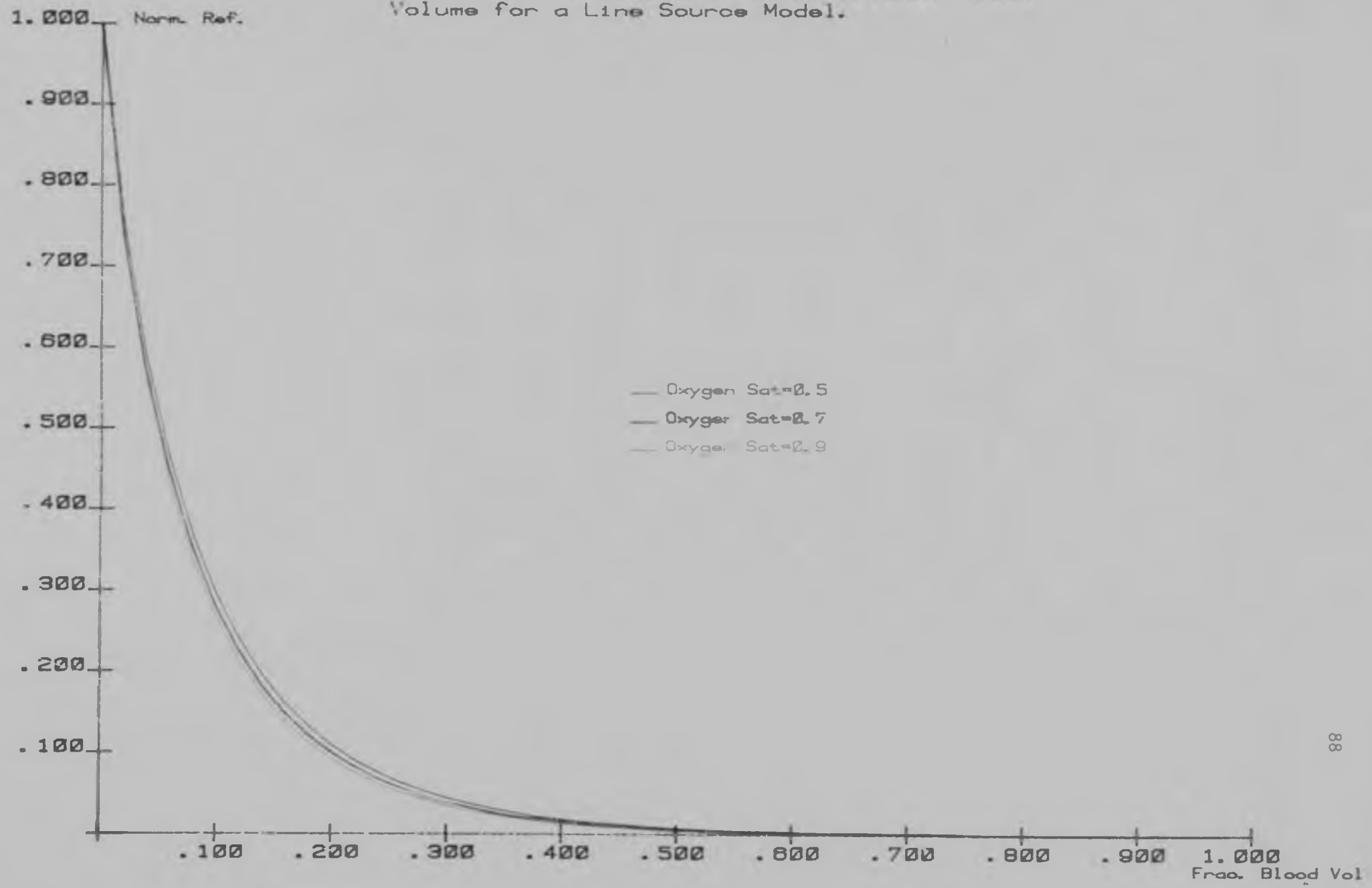
purposes, the operating region must be approximately known because of the gross non-linearities present. This is borne out by considering changes in peripheral fractional blood volume. Figure 3.9 shows the model predicted reflectance, using published parameter values (appendix 3) at a wavelength of 940nm and at three different oxygen saturation levels. The line source model was used with the following parameter values: (see appendix 3)

absorption of oxyhaemoglobin	0,85 mm^{-1}
absorption of reduced haemoglobin	0,59 mm^{-1}
scattering of blood	1,50 mm^{-1}
absorption of tissue	0,03 mm^{-1}
scattering of tissue	1,00 mm^{-1}

The curves show that reflectance decreases with increased fractional blood volume. However, the results of section 5.4 indicate that when the hand is heated, both channel's outputs increased. Physiologically, it is well known (section 2.6.1) that a local increase in temperature will result in an increased blood flow. This, together with the interpretation of the other results presented in chapter 5, suggests that the oximeter output should increase with increase in fractional blood volume. The structure of the measurement model allows for such behaviour provided that the absorption and scattering parameters are changed from the values presented above. At present there is insufficient experimental data to support such a change. An accurate determination of the parameter values is important and as such forms part of the recommendations for further work.

It would therefore appear that it is important to obtain better values for the parameters. In the past much emphasis has been placed on developing solutions to complex models, with little work on experimentally verifying its predictions. In other words, it is not desirable that the model accuracy should greatly exceed the accuracy of the parameter values.

Figure 3.9 Reflectance Vs Fractional Blood Volume for a Line Source Model.



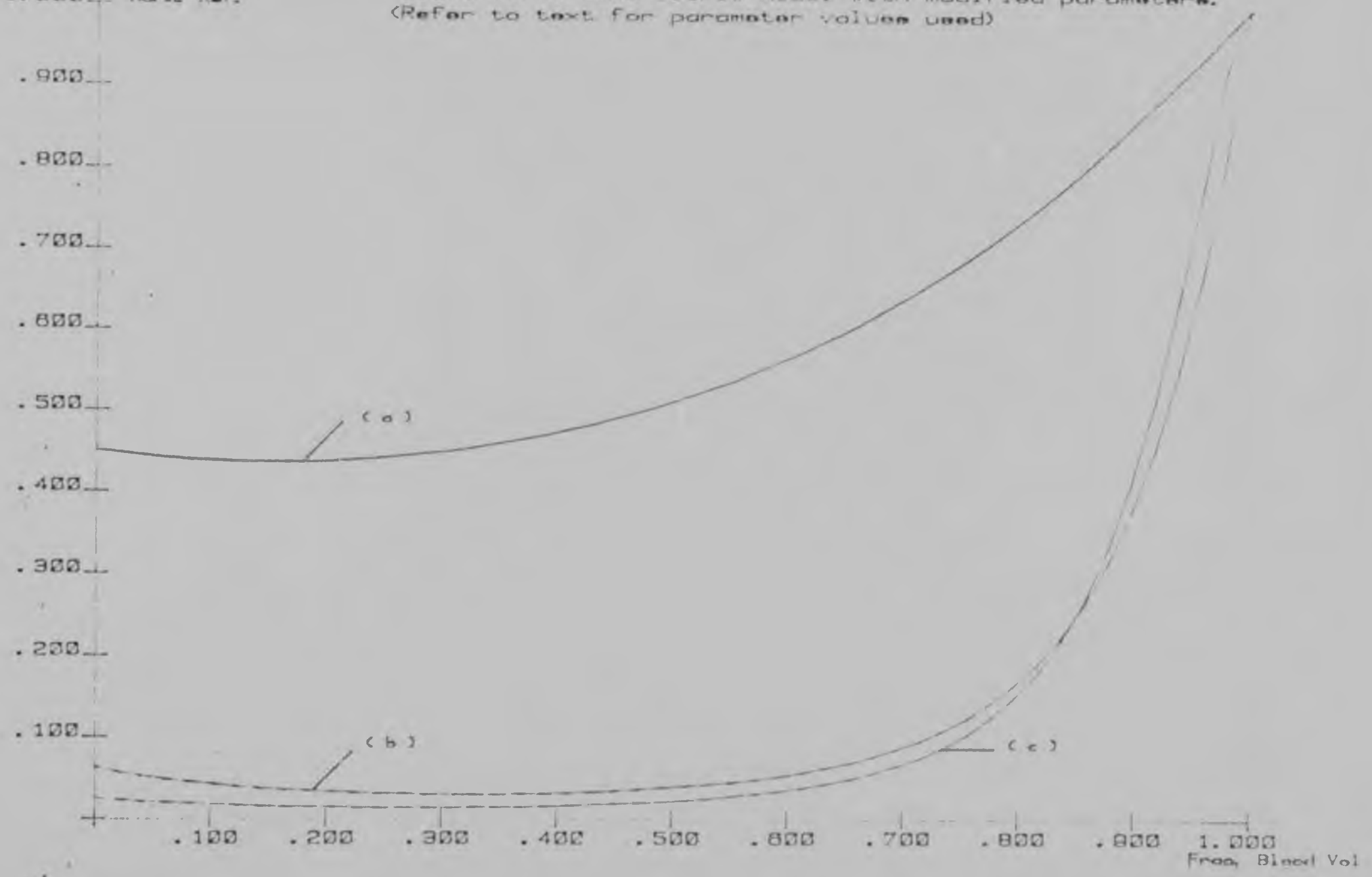
It is interesting to investigate how the above set of parameters would have to be adjusted in order to obtain qualitative concurrence between predicted and experimental results. It is clear that in order to obtain an increased reflectance when fractional blood volume increases, the contribution from the blood compartment must exceed that from the skin compartment. Thus, the relevant aspect is the relative magnitudes of the absorption and scattering parameters in the two compartments. In the discussion presented below, the absorption coefficients for blood are kept within the published range, while the absorption coefficient for skin is modified to lie outside the published range (see appendix 3). The scattering coefficients for both blood and skin are pushed to their respective limits.

This approach was adopted because the values for blood absorption have been well established, while those for skin have not been extensively measured. Previous measurements have neglected the effects of tissue type [98], wavelength and melanin concentration [75]. The scattering coefficients have been largely deduced from one dimensional models.

Figures 3.5 and 3.6 suggest the direction and magnitudes of the changes required. The model is operating on the right hand portion of the peaked curve in figure 3.5. Hence, it is intuitively obvious that both the scattering and absorption coefficient for skin must increase in order to obtain the desired output. Figure 3.10 shows the output from the model at an oxygen saturation of 70% under the following conditions:

	Absorption Coefficient (mm^{-1})			Scattering Coefficient (mm^{-1})	
	HbO_2	Hb	Tissue	Blood	Skin
Curve (a)	0,85	0,59	0,7	0,5	2,0
Curve (b)	0,85	0,59	0,4	0,5	5,5
Curve (c)	0,85	0,59	0,4	0,1	5,5

Figure 3.10 Reflectance /s Fractional Blood Volume for a Line Source Model with modified parameters. (Refer to text for parameter values used)



All the curves in figure 3.10 exhibit an increased reflectance with increased blood volume. Curve (a) illustrates the effect of increasing the skin absorption by a factor of twenty while retaining the other parameters within the published ranges. Curves (b) and (c) show the effect of varying the scattering coefficients. Values at the extreme of the published ranges can affect the model's qualitative response, although the sensitivity to these parameters does decrease at these values (c.f. curves (b) and (c)). In addition, the non-linear behaviour of the curves illustrate the importance of defining the operating region (especially in (b) and (c)).

In summary, when published parameter values are used, the output from the model is qualitatively inconsistant with experimental results. However, increasing the absorption coefficient of skin by a factor of between fifteen to twenty brings about qualitative concurrence. Scattering coefficients affect the output to a lesser degree. Thus, before rejecting the model structure, more careful consideration should be placed on the measurement of the parameters.

CHAPTER 4 HARDWARE DESCRIPTION

4.1 INTRODUCTION

4.1.1 The Need for Acquiring and Storing Data.

The initial work of Turner and Wigdorowitz [99] and subsequent spectral work of Dr Garner suggested that more information, concerning the respiratory and vascular systems, could be extracted from the oximeter measurements. However, these measurements could not simply be used in their raw form, but required some form of processing. At this stage all results were viewed on a chart recorder which, while giving a qualitative indication of the phenomenon, were not really ameniable to analysis.

The present project was initiated so as to further investigate the oximeter. After some preliminary work, aimed mainly at verifying and reproducing the previous result quoted above, (also see chapter 5), it was found that these results were not always reproducible. It was decided that in order to systematically analyse the data, records of experiments should be numerically stored so as to be available for further analysis. Consequently the data capture system (section 4.4) was assembled.

4.1.2 The Instrumentation

When the outputs from the oximeter were greatly amplified, pulsatile behaviour could be observed (see figures 5.14 and 5.15). These have the appearance of a blood pressure pulse. If these pulses could be correlated with known blood pressure pulses, they could be more positively identified, hence lending

greater credibility to the oximeter. It had also been postulated that in order to extract more information from the oximeter outputs, a physiological model would be required. A useful input to such a model would be the pulsatile blood pressure.

The above two points were the main motivations for constructing a device to monitor the pulsatile blood pressure. The pulse monitor is described in section 4.2 The oximeter itself is described in section 4.3, while the data capture system is discussed in section 4.4

4.2 THE PULSE MONITOR

4.2.1 The Transducer

Many commercially available transducers could have served the required purpose. However, as a result of lack of funds and the nature of the project, a simple inexpensive device was developed. An obvious site for the measurements is the radial artery as it passes through the wrists because:

(i) The artery is near the skin surface and hence the signal is amenable to measurement.

(ii) This site is close to the finger (the site of measurement for the oximeter) and hence spatial lags could be ignored

The first arrangement attempted involved the use of strain gauges and a plunger, as shown in figure 4.1. However, the mass of the plunger and spring constant of the cantilever proved to suppress any response.

The second arrangement, and one adopted was to use a Phillips ceramic gramophone pickup. The stylus was removed from its seating and replaced by a flat pad, moulded from Pratley expoxy (see figure 4.2).

A fix-velours strap was fixed to the pickup so as to enable it to be simply attached to the wrist. It is usually necessary to adjust the positioning of the pickup until a satisfactory output is obtained.

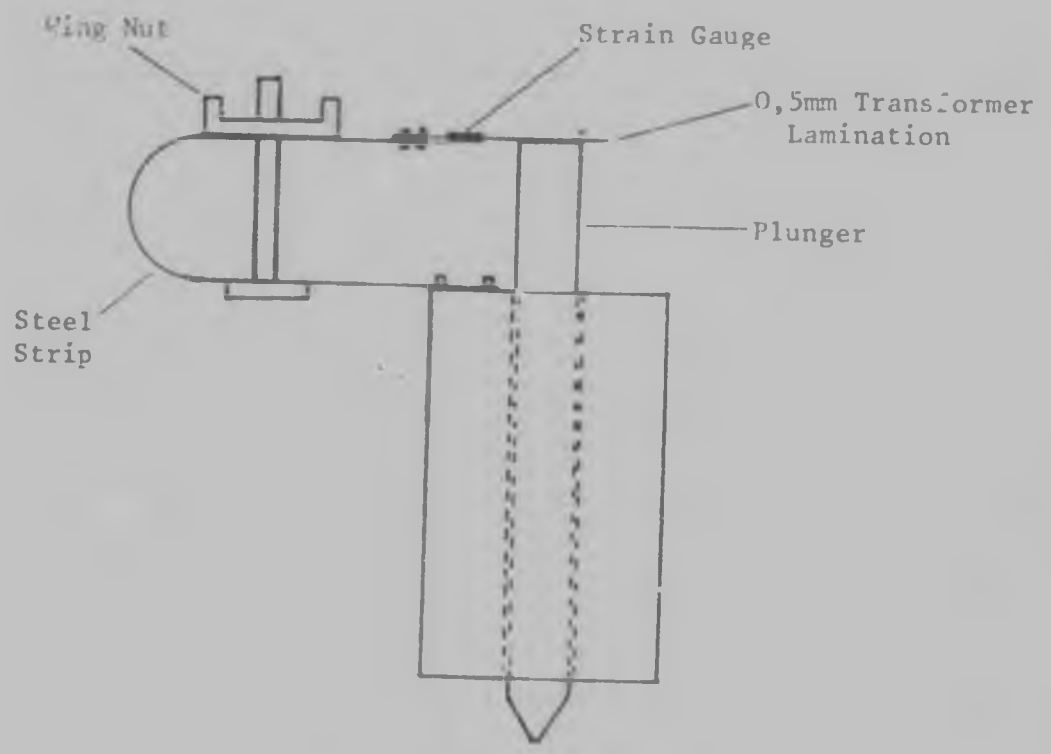


Figure 4.1 Strain Gauge Pulse Monitor.

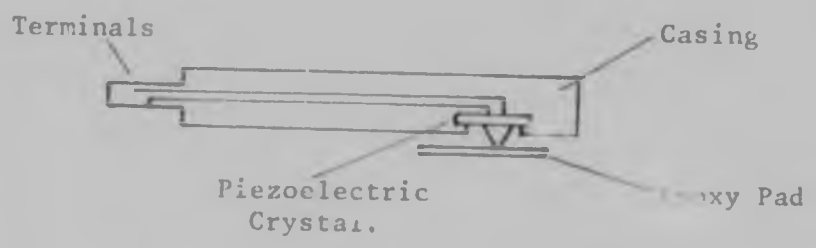


Figure 4.2 Gramophone Pickup Pulse Monitor.

4.2.2 The Electronic Signal Processing

The signals associated with the pickup output are low level and have a high source impedance. Therefore, the first stages of amplification should guard against noise interference. The circuit diagram is given in figure 4.3. The front end of the circuit is a standard instrument amplifier configuration. The two non-inverting amplifiers at the input are located physically on top of the pickup and so buffer the transducer input. The first stages low source impedance, together with the low input impedance of the second stage ensure a substantial current in the (relatively long) connecting wires and hence reduce the effects of electromagnetic interference. In order to minimise the mechanical forces, these wires were chosen to be as light as possible. Consequently insulated Lewmex copper wire of diameter 0,0084 inch (London Electric Wire Company and Smiths Limited) was used. The second stage is followed by a differential amplifier which is also aimed at reducing common mode interference.

The piezoelectric transducer acts as a high pass filter and hence to reconstruct the original signal, a low pass filter is included in the fourth stage. The time constant of this integrator was made as large as possible in order to match the time constant of the transducer. The overall step response is shown in figure 4.4.

The final stage provides extra gain and a variable D.C offset. This D.C. adjustment is required so as to allow the output to be compatible with the data capture facility, which will only accept a unipolar input potential.

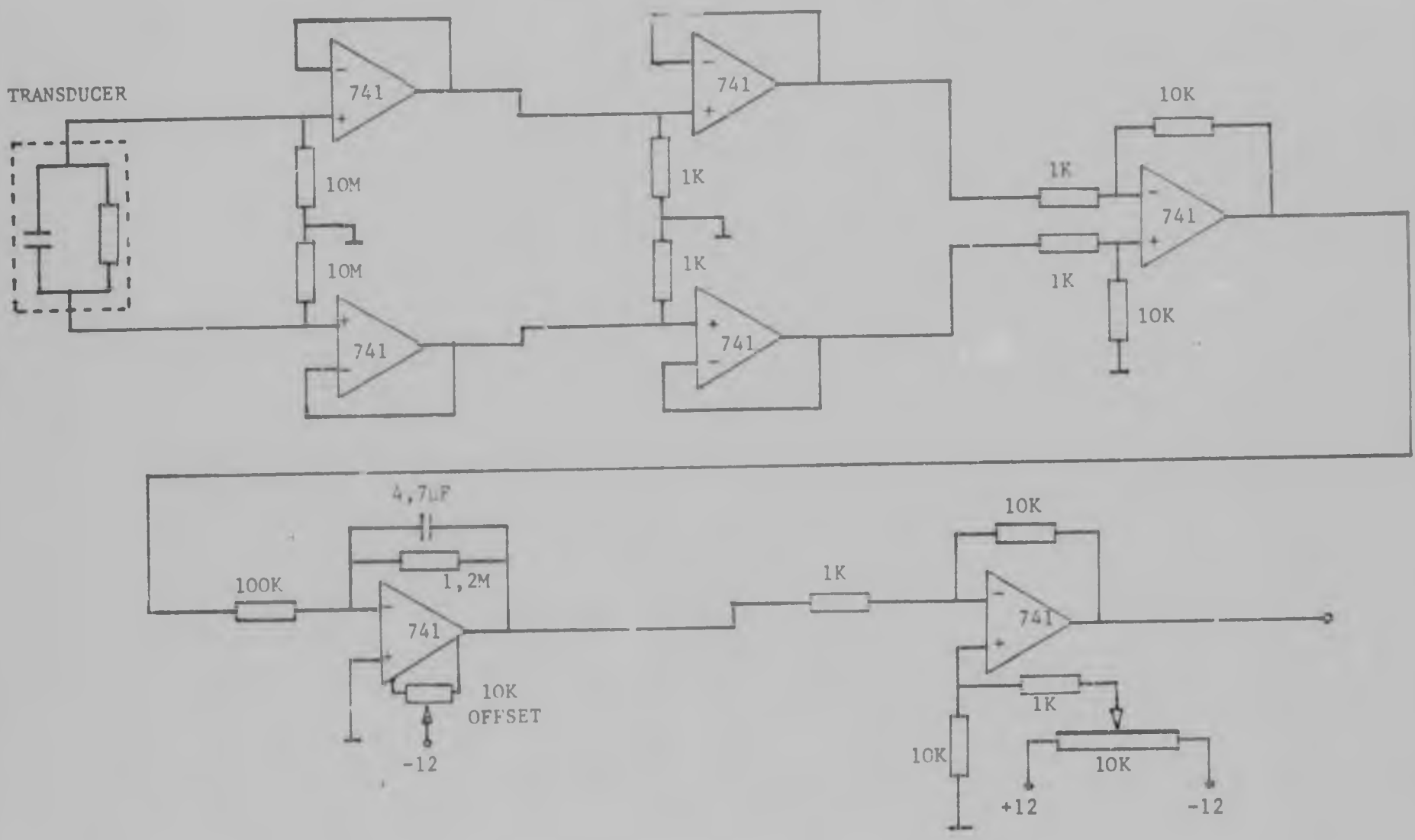
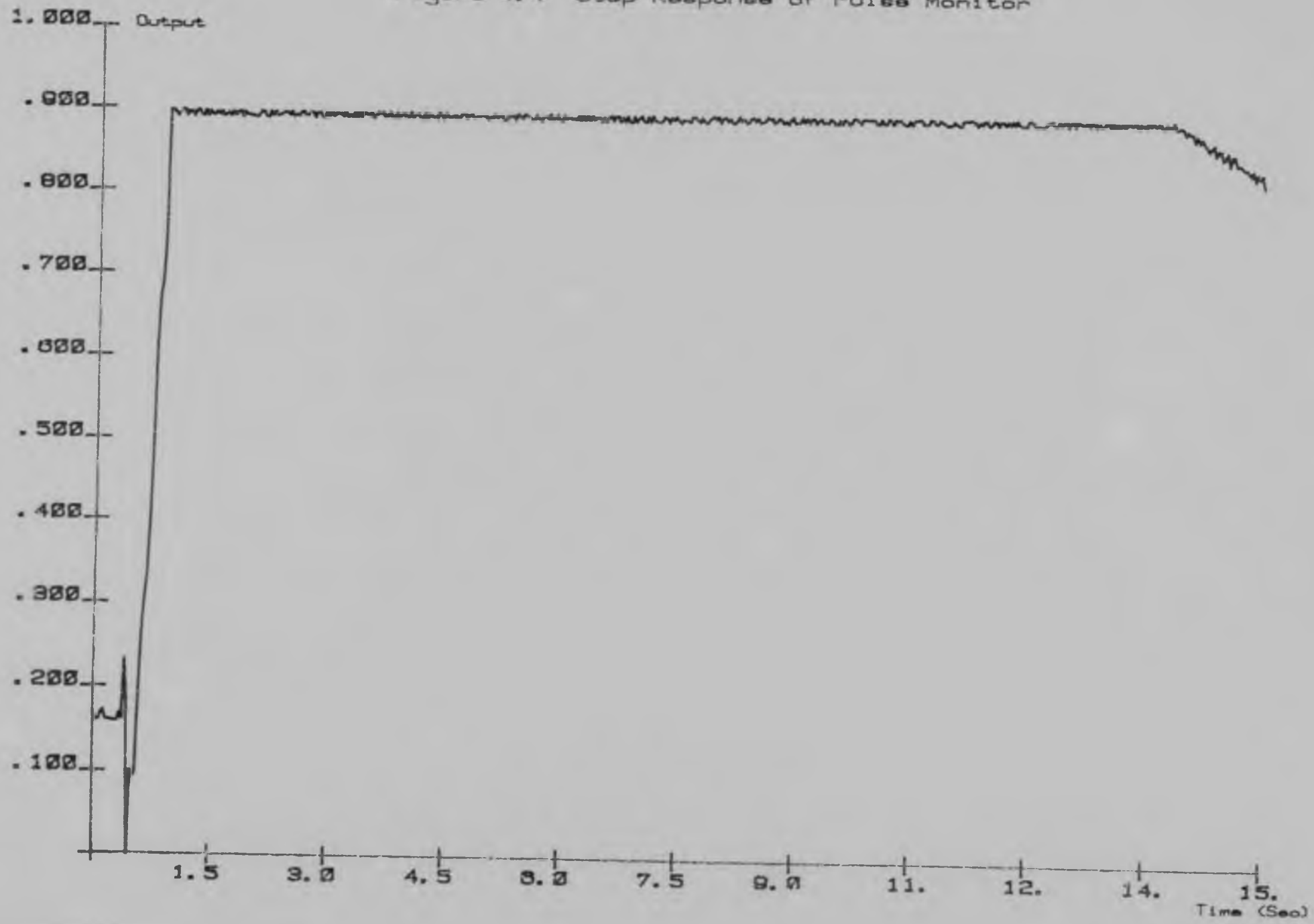


Figure 4.3 Circuit Diagram of Pulse Monitor.

Figure 4.4 Step Response of Pulse Monitor



4.3 THE OXIMETER

4.3.1 An overview

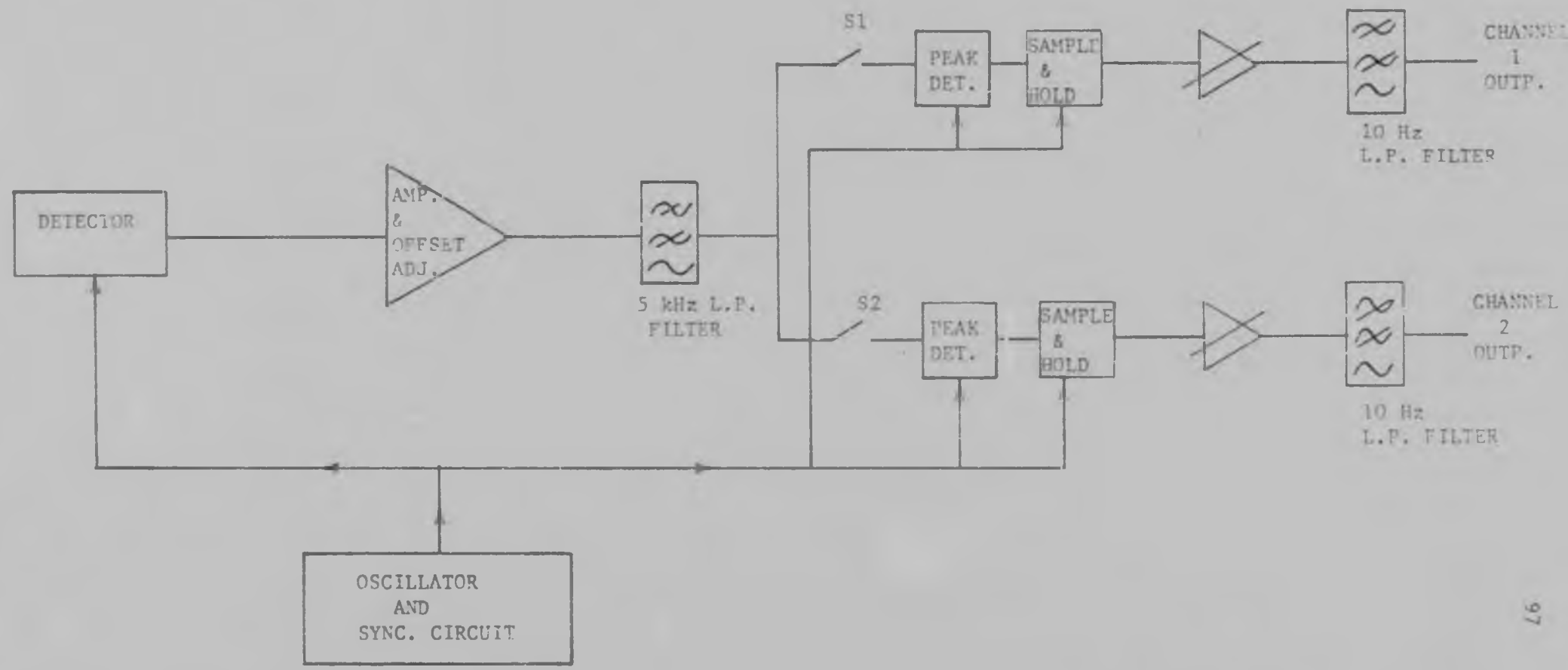
As has previously been pointed out, (Chapter 1), the basic oximeter was developed as an undergraduate project. Thus fuller details may be found in reference [99]. In this section only the salient features will be discussed.

The instrument is a two wavelength oximeter, using sources in the red and infra-red portions of the spectrum. For reasons of economy, commercially available light emitting diodes (LEDs) were used in place of the more conventional (and more accurate) single source with interference filters. Added advantages of using LEDs are that; (1) The conventional mechanical light chopping arrangement (used so as to enable low level signal amplification) may be dispensed with and replaced by an electronic switching network which is synchronized with the detector circuits. (2) Their small size ensures that both sources illuminate approximately the same region. If fibre optic sources, in particular, if fibre bundles are used this factor would be further enhanced.

The disadvantages of this type of source lie in their spectral properties. Firstly their bandwidth (typically 60-80nm) is larger than that obtainable using interference filters. Secondly the choice of peak emission wavelength is limited. Fortunately commercially available LEDs are available which emit in the red and infra-red region. The red LED has a peak output at 650nm which is ideal, but the infra-red LEDs peak at 940nm which is close but not at the isobestic wavelength (805nm).

The block diagram of the oximeter is given in figure 4.5. A phototransistor detects the reflected light, which is amplified

Figure 4.5 Block Diagram of the Oximeter.



and low pass filtered (cutoff frequency 5KHz).

A D.C. offset is also provided. The red and infra-red channels are then separated using switches S1 and S2 which are synchronized to the LED driving circuits. Peak detectors and sample and holds are provided in each of the channels. These are included since the light output from the LEDs is not a step but has a finite rise time. (figure 4.6). Finally, low pass filtering is used to eliminate higher frequency interference (mains and switching noise). The complete (and modified) circuit diagram is given in figure 4.7

4.3.2 Modifications

Some modifications were made to the original circuit. These are mainly technical and do not significantly affect the overall performance, only the more major changes are reported here.

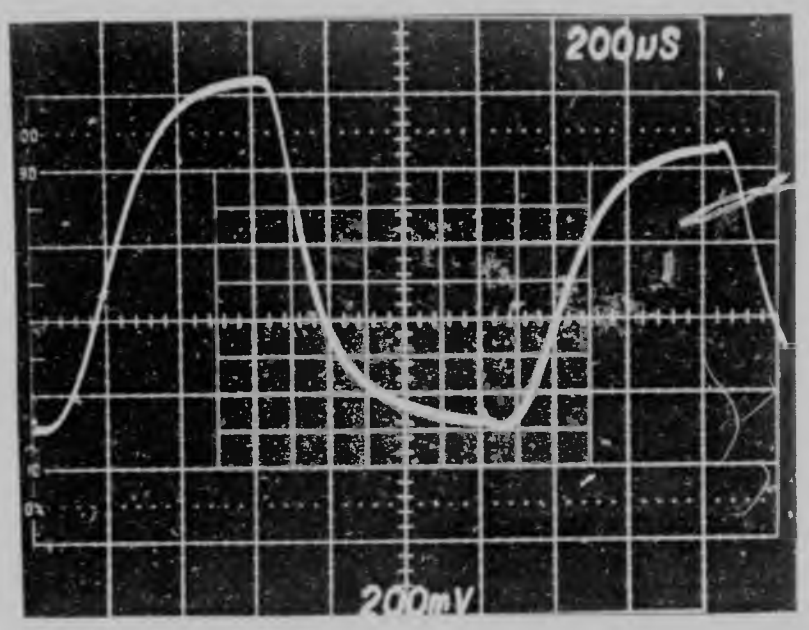


Figure 4.6 Response of the Phototransistor. The oscilloscope trace shows the finite response time of the phototransistor. The photograph shows a pulse from the infra-red source followed by one from the red LED (hence the different amplitudes of the two pulses).

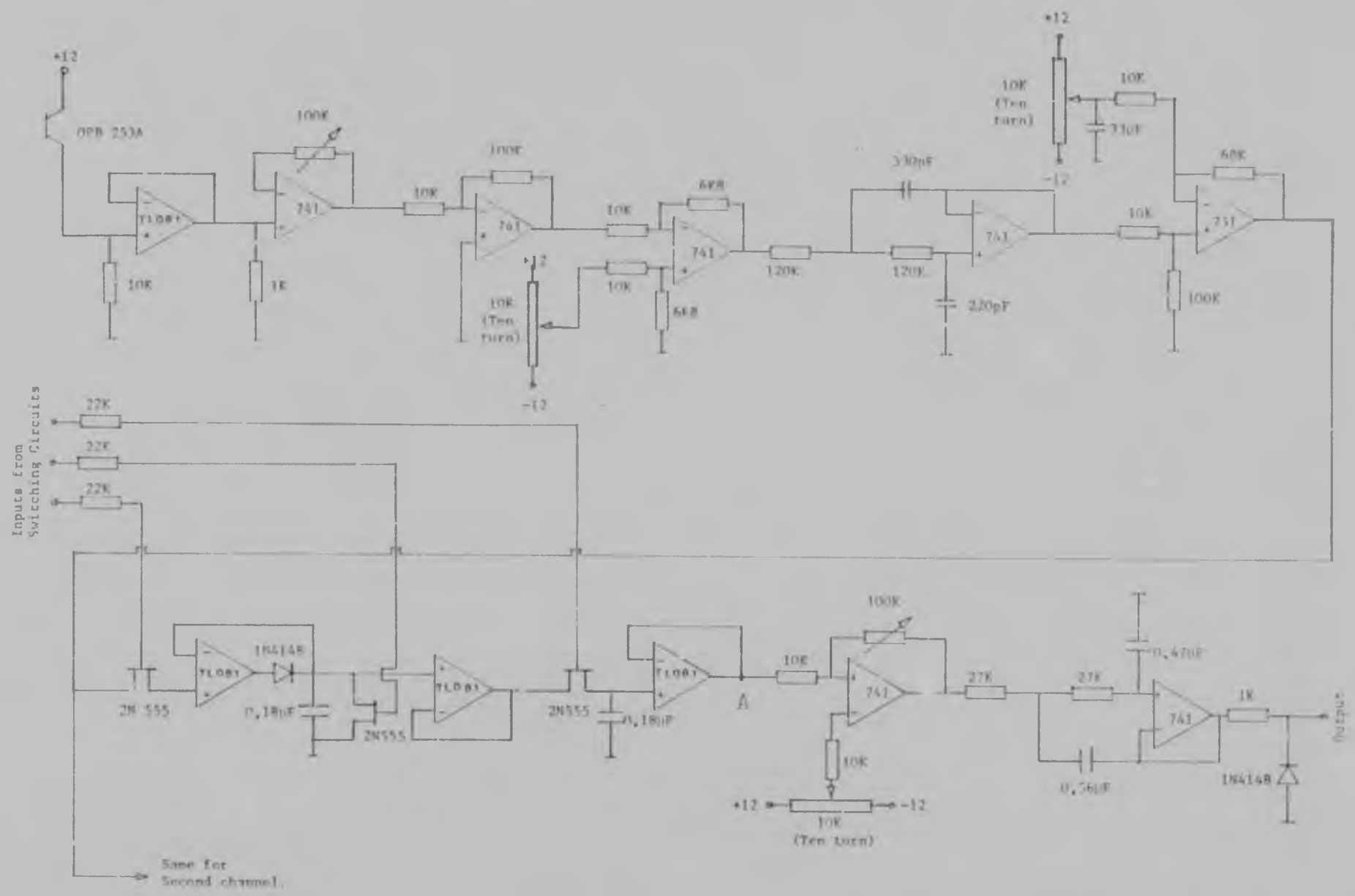


Figure 4.7 Circuit Diagram of Oximeter.

The original instrument had only a single output, which was the difference between the red and infra-red channels. It would appear that combining these two signals would result in a loss of information. It is also doubtfull as to whether this is the best way to combine the signals. (Section 3.2.3 suggests a ratio of the two signals). Therefore the subtraction network was removed.

A new printed circuit layout was designed by Dr Garner. The major aim of the new design is to modularise the detector circuit so that they would conveniently fit into a standard rack. Eventually many detectors could be located at different locations on the body and simultaneous measurements taken. A single switching circuit would supply all the detectors. Many decoupling capacitors were added to this design to reduce the mains-borne interference caused by the switching circuits.

The weak link in the original design had always been the transducer geometry. Other geometries were tried and are discussed in section 4.3.3.

To aid in the elimination of noise interference in the low level transducer signals, a buffer amplifier was mounted on the actual transducer. Its low output impedance driving the low input impedance of the first stage of the oximeter circuitry serves the same purpose as that used for the pulse moritor (see section 4.2.2).

An "auto-zero" facility was included in the design of Turner and Wigdorowitz. The justification for this was that any disturbance

in the transducer would result in a D.C. shift. This circuitry was designed to minimise this offset. However, this introduced unwanted dynamics into the system. Careful design of the transducer made this section unnecessary and hence it was removed.

An on-board oscillator was provided for the LED driving circuits. (Previously the driving waveform was derived from a microprocessor clock and frequency divide circuits.) All the LED driving circuitry was moved to a seperate board.The circuit diagram for theoscillator is given in figure 4.8. The outputs "a" and "b" refer to figure 5, page 17 in reference [99].

The sampling FET transistor in the sample and hold circuit (transistor Q3 in figure 8, page 24 in [99]) was found to malfunction for high "hold" voltage levels. The problem was traced to the driving circuit for this particular transistor (figure 6(a), page 17 in [99]). The driving circuit did not allow the transistor to be turned on when the output from the sampler neared saturation. Thus the circuit (figure 6(a), in [99]) was modified to that given in figure 4.9.

As the data aquisition system was to be a sampled data system, a low pass filter was added to the outputs of the sample and holds with a cutoff frequency of 10 Hz. This value was chosen as it is unlikely that ther are body rhythms above 10 Hz. Hence the sampling rate for spectral purposes need be 20 Hz.

Finally a wooden rack was constructed to house all the circuitry. Five power supply terminals were provided (+12V, -12V, +15V, -15V and ground). A plastic 3M connector allows the transducer to be easily connected and disconnected from the circuitry.

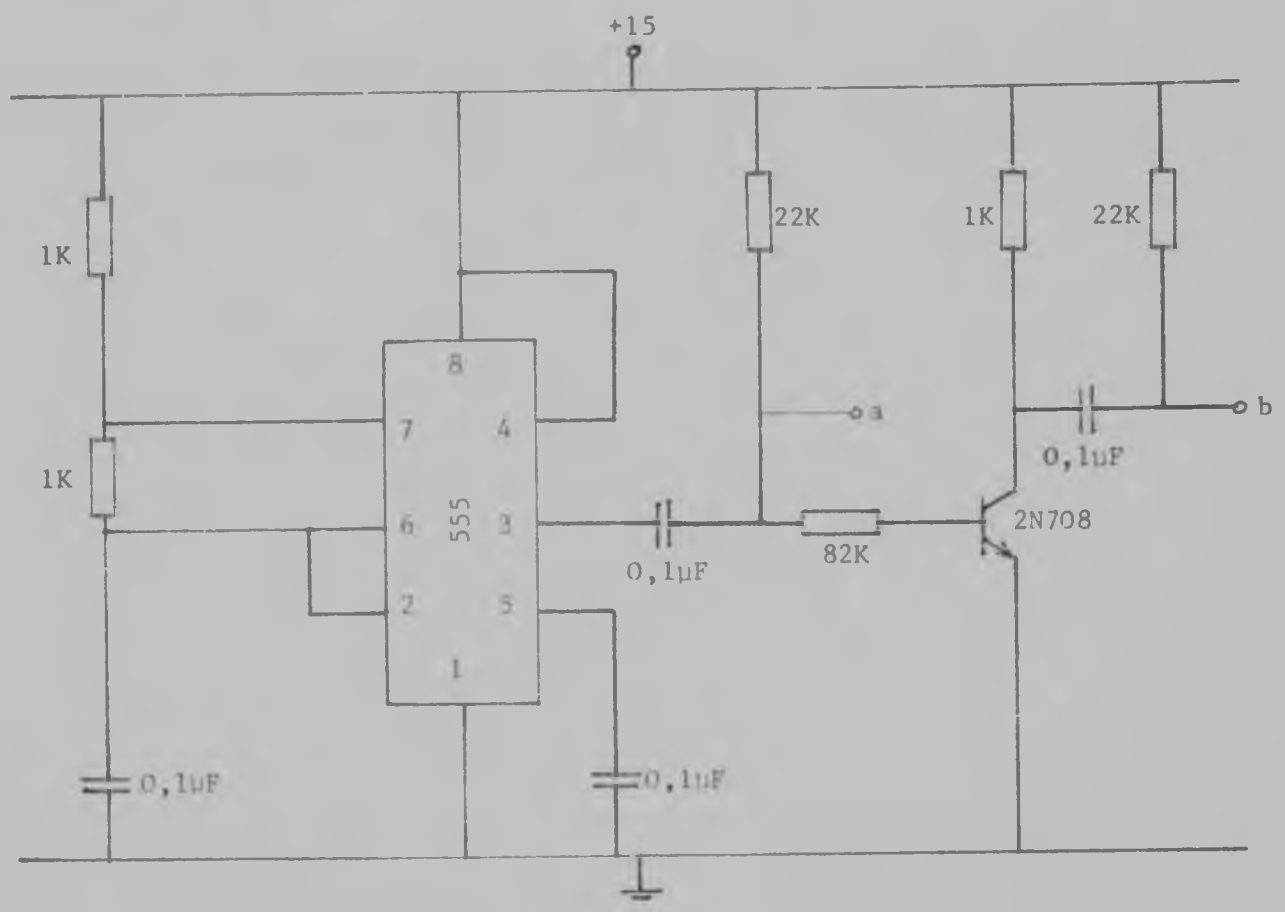


Figure 4.8 Oscillator.

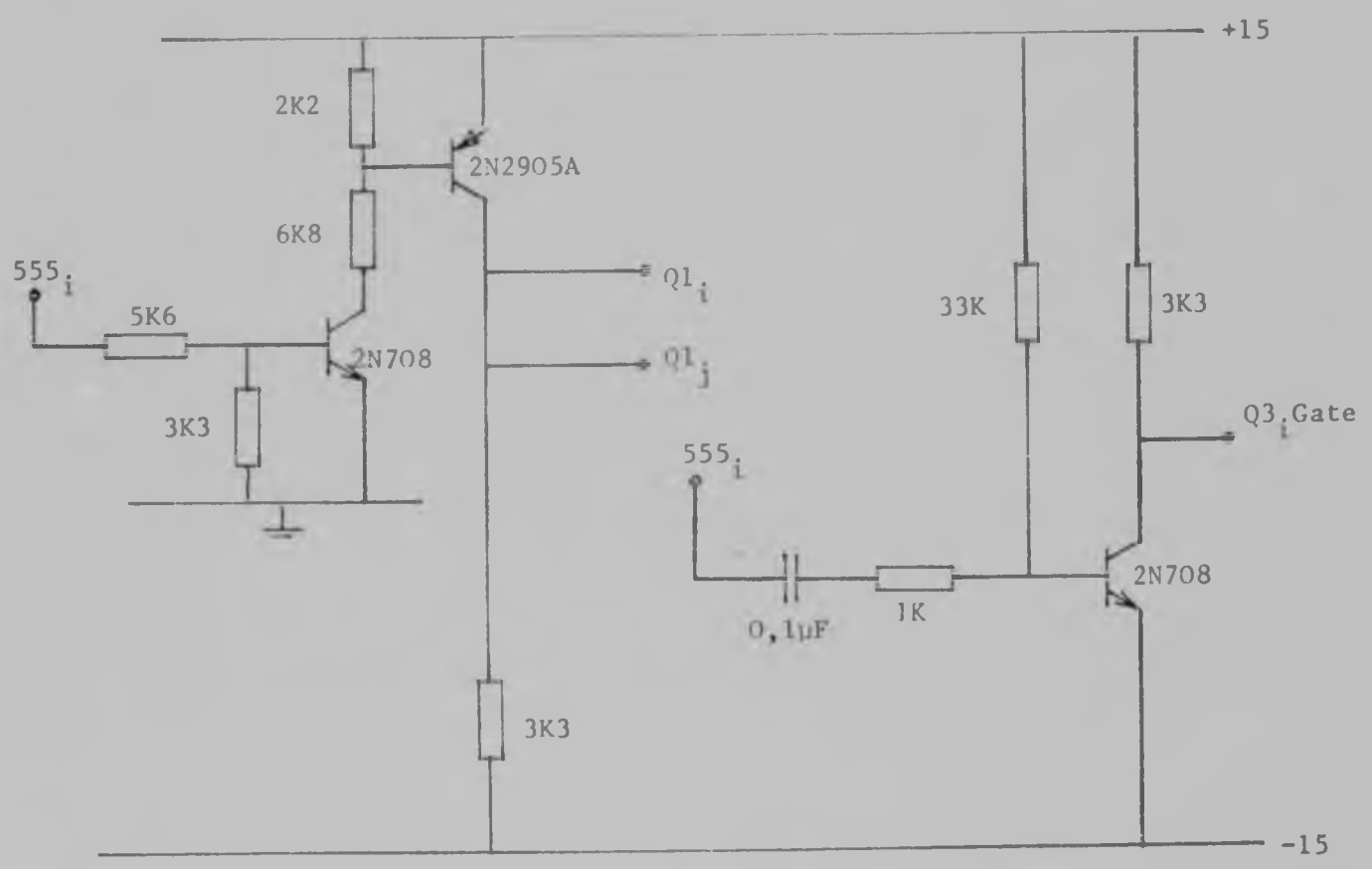


Figure 4.9 FET Drivers.

4.3.3 Transducer Design

The geometry of the transducer is of critical importance in the proper functioning of the oximeter. Ideally, it should not, in any way, disturb the blood flow in the tissue to which it is attached. Therefore, the pressure that it exerts should be kept at a minimum. However, at the same time, it should not move relative to the tissue surface, since any movement results in meaningless results. In addition the geometrical relationship between source and detector will influence the intensity of backscattered light (and hence signal to noise ratio) and the depth of penetration of the beam. The theory requires that the interface at the skin surface be perfectly absorbing, therefore, the transducer holder surface should be black.

The original transducer was not satisfactory as it could not be easily kept in place. Furthermore it did not produce reliable output. It used commercially available photo-transistors, and LED's placed in a moulded Pratley epoxy holder. A major drawback of the detector is its poor response in the red region.

Two new transducer designs were tried. Firstly, it was attempted to simulate a point source surrounded by a ring of detectors (figure 4.10). Four TIL 63 photo-transistors, four red LED's, (TIL 209) and a single infr red (TIL 32), (see appendix 6 for detailed data), were placed on a printed circuit board. This method did not work well, primarily because the individual components are physically too large. It is suggested that such a system might be feasible using fibre optic bundles. The infra-red and red source bundles could be intermingled in order that both sources illuminate the same region. The detector would be constructed from an annulus of fibre optic clusters, surrounding the source cluster. This would beter approximate to the geometry of the transducer model (section 3.4). Alternatively, the complications of the three dimensional geometry may be partly overcome by intermingling source and detector bundles so as to essentially have a single dimensional geometry.

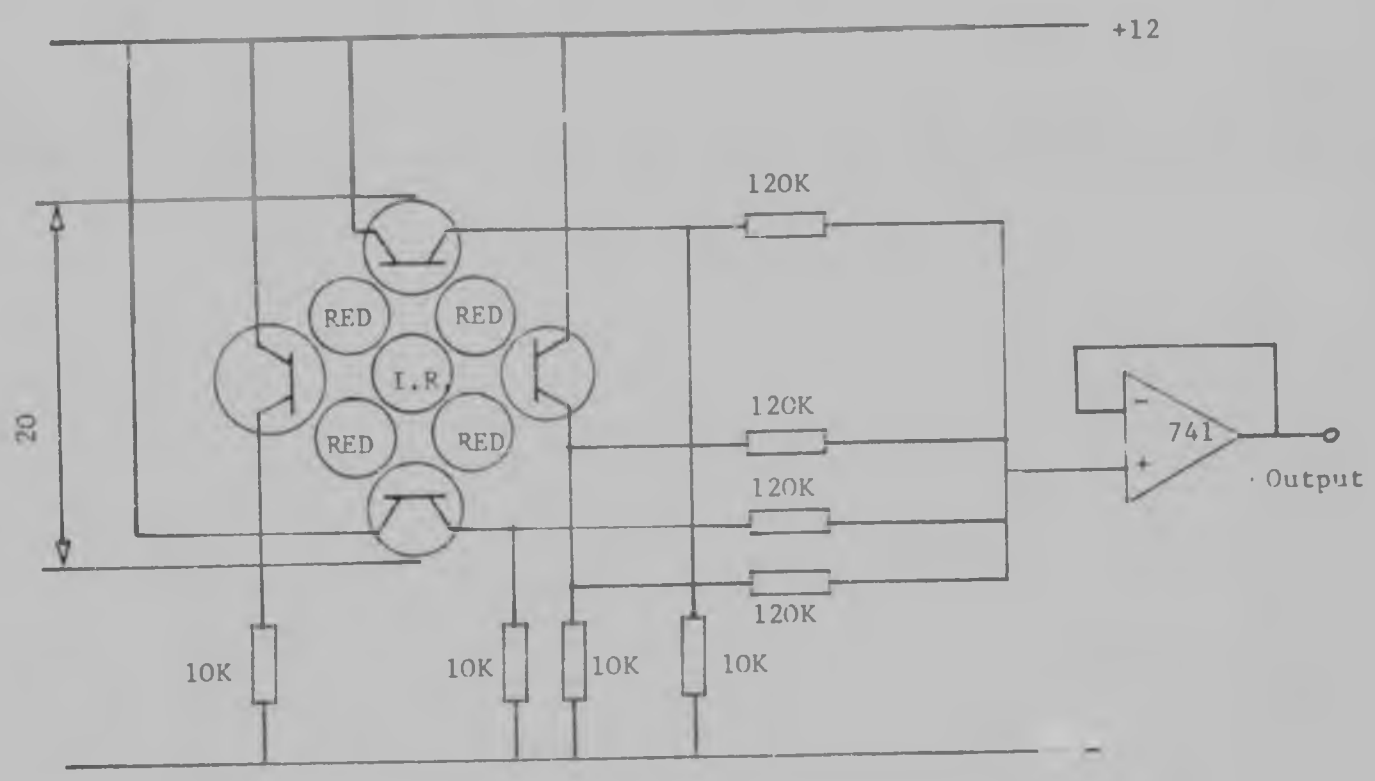
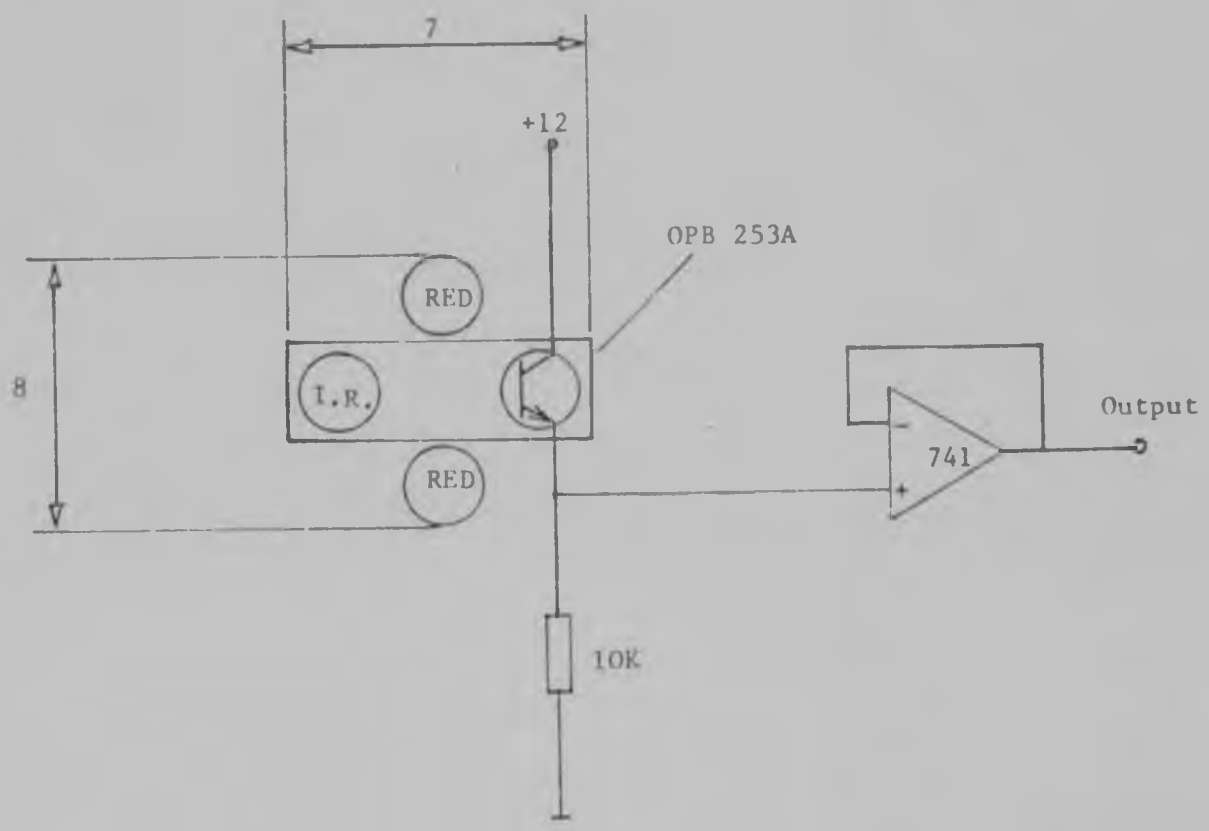


Figure 4.10 Transducer Using an Annulus of Detectors (Schematic)

Figure 4.11 Schematic of Transducer Using an OPB 253A Reflective Sensor.



The transducer which produced the best results was constructed using an Optron type OPB 253 A, (see appendix 6) reflective object sensor. This device consists of an infra-red (930nm) LED and a silicon phototransistor in a moulded plastic housing. The advantage of this detector is that its response in the red spectral region is greater than that of previous transducers. Two red LEDs (TIL 209) were placed on either side of the plastic casing and then fixed in a moulded epoxy finger cap (figures 4.11 and 4.12). The finger cap holds the transducer on the finger without much local pressure. The disadvantage is the heat generated by the LEDs and the finger cannot be easily dissapated and hence physiological changes can take place. This difficulty is largely overcome by ensuring that the duration of experiments does not become too long.

The linearity of the transducer response was checked in both the red and infra-red regions. The transducer plus buffers were connected to the electronic processing circuitry. An LED was mounted in front of the transducer (figure 4.13). The current through the LED was adjusted and the voltages at point A in figure 4.7 were recorded.



OPB 253A Sensor

Buffer Stage

Figure 4.12 Finger Cap in Position.

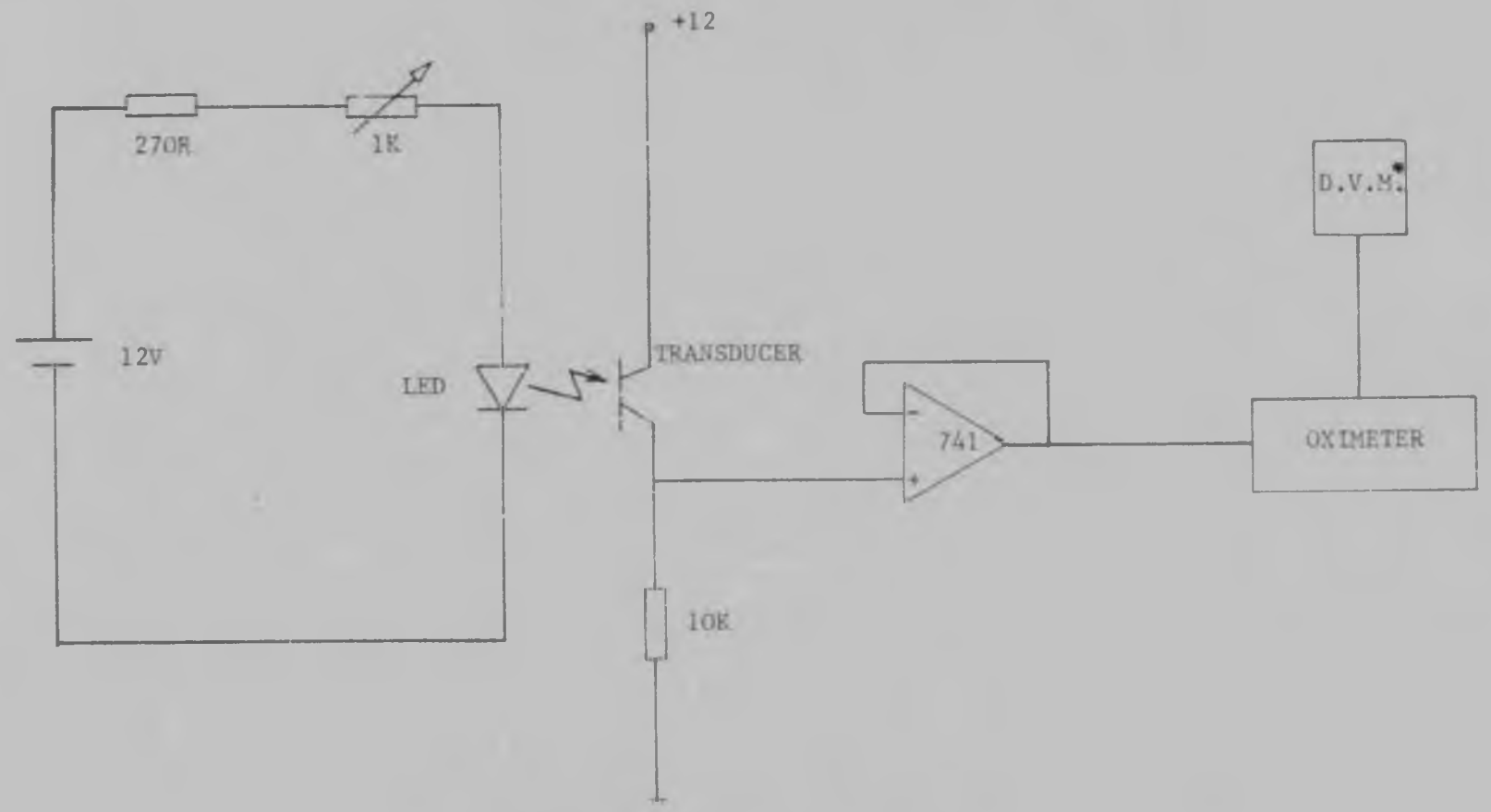


Figure 4.13 Experimental Setup for Checking Transducer Linearity.

(* Digital Volt Meter)

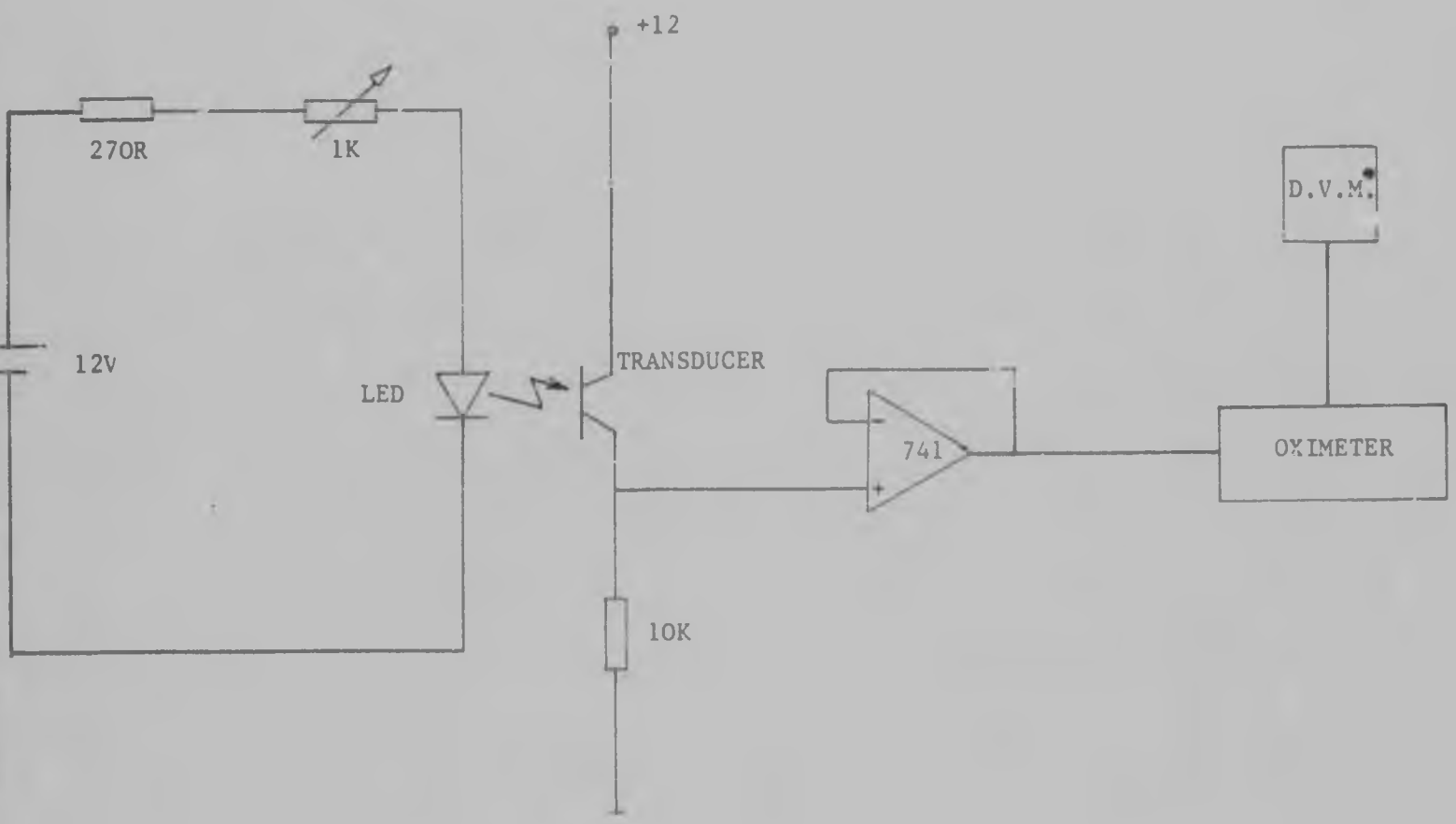


Figure 4.13 Experimental Setup for Checking Transducer Linearity.

(* Digital Volt Meter)

Figure 4.14 Response of Transducer in the Infra-Red region

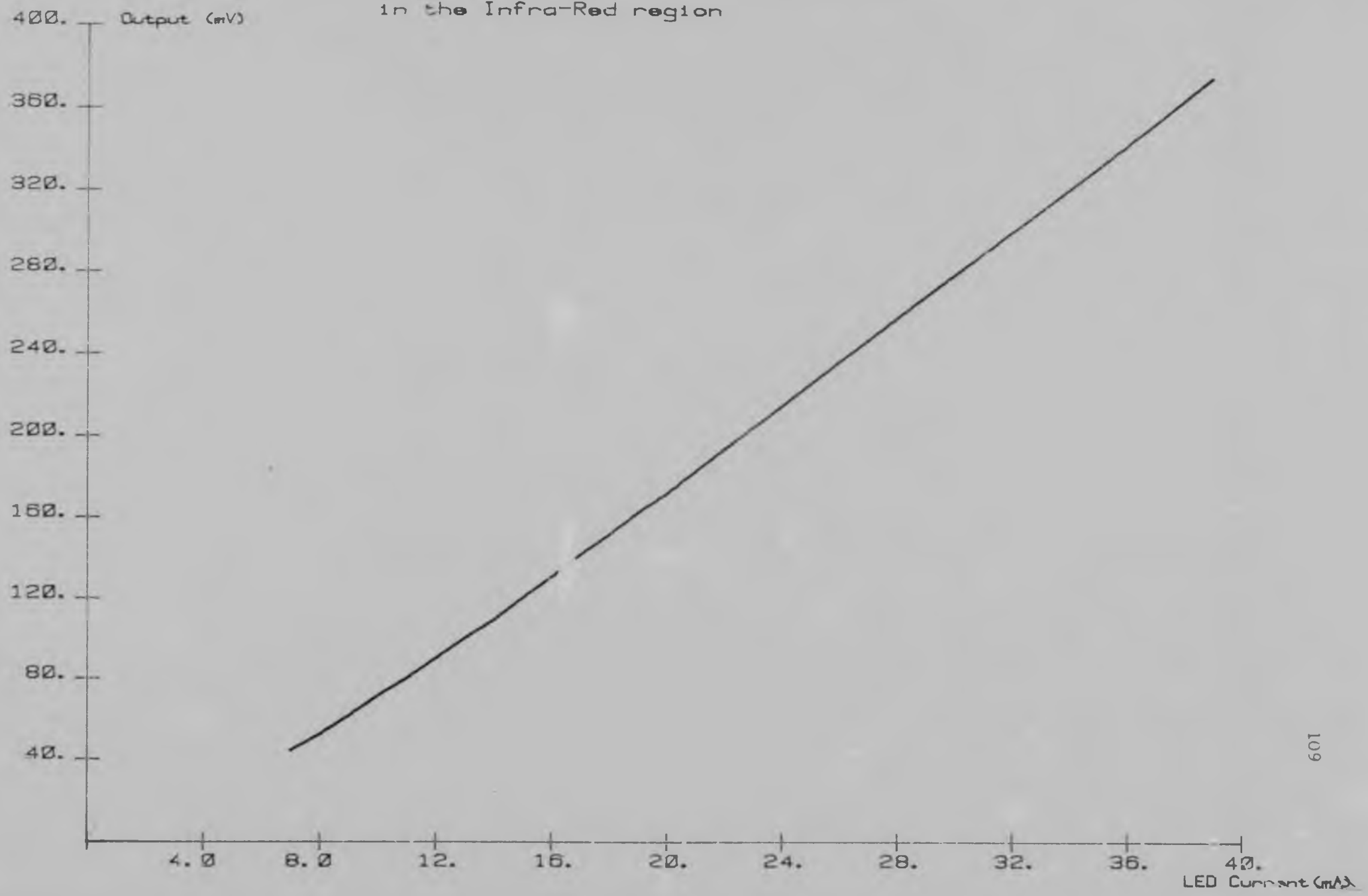
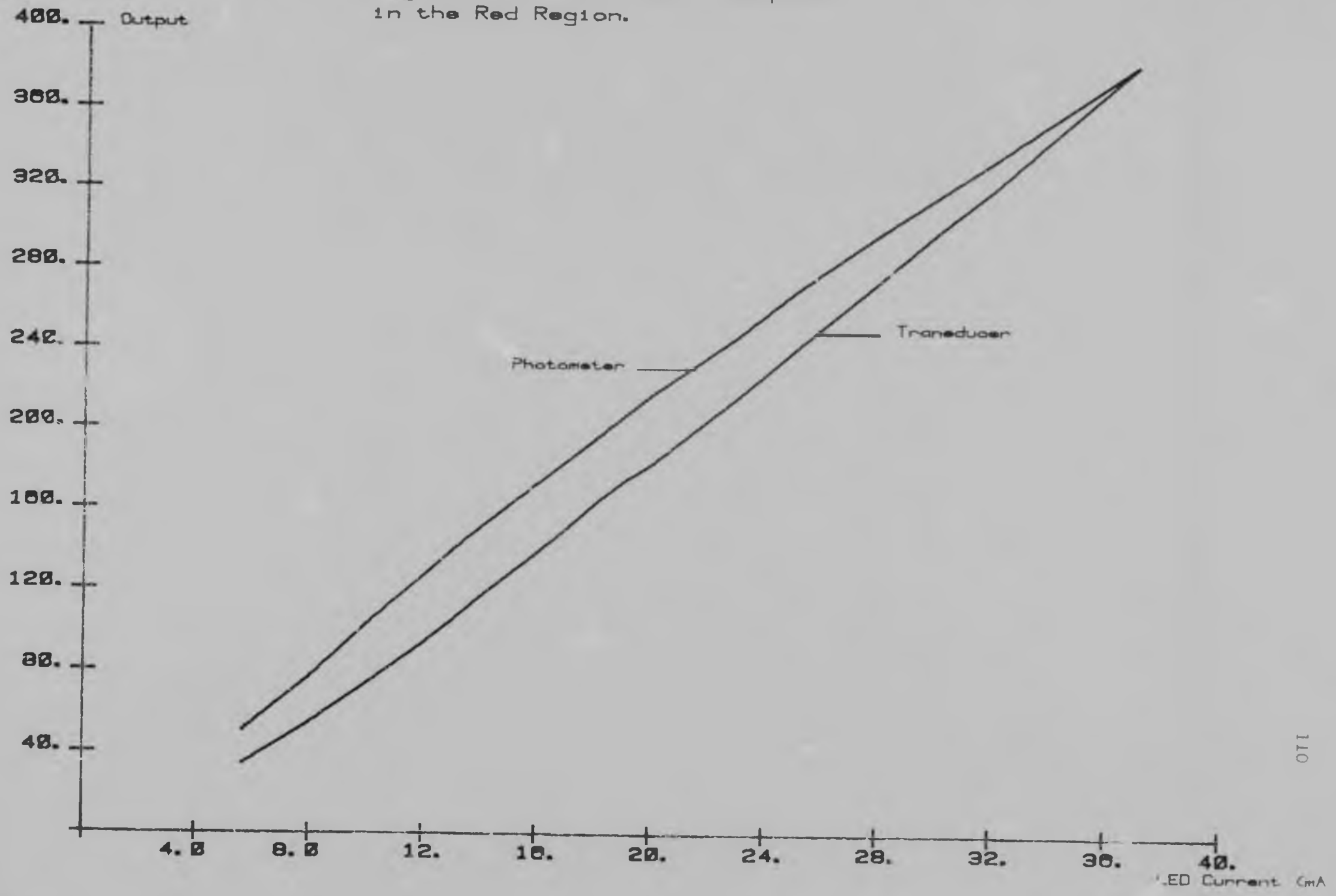


Figure 4.15 Transducer Response in the Red Region.



The results are presented in figures 4.14 and 4.15. In the red region readings were checked using a Tektronix J 16 Digital Photometer. The measured intensities (foot-lamberts) were scaled so as to agree with the photo-transistor output at the highest LED current.

4.4 COMPUTER BASED DATA CAPTURE AND STORAGE

It is convenient to record and store data from various experiments in a form which is amenable to computer processing. This would aid in any modelling process of the system under consideration.

There are many ways of implementing such a facility. (A 8085 microprocessor technique was suggested by Turner and Wigdorowitz) Based on the requirement of using currently available departmental equipment, a rather overdesigned system involving an RTP controller, microNova computer and a Hewlett Packard 264/A graphics terminal was assembled. (However, this system is not dedicated to the oximeter and thus has the advantage that it is a general purpose data capture facility, available for other applications in the department.)

A RTP7435/47 sixteen channel analog to digital card [102] was connected to the oximeter, and pulse monitor outputs (figure 4.16). This card has an input range of 0 - +10,24 volts. The digital output is a 12-bit two's complement binary word with a sign extension to give a total word length of 16 bits. In addition, one of the channels was connected to an "event marking" switch. This switch simply either connected +5 volts or 0 volts to the RTP inputs and was used to mark the beginning of experimental events (e.g. arterial occlusion). Management of the analog to digital conversions was performed via the Universal

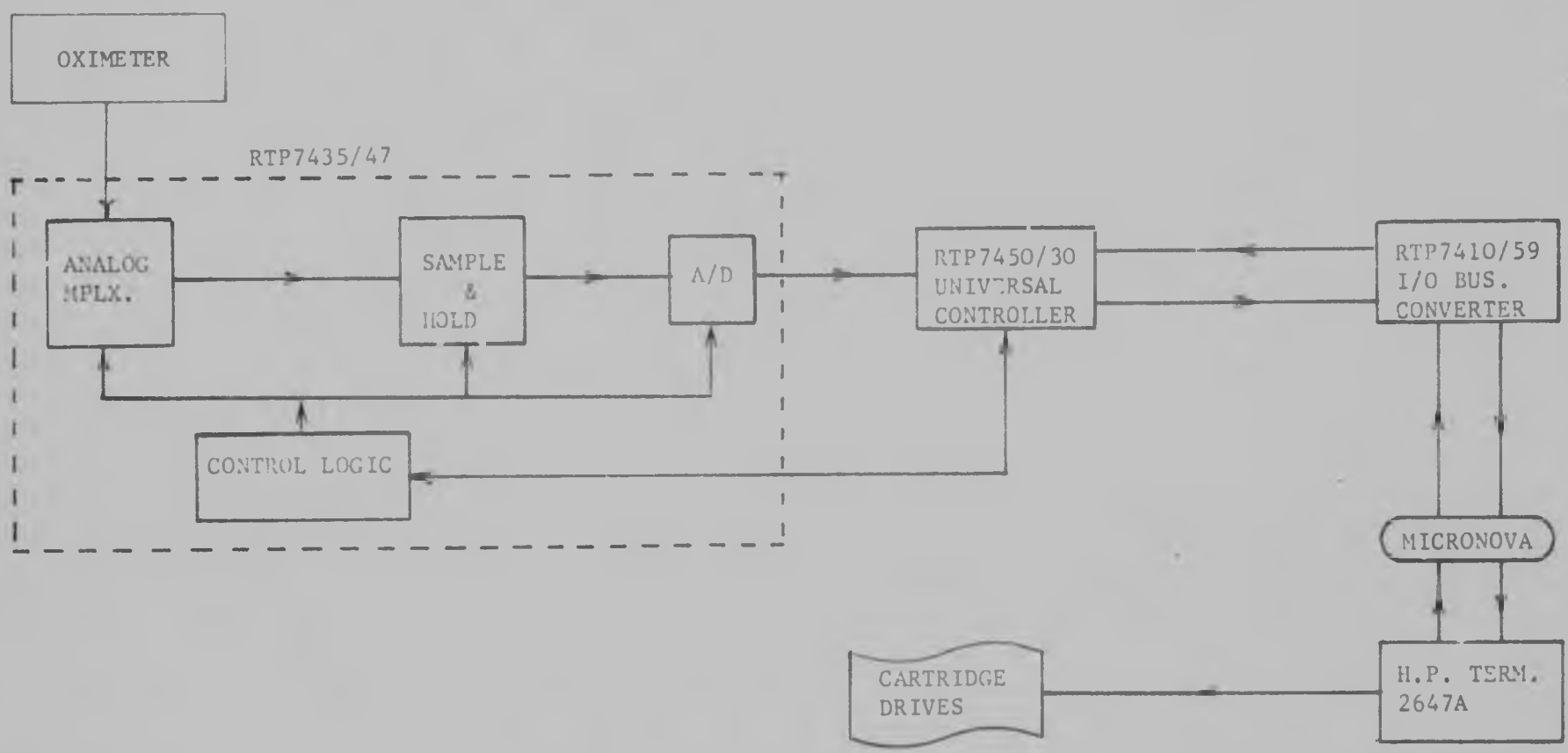


FIG. 4.16 INFORMATION FLOW IN DATA CAPTURE SYSTEM.

Controller [103] RTP7430/30 and RTP7410/59 I/O Bus Converter [101] for microNova computers. These cards make the initiation and control of the analog to digital process almost transparent to the user. A single output and a single input instruction is all that is required from the host (microNova) computer.

The microNova does not have a sophisticated monitor. The terminal debug option only allows interrogation and modification of memory locations. Furthermore it does not have any mass storage facilitys (although it does have 24K words of 16 bit wide RAM memory). The computer is, therefore, not geared towards program development and consequently only the minimum was implemented. All data processing was performed using a high level language in the H.P. terminal or in the University Computer Centre's IBM 370/158. The final microNova program accepts, as input, the number of samples to be taken and the sampling interval. It then initiates and monitors the sampling process, storing the data values in the computer's RAM memory. At the end of the sampling interval, it transfers the data values to the Hewlett Packard (HP) terminal. The program converts each 12 bit data word to 3 ASCII hexadecimal digits before transmitting it to the terminal.

The HP terminal can be loaded with a BASIC interpreter. This facility in conjunction with its two cartridge tape drives make it fairly powerful. A BASIC program was written which acted as a crude "Task management system" for the data capture facility. This program enabled the microNova program to be loaded from catridge tape, the passing of parameters to the microNova, initiation of a sampling session, elementary processing and storage of the raw data on cartridge tape. The processing consists essentially of removing the D.C. value of the data and converting their hexadecimal representation to decimal (ASCII) representation.

Details of the manner in which the data is stored and transmitted is given in appendix 4. A sample session, flow charts and program listings for both the HP and microNova are given in appendix 5 and appendix 8 respectively.

Once in decimal the data was transferred for permanent storage onto "floppy discs". A total of 6 discs, each of 250K bytes, were used to store all the experimental data collected. The data could then be transferred, when required, for processing by the University's central IBM 370/158 computer.

CHAPTER 5 RESULTS AND MODELLING

5.1 INTRODUCTION

A series of experiments were performed using the oximeter, pulse monitor and data capture facility which were described in chapter 4. The aims of these experiments were primarily:

(i) To establish whether results from controlled experiments are repeatable.

(ii) Testing the transducer models investigated in chapter 3 against the results of the controlled experiments.

(iii) A qualitative appraisal of the results in terms of known physiological phenomenon (e.g. response to a deep inspiration).

(iv) To aid the construction of a simple physiological and optical measurement models of the composite system, comprising the oximeter and tissue.

Initially, the above objectives could not be clearly defined, but were formulated as the project progressed. At first, it was thought that the main thrust of the investigation would be concerned with aim (iv). However, first experiences with the oximeter indicated that more work was required to achieve a significant level of confidence in the output of the instrument particularly with respect to repeatability of results and in applying a measurement model. Although some tests exhibited interesting phenomenon, other experiments, or the same subject

and under similar circumstances would either show no response, a contradictory or different response. Therefore, before aims (ii)-(iv) could be tackled the question of repeatability had to first be resolved.

Hence, it transpired that the main experimental work done, was concerned with objective (i) and evaluations were performed in respect of objective (ii) (sections 3.5 and 3.7). A number of experiments were designed to highlight different physiological phenomina. The tests performed include:

(i) Arterial occlusion

(ii) Breath holding

(iii) Increase of local peripheral temperature.

(iv) Controlled breathing (spectral studies)

(v) Observation of pulsatile flow

More than 10 of each type of test was performed on the same subject on consecutive days, each test category taking place under similar conditions. In addition, a second subject, not familiar with the project, was also tested, although not as extensively. The results from the two subjects were similar. The details and discussion of the tests are presented in the following sections.

A number of observations were consistently observed and rational explanations, in a qualitative sense were sought. In view of section 3.7, which highlights the inadequacies of present transducer models, the explanations, at this stage, cannot be quantitative. However, the value of the present discussion is that in recognising certain phenomena and attempting to place them in the context of a physiological model, it is exposing the

potential of the instrument for use as a dynamic diagnostic aid. The models are presented with the full realisation of their possible inadequacies, which may be exposed when a beter understanding of the measurement model has been attained.

Further experimental data (representing less than half the total data collected) may be found in appendix 7

5.2 ARTERIAL OCCLUSION

Arterial occlusion experiments were chosen because it was argued that such a test should constrain the total blood volume to remain constant. This would mean that one of the possible variables in the system would be a priori known, or more correctly its dynamic component would be zero. Since the objective is to only identify trends (section 3.6) and not absolute values, knowing the change and rate of change in a variable is valuable. However, this is only strictly true in linear systems and so because of the non linearities present, any quantitative analysis would have to take into consideration the actual values.

The test duration was 1,5 minutes. The subject was seated and his right arm was allowed to rest on a table. The oximeter was placed on the subject's right index finger, the pulse monitor was attached to the wrist and a mercurial sphygmomanometer wound around the arm, just above the elbow. Thirty seconds after the start of the test, the sphygmomanometer was inflated to above systolic pressure (usually inflated to 140-160mm Hg). The time taken to inflate to full pressure varied between 3-6 seconds and thus cannot be taken as a "step input". The period of occlusion varied between 40-60 seconds. Although. this period is comparitively short, it was not advisable to attempt longer periods of occlusion as medical supervision was not available. Figure 5.1 illustrates the experimental setup.

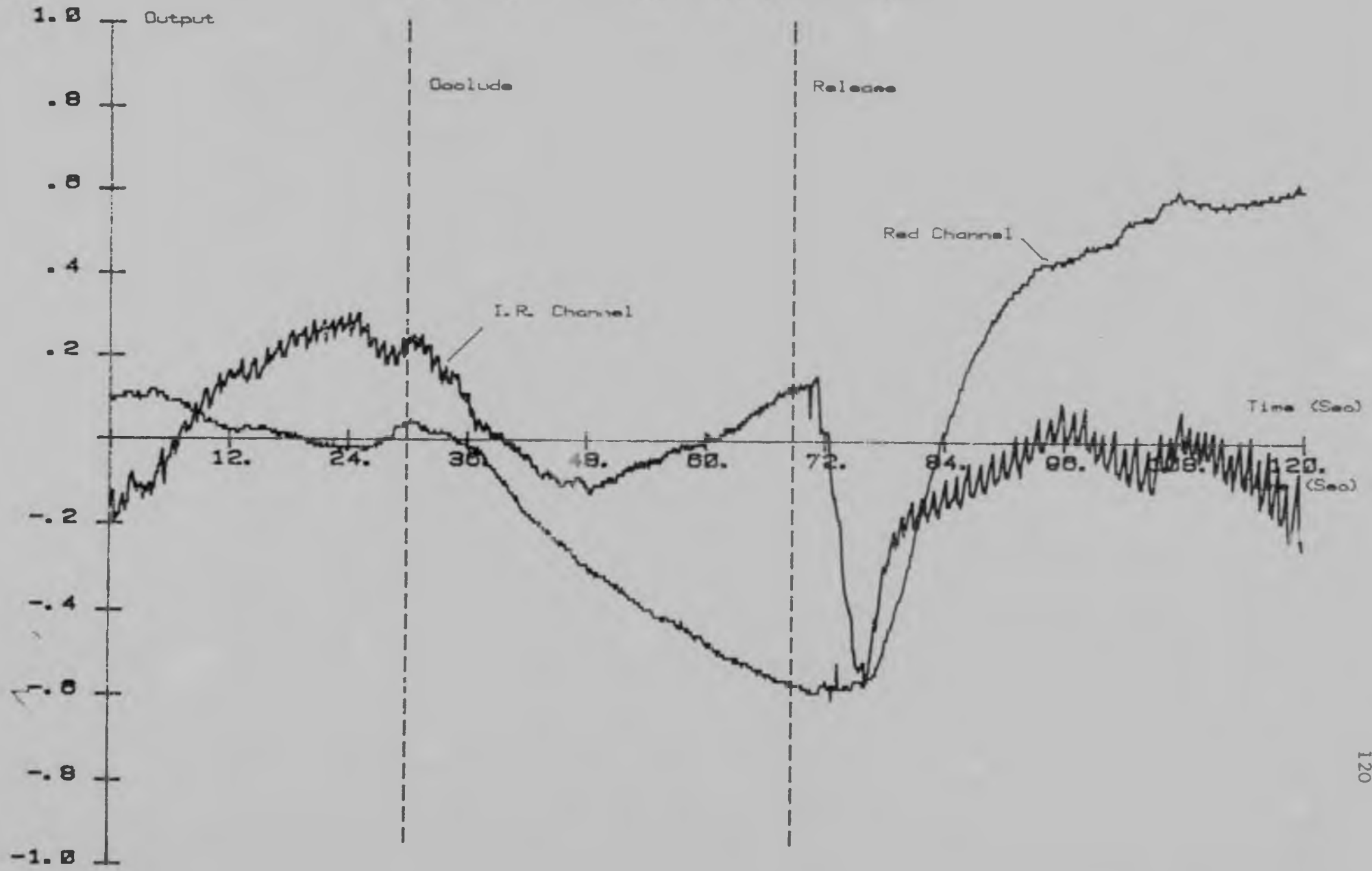


Figure 5.1 Experimental Setup for Arterial Occlusion Experiment. The Sphygmomanometer cuff was inflated above systolic pressure for approximately 40 seconds.

The results of these tests exhibited two interesting features (figure 5.2). Firstly, observing the output from the red channel of the oximeter, there is a definite change in slope of the output during the period of occlusion (between the vertical dotted lines in figure 5.2). This change occurs consistantly in almost all the results (appendix 7). In addition the change occurs 15-20 sec (average 18 sec standard deviation 2,1 sec over ten experiments) after the beginning of the occlusion. Simultaneous with the change in the red channel output is a local minimum in the infra-red channel output.

Such a result suggests that the volume of blood in the superficial skin does not remain constant during the occlusion. Since the total volume of blood in the arm and hand cannot change, any change in the skin blood volume must take place with a complementary change in the deep tissue. The venous system provides a pool in which large volumes of blood may be deposited. The form of the results suggest that initially the skin blood volume decreases and then increases again. This increased blood volume could be attributed to a vasodilation as a result of the buildup of metabolites (see sections 2.6.1 and 2.7.4). However, a possible objection to this is, why dilation in the skin should be greater than that in the deep tissue. A reflex response (section 2.7.4) might actually be responsible for diverting the blood from the higher metabolic tissue to the skin, so as to conserve oxygen. Initially, the metabolite buildup would be prominent, and since the deeper tissue (muscular tissue) is metabolically more active, the vasodilation would be greater here. The continual decrease in available oxygen would then stimulate the local controller, which would then attempt to conserve oxygen by diverting more blood to the less active skin areas. This would qualitatively explain the observed phenomenon. However, these changes might actually be partly attributable to the transducer. In section 3.5.4 it was shown that changes in reflection depend upon the relative magnitude of the absorption and scattering coefficients of blood and tissue and on the nominal values of blood fractional volume and oxygen saturation. In other words, the parameter value choice could be such that as the oxygen saturation decreases (as it must, and is confirmed by the decrease in the red channel), so

Figure 5.2 Arterial Occlusion Experiment



small changes in fractional blood volume might have different effects at the two wavelengths. Nevertheless, it may definately be concluded that peripheral circulatory changes do take place and that these are detected by the transducer in a repeatable fashion.

The second interesting feature occurs at the end of the occlusion period. The pressure in the sphygmomanometer cuff is released by opening a valve. This results in sharp decrease in cuff pressure and thus better approximates a "step change". The infra-red channel output exhibits a sharp drop, followed by an almost equally sharp recovery. A corresponding change in the red channel is very largely attenuated or is not present. This effect is clear in figure 5.2, and appears in most, but not all of the other results (appendix 7).

This behaviour could be a myogenic response (section 2.6.1) to the sudden increase of blood pressure following the release of the syhygmomanometer cuff pressure. This explanation would suggest that the "setpoint" for constrictor tone around the local blood pressure loop, adapts to the prevailing conditions. During the period of occlusion, the average transmural pressure drops and hence the setpoint for myogenic response. When the arterial pressure is restored, this represents an increased transmural pressure and thus the vasculature responds by constricting. The rapid recovery tends to show that the system adapts quickly to the new average value.

A third observation from the results is that the reactive hyperaemia (section 2.7.4) is not obvious in both channels. This may be owing to the period of occlusion being too short. However, as was stated in section 2.7.4, reactive hyperaemia is not a necessary response.

5.3 BREATH HOLDING TESTS

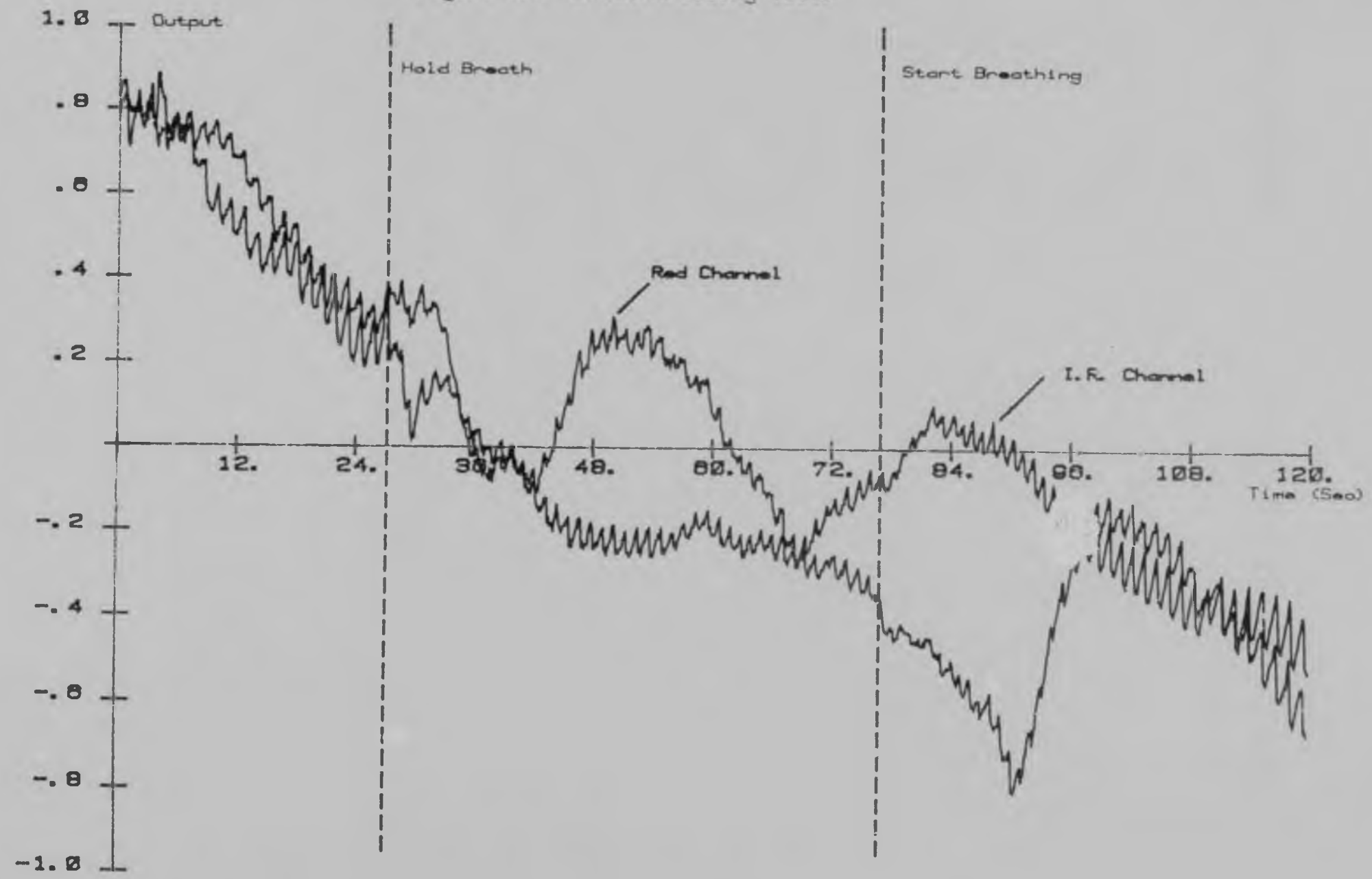
The breath holding tests were one of the first tests performed using the oximeter. Initially, it was thought that the transport delay time from lungs to periphery could be easily measured using this manoeuvre. It was reasoned that this lag could be measured as the time interval between the instant at which the subject began holding his breath untill the oximeter registered that relatively deoxygenated blood arrived at the site of measurement. However some experiments exhibited an initial sharp decrease almost immediately following the start of a breath-holding session. These obsevations plus obvious rhythmic behaviour stimulated the present research project. Parathentically it should be noted that the lag time interval measurements will not be simple using the oximeter.

A series of six standard test were performed on the same subject. The subject was seated and the oximeter placed on his right index finger. A few minutes prior to the beginning of recording, were allowed for the subject to reach steady state. Thirty seconds after the start of recording the subject took a deep inspiration and held his breath for as long as was possible (approximately 60 seconds). Following expiration, breathing was deep and rhythmic. This usually lasted for 20-30 seconds. Thereafter a normal breathing pattern was resumed.

A typical result is shown in figure 5.3. The initial decrease in the red channel output following the deep inspiration must be neural. Following this initial decrease there is a recovery and thereafter a further decrease as deoxygenated blood reaches the site.

The infra-red channel response also exhibits an initial decrease, this tends to indicate that the fractional blood volume initially decreases which agrees with previous observations (see section

Figure 5.3 Breath Holding Test.



2.7.3). The curve then flattens out showing a constant blood volume situation. However, after 35-45 seconds, the output from the infra-red begins to increase (at this stage the red channel is decreasing). The conclusion from this in terms of the simple model structure (section 2.5) is that although oxygen is decreasing, the skin blood flow is increasing. This would be a mechanism whereby the central controller attempts to conserve oxygen by diverting the blood to the less metabolically active skin.

It should be pointed out that these results were not always repeatable. In some cases, the above response was extremely small (Other subjects were also tested and similar results were obtained) In addition, the non-isobestic wavelength of the infra-red channel has been ignored. However, these tests definitely indicate an interacton between a central and local control in the allocation of resources during asphyxia.

5.4 THE EFFECTS OF LOCAL TEMPERATURE CHANGE

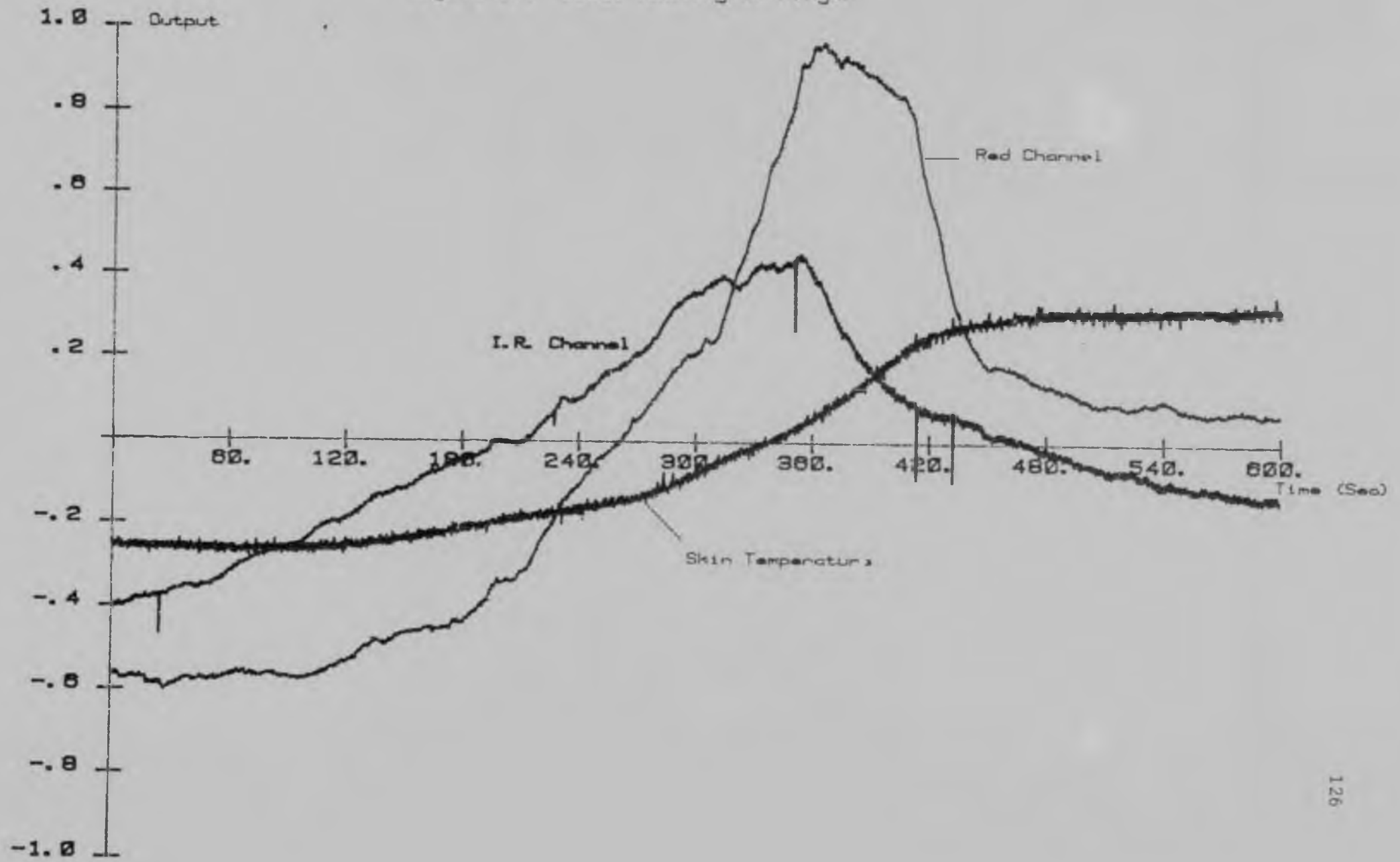
The background physiology of Chapter 2 suggests that temperature change is an important factor in the regulation of blood flow. In order to test the oximeter's performance, a series of experiments were devised to determine whether the oximeter can detect the effect of temperature change. In similarity with the other experiments, an extensive investigation was not undertaken, but the tests were primarily aimed at testing the oximeter performance via known physiological phenomena and obtaining repeatable results. The results from this series of tests qualitatively conflict with the predictions of the models when published parameter values are used. This leads to the requirement for a new assesment of parameter values, as discussed in section 3.7.

When considering changes in tissue perfusion, two types of temperature change are important; viz. body heating and local heating. Because of the practical difficulties involved with body

heating, only the latter was investigated. Initially, local heating was attempted using hot water. Various systems of immersing the subject's hand in hot water were attempted; all were unsuccessful as the transducer became wet and the water interfered with the optical system. There were various attempts at encapsulating the hand and transducer in plastic before immersion in water, but these involved unnatural contortions which interfere with the normal blood flow. Finally a household barheater was used to heat the patient's hand via radiation. The heater was 15-20cm above the subject's hand, which was allowed to rest in the horizontal position, so as to significantly raise the local temperature. A Fluke 80T-150 temperature probe was placed on the skin adjacent to the oximeter transducer to record skin temperature. The purpose of the temperature probe was not to obtain accurate absolute temperature readings but rather to provide an indication of the skin temperature profile with time. Hence the effects of direct heat radiation onto the probe body and conduction through the probe body were neglected. Consequently the temperature curve in figure 5.4 is not calibrated to a temperature scale (although it is proportional to the centigrade temperature scale).

A typical result is shown in figure 5.4. The bar heater was turned on at the start of the experiment and removed after 5 minutes. Both the infra red and red channels increase, indicating that the expected increased blood flow has been detected. An interesting phenomina is the delayed and large increase in the red channel, compared to the infra red channel. Physiological explanations for this delay have not been satisfactory. It is possible that the phenomenon is a transducer artifact, caused by the two channels operating in different regions of the non-linear response curve (section 3.5.4). Obviously the change in transducer temperature during the course of the experiment will affect its output. However, changes in the transducer output with temperature change (in the range experienced in the experiments) was found to be negligible compared to the changes observed during the experiments and hence this effect may be neglected.

Figure 5.4 Local Heating of Finger



Alternatively, it may, be deduced that although the fractional blood volume increases almost immediately at the start of the experiments, the average oxygen saturation of the cutaneous blood has a delayed substantial increase. A number of hypotheses may be put forward as to why this occurs. The increased skin blood flow may be at the expense of the blood supply to the deep, higher metabolising tissue. Hence as the blood is diverted from this tissue to the skin, so will its average oxygen concentration increase.

The non-linear oxygen dissociation curve should also be considered. However, the shape of the curve (figure 2.7) suggests that any increase above the average tissue oxygen partial pressure (approximately 40 mmHg [67]) would shift the "operating point" onto the plateau region of the curve which would produce a non-linear decrease, and not increase in oxygen saturation. The situation is further complicated by the effect of temperature on the dissociation curve. An increased local temperature facilitates the unloading of oxygen into the tissue, with a corresponding rise in oxygen partial pressure. The overall effect can only be predicted using a simulation technique. This still remains to be done, once a model has been constructed.

5.5 SPECTRAL STUDIES

When a "black box" approach to system identification is adopted, it is useful to observe the power spectra of the system output. In a single input, single output, linear system, the system impulse response can be obtained if the input is known. In the present situation, there is no reason to assume linearity and the input is unknown. Nevertheless, it is still valuable to examine the power spectrum of the oximeter output as any periodic or pseudo-periodic behaviour will be apparent.

The test results obtained definately indicate that the oximeter's output does exhibit periodic behaviour. The heart rate and its

harmonics are always prominant in the spectra. Other dominant periodic components lie mainly below 1Hz. The breathing rhythm is one of the dominant cycles.

A series of test spectra are shown in figures 5.5 - 5.8. These spectra were recorded using a Bruel and Kjaer Narrow Band Spectrum Analyser type 2031. This instrument uses a fast fourier transform to obtain spectra from a 40 second time record using 1024 sample values. The sampling frequency was chosen to be 20Hz (The lowest available on the machine). Therefore, 10Hz, full scale spectra, having 400 lines were obtained. Successive spectra were averaged using an exponential algorithm as follows:

$$Y(n) = \frac{(n-1)\ Y(n-1) + X(n)}{n}$$

where: Y(n) is the n'th averaged spectrum

X(n) is the n'th instantanuous spectrum

Usually a total of ten spectra were averaged. Note that the magnitude scale is a dB scale. Only relative magnitudes are significant (i.e. the magnitude between different spectra should not be directly compared, only relative magnitudes may be compared.)

The spectrum analyser was initially connected to the infra-red channel of the oximeter. The subject was seated and the oximeter placed on the right index finger. In figure 5.5 the subject simply sat still and spoke quietly. This was done in order that there should be no significant rhythmic breathing pattern. In the following three experiments the subject breathed rhythmically at rates of 0,1Hz, 0,2Hz and 0,5Hz respectively. The breathing rhythm peaks in the power spectra are clearly visible together

Figure 5.5 Spectrum From I.R. Channel
When Sitting Still.

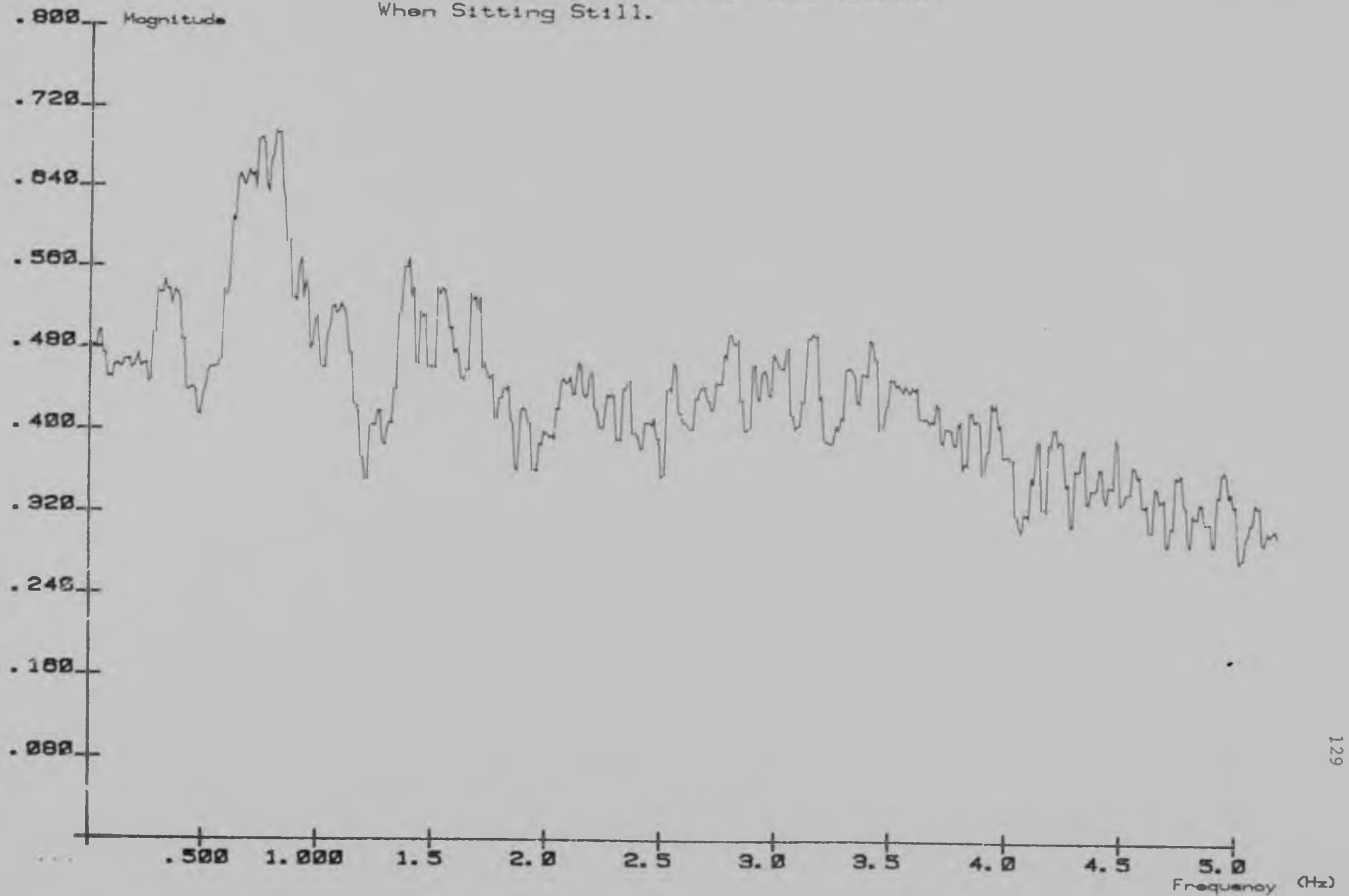


Figure 5.8 Spectrum From I.R. Channel
When Breathing at 0.1 Hz.

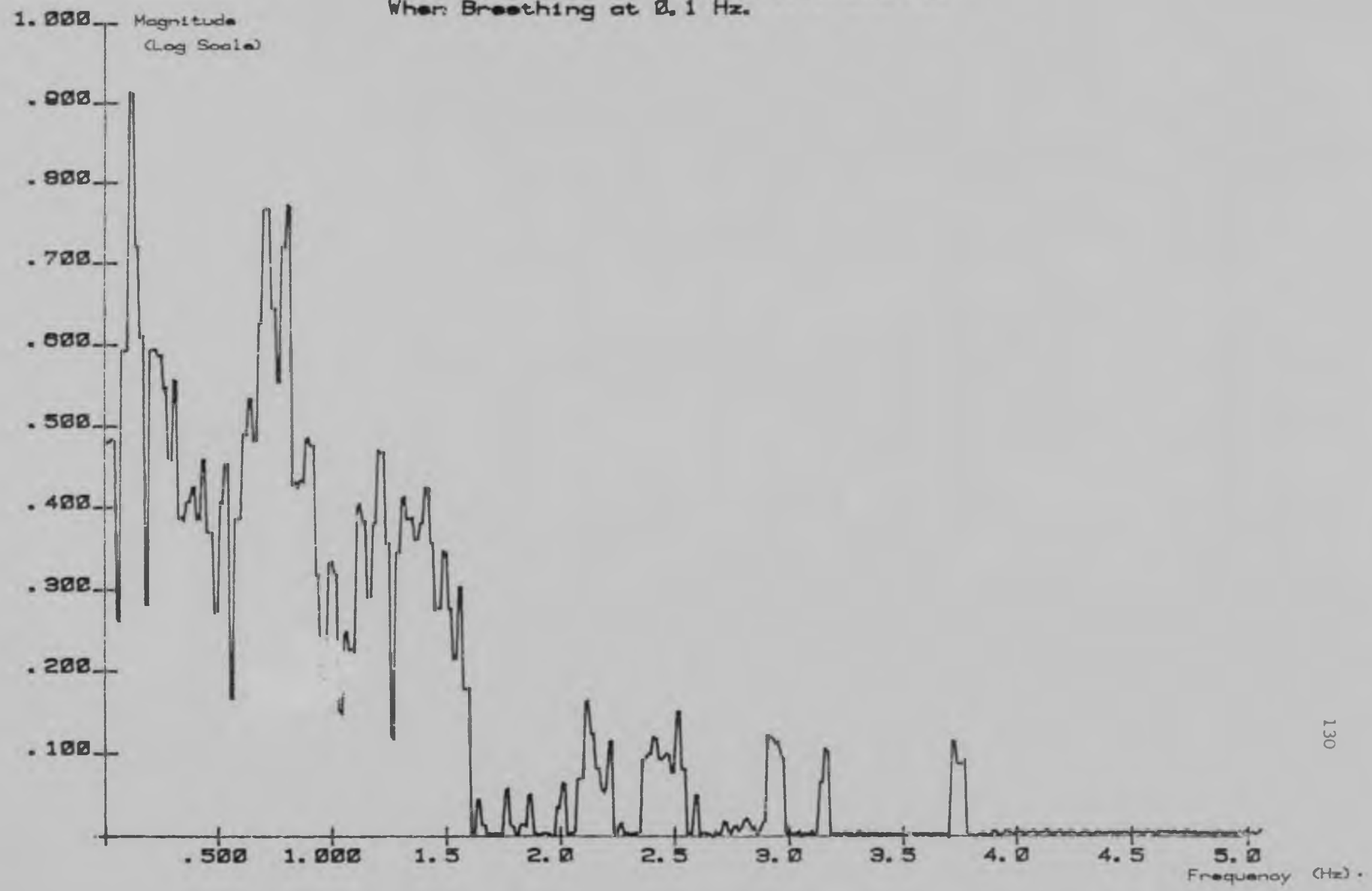


Figure 5.7 Spectrum From I.R. Channel
When Breathing at 0.2 Hz.

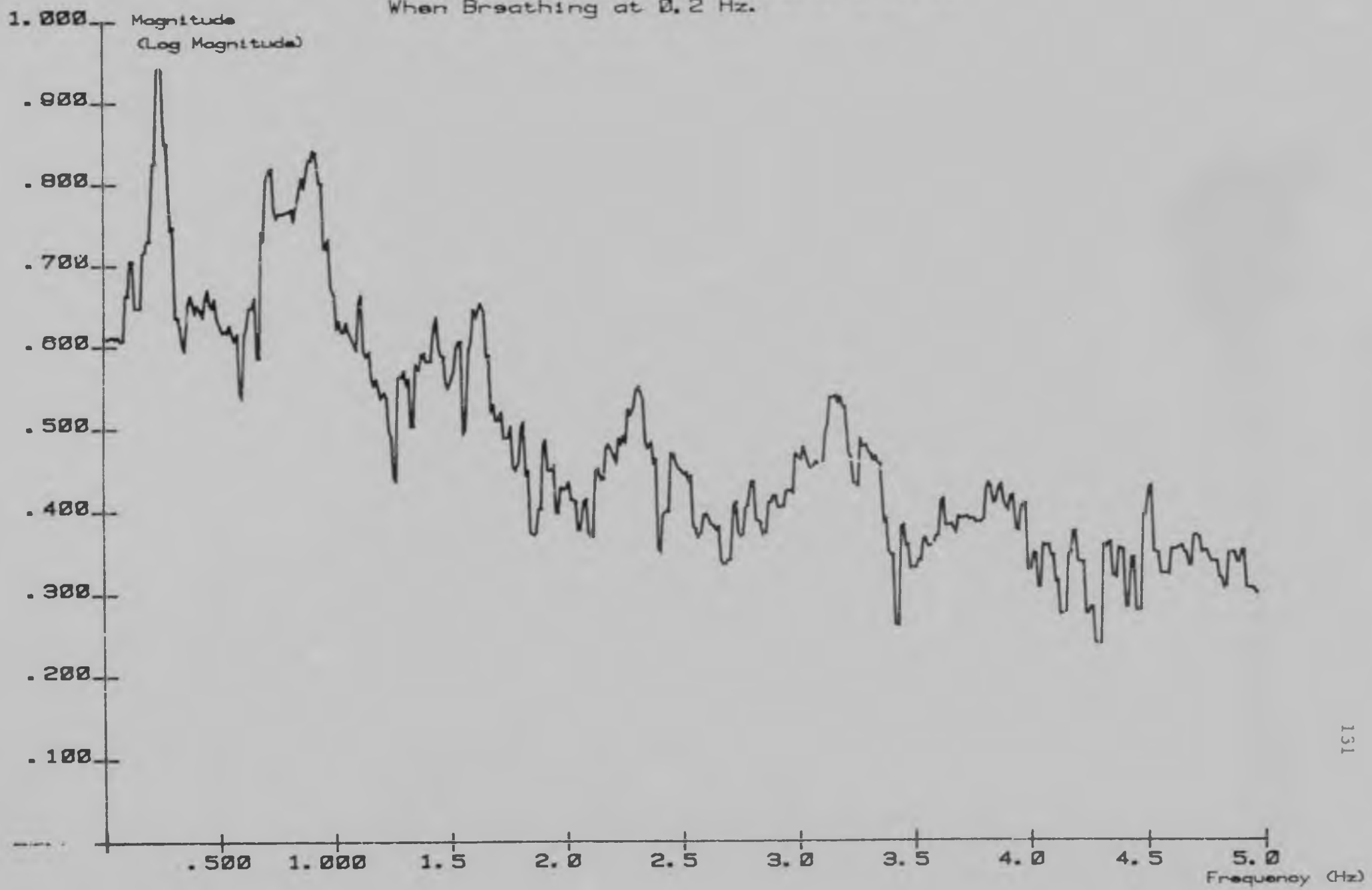
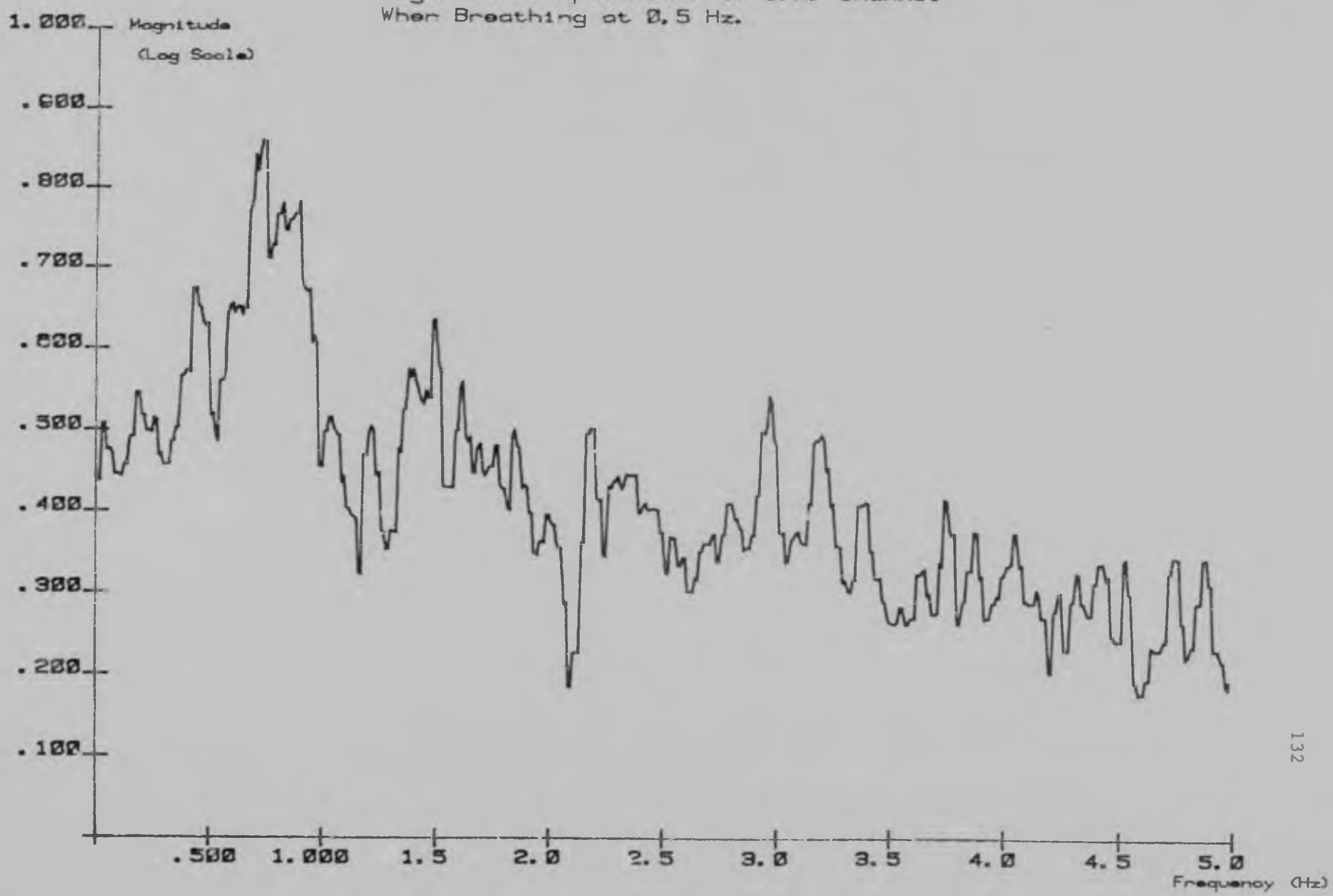


Figure 5.8 Spectrum From I.R. Channel
When Breathing at 0.5 Hz.



with the heart rate rhythm. The breathing rhythm agrees with the findings of Burton [6] (see section 2.6.2).

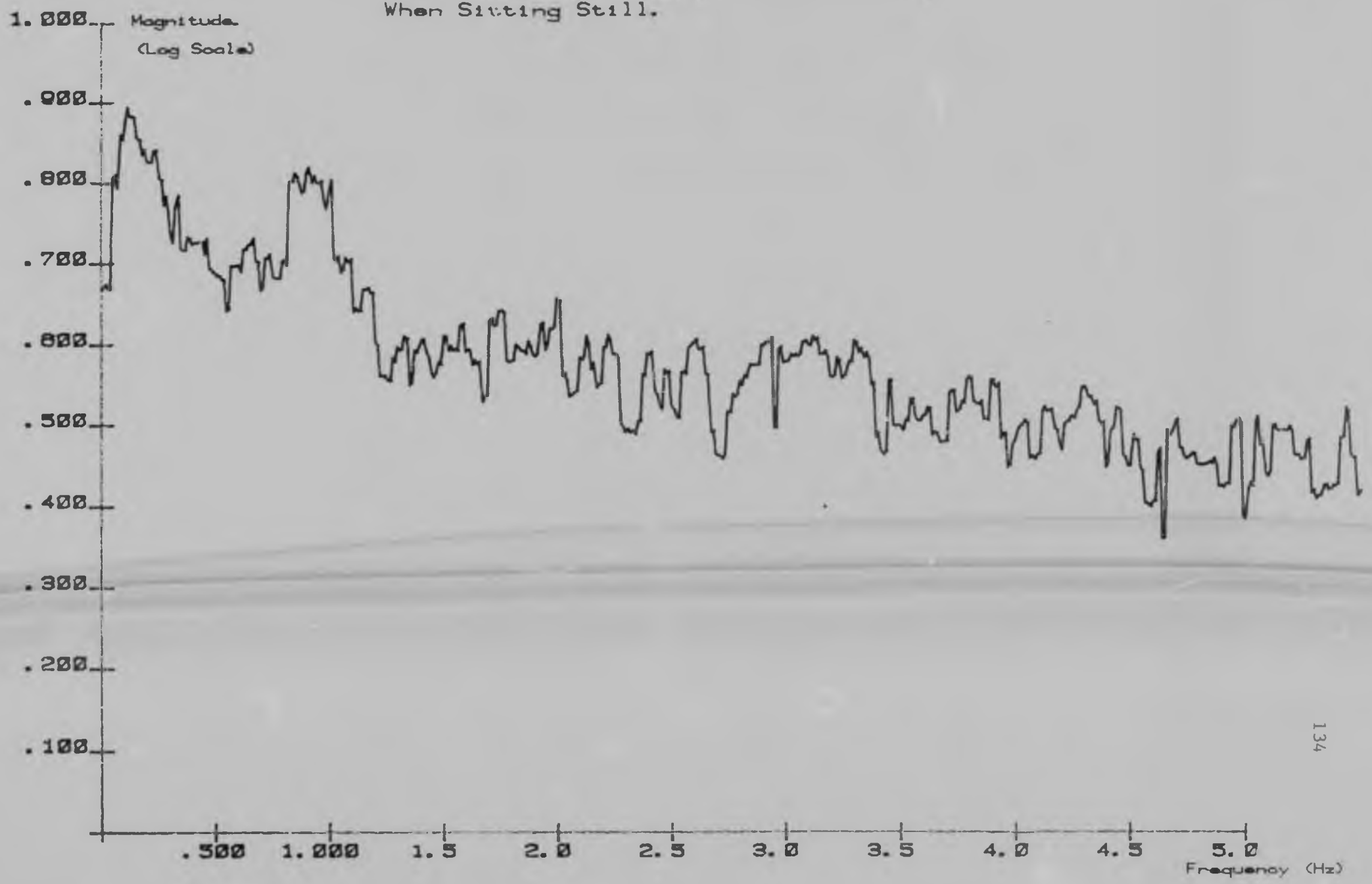
The spectrum shows other peaks below 1Hz. The cause of these were not identified. The temperature controller almost certainly has components in this range. It is doubtful if very low frequencies (i.e. less than 0,05Hz) can be identified in a simple manner, as any long term changes will require that the subject must remain very still for long periods. Thus the identification of the temperature controller oscillations discussed in chapter 2 (having periods of the order of minutes) will be more difficult. These observations were checked using a second subject. Again the heart rate and breathing rhythm are clearly observable.

In a second set of tests a subject performed vigorous exercise. Spectra were recorded immediately after cessation of the exercise (see appendix 7). A heart rate peak was obtained at 1,55Hz (93 beats/min). Large harmonies (up to the third harmonie) were also clearly visible. A broad peak extended from 0,25-0,45Hz. This represents the range of breathing rhythm as the subject recovered. The decrease in the heart rate was apparent in a spectrum obtained half an hour later. In addition the harmonics were smaller.

Spectra were also taken from the red channel output. (see figures 5.9 and 5.10). The breathing rhythm is again present, and is large compared to the heart rate peak. The significance of this is discussed below. When no particular breathing rhythm was maintained, the spectrum had a broad "peak" from 0,1-0,3Hz.

Therefore, both channels contain spectral information. The red channel contains stronger spectral information at frequencies below the heart rate. A breathing rhythm has been identified at low frequencies in both channels. When breathing is not rhythmic, there still appears to be spectral power in the frequency range 0,1 - 0,3Hz. This power is probably partly a result of breathing, but other factors for example, the thermal controller, contribute in this range.

Figure 5.9 Spectrum From Red Channel
When Sitting Still.



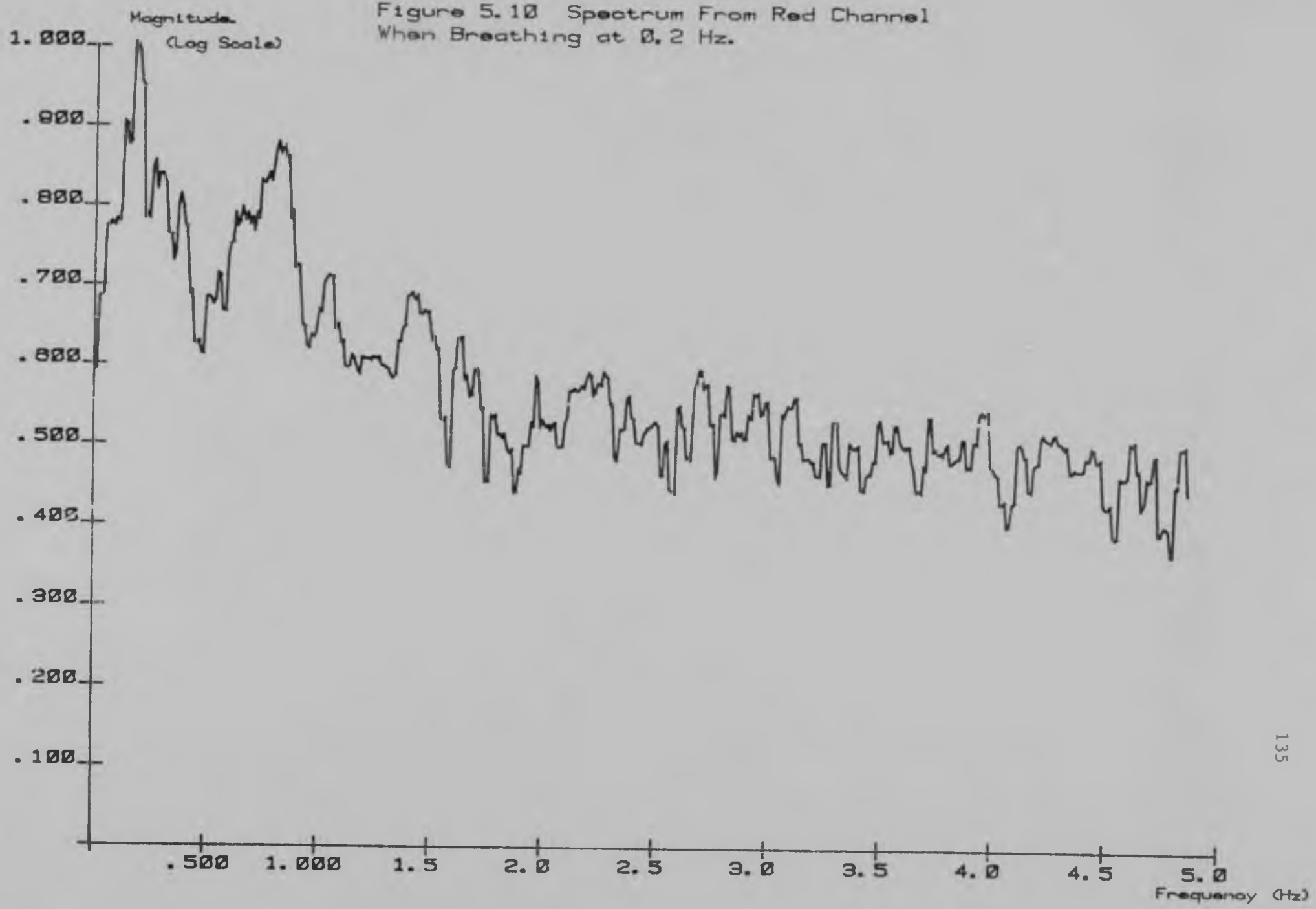


Figure 5.10 Spectrum From Red Channel When Breathing at 0.2 Hz.

The origin of the breathing rhythm in the spectrum is interesting. Possible causes may be postulated. Firstly, it is known [67] that respiratory movements affect the end-diastolic ventricular volume and hence the stroke volume. Thus the cardiac output is modulated by the breathing pattern and this would be reflected in the spectral content of the peripheral blood volume. Secondly, respiratory movements may directly affect the peripheral vasculature (as in "response to a deep inspiration", section 2.7.3). Both effects contribute components to the power spectrum at the respiratory frequency. To check the contribution from heart rate modulation, spectra were taken using the output from the pulse monitor. The results are presented in figures 5.11-5.13. The breathing rhythm is obvious in these plots. It should be noted that the integrator in the pulse monitor circuit (figure 4.3) has a time constant of 5,6 seconds (0,17Hz). Thus part of the power around 0,2Hz is attributable to the integrator. As the relative magnitude of the breathing rhythm is larger from the oximeter spectra, it may be concluded that both phenomina, postulated above, play a role.

Comparing the spectra obtained from the red channel with that obtained from the infra-red channel, it can be seen that the relative magnitude (relative to the heart rate peak) of the breathing rhythm is larger for the red channel. This indicates that the instrument is sufficiently sensitive to oxygen saturation to detect the cyclic changes of oxygen saturation in the blood corresponding to the respiratory cycle. This is encouraging as it means that extremely small variations in blood gas content may be detected. This feature would be valuable in a patient monitoring environment.

The above results do not attempt to be exhaustive but rather serve as an illustration as to the wealth of information contained in the oximeter outputs. The results are repeatable and their causality is encouraging. Incorporating a model structure will almost certainly yield more information.

Figure 5.11 Spectrum From Heart Rate Monitor When Sitting Still.

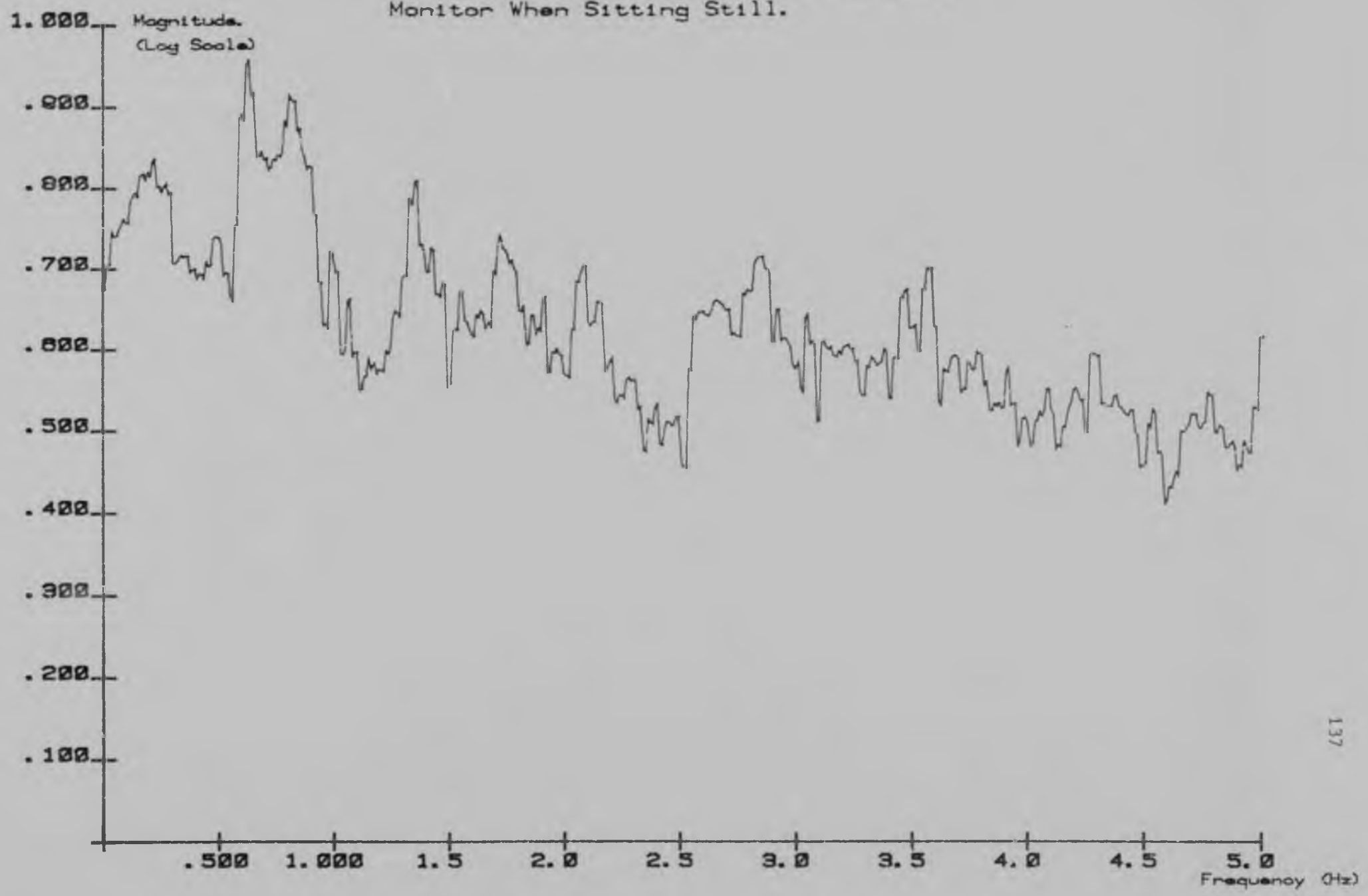


Figure 5.12 Spectrum From Heart Rate Monitor When Breathing at 0.1 Hz

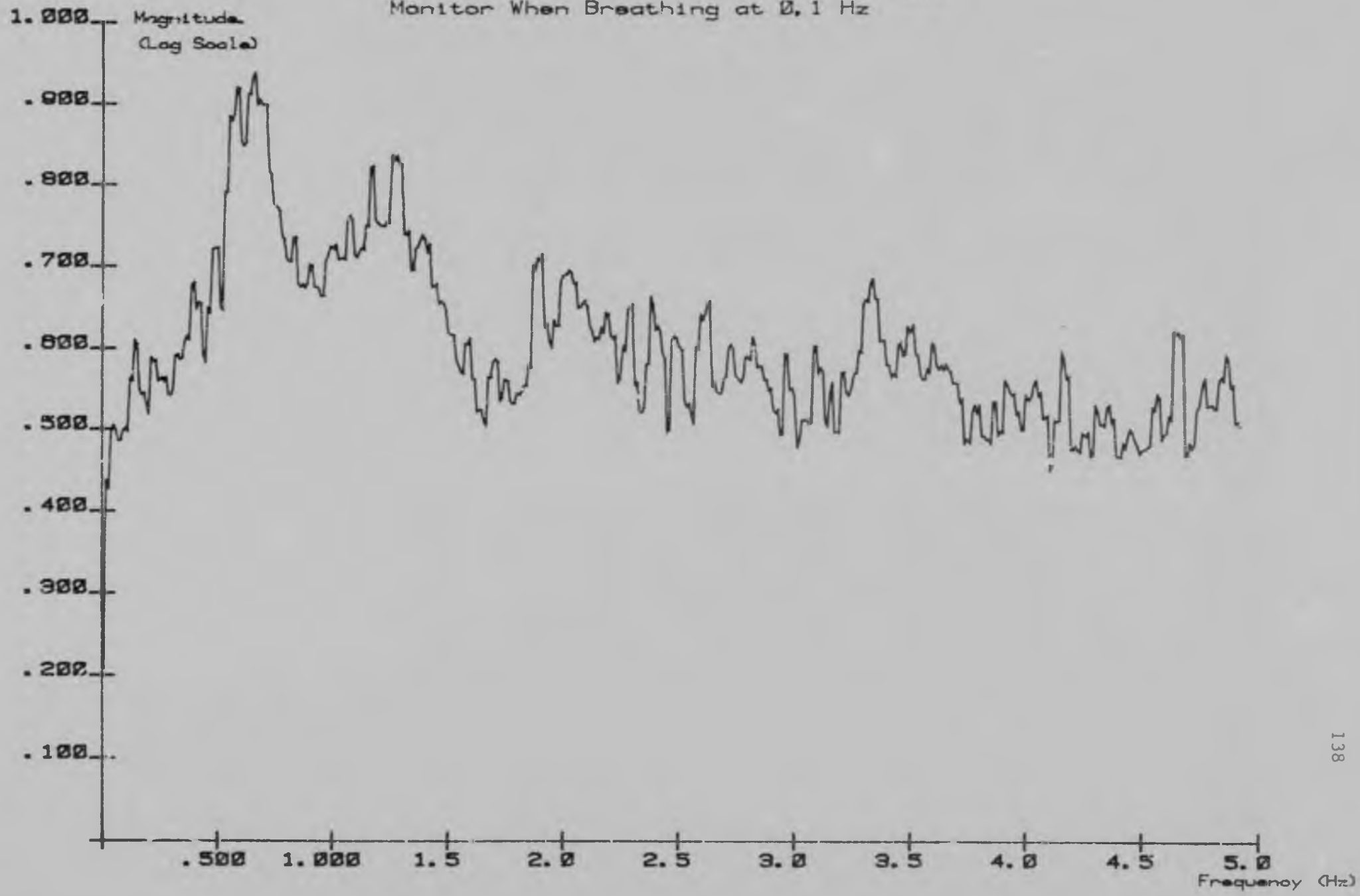


Figure 5.13 Spectrum From Heart Rate Monitor When Breathing at 0,2 Hz

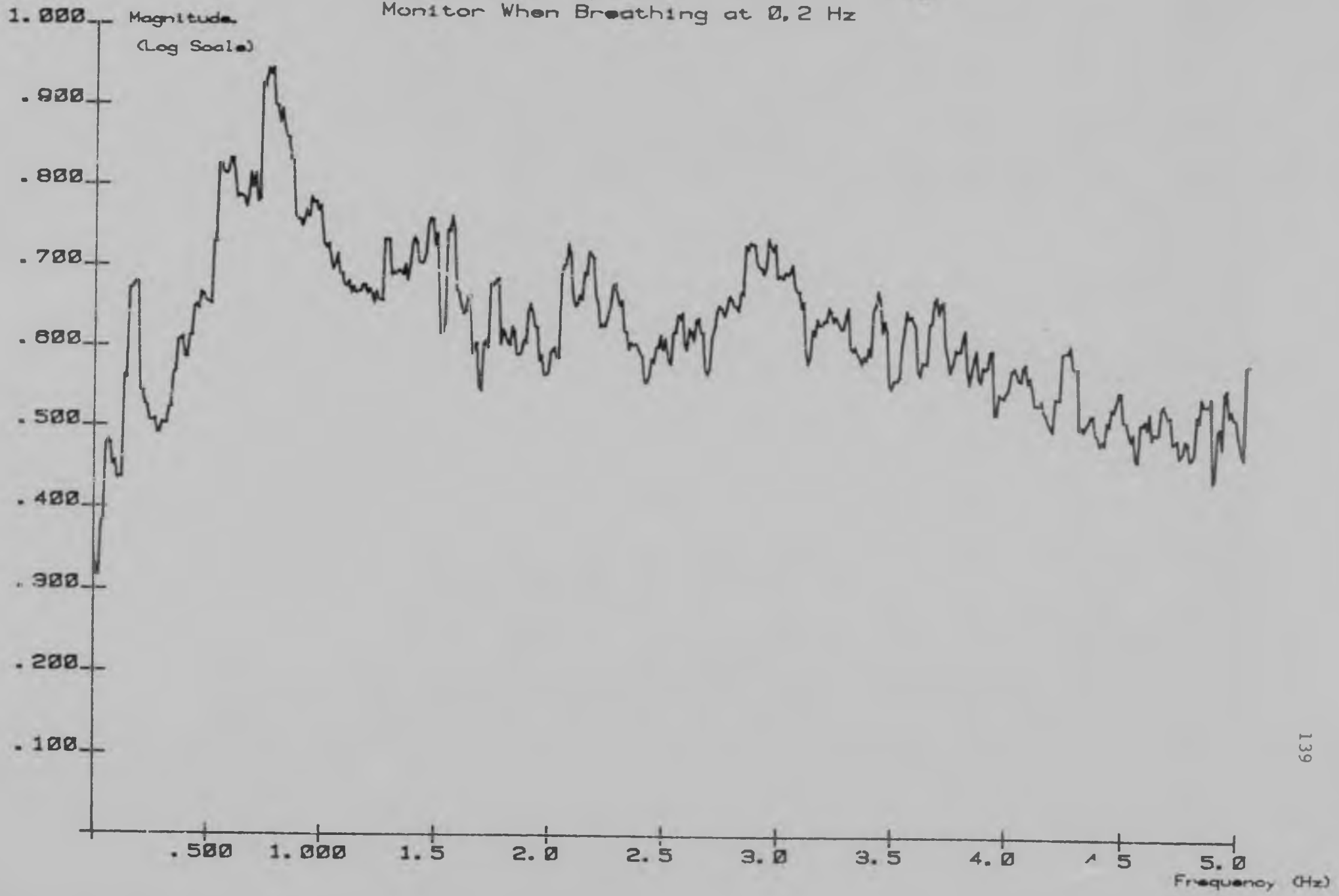
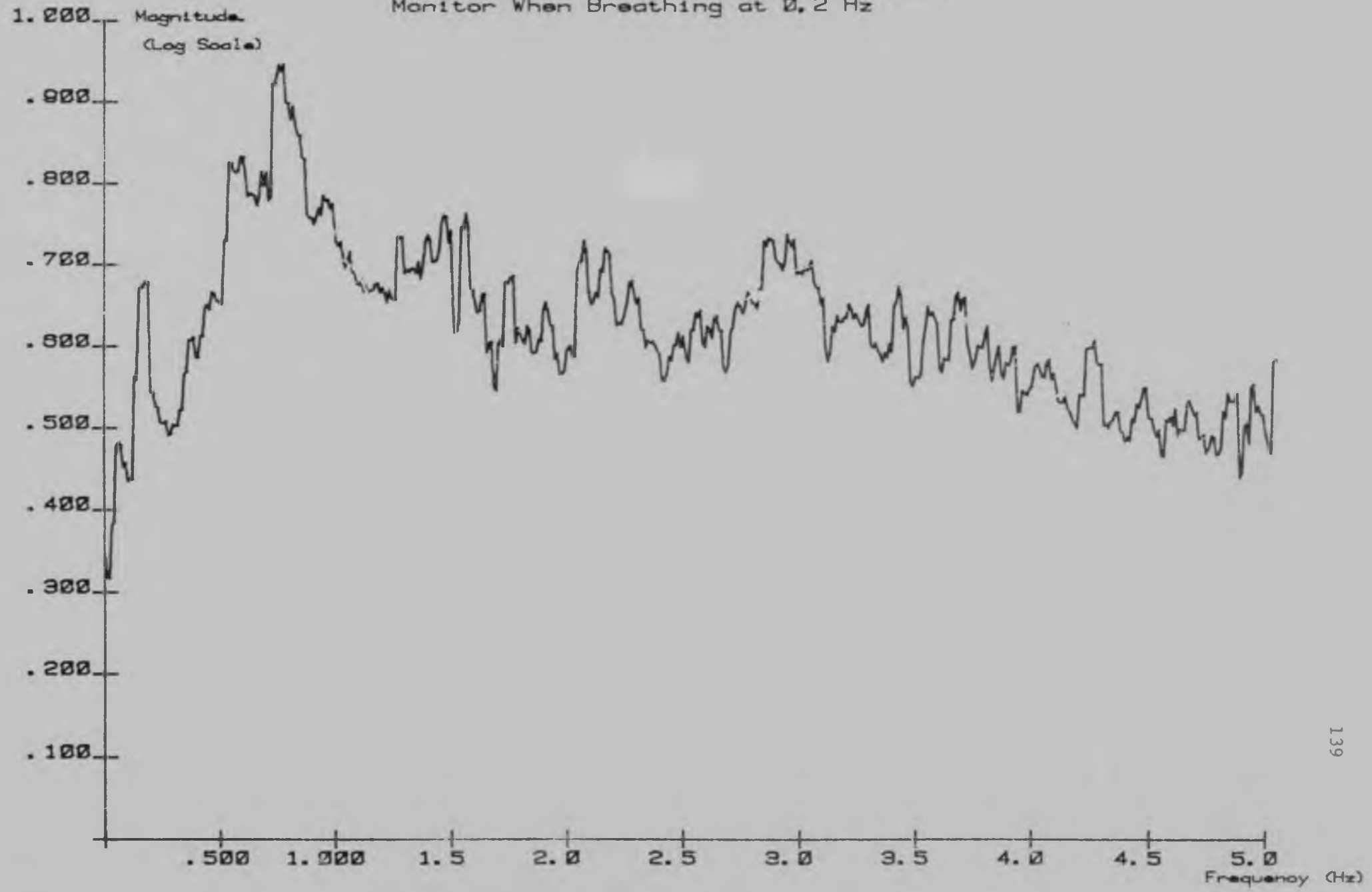


Figure 5.13 Spectrum From Heart Rate Monitor When Breathing at 0.2 Hz



5.6 PULSATILE FLOW

When the oximeter output is greatly amplified, pulsatile behaviour can be observed. It was postulated that this is a result of pulsatile blood flow in the skin. In order to confirm this hypothesis, the pulse monitor was built. The results obtained are interesting.

Simultaneous outputs from the infra-red channel and pulse monitor are shown in figure 5.14. The oscillations in the two outputs appear to be out of phase. Figure 5.15 shows the same results except that the output from the infra-red channel has been inverted. These results indicate that the pulsatile blood flow as observed by the oximeter is out of phase with the arterial pulsations. This inversion cannot be the result of the measurement process, because the output from the pulse transducer has the shape of the familiar pressure wave and it was checked that there is no inversion in the oximeter channels. Two explanations for this phenomina are possible. Firstly, the observation might be a result of a myogenic vascular response (section 2.6.1) acting at an extremely fine level. As the pressure in the peripheral tissue rises during systole the vessel walls would react by contracting, thus reducing the fractional blood volume. This type of dynamic "Bayliss response" has not been previously described. A second possibility is that the observation is the result of a change in extracellular pressure caused by pressure pulsations in the main arteries of the finger. According to this hypothesis, the pulsatile flow has been largely damped out by the time blood reaches the capillaries of the skin. As the pressure in the finger arteries increase, the increased pressure would be transmitted through the tissue, thereby increasing the tissue pressure on the exterior of the minute capillary vessels. As there is no concomitant increase in capiliary pressure, the vessel diameter and hence blood volume would decrease. This explanation is supported by previous reports of the observation

of pulsatile flow in the finger via volume plethysmography.

Nevertheless, the ability of the oximeter to resolve these small changes in blood flow are encouraging. This apparent fine resolution of the instrument would make it a valuable diagnostic aid, for if changes can be detected before they become severe, then appropriate preventative action may be taken at an early stage.

Figure 5.14 I.R. Channel and Pulse Monitor
Showing Pulsatile Blood Flow.

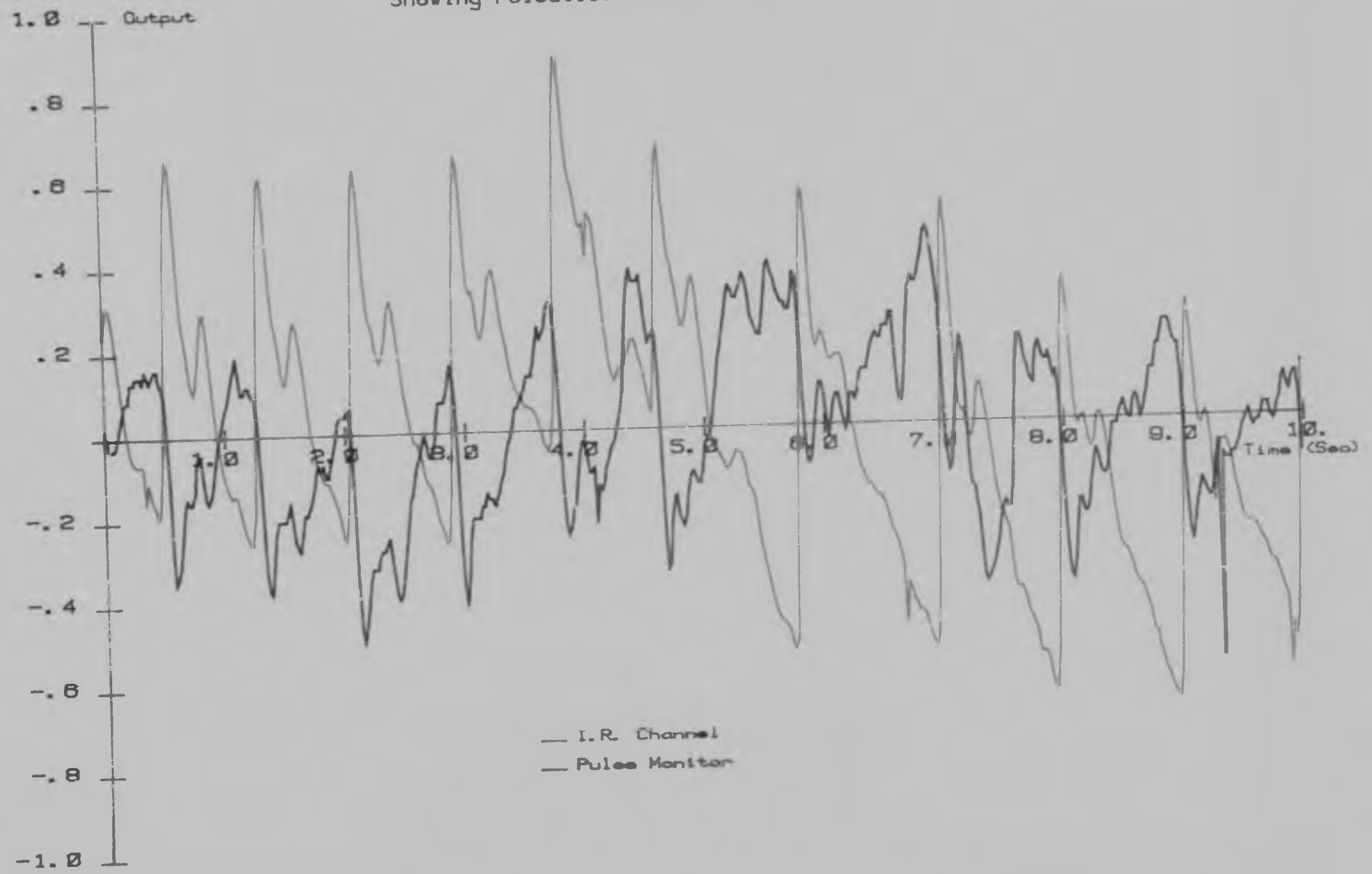
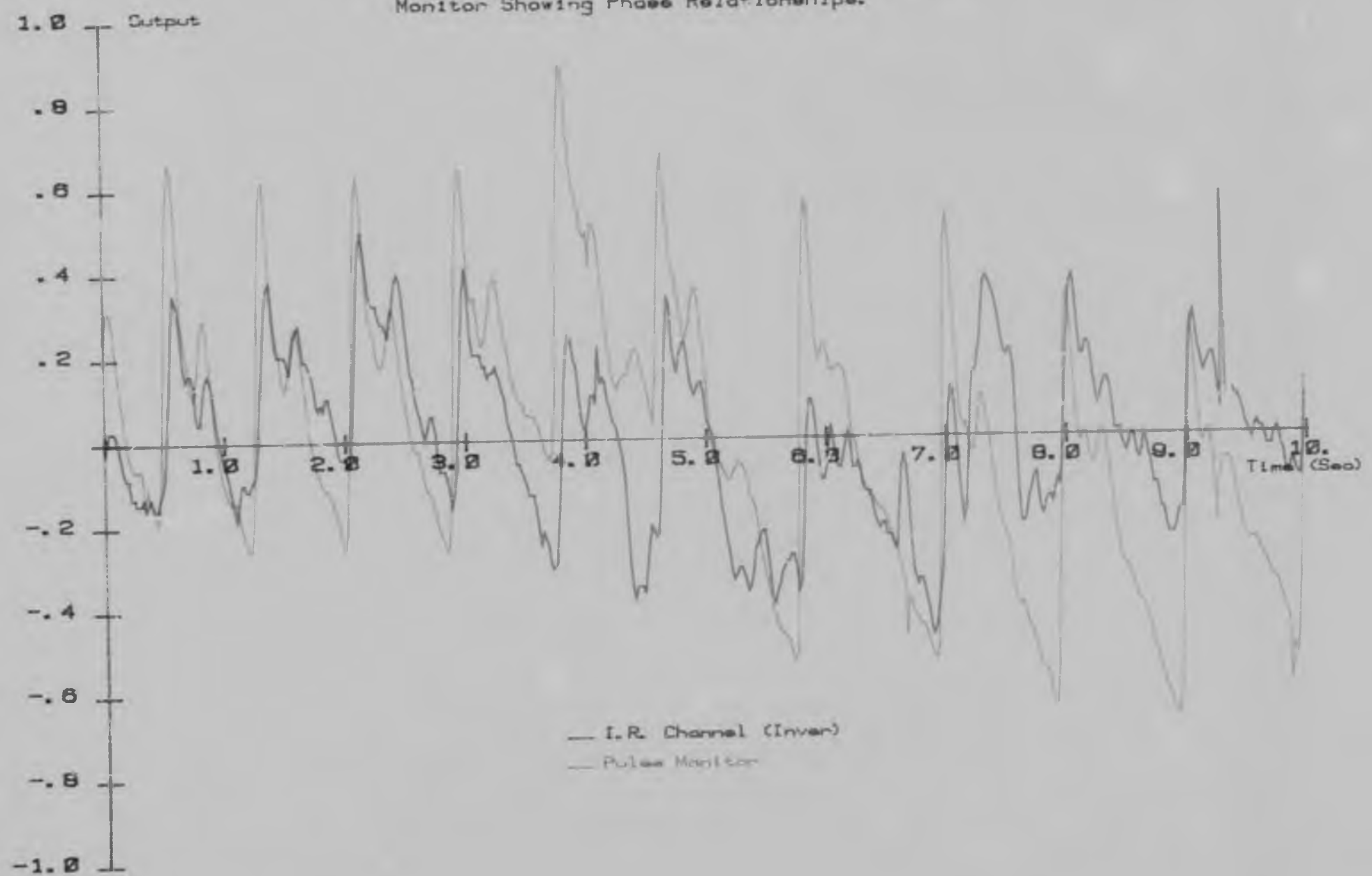


Figure 5.15 Inverted I.R. Channel and Pulse Monitor Showing Phase Relationships.



CHAPTER 6 CONCLUSIONS AND SUGGESTIONS FOR FURTHER WORK

6.1 INTRODUCTION

This project cannot in any way claim to be complete. The very nature of the research makes it difficult to plan the development of the work, but it must rather evolve. Rigorous and even quantitative results are difficult to obtain as all measurements are the result of the integrated response of many variables, while being, in the first instance, very difficult to control are also not easily defined. Factors such as the mental state of the subject, when he last ate, etc, all contribute to any measured response. Thus, the writer views the role of this mini-thesis as the first iteration in an ongoing investigation into the field of non-invasive patient monitoring using a peripheral tissue reflectance oximeter.

A wealth of research data and theoretical developments exist in the literature. An attempt has been made in this project to gather this work together and relate it to a specific area of research. At the same time, several speculative questions and suggestions are put forward. Even at the conclusion of this project, it is difficult to clearly define the future road and objectives, however, it is hoped that it is slightly less diffuse than what it was previously.

The major portion of this dissertation reviews and collects previous work. Chapter 2 gives a simplified background into the underlying physiology of the extremeties. This knowledge is required if a model of the physiology is to be constructed. The section is mainly aimed at the natural scientists who is entering this field for the first time and requires a brief introduction to the physiological arena. Gaps and contradictions are present

in this body of knowledge, but on the whole it presents a rational narrative.

Chapter 3 reviews previous theories of the propogation of light in a complex medium such as a mixture of tissue and blood. Light transmission through a solution (such as hemolysed blood) is well understood. The particle nature of whole blood introduces the problem of scattering. In the presence of tissue and blood, there is no simplistic approach. When considering a model of the skin which consists of a number of layers with differing optical properties, then solutions become extremely tedious. The complications introduced by the geometry of reflectance oximetry are discussed in detail.

Experimental work was performed to test and validate the functioning of the instrumentation. Chapters 4 and 5 respectively describe the equipment and results obtained fro these tests.

6.2 CONCLUSIONS

The present experience and results with the two wavelength oximeter support the original hypothesis that a substantial amount of information may be extracted from the instrument's outputs. Measurements under controlled experimental conditions, together with a physiological and instrument model can yield valuable insight into the underlying mechanisms and control strategies of the peripheral vasculature.

At this stage, quantitative results are not available, however in a qualitative sense, the instrument is sensitive enough to dete t small changes in the oxygen saturation of the peripheral blood, as well as small changes (eg pulsatile flow) in the fractional blood volume in the peripheral tissue. Much information is contained in the time and frequency records of the oximeter's outputs. The intention of the device, is not to obtain absolute measurements, but rather to use it in gathering dynamic infor-

mation concerning the living body. It is postulated, at this point in time, that by monitoring variables other than the classically controlled variables such as temperature, heart rate, blood pressure etc, the physician may be able to recognise certain development patterns at an early stage, before the situation degrades to such an extent that the various physiological control loops cannot keep the controlled variables at the desired values. At this stage, the overall system might have degraded to such an extent that major treatment would be necessary. This philosophy emphasises the need to examine the dynamic, rather than the steady state behaviour of the body. Consequently, absolute measurements are not as important as in the classical steady state approach. A tangible example would be in the area of cardiovascular and plastic surgery. A vital quantity is the level of perfusion in a given tissue mass. The adverse effects of gangrenous conditions may be reduced if the level and direction of change of the blood perfusion could be estimated. Further, the levels of perfusion are important in shock treatment.

Models of the transducer system, which have appeared in the literature, are mathematically complex. Attempts to simplify the mathematical tractibility of the solutions, by neglecting the three dimensional geometry of the problem are not valid. In addition,the models depend upon parameters which are not well known. Model predictions, using published values, yield qualitatively contradictory results to the experimental results obtained in the present work. As it is not a trivial problem to obtain parameter values, it is thought that before any attempt is made at extending or changing the present models, an attempt should be made to better parameterise the existing models.

A simple, lumped physiological model of the skin vasculature based upon the underlying physiology has been presented. Its form suggests that the individual arterial and venous blood volumes may change while either keeping their combined volume constant or allowing it to change. A qualitative discussion of the observed oximeter outputs as a result of controlled stimuli was presented in terms of this model. However, it is thought that the measurement model should be improved (in terms of the parameters) prior to extending the physiological model.

mation concerning the living body. It is postulated, at this point in time, that by monitoring variables other than the classically controlled variables such as temperature, heart rate, blood pressure etc, the physician may be able to recognise certain development patterns at an early stage, before the situation degrades to such an extent that the various physiological control loops cannot keep the controlled variables at the desired values. At this stage, the overall system might have degraded to such an extent that major treatment would be necessary. This philosophy emphasises the need to examine the dynamic, rather than the steady state behaviour of the body. Consequently, absolute measurements are not as important as in the classical steady state approach. A tangible example would be in the area of cardiovascular and plastic surgery. A vital quantity is the level of perfusion in a given tissue mass. The adverse effects of gangrenous conditions may be reduced if the level and direction of change of the blood perfusion could be estimated. Further, the levels of perfusion are important in shock treatment.

dels of the transducer system, which have appeared in the literature, are mathematically complex. Attempts to simplify the mathematical tractibility of the solutions, by neglecting the three dimensional geometry of the problem are not valid. In addition, the models depend upon parameters which are not well known. Model predictions, using published values, yield qualitatively contradictory results to the experimental results obtained in the present work. As it is not a trivial problem to obtain parameter values, it is thought that before any attempt is made at extending or changing the present models, an attempt should be made to better parameterise the existing models.

A simple, lumped physiological model of the skin vasculature based upon the underlying physiology has been presented. Its form suggests that the individual arterial and venous blood volumes may change while either keeping their combined volume constant or allowing it to change. A qualitative discussion of the observed oximeter outputs as a result of controlled stimuli was presented in terms of this model. However, it is thought that the measurement model should be improved (in terms of the parameters) prior to extending the physiological model.

A second method of analysing the data, which has not received much attention here, is via the "Black Box" approach, using signal processing techniques. This method does not seek an "a priori" model but rather looks for correlations in observed outputs. The brief spectral work done in the present report suggests that this avenue is encouraging.

It should be emphasised at this stage, that the ideas expressed here are mainly speculative. Many man-years must be invested before such ideas may be realised. However, the central conclusion from the present work is that the oximeter definetely has a large potential for a patient monitoring application, and that further work is justified.

Parenthetically it should be added that any understanding of the intricate biological control processes could aid the improvement of engineering control problems. The manner in which feedforward and adaptive control strategies are handled would be of importance. Also, it is widely postulated [25] that biological systems operate so as the maximise / minimise some performance criteria. This is generally also the goal of engineering projects.

6.3 SUGGESTIONS FOR FURTHER WORK

It has been consistantly emphasized throughout this dissertation that this type of instrument raises a host of possibilities and questions, and the more one investigates, the wider the field becomes. Hence a section on suggestions for further work could never hope to be complete. A sample of points which arose during the present investigation are presented here. It proves convenient to divide these up into short term and long term objectives. The short term suggestions are more closed in nature, while the long term are speculative.

6.3.1 Short Term

Two main areas require further work. Firstly, the light source and detector systems need to be improved, both with respect to performance and from an ergonometric point of view. The present shortcomings are that heat from the light sources will affect the vasculature and that the present finger cap still allows some movement of the transducer relative to the skin surface.

It is suggested that a fibre-optic, optical system be investigated. A point source would be better approximated, by using clusters of optical fibres. Intermingling the red and infra red clusters would ensure that both sources illuminate the same vascular region. Ideally, both sources should use the same optical guides. The detector system might be realised by an annulus of optical bundles surrounding the source. Alternatively, a single dimensional measuring system (i.e. source and detector in the same straight line) might be approximated to by intermingling source and detector bundles. In addition, the non-isobestic wavelength of the infra-red LED might be considered.

The second area relates to the measurement and physiological models. Experiments are required, which will allow the existing models to be parameterised so that their peformance might be evaluated. Examples of such experiments would be, carefully controlled breathing or temperature tests in which ventilation and changes in peripheral skin flow rate are measured via other techniques. These measurements would then be correlated with the oximeter outputs. Such tests would most probably require a well equipped physiology laboratory, in which external influences may be controlled.

Finally, the "black box" approach could be further pursued via more spectral and correlation studies of the outputs. These were not emphasized in the present report, mainly because it was felt that these studies should be postponed until more confidence was

gained in the instruments' outputs. Various rhythmic modes of perfusion have been qualitatively identified in physiological studies (see chapter 2). The various temperature controller modes (such as hunting reaction) should produce interesting spectral studies.

6.3.2 Long Term

These suggestions cannot be explicitly stated. They are mainly associated with the application of the instrument as an aid to patient monitoring. This would involve exploiting the ability of the instrument to reflect the dynamic behaviour of local tissue perfusion. Possibly, this could be ultimately extended to obtain a spatial, dynamic picture of the state of the body through utilising a number of transducers situated at different points of the body. Together, the outputs may possibly yield information concerning the overall state of the cardiovascular system. This work would have to proceed in conjunction with the needs and suggestions of clinicians.

Two possible approaches may be adopted. The shorter of these two could be via the "black box" approach. This would involve the collection and processing of large amounts of data from patients with varying degrees of pathological conditions. By noting the correlation, spectra and time responses to various manoeuvres, it might be possible to identify and predict various disorders.

The second approach is via parametric modelling of the system under investigation. This approach is fundamental and would lend a great amount of understanding to the system. However, the realisation of such a goal is most probably far into the future.

LIST OF REFERENCES

1. ABRAMSON D.J., FERRIS E.B. Responses of Blood vessels in the resting hand and forearm to various stimuli. The American Heart Journal. 19; 541, 1940

2. ALLWOOD M.J., BARCROFT H., HAYES J.P.L.A., HIRSJARVI E.A. The effect of mental arithmetic on blood flow through normal sympathectomised and hyperhidrotic hands. J. Physiol., London, 148; 108, 1959

3. ATKINS A.R. A method for simulating heat flow and control in a nude man with an analogue computer. MSC Thesis, University of the Witwatersrand, 1962

4. BAYLISS W.M. On the local reactions of the arterial wall to change of internal pressures. J of Physiol. 28; 220, 1902

5. BOLTON B., CARMICHAEL E.A., STURUP G. Vasoconstriction following a deep inspiration. J of Physiol, London, 86; 83, 1936

6. BURTON A.C. The Range and Variability of the blood flow in human fingers and the vasomotor regulation of body temperature. Am. J Physiol. 127; 437, 1939

7. BURTON A.C. Physiology and Biophysics of the Circulation. Year Book Medical Publishers, 1965

8. CHALMERS J.P., KORNER P.I. Effect of arterial hypoxia on the cutaneous circulation of the rabbit. J. Physiol (London) 184;

9. CHARM S.E., KURLAND G.S. Blood flow and Microcirculation. John Wiley & Sons, 1974

10. CHOW C.K., JACOBSON D.H. Studies of Human Locomotion Via Optimal Programming. Mathematical Biosciences 10; 239-306, 1971.

11. COHEN L., BEATON G., MITCHELL D. The South African Textbook of Sports Medicine. Sports Medicine Clinic, 1979

12. COLES D.R., GREENFIELD, A.D.M. The Reactions of the blood vessels of the hand during increases in transmural pressure. J. Physiol. 131; 277-289, 1956.

13. COMROE J.H. Physiology of Respiration. Year Book Medical Publishers, 1965

14. CROSSLEY R.J., GREENFIELD A.D.M., PLASSARAS G.C., STEPHENS D. The interrelation of thermoregulating and baroreceptor reflexes in the control of blood vessels in the human forearm. J. Physiol. (London), 183; 628-636, 1966

15. CUMMING G. The Measurement of Oxygen in the Clinical situation. In Oxygen Measurements in Biology & Medicine. (Payne J.W., Hill D.W. eds) Butterworths, 1975

16. DAVIS D.L. & CARLETON H.B. Comparison of changes in blood volume and opacity in dog digital pad and tongue. J. Appl. Physiol. 27(5); 613-618, 1969.

17. DI SALVO J., PARKER P.E., SCOTT J.B., HADDY F.J. Carotid baroreceptor influence on total and segmented resistance in skin and muscle vasculatures. Am J. Physiol. 220, 6; 1970-1978, 1971.

18. DULING B.R. Microvascular response to alterations in oxygen tension. Circulation res. 31; 481, 1972

19. DULING B.R. Oxygen sensitivity of vascular smooth muscle II. In Vivo Studies. Am J. Physiol. 227; 1; 42, 1974

20. EDHOLM O.G., FOX R.H., MACPHERSON R.K. Vasomotor control of the cutaneous blood vessels in the human forearm. J. Physiol. (London) 139; 455-465, 1957

21. EDWARDS A.E., DUNTLEY S.Q. The pigments and colour of living human skin. Am J. of Anatomy. 65, 1; 1-33, 1939

22. FOLKOW B. Range of Control of the Cardiovascular system by the central nervous system. Physiol Rev. 40, Suppl 4; 93-99, 1960

23. Fox R.H. & Hilton S.W. Bradykinin formation in human skin as a factor in heat vasodilation. J. Physiol., London, 142; 219, 1958.

24. FROESE G., BURTON A.C. Heat losses from the human head. J. Appl. Physiol., 10; 235, 1957

25. GEDDES L.A., BAKER Principles of Applied biomedical instrumentation John Wiley, 1968

26. GRAY H Anatomy - Descriptive and Applied. Longmans, Green & Co. 1916

27. GREEN H.D., RAPELA C.E. Blood flow in Passive Vascular Beds. Circulation Res. Suppl 1; 11-16

28. GREENFIELD A.D.M. The Circulation through the skin. American Physiological Society. Handbook of Physiology sec 2, vol 2, 1963.

29. GREENFIELD A.D.M., WHITNEY R.J., MOWBRAY J.F., Methods for the investigation of peripheral blood flow. Br. Med Bull. 19; 101-109, 1963.

30. GREENFIELD A.D.M., SHEPHERD J.T., WHELAN R.F. The proportion of the total hand blood flow passing through the digit. J. Physiol. 113; 63-72, 1951

31. GREENFIELD A.D.M., SHEPHERD J.T., WHELAN R.F. Cold Vasoconstriction and Vasodilation. Irish Journal of Medical Science 309; 415 1951

32. GRODINS F.S., BUELL J., BART A.J. Mathematical Analysis and digital simulation of the respiratory control system. J. Appl. Physiol. 22; 260-276, 1967

33. GUYTON A.C., ROSS J.M., CARRIER O., WALKER J. Evidence for tissue oxygen demand as a major factor causing autoregulation. Circul. Res. Suppl. 1; 60-68, 1964

34. HALE R.A., BURCH G.E. The arteriovenous anastomosis and blood vessels of the human finger. Medicine, 39; 191-240, 1960.

35. HAMILTON W.J. (edit) Textbook of Human Anatomy. London, Macmillian & Co., 1956

36. HATZE H. Optimal Processes of Neuro-Musculoskeletal Control System. Symposium on Mathematical Modelling in Biology and Ecology. CSIR, Pretoria, July 1979.

37. HEISTAD D.D., ABBOUD F.M. Factors that influence blood flow in skeletal muscle and skin. Anesthesiology. 41; 139-156, 1974.

38. HERTZMAN A.B., RANDALL W.C., JOCHIM K.E. The estimation of the cutaneous blood flow with the photoelectric plethysmograph. Am. J Physiol 145, 716-726, 1946.

39. HOCHERMAN S. AND PACTI Y. Correlation between blood volume and opacity changes in the finger. J. Appl. Physiol. 23(..); 157-162 1967.

40. HSIEH A.C.L., NAGASAKA T., CARLSON L.D. Effects of immersion of the hand in cold water on digital blood flow. J. Appl. Physiol. 20; 61-64, 1965

41. JACQUEZ J.A., KUPPENHEIM H.F., DIMITROFF J.M., McKEEHAM W., HUSS J. Spectral Reflectance of Human Skin in the Region. 235-700nm. J. Appl. Physiol. 212-214, 1955

42. JARRET A., (ed) The Physiology and Pathophysiology of the Skin. Academic Press Vol. 2 1973.

43. JOHNSON P.C., (ed) Peripheral Circulation. John Wiley & Sons 1978.

44. JOHNSON P.C. Review of Previous Studies and Current Theories of Autoregulation. Circulation Res. 14 Suppl 1,2, 1964

45. KELMAN G.R. Applied Cardiovascular Physiology. Butterworth & Co. 1971.

46. KORNER K.J. Control of blood to special vascular areas, brain, kidney, muscle, skin, liver and intestine. In Guyton A.C., Jones C.E. (eds). Cardiovascular Physiology. Physiology series Vol 1 Butterworth, London, 1974

47 KRAMER K., LOCHNER W., WETTNER E. Methods of measuring blood flow. In American Physiological Society Handbook of Physiology Sec. 2 Vol. 2 Circulation; 1277- 1324, 1963.

48. LEWIS T. Observations upon the reactions of the human skin to cold. Heart 15; 177, 1930

49. LEWIS T. The Blood vessels of the Human Skin and their responses. Shaw and Son, London 1927.

50. MELLANDER S., JOHANSSON B. Control of Resistance, exchange and capacitance functions in the peripheral circulation. Pharmocol. Reviews 20; 117, 1968

51. MELLANDER S., OBERG B., ODELRAM H. Vascular adjustments to increased transmural pressure in cat and man with special reference to shifts in capillary fluid transfer. Acta Physiol. Scand. 61; 34-48, 1964

52. MERRIL P.S., ADAM B.D. Jnr. Pulsatile Blood flow in the vascular system. In American Physiological Society Handbook of Physiology, section 2, Vol 2 Circulation 839-864, 1963

53. MULINOS M.G., SHULMAN I. Vasoconstriction in the hand from a deep inspiration. J. of Physiol. 125; 310, 1939.

54. NUNN J.F. Applied Respiratory Physiology. Butterworths 1969.

55. PERERA P., KURBAN A.K., RYAN T.J. The development of the Cutaneous System in the newborn. Br J. Derm 82, Suppl. 5; 86, 1970

56. PETERSON L.H., JENSON R.E., PARNELL J. The mechancial properties of arteries in vivo. Circulation Res. 8(3); 622-639, 1960

57. PETERSON L.H. Regulation of Blood Vessels. Circulation 21 (1); 749-759, 1960

58. PICKERING G.W. The vasomotor regulation of heat loss from human skin in relation to external temperature. Heart 16: 115, 1933.

59. RODDIE I.C., SHEPHERD J.T., WHELAW R.F. The vasomotor nerve supply to the skin and muscle of human forearm. Clinical Science 16; 67-74 1957.

60. ROMANES C.J., (ed), Cunnighams Textbook of Anatomy. Oxford Univ. Press (10th edition) 1966.

61. ROUGHTON F.J.W. Transport of oxygen and carbon dioxide. In American Physiological Society; Handbook of Physiology. Sec 3, Vol 1, Respiration; 767-825, 1963

62. SHEPHERD J.T. Physiology of Circulation in human limbs in health and disease. W.B. Saunders Co. 1963

63. SHERMAN J.L. Normal Arteriovenous Anastomosis. Medicine 42; 247-267, 1963

64. SILVER I.A. Oxygen tension & Epitheliazation. In: Maibach H.I., Rovee D.T. (eds) Epidermal Wound Healing, Chicago Year Book, 291-305, 1972

65. TRUEB T.J., CHERMACK N.S., DSOUZA A.F., FISHMAN A.P. A Mathematical Model of the controlled plant of the respiratory System. Biophys. J. 11: 810-834, 1971.

66. UNNAS B. Sympathetic Vasodilastor system and blood flow. Physiol. Reviews 40 Supp 4; 69, 1960

67. VANDER A.J., SHERMAN J.H., LUCIANO D.S. Human Physiology. Second Edition. McGraw-Hill, 1970

68. WEINMAN J., MANOACH M. A Photoelectric Approach to the study of peripheral circulation. American Heart Journal 63; 219-231, 1962.

69. WHILLIS JAMES Elementary Anatomy and Physiology. J & A Churchill Ltd London 1938

70. ZELIS ROBERT (edit) The Peripheral Circulations. Grune & Stratton 1975.

71. ANDERSON N.M. & SEKELJ P. Light absorbing and scattering properties of non-haemolysed blood. Phys. Med. Biol., 12; 173-184, 1967.

72. ANDERSON N.M., SEKELJ P. Studies on the light transmission of nonhaemolysed whole blood. Determination of oxygen saturation. J. Lab & Clin. Med; 153, Jan 1965.

73. ANDERSON N.M., SEKELJ P. Reflection and Transmission of Light by thin Films of Nonhaemolysed Blood. Phys. Med. Biol. 12; 185-192 1967.

74. BARBENEL J.C., TURNBULL F.W., NISBET R.M. Backscattering of light by red cell suspensions. Med & Biol. Eng & Compot. 17; 76? 68, 1979

75. COHEN A., LONGINI R.L. Theoretical determination of the blood's relative oxygen saturation in Vivo. Med & Biol Engng.; 61-69 1971.

76. EASON G., VEITCH A.R., NISBET R.M., TURNBULL F.W. The theory of the back-scattering of light by blood. J. Phys. D: Appl. Phys, 11; 1463, 1978

77. ELAM W.N., WHITE H.L. Photo-electric measurements of the arterial oxygen saturation dyramics in man for study of cardio-pulmonary function. Federation Proc. 8; 40, 1949

78. ENSON Y., BRISCOE W.A., POLANYI M.L., COURNAND A. In vivo studies with an intrasvascular and intracardiac reflection oximeter. J. Appl. Physiol. 17; 552-558, 1962

79. FRETTERD R.J., LONGINI R.L. Diffusion Dipole Source. J. Optical Soc. Amer., 63; 336-337. 1973

80. GORDY E., DRABKIN D.L. Determination of the oxygen saturation of blood by a simplified technique applicable to standard equipment. J. Biol. Chem., 227; 285-299, 1957

81. GRAUPE D. Identification of Systems. Van Nostrand Reinhold Company, 1972

82. HIRKO R.J., FRETTERD R.J., LONGINI R.L. Application of the diffusion dipole to modelling the optical characteristics of blood. Med & Biol Eng., 192-195, March 1975.

83. JANSSEN F.J. A Study of the Absorption and Scattering factors of light in whole blood. Med & Biol. Eng. 10; 231-240, 1972

84. JANSSEN F.J. The Principle design and features of a new Hb-Oximeter Med. & Biol. Engng. 10; 9-22, 1972.

85. JOHNSON C.C. Optical Diffusion in Blood. IEEE Trans Bio Med. Engng. 17; 129-133, 1970

86. KRAMER K., ELAM J.D., SAXTON G.A., ELAM W.N. Influence of oxygen saturation, erythrocyte concentration and optical depth upon the Red and Near-Infrared Light Transmittance of whole blood. Am. J. Physiol. 165; 229-246, 1951

87. LIEBERSTEIN H.M. Mathematical Physiology. Blood flow and electrically active cells. American Elsevier Publishing Co. 1973

88. LOEWINGER E., GORDON A., WEINREB A., GROSS J. Analysis of a micromethod for transmission oximetry of whole blood. J. Appl. Physiol. 19; 1179-1184, 1964

89. LONGHURST R.S. Geometric and Physical Optics. Longmans 1957

90. LONGINI R.L., ZDROJKOWSKI R. A note on the theory of Back-scattering of Light by Living Tissue. IEEE Trans on Bio-Med Engng. 15; 4-10 1968

91. LUBBERS P.W., WODICK R. Absolute reflection photometry applied to the measurement of capillary oxyhaemoglobin saturation of the skin in man. In Payne J.P. and Hill D.W. Oxygen measurements in Biology and Medicine, Butterworths, 1975.

92. LUBBERS P.W. Spectrophotometric examination of tissue oxygenation. In Oxygen transport to tissue vol. 2. Bicher H.J., Bruley D.F. (eds) Plenum Press, 1973

93. MEDGYESI S. Photoelectric Oxillometry. Scand. J. Plast Reconstr. Surg. 7; 29-34, 1973

94. NILSSON G.E., TENLAND T, OBERG P.A. A new instrument for continuous measurement of tissue blood flow by light beating spectroscopy. IEEE BME-17, 1; 12-19 1980.

95 RODRIGO F.A. The determination of the oxygenation of Blood in Vitro using reflected light. Am. Heart J., 45; 809-822, 1953.

96. SLEATOR W., ELAM J.O., KILIAN D.J., ELAM W.N. Comparison transmission spectra of blood in the human ear flushed by histamine with those obtained after heat flushing. Feder. Proc 8; 147, 1949

97. TAIT G.R., SEKELJ P. An Analog Computer for ear oximetry. Med & Biol. Engng, 5; 463-472, 1967

98. TAKATANI & GRAHAM Theoretical Analysis of Diffuse Reflectance from a 2-Layer Tissue Model. IEEE BME-26, 12; 656-664, 1979.

99. TURNER G & WIGDOROWITZ B. Skin Reflectance oximeter. Electrical Engineering Laboratory report 78/12A. Univ of Witwatersrand 1978.

100. ZDROJKOWSKI R.J., PISHAROTY N.R. Optical Transmission and Reflection by Blood. IEEE Trans Biol Med Eng. Vol BME 17(2); 122-128 1970

101. COMPUTER PRODUCTS Technical Manual RTP 7410/59 I/O. Bus Converter for MicroNova series computers, November 1978

102. COMPUTER PRODUCTS Technical Manual RTP 7435 Series A/D converter cards. Seventh Edition, April 1978

103. COMPUTER PRODUCTS Technical Manual RTP 7430 Series Universal input/output controllers. Twelfth edition, March 1979

104. OPTRON INC., Complete Optoelectronics for Industry (catalogue)

105. TEXAS INSTRUMENTS. The Optoelectronics Data Book For Design Engineers. Second edition. 1975

106. WELCH P.D. The use of the Fast Fourier Transform for the estimation of Power Spectrum. A method based on time averaging over modified Periodograms. IEEE Trans. on Audio Electroacoustic AU-15 70-73, 1967.

APPENDIX 1 BLOOD VESSELS OF THE HAND

The Brachial artery divides into the radial and ulnar arteries near the elbow joint. (see figures 2.1-2.3). These arteries run on either side of the forearm towards the wrist. The radial artery gives rise to:

(1) Princeps Pollicis artery which supplies the palmer (i.e. palm side of the hand) side of the thumb.

(2) Radialis indicis artery which runs down the palmer side of the index finger nearest the thumb.

(3) First dorsal metacarpal artery which proceeds along the posterior of the hand (i.e. opposite side to the palm) and has branches supplying the thumb and index finger.

Roughly speaking, the radial and ulnar arteries are connected via three arches which lie in the middle of the palm in a line with the end of the thumb.

The superficial palmer arch extends closest to the fingers. It gives rise to three common palmer digital arteries which form a network to supply all the fingers. The deep palmer arch gives rise to three palmer metacarpal arteries which anastomose with the palmer digital arteries in the clefts at the roots of the fingers.

The third arch is nearest to the wrist It is found on the posterior side of the hand. It is usually termed the dorsal carpal r'te and provides the second, third and fourth metacarpal

arteries, which supply the fingers on the posterior side in a similar manner as the palmer arteries. There is communication between the metacarpal and palmer arteries in more than one place. The above, short account demonstrates that the radial and ulnar arteries form a relatively complicated interconnected mesh of blood vessels in the hand. It should be remembered that these arteries then form many "rete cutaneum" in the corium. (see appendix 2). These in turn give rise to subpapillary plexus which branch to form numerous papllary loops and arteriovenous shunts. Thus the blood vessels of the hand form a complex, integrated vascular grid covering the hand and fingers.

arteries, which supply the fingers on the posterior side in a similar manner as the palmer arteries. There is communication between the metacarpal and palmer arteries in more than one place. The above, short account demonstrates that the radial and ulnar arteries form a relatively complicated interconnected mesh of blood vessels in the hand. It should be remembered that these arteries then form many "rete cutaneum" in the corium. (see appendix 2). These in turn give rise to subpapillary plexus which branch to form numerous papllary loops and arteriovenous shunts. Thus the blood vessels of the hand form a complex, integrated vascular grid covering the hand and fingers.

APPENDIX 2 VASCULATURE OF THE FINGER

Hale and Burch [34] have investigated the details of the morphological (structural) and functional aspects of the cutaneous blood supply with special reference to the supply in the finger.

The digital arteries divide into a periosteal and terminal branch (see figure 2.5). Throughout their courses, the periosteal and terminal branches communicate with each other via arcuate anastomotic arteries (AVA) of medium size. The terminal branch gives rise to smaller arteries (perforating arteries) which continue perpendicularly to the skin surface. As the perforating artery enters the lower dermis, it branches into terminal arteries, which continue perpendicularly towards the skin surface, and anastomotic dermal branches which run parallel to the skin surface to form an arterial arcade with similar branches from adjacent arteries.

As the terminal arteries rise, their smooth muscle coats become thinner. Those branches near to sweat glands and hair follicles supply these structures. They terminate just under the epidermis in a subpapillary capillary plexus. The individual papillary loops rise perpendicularly out of the plexus into the papillae ridges in the bottom layer of the epidermis (see figure A2.1). These capillaries are very thin (15μm [62] in diameter), shaped like hairpins and are linearly spaced along the undersurface of the epidermis. The passage of red blood cells through these vessels cannot be termed a "flow".

As the capillaries turn they drain into a venous plexus which intermingles with the subpapillary capillary plexus. Venules descend from this plexus in a candelabra fashion into an intermediate venous plexus. Venous drainage from hair follicles

and sweat glands also enter this plexus. Finally, vessels descend into a third, deep plexus, located in the deep dermis. Valves appear in these veins. The vessels connecting the deep and intermediate plexi often contain a sphincter of smooth muscle which may help to regulate the circulation and transfer of waste and solutes. The volume of the superficial, intermediate and deep plexi is about fifteen times that of the arterial supply. The proximity of the arteries and veins in the various plexi promotes the possibility for heat exchange between arterial and venous blood.

There are numerous arteriovenous anastomoses connecting the various arterial and venous plexi. These vessels are 20-40μm in diameter, with thick muscular walls richly supplied with nerve fibres. The function of the most simple anastomoses is simply to shunt blood from the arterial to venous circulations so as to be able to control the volume and rate of flow of the cutaneous blood. The more complex structures resemble organs. The functions of these (glomus organs) is not clear. Hale and Burch [34] believe that the digital glomus organs may serve a neurovascular function similar to the carotid bodies.

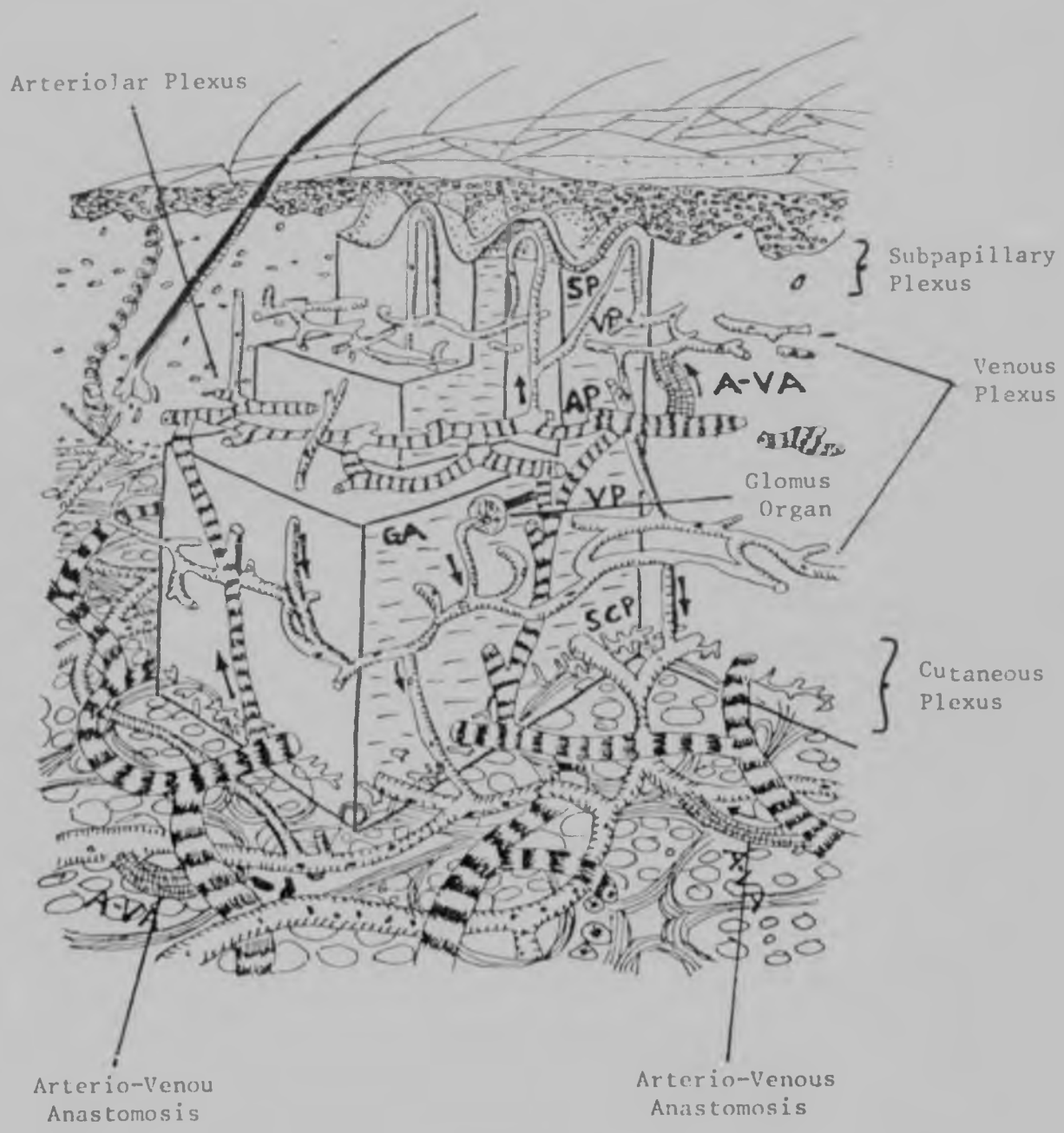


Figure A2.1 Blood Vessels of the Skin (Schematic)
(Hand copied from [43], section 7, page 194, fig 1)

APPENDIX 3 ABSORPTION AND SCATTERING FACTORS

The diffusion equation and Kubelka-Munk theory for reflectance and transmission require absorption and scattering factors for tissue and blood. These values have been indirectly measured by a number of workers. A collection of results is presented in this appendix. As can be seen, these factors are difficult to measure accurately, because the values also depend on the type of instrumentation used [80] (i.e. on the bandwidth of the light source, the type of receptor, etc.) The values show a large scatter. Only the absorption factors for blood may be treated with confidence, as these have generally been measured carefully.

A.3.1 ABSORPTION FACTOR

A.3.1.1 Tissue

The absorption of tissue is small and can usually be neglected [90]. Cohen [75] and Takatani et al [98] present a value of 0,3 per cm for the absorption of gut tissue. It is questionable as to whether the optical properties of skin are similar to those of gut tissue. The experimental results of chapter 5 and the tranducer models of chapter 3 suggest that the absorption of skin is not negligible.

APPENDIX 3 ABSORPTION AND SCATTERING FACTORS

The diffusion equation and Kubelka-Munk theory for reflectance and transmission require absorption and scattering factors for tissue and blood. These values have been indirectly measured by a number of workers. A collection of results is presented in this appendix. As can be seen, these factors are difficult to measure accurately, because the values also depend on the type of instrumentation used [80] (i.e. on the bandwidth of the light source, the type of receptor, etc.) The values show a large scatter. Only the absorption factors for blood may be treated with confidence, as these have generally been measured carefully.

A.3.1 ABSORPTION FACTOR

A.3.1.1 Tissue

The absorption of tissue is small and can usually be neglected [90]. Cohen [75] and Takatani et al [98] present a value of 0,3 per cm for the absorption of gut tissue. It is questionable as to whether the optical properties of skin are similar to those of gut tissue. The experimental results of chapter 5 and the tranducer models of chapter 3 suggest that the absorption of skin is not negligible.

A.3.1.2 Blood

As was discussed in chapter 3, the absorption of light by blood depends on the oxygen saturation of the blood and the wavelength of light used. The coefficients are thus presented for oxygenated and reduced haemoglobin as a function of wavelength. The absorption factor of a blood sample with average blood saturation S is then calculated from:

$$a = S(ao) + (1-S)\,ar$$

where ao - absorption of oxygenated haemoglobin

ar - absorption of reduced haemoglobin

The factors ao and ar are calculated from the extinction coefficient for haemolysed blood. Table A3.1 presents a collection of normalised absorption coefficients. (i.e. for a haemoglobin concentration of 1g/100ml). Thus the absorption of a blood sample with a haemoglobin concentration C g/100ml will be given by

$$(a \times C)$$

Zdrojkowski and Pisharoty have calculated absorption factors from extinction coefficients that were measured using collimated light. In their calculations, they appear to neglect the difference between diffuse and collimated absorption coefficients (section 3.3.1). In addition they introduce, for some unknown reason, a factor of 1,5 into their calculations. Therefore the values given by Zdrojkowski and Pisharoty, are 0,75 times the values predicted by Janssen [83]. The other sources do not specify exactly how their values were arrived at.

λ (nm)	Cohen [75] (cm^{-1})		Zdroj [100] (cm^{-1})		Hirko [82] (cm^{-1})		Takat. [98] (cm^{-1})	
	ao	ar	ao	ar	ao	ar	ao	ar
600	-	-	2,24	7,21	-	-	1,52	2,7
620	0,38	1,10	-	-	0,57	1,83	-	-
625	-	-	0,48	2,58	-	-	0,34	2,09
650	-	-	0,25	1,84	0,23	1,83	-	-
655	-	-	-	-	-	-	0,16	1,54
660	-	-	0,21	1,73	0,21	1,69	-	-
665	-	-	-	-	-	-	0,16	1,49
805	0,38	0,38	0,41	0,41	0,42	0,42	0,42	0,43
850	-	-	0,49	0,35	0,50	0,33	0,51	0,39
900	-	-	0,54	0,36	0,54	0,35	0,56	0,42
935	-	-	-	-	-	-	0,57	0,40
945	-	-	-	-	-	-	0,57	0,36

Table A3.1 Normalised Absorption Coefficients of Blood

A.3.2 SCATTERING FACTOR

A.3.2.1 Tissue

Values are difficult to obtain. Cohen and Longini give values of 30-55 cm^{-1} for white skin and 60-70 cm^{-1} for dark skin. On the other hand, Takatani and Graham give the normal physiological range as 10-15 cm^{-1} for tissue. Their measurements were performed on gut tissue, washed with saline. There is no indication as to how this will change for different types of tissue. The present author proposes that there is a substantial variation of scattering coefficients between the different types of tissue. In addition, most authors neglect possible variations with wavelength (see section 3.3.1).

A.3.2.2 Blood

The scattering by blood depends on the haematocrit. Several formualae have been presented for the scattering factor such as (in cm^{-1})

(i) 64 H (1-H) Cohen and Longini [75]

Takatani and Graham [98]

(ii) 25 H (1-H) Zdrojkowski and Pisharoty [100]

(iii) H(1-H)(54,1 - 38,97H) Hirko et al [82]

(iv) $43,1H^3 - 99,7H^2 + 56,1H - 0,15$ Barbenel et al [74]

Table A3.2 compares the values obtained via the above formula for a haemotocrit of 0,45

Cohen cm^{-1}	Zdroj cm^{-1}	Hirko cm^{-1}	Takatani cm^{-1}	Barbenel cm^{-1}
15,84	6,19	9,05	15,8	8,83

Table A3.2 Comparison of P[illegible] Scattering Scattering Factors.

A.3.3 CONCLUSION

It therefore appears that there exist substantial differences in the literature concerning the optical parameters of tissue and blood. Previous work was mainly aimed at obtaining solutions to the relatively complex model equations. To the authors knowledge, no study has been undertaken to systematically investigate these parameters.

APPENDIX 4 DETAILED DESCRIPTION OF DATA HANDLING ROUTINES

A.4.1 Introduction

The data handling problem is to convert the analog oximeter outputs to digital representation, which would then be available as input to data processing routines (such as graph plotting, model fitting, etc). All data records are time records and hence sample values must be ordered with respect to time. Furthermore the number of channels to be recorded during an experiment varies between 2-4. At the sampling instant, all channels are sequentially sampled and stored in adjacent locations. At processing time each channel is to be individually treated, and hence the adjacent storage pattern has to be decoded. The complete data handling process is outlined in figure A4.1

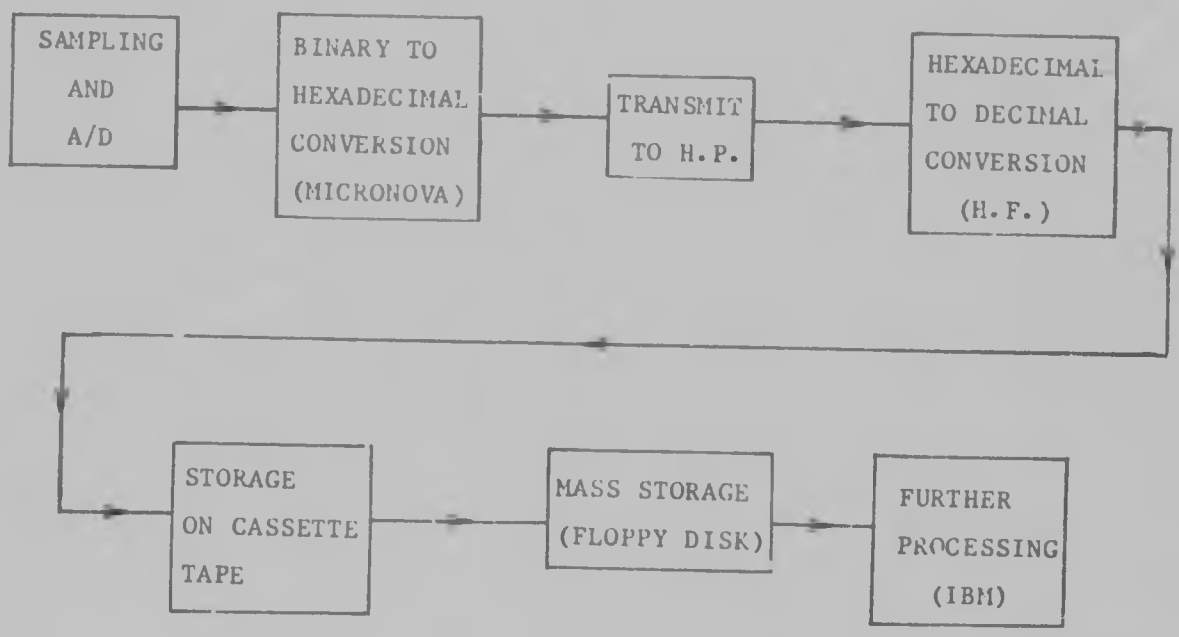


Figure A.4.1 The Data Handling Process

As described in section 4.4, the data gathering system consists of two computers, viz., the microNova and intelligent Hewlett Packard 26047A graphics terminal, which can be loaded with BASIC interpreter. The microNova is used to control the A/D process, while the H.P is used as a task manager. The third section of the overall data handling, is the processing performed by the IBM 370/158. Program listings are given in appendix 8.

A.4.2 MicroNova Routine

As was mentioned in section 4.4, the microNova is not geared for program development. The monitor can only examine and modify the registers and memory locations. Consequently all routines had to be assembled on the department's Nova 3 minicomputer into an absolute binary file. This file was then recorded on cassette tape and downloaded via the BASIC program (see section A4.3).

The program that runs in the MicroNova computer consists of two sections:

(i) Sampling.

(ii) Conversion of binary to hexadecimal ASCII characters and transmission to the H.P. terminal.

The sampling routine uses the internal real time clock (RTC) to time out the sampling intervals. Once the clock has been enabled,

it causes an interupt every 2,4 msec. This, therefore, sets an upper bound to the sampling rate and also demands that the sampling rate be an integral multiple of 2,4 msec. A flow chart of the sampling procedure is given in figure A4.2

Three counters are used. These store:

(i) The starting address in memory where sample values are to be stored.

(ii) The total number of samples to be taken.

(iii) The number of RTC interupts between sampling intervals.

These values are entered via the BASIC program (section A4.3)

The binary to hexadecimal and transmission section converts the binary word corresponding to each sample value to three hexadecimal ASCII characters (the resolution of the A/D converter is 12 bits) and transmits the characters to the H.P. terminal. It should be noted that as the A/D card only accepts positive voltages, the sign bit can be ignored. An ASCII "H" is transmitted before each sample value (This signifies to the BASIC hexadecimal to decimal converter that the data value is in fact hexadecimal). The format of the data records is 18 sample values per data record. Thus after every 72 characters a carriage return (CR), line feed (LF) is transmitted. The actual conversion of binary to hexadecimal involves, masking and shifting the data values so as to make all except the 4 least significant bits, zero. These 4 bits are then recognised as a hexadecimal digit, and the equivalent ASCII representation is transmitted. A simplified flow chart is given in figure A4.3 The H.P. buffer is cleared before transmission begins. The 'EDIT' mode is enabled as this allows the the buffer to overflow onto the cartridge tapes.

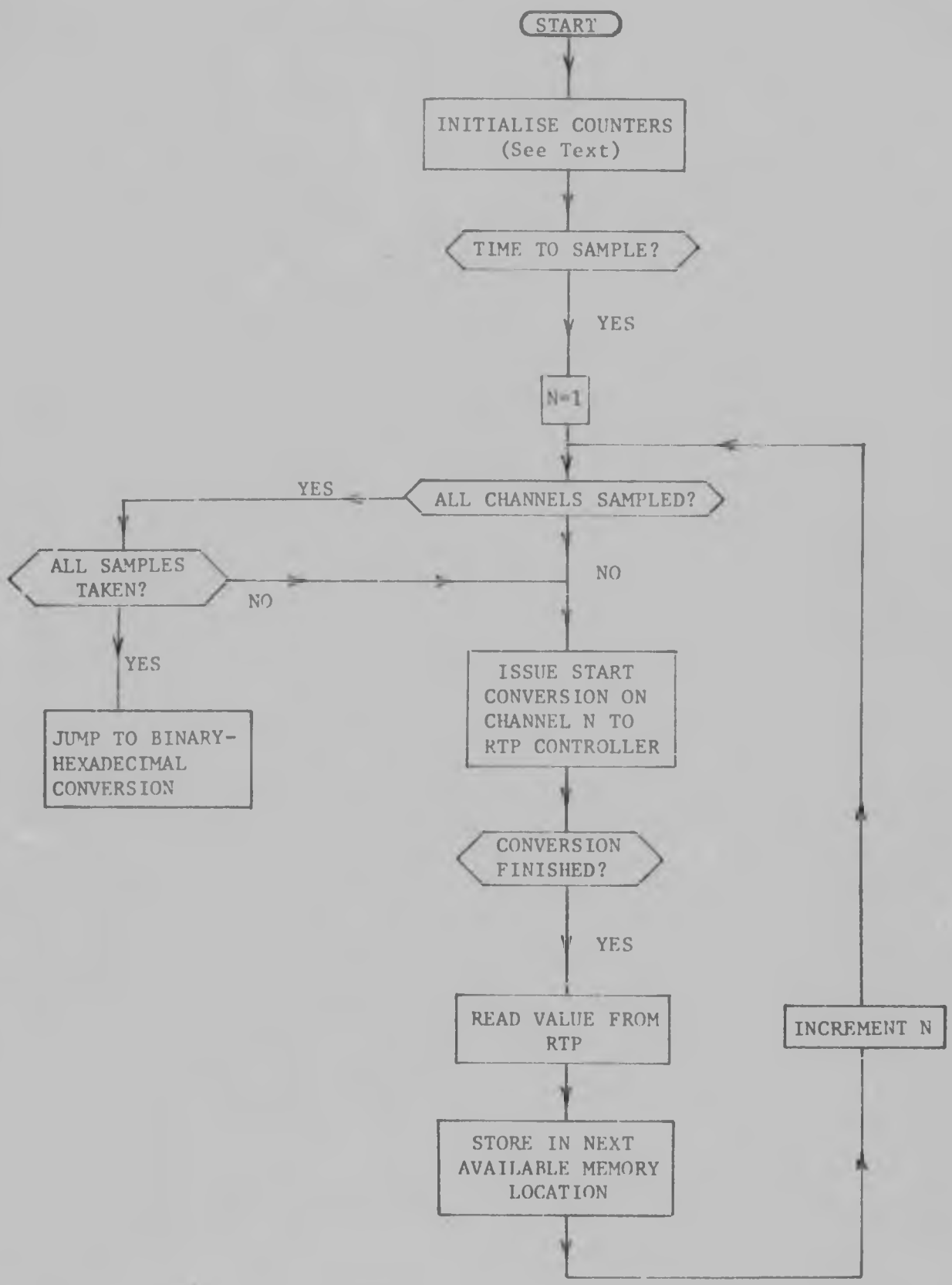


Figure A4.2 The Sampling Process.

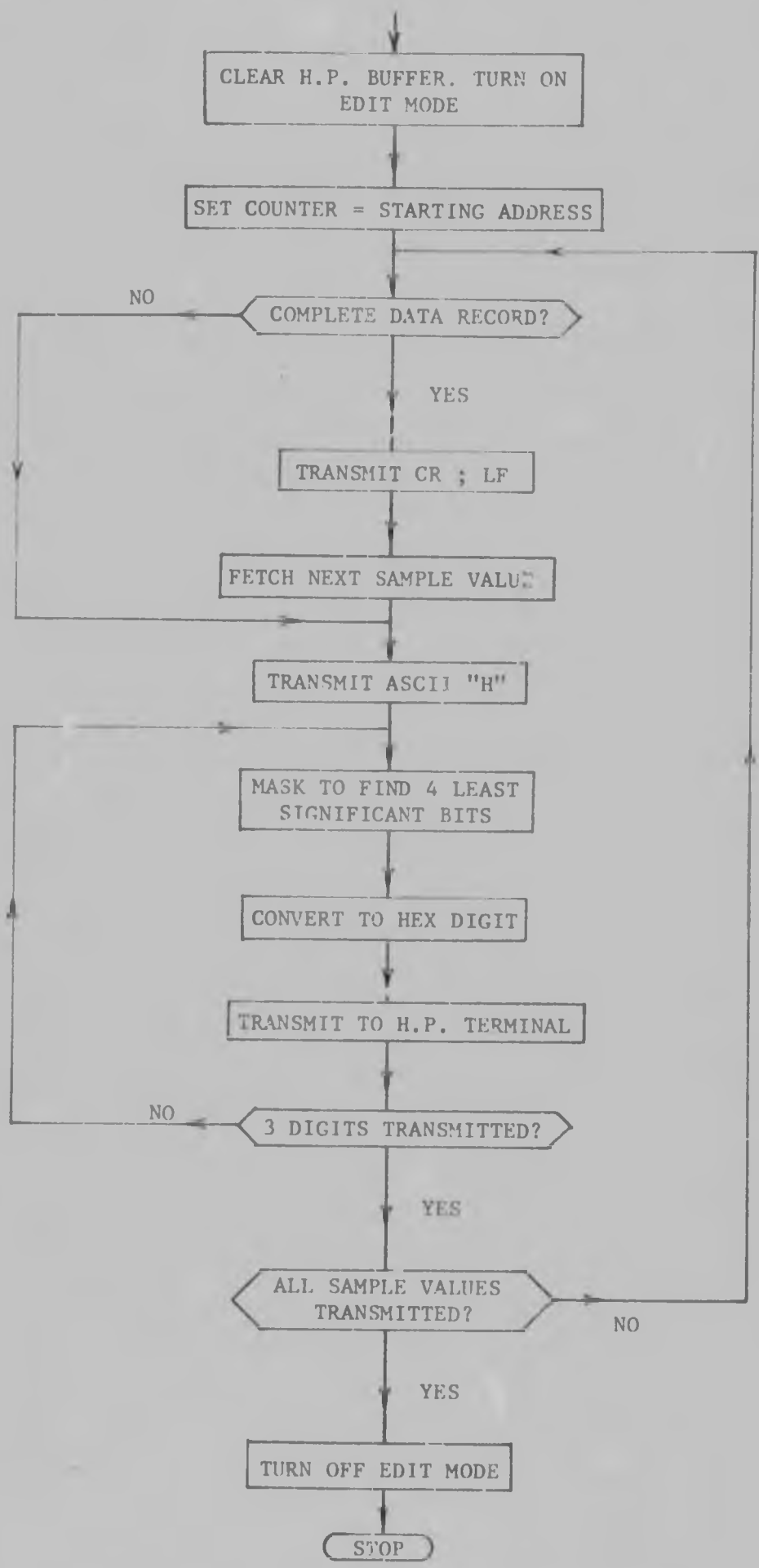


Figure A4.3 Conversion and Transmission

A.4.3 The Task Manager and Utilities

The H.P. 2647 graphics terminal is an intelligent terminal with two cartridge tape drives and can be loaded with a BASIC interpreter.

A BASIC program was written which manages the whole data capture facility. Five basic commands are accepted by the executive. The format of the commands is

XXXXn

where XXXX is a 4 letter command

and n is a digit which is required by three of the commands and specifies a file number on the right tape drive.

The commands recognised are:

LOADn
SAMP
AVERn
PLOTn
GRAP

Each command is briefly discussed in the following subsections

A.4.3.1 LOADn

This command initiates the downloading of an absolute binary file obtained from the NOVA 3 assembler. The file to be loaded is file n on the right cassette drive. The listing from the assembler basically consists of two columns, the first column contains the location, and the second column, the contents. The program loads each address via the microNova monitor. As each memory address is loaded, ics contents are displayed on the screen.

A.4.3.2 SAMP

This command initiates a sampling session. Self evident questions allow relevant parameters to be passed to the microNova.

The parameters passed are:

(i) The total number of samples to be taken.

(ii) The number of channels to be sampled.

(iii) Number of RTC interupts between samples.

After all the data has been entered, the actual sampling is initiated by striking key "S". The example session in appendix 5 illustrates the above.

Once the microNova has transmitted all the data values to the H.F. terminal, the user again strikes key 'S', so as to record all the sample values on the right drive. A header record consisting of the following is included:

(i) Number of samples in file.

(ii) Duration of the experiment in seconds.

The last record in the file consists of a description of the data (typed in by the user at the appropriate point).

A.4.3.3 AVERn

This command initiates elementary processing of the raw data following a sampling session. The raw data is to be found in file n on the right drive. The processing consists of two stages.

Firstly, the DC value (average value) of each data channel is computed. In the second stage, the second data channel is plotted according to the selected function (see below) on the normalised scale (-1;1). At the same time all the data values are converted from hexadecimal to decimal and stored on the left drive. This facility is optional. Self evident questions control the plotting and storage of the data (see example session in appendix 5). For further details concerning the control of the plotting function, see command PLOT.

When the data values are converted and copied onto the left drive, they are also stored as 18 data values per record. In this case each data value is a 4 digit (decimal) integer. Again the data from all the channels are stored next to each other. A typical data record for the case of 4 data channels is shown in figure A.4.4

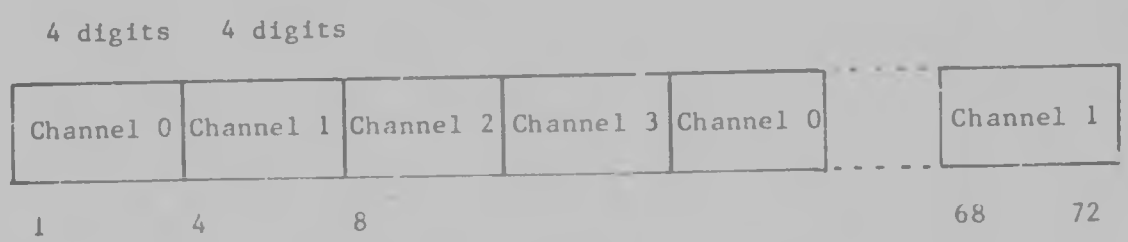


Figure A.4.4 Data Record Format

The header and tail records are also copied, however the header record is extended to include the average values of all the data channels.

A.4.3.4 PLOTr

This command intiates the second stage of AVER. Self evident questions control the plotting. It should be noted that the user may select the data channel to be plotted. The numbering scheme numbers the channels sequentially, starting from zero. A scale factor is requested. The normalised data values are first multiplied by the scale factor before plotted. This is simply a technique for providing extra gain. In response to the prompt "FUNCTION TO BE PERFORMED ?", the user may respond with one of the following:

(i) AVER
(ii) MARK
(iii) DIVS

AVER - selects that the AC component should be plotted.

MARK - implies that the selected channel is an event marker, i.e. either 0 volts or +5 volts is applied via a switch. The initial

state is assumed to be 0 volt, subsequent events are designated by switching the switch. As the routine encounters a switch change, it draws a vertical line on the plot at the appropriate time position.

DIVS - selects that the AC component of the ratio:

$$\frac{\text{CHANNEL 1}}{\text{CHANNEL 2}}$$

is to be plotted.

A.4.3.5 GRAP

This command is not strictly associated with the data capture facility. Its purpose is to allow graphs to be simply plotted. Two options are available in response to the question "FUNCTION TO BE PERFORMED".

FUNC - implies that the graph is available in functional form in subroutine FUNCT (program statements numbers 4080 - 4140)

DATA - implies that the graph is to be plotted from a set of X,Y data points stored on the right cartridge tape.

A.4.4 IBM Routines

The decimal data files obtained via the BASIC routines described above, were used as input for further processing by the University's central IBM 370/158 computer system. This processing consists of fast fourier transforms, least squares model fitting and plotting routines. These programs are not relevant to the data handling section and are therefore not discussed. However, one utility program which divided the data file according to the

channel number will be described.

The sample values from the different channels in the data files obtained from the data acquisition system are intermingled one with another. The aim of the utility program is to separate the channels. The program is written in FORTRAN IV and can run in the WITS system. (The WITS system is an interactive terminal system available on the central computer). The program will either prepare the data for plotting on the Hewlett-Packard 7221A flatbed, graphics plotter or for further processing. In the latter case, the data values for the chosen channel appears in the output workspace. The channel number and option are inputted via self evident questions. It should be noted that the channel numbering scheme assumes that the first channel is designated number one.

The options are chosen in response to the question:

COMMAND, CHANNEL NO., SCALE FACTOR?

The user replies with

XXXX N M

where:

XXXX is a four letter command
N is the channel number to be processed
M is the scale factor

Available commands are:

(i) PLOT
(ii) DIVS
(iii) MARK
(iv) CHOS
(v) PICK

The raw data is normalised to the range (0;1) and then multiplied by scale factor M.

The action of the commands are described in the following subsections

A.4.4.1 PLOT

This command prepares the data so as to enable the AC component to be plotted (scaled by the value of the scale factor).

A.4.4.2 DIVS

DIVS prepares the AC component of the ratio of the first channel to the second channel for plotting. The scale factor is applied to the ratio.

A.4.4.3 MARK

This command initiates the same action as the option MARK described in section A4.3.4. Scale factor M is obviously irrelevant (although a value must be entered).

A.4.4.4 CHOS

CHOS is the option which selects the channel data and writes it to the output workspace. The data is written via a FORTRAN WRITE statement, using format E13.7

A.4.4.5 PICK

PICK will select the data values from the first two channels, but, only those data values that lie between the first two event markers. Each record written consists of three values ie. the time elapsed at which the following two normalised data channel values were recorded. In this case, channel number N designates the channel number which was used to mark events. Scale factor M is irrelevant.

Hardcopy plots are obtained via execution of a modified version of a general plotting utility. The format of the data prepared by the above commands is directly compatible with this utility.

Finally, it should be noted for every command processed, the program reads the whole raw data file. As the WITS system does not allow rewinding of data files, the user is required to insert the raw data file the same number of times as there are commands (This is conveniently arranged using the /INC statement.)

APPENDIX 5 SAMPLE SESSION

This appendix illustrates a typical experimental session. The example shows a "cold start", assuming that the BASIC program has already been loaded. Firstly, a sampling session is initiated. One thousand sample values from three channels are collected and stored in file 1 on the right drive. Thereafter the raw (Hexadecimal) data is processed according to the command AVER.

```
>RUN
GIVE ADDRESS OF ONE UNUSED PAGE ZERO MEMORY LOCATION ? 4
10A 115633 4
COMMAND ? SAMP
TYPE IN THE NUMBER OF SAMPLES REQUIRED
? 1000
TYPE IN THE SAMPLING INTERVAL
NUMBER OF HOURS?0
NUMBER OF MINUTES?5
NUMBER OF SECONDS?0
TYPE IN THE NUMBER OF CHANNELS BEING USED
? 3
WHAT FILE NUMBER DO YOU WANT TO USE ON THE RIGHT DRIVE?
? 1
40/000040 177777
1750!41/000041 177777
247!43/000043 177777
3!
**START THE SAMPLING BY PUTTING TERMINAL INTO REMOTE**
              **AND HITTING KEY 'S'**
60R

    TYPE IN A HEADING FOR THE PAST EXPERIMENT
? EXAMPLE SESSION
```

The data collected above is now processed according to the command AVER

```
COMMAND ? AVER1
SHOULD THE GRAPHICS BE CLEARED?Y
SCALE FACTOR?5
COPY DATA TO LEFT TAPE?Y
FILE NO. ?1
```

APPENDIX 6 LED DATA

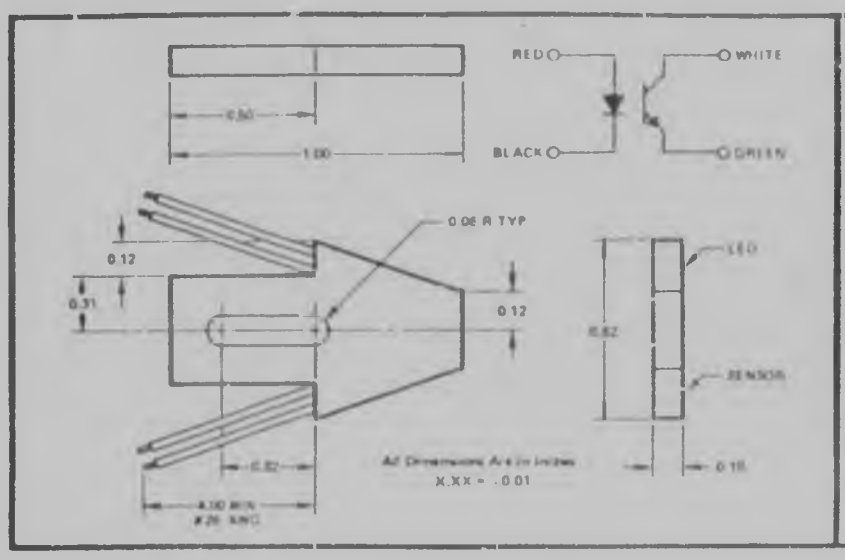
The data sheets presented in this appendix cover the light sources and detectors used in the transducers (section 4.3.3). The OPB 253A data are reproduced from [104], while the rest of the data is from [105].

OPTRON INC.
1201 Tappan Circle • Carrollton Texas 75006 • USA
Telephone • 214/242-6571
Telex • 73-0701 TWX • 910-860-5958

Type OPB 253 A
Reflective Object Sensor

Bulletin No. 1054 April, 1976

Physical Description





SHOWN ACTUAL SIZE

General Description

The OPB253 consists of a gallium arsenide infrared LED and a silicon phototransistor in a molded plastic housing. The phototransistor responds to radiation from the LED only when a reflective object is within its field of view.

Features

- High Sensitivity
- Fast Response
- High Reliability
- Small Size Designed for Stacking

absolute maximum ratings (25°C unless otherwise noted)

Storage Temperature	−40° to 125°C
Operating Temperature	−40° to 100°C
Lead Soldering Temperature (30 sec)	260°C

Input Diode		put Sensor	
Forward DC Current	50 mA*	Collector Emitter Voltage	25V
Reverse DC Voltage	3V	Emitter Collector Voltage	5V
Power Dissipation	80 mW**	Power Dissipation	50 mW***

*Derate linearly 0.67 mA/°C above 25°C
**Derate linearly 1.07 mW/°C
***Derate linearly 0.67 mW/°C above 25°C

Type OPB 253A
Reflective Object Sensor

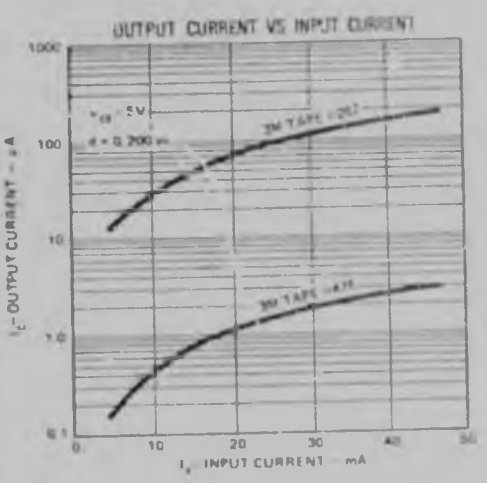
OPTRON, INC.

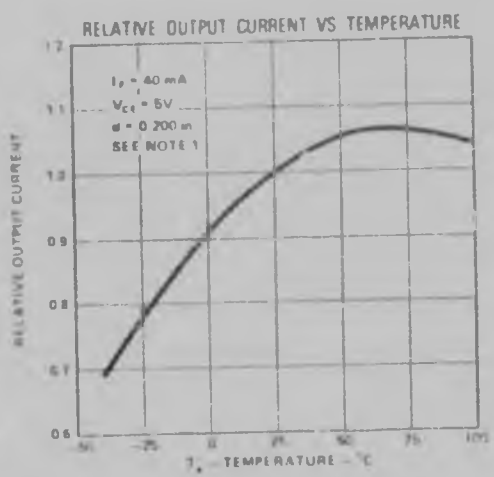
Bulletin No. 1054 April, 1976

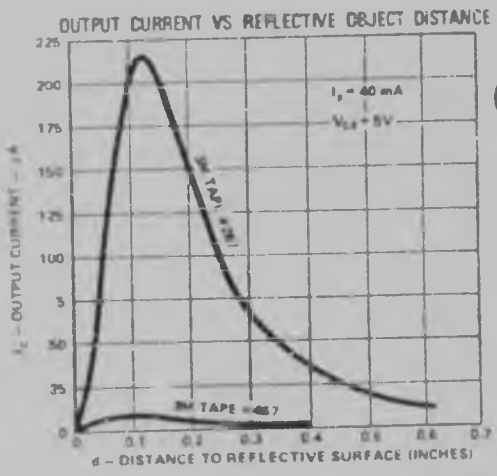
electrical characteristics (25°C free-air temperature unless otherwise noted)

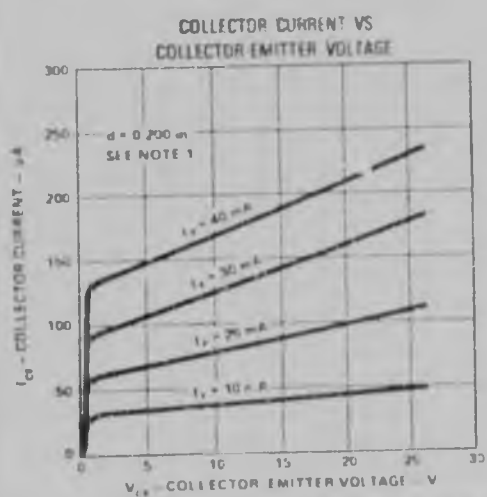
SYMBOL	PARAMETER	MIN	MAX	UNITS	TEST CONDITIONS
Combination					
I_{CL1}	Photocurrent (See Note 1)	25		μA	I_F = 40 mA, V_{CE} = 5V, d = .200 in (See Fig 1)
I_{CL2}	Photocurrent (See Note 2)		10	μA	I_F = 40 mA, V_{CE} = 5V, d = .200 in (See Fig 1)
I_{CX}	Crosstalk (See Note 3)		2.0	μA	I_F = 40 mA, V_{CE} = 5V, No Reflecting surface
Input Diode					
V_F	Forward Voltage		1.6	V	I_F = 50 mA
I_R	Reverse Current		100	μA	V_R = 3V
Output Sensor					
BV_{CEO}	Collector Emitter Breakdown Voltage	25		V	I_{CE} = 100 μA
BV_{ECO}	Emitter-Collector Breakdown Voltage	5		V	I_{EC} = 100 μA
I_{CEO}	Dark Current		100	nA	V_{CE} = 10V, I_F = 0, H ≤ 0.1 μw/CM²

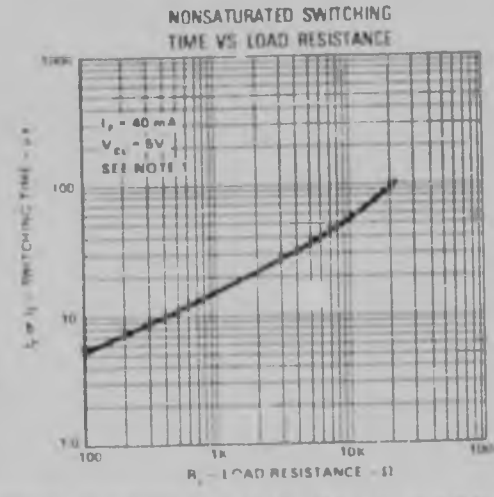
Typical Characteristics

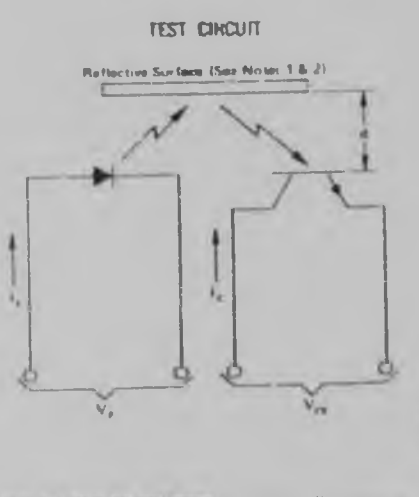












Note 1 Photocurrent (I_{CL1}) is measured using 3M Tape #267 for a reflecting surface. The reflective qualities of 3M Tape #267 are very similar to an Eastman Kodak neutral white test card having 90% diffuse reflectance.

Note 2 Photocurrent (I_{CL2}) is measured using 3M Tape #476 for a reflecting surface. 3M Tape #476 has a very black dull surface with optical reflectance qualities comparable to a surface painted with carbon black pigment and

Note 3 Crosstalk (I_{CX}) is the photocurrent measured with the indicated current in the input diode and with no reflecting surface.

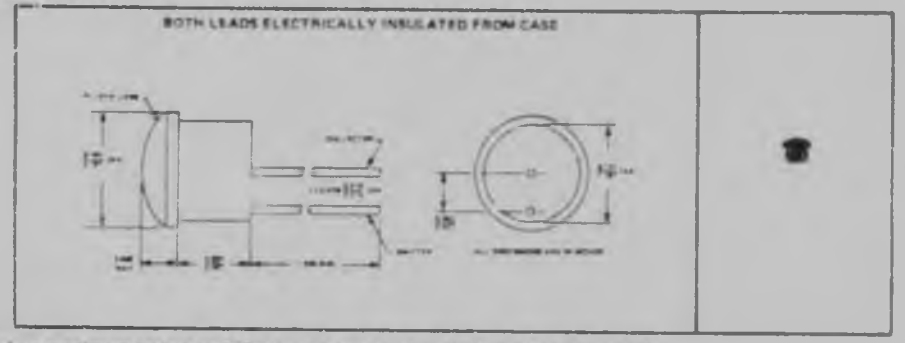
OPTRON RESERVES THE RIGHT TO MAKE CHANGES AT ANY TIME IN ORDER TO IMPROVE DESIGN AND TO SUPPLY THE BEST PRODUCT POSSIBLE

PRINTED IN U.S.A.

TIL63 THRU TIL67
BULLETIN NO. DL-S 6911721, DECEMBER 1969

- Recommended for Application in Character Recognition, Tape and Card Readers, Velocity Indicators, and Encoders
- Epoxy Dome-Shaped Lens
- Glass-to-Metal Seal Header

mechanical data



absolute maximum ratings at 25°C free-air temperature (unless otherwise noted)

Collector-Emitter Voltage	50 V
Emitter-Collector Voltage	7 V
Continuous Device Dissipation at (or below) 25°C Free-Air Temperature (See Note 1)	50 mW
Operating Free-Air Temperature Range	−40°C to 85°C
Storage Temperature Range	−40°C to 100°C
Lead Temperature 1/16 Inch from Case for 10 Seconds	240°C

electrical characteristics at 25°C free-air temperature (unless otherwise noted)

PARAMETER		TEST CONDITIONS		TYPE	MIN	TYP	MAX	UNIT
$V_{(BR)CEO}$	Collector-Emitter Breakdown Voltage	I_C = 100 μA, H = 0		ALL	50			V
$V_{(BR)ECO}$	Emitter-Collector Breakdown Voltage	I_E = 100 μA, H = 0		ALL	7			V
I_D	Dark Current	V_{CE} = 30 V, H = 0		ALL			25	nA
		V_{CE} = 30 V, H = 0	T_A = 85°C	ALL			0.5	μA
I_L	Light Current	V_{CE} = 5 V, H = 20 mW/cm², See Note 2		TIL63	0.4			mA
				TIL64	0.4		1.6	
				TIL65	1		4	
				TIL66	2.8		10	
				TIL67	8			
$V_{CE(sat)}$	Collector-Emitter Saturation Voltage	I_C = 0.4 mA, H = 20 mW/cm², See Note 2		ALL		0.15		V

NOTES: 1. Derate linearly to 85°C free-air temperature at the rate of 0.91 mW/°C.
2. Irradiance (H) is the radiant power per unit area incident upon a surface. For this measurement the source is an unfiltered tungsten-filament lamp operating at a color temperature of 2870 K.

switching characteristics at 25°C free-air temperature

PARAMETER		TEST CONDITIONS	TYP	UNIT
t_r	Rise Time	V_{CC} = 30 V, I_L = 800 μA, R_L = 1 kΩ, See Figure 1	1.5	μs
t_f	Fall Time		15	

PARAMETER MEASUREMENT INFORMATION

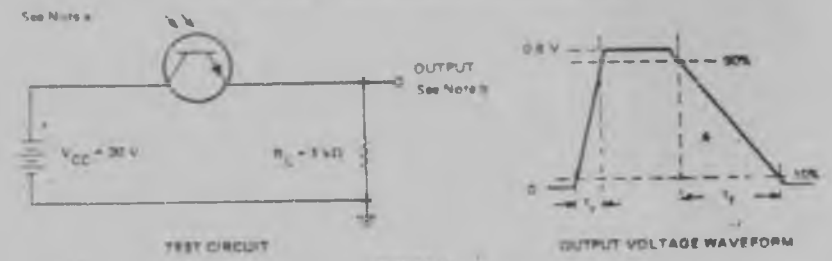


FIGURE 1

NOTES: a. Input impedance is supplied by a pulsed tungsten bulb source. Incident irradiation is adjusted for I_L = 800 μA.
b. Output waveform is monitored on an oscilloscope with the following characteristics: $t_r \leq 25$ ns, $R_{in} \geq 1$ MΩ, $C_{in} \leq 20$ pF.

TYPICAL APPLICATION DATA

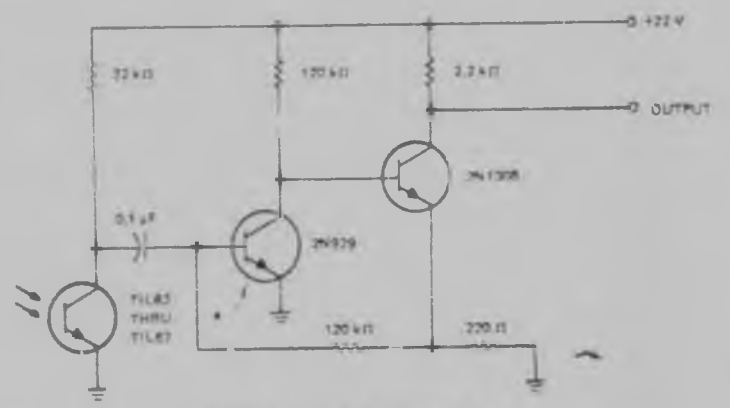


FIGURE 2–LIGHT PULSE DETECTOR

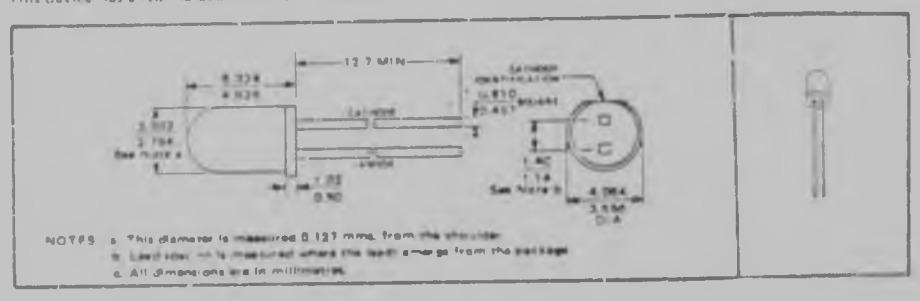
TYPE TIL209
GALLIUM ARSENIDE PHOSPHIDE VISIBLE-LIGHT SOURCE

DESIGNED TO EMIT VISIBLE RED
LIGHT WHEN FORWARD BIASED

- Recommended for Application in Visual Indicators, Alpha-Numeric Displays, and Built-In Diagnostics
- High Brightness with Solid State Reliability
- Compatible with Most TTL and DTL Circuits
- Ideal as Fault or Trouble Indicator
- Filled Epoxy Lens Provides Diffused Source
- Ideal for Socket, Printed Circuit Board, and 1/16" Panel Mounting Techniques

mechanical data

This device has a red molded filled epoxy body.



absolute maximum ratings

Reverse Voltage at 25°C Free Air Temperature	3 V
Continuous Forward Current at (or below) 25°C Free Air Temperature (See Note 1)	40 mA
Storage Temperature Range	−40°C to 80°C
Lead Temperature 1/16 Inch from Case for 5 Seconds	230°C

operating characteristics at 25°C free air temperature

	PARAMETER	TEST CONDITIONS	MIN	TYP	MAX	UNIT
I_V	Luminous Intensity (See Note 2)	I_F = 20 mA	500			mcd
λ_{peak}	Wavelength at Peak Emission	I_F = 20 mA	6300	6500	6700	Å
V_F	Static Forward Voltage	I_F = 20 mA		1.8	2	V
I_R	Static Reverse Current	V_R = 3 V		0.1		μA

NOTES 1. Derate linearly to 70°C free air temperature at the rate of 0.89 mA/°C.
2. Luminous intensity is measured with a solar cell and filter combination which approximates the CIE (International Commission on Illumination) eye response curve.

TYPICAL CHARACTERISTICS

RELATIVE SPECTRAL CHARACTERISTICS

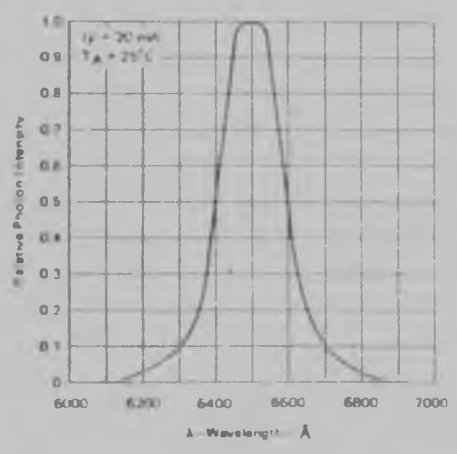


FIGURE 1

RELATIVE LUMINOUS INTENSITY
vs
FREE AIR TEMPERATURE

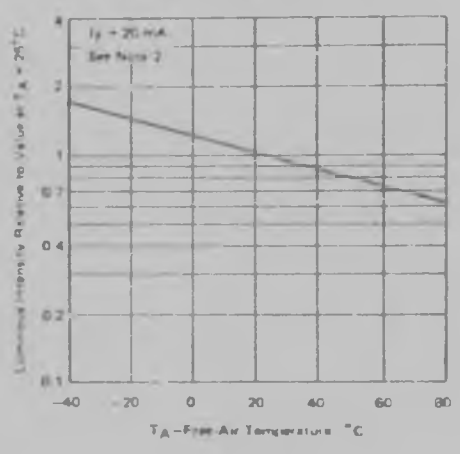


FIGURE 2

RELATIVE LUMINOUS INTENSITY
vs
FORWARD CURRENT

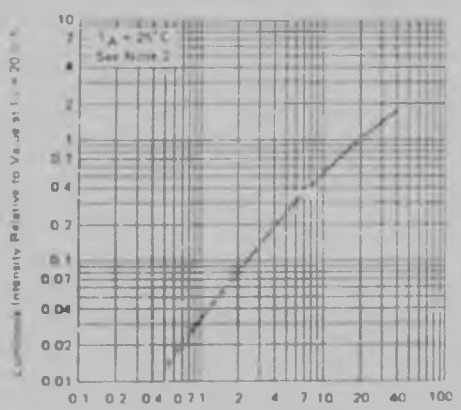


FIGURE 3

FORWARD CONDUCTION CHARACTERISTICS

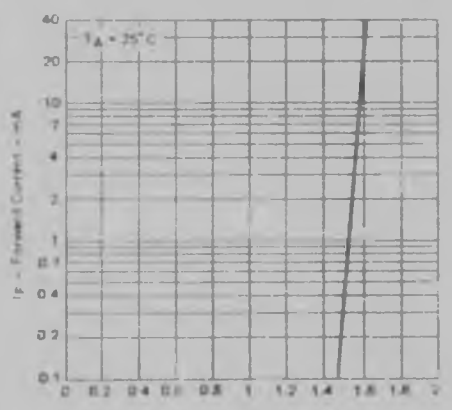


FIGURE 4

NOTE 2: Luminous intensity is measured with a solid-state detector and filter combination which approximates the CIE (International Commission on Illumination) eye-response curve.

TEXAS INSTRUMENTS

TEXAS INSTRUMENTS RESERVES THE RIGHT TO MAKE CHANGES AT ANY TIME

TYPICAL CHARACTERISTICS

COLLECTOR CURRENT
vs
COLLECTOR-EMITTER VOLTAGE

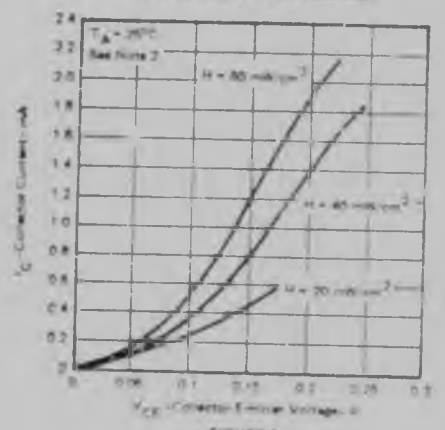


FIGURE 3

TIL66
COLLECTOR CURRENT
vs
COLLECTOR-EMITTER VOLTAGE

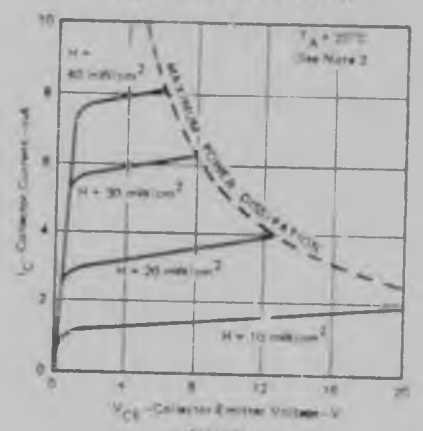


FIGURE 4

COLLECTOR-EMITTER SATURATION VOLTAGE
vs
IRRADIANCE

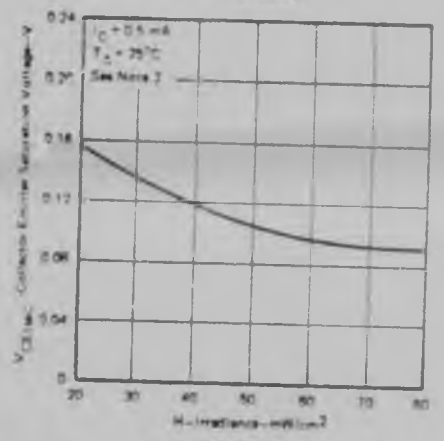


FIGURE 5

DARK CURRENT
vs
FREE-AIR TEMPERATURE

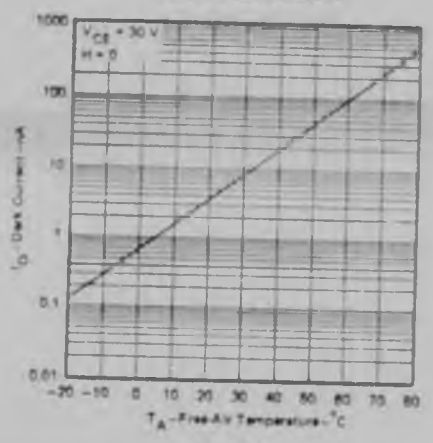


FIGURE 6

NOTE 2: Irradiance (H) is the radiant power per unit area incident upon a surface. For this measurement the source is an unfiltered tungsten-filament lamp operating at a color temperature of 2870°K.

TEXAS INSTRUMENTS

TYPICAL CHARACTERISTICS

RELATIVE OUTPUT
vs
MODULATION FREQUENCY

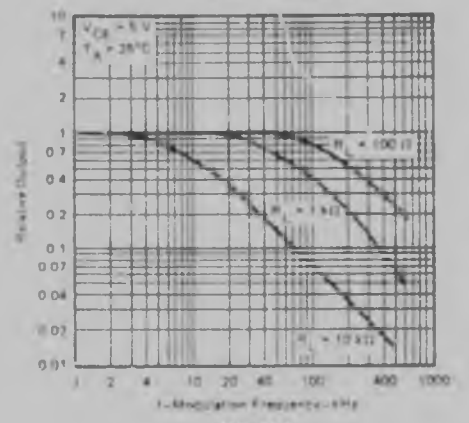


FIGURE 7

NORMALIZED LIGHT CURRENT
vs
ANGULAR DISPLACEMENT

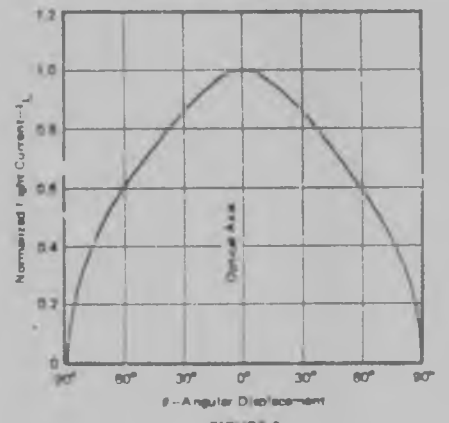


FIGURE 8

RELATIVE SPECTRAL CHARACTERISTICS

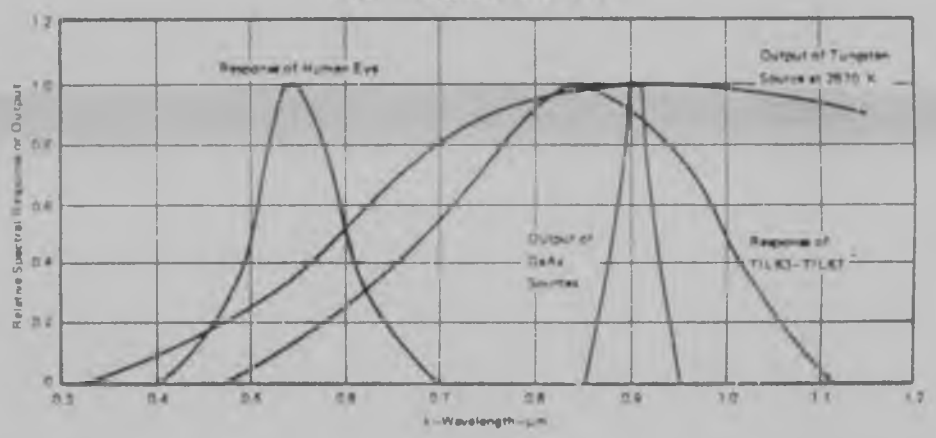


FIGURE 9

TEXAS INSTRUMENTS

TI cannot assume any responsibility for any circuits shown or represent that they are free from patent infringement
TEXAS INSTRUMENTS RESERVES THE RIGHT TO MAKE CHANGES AT ANY TIME IN ORDER TO IMPROVE DESIGN AND TO SUPPLY THE BEST PRODUCT POSSIBLE

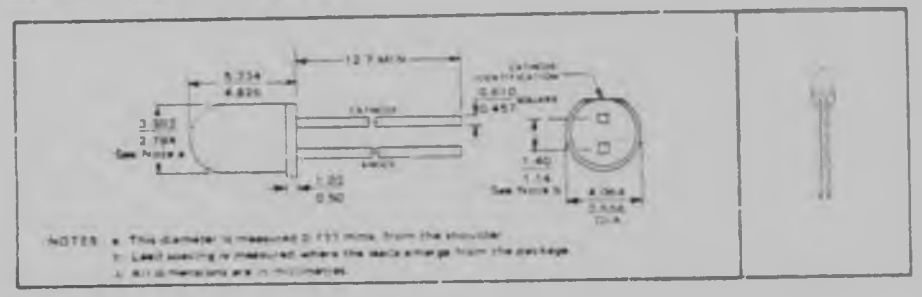
TIL32
PN GALLIUM ARSENIDE LIGHT SOURCE

Designed to emit near-infrared light when forward biased

- Output spectrally compatible with silicon sensors
- High power efficiency . . . typically 5% at 26°C
- High power output . . . typically 1.2 mW at 25°C
- High radiant intensity . . . typically 4 mW per steradian†
- Plastic package with two leads for ease of handling

Mechanical data

This device has a clear molded epoxy body



NOTES: a. This diameter is measured 0.127 mm from the shoulder.
b. Lead spacing is measured where the leads emerge from the package.
c. All dimensions are in millimeters.

Absolute maximum ratings

Reverse Voltage at 25°C Free-Air Temperature	2 V
Continuous Forward Current at (or below) 25°C Free-Air Temperature (See Note 1)	40 mA
Operating Free-Air Temperature Range	−40°C to 80°C
Storage Temperature Range	−40°C to 120°C
Lead Temperature 1/16 Inch from Case for 5 Seconds	240°C

Operating characteristics at 25°C free-air temperature

	PARAMETER	TEST CONDITIONS	MIN	TYP	MAX	UNIT
P_O	Radiant Power Output	I_F = 20 mA	0.5	1.2		mW
λ_{peak}	Wavelength at Peak Emission			0.94		µm
BW_λ	Spectral Bandwidth between Half Power Points			800		Å
θ_{HP}	Emission Beam Angle between Half Power Points			35°		
V_F	Static Forward Voltage			1.2	1.8	V
t_r	Light Rise Time‡	I_{FM} = 20 mA, t_w = 2 µs, f = 45 kHz		800		ns
t_f	Light Fall Time‡			250		

†Radiant intensity is calculated from $I = P_O/2\pi(1-\cos 0.5\theta_{HP})$. One steradian is the solid angle at the center of a sphere subtended by a portion of the surface area equal to the square of the radius of the sphere. There are 4π steradians in a complete sphere.
‡Light rise time is the time required for a change in light intensity from 10% to 90% for a step change in current. Light fall time is the time required for a change in light intensity from 90% to 10% for a step change in current.
NOTE 1: Derate linearly to 80°C free-air temperature at the rate of 0.73 mA/°C.

TYPICAL CHARACTERISTICS

RELATIVE SPECTRAL CHARACTERISTICS

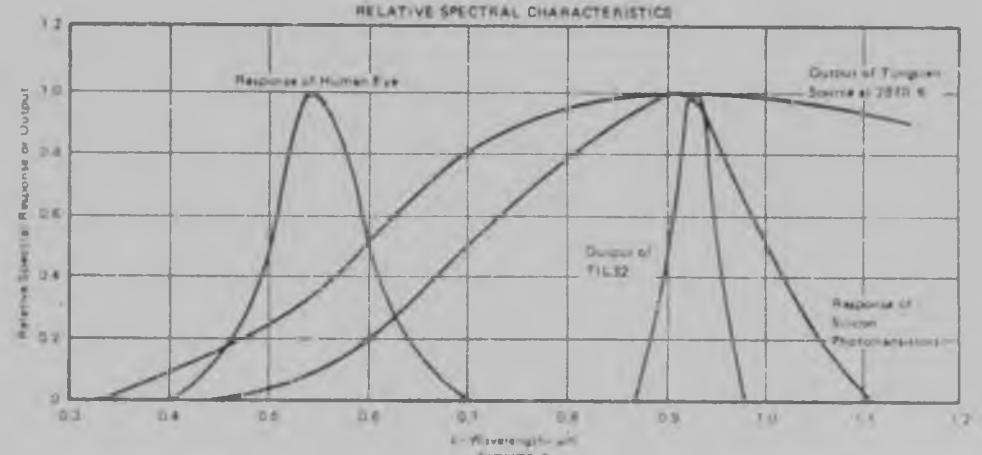


FIGURE 1

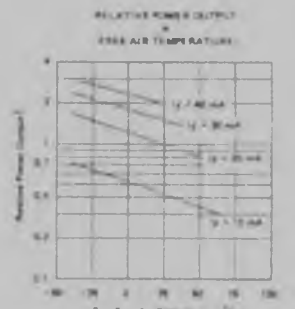


FIGURE 2

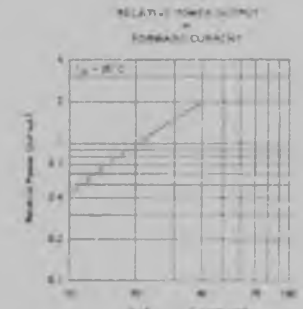


FIGURE 3

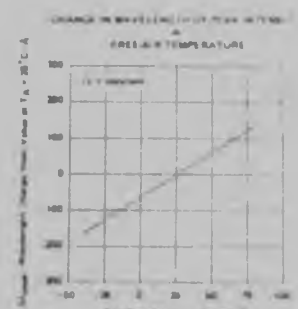


FIGURE 4

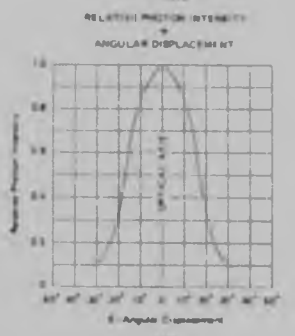


FIGURE 5

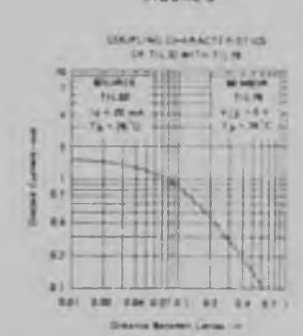


FIGURE 6

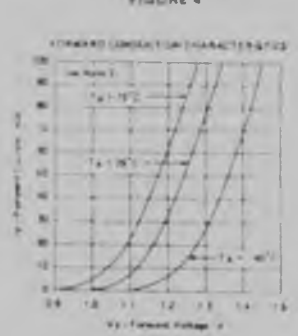


FIGURE 7

NOTE 2: This parameter must be measured using pulse techniques. t_w = 0.04 ms, duty cycle ≤ 10%.
†Normalized to Output at I_F = 20 mA, T_A = 25°C.

APPENDIX 7 RESULTS

A sample of the experimental results collected are presented in this appendix. The results were obtained from tests performed on two subjects. The following results are given:

Figures A7.1 - A7.4 Arterial Occlusion.

Figures A7.5 - A7.7 Breath Holding Tests.

Figures A7.8 -A7.11 Local heating of the Hand.

Figures A7.12 - A7.16 Spectral Results.

Figures A7.17 - A7.18 Correlation Between the Oximeter (I.R. Channel) and Pulse Monitor.

Figure A7.1 Arterial Occlusion Test.

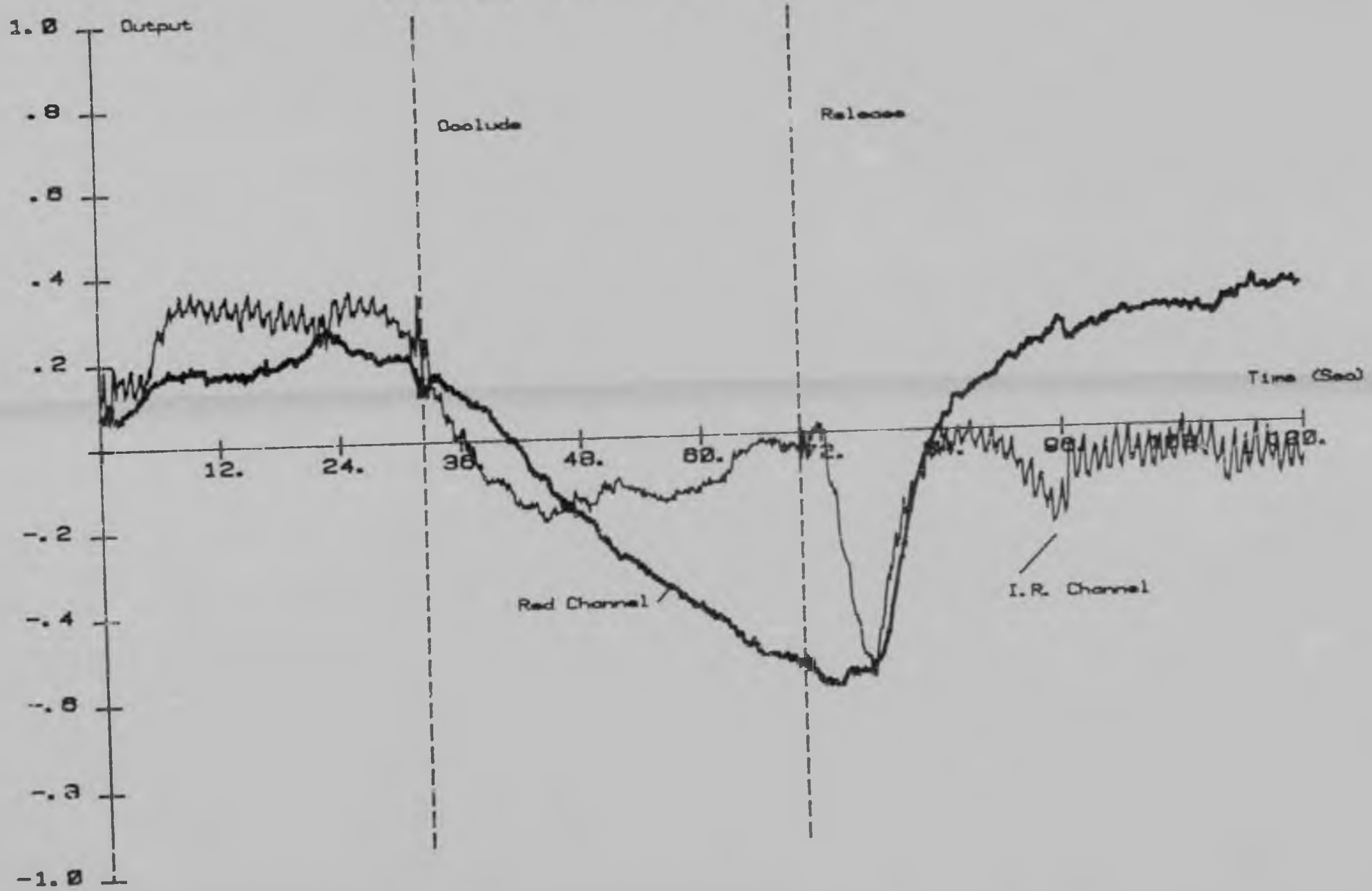


Figure A7.2 Arterial Occlusion Test.

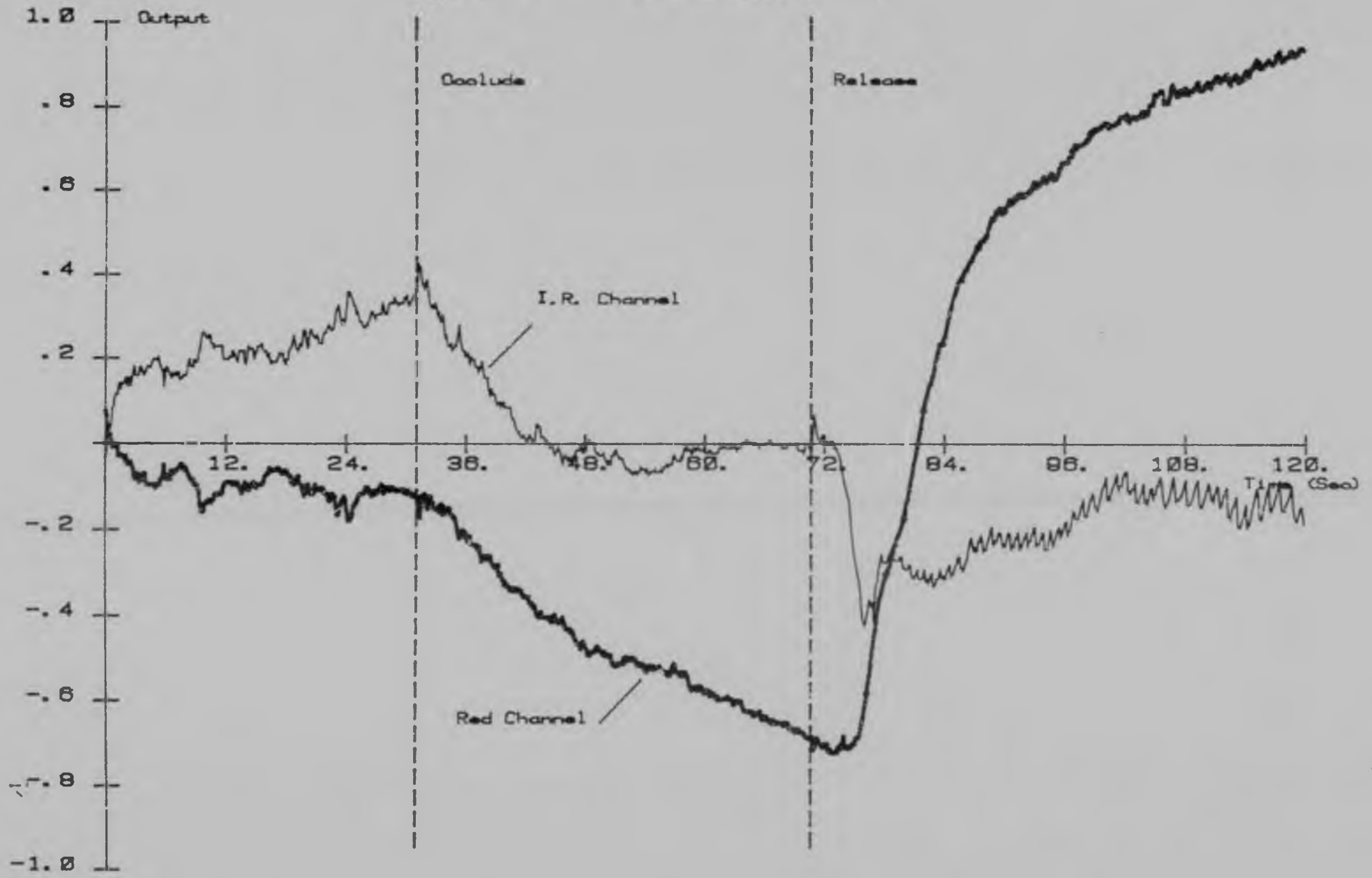


Figure A7.9 Arterial Occlusion Test.

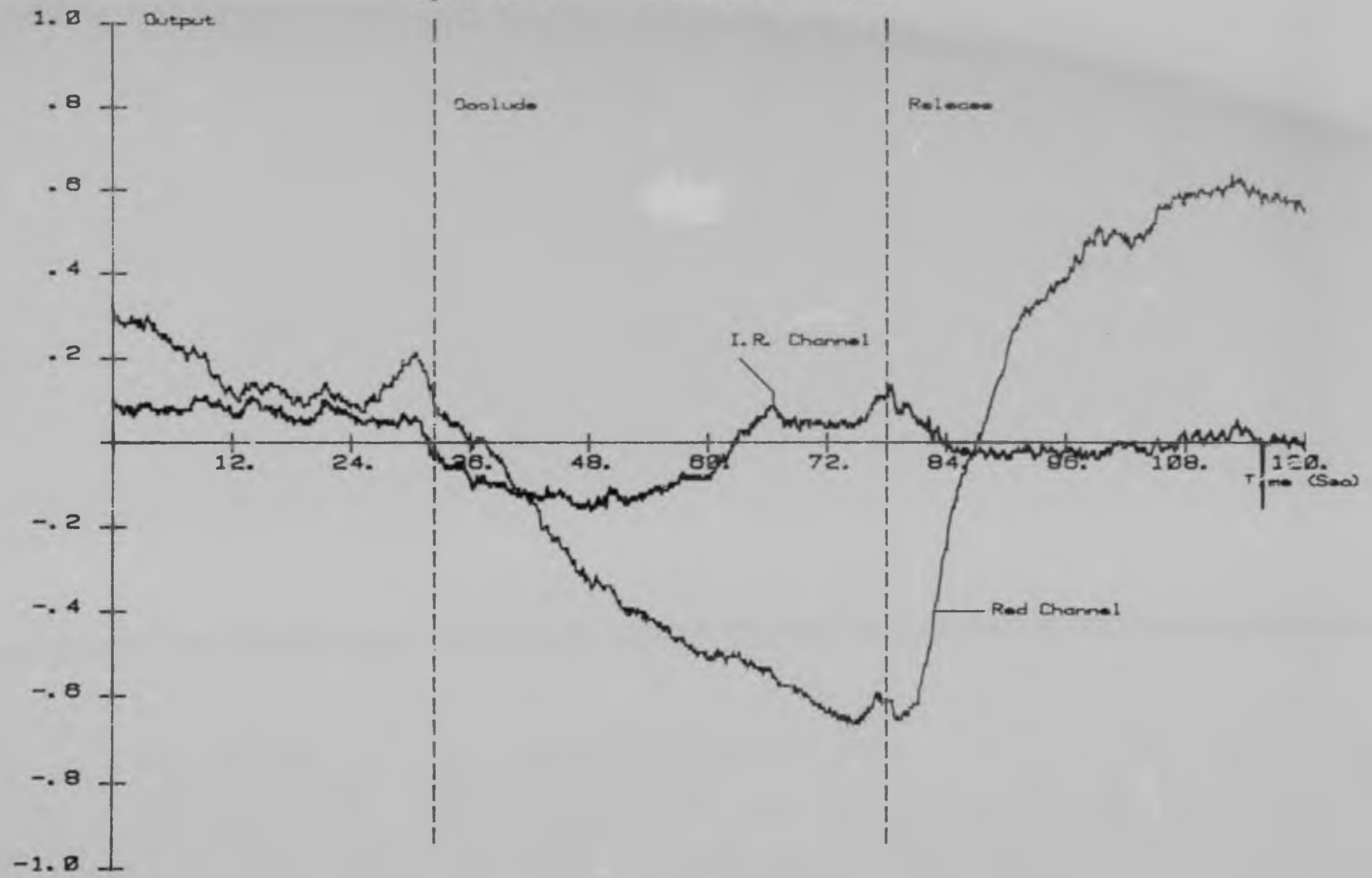


Figure A7.4 Arterial Occlusion Test.

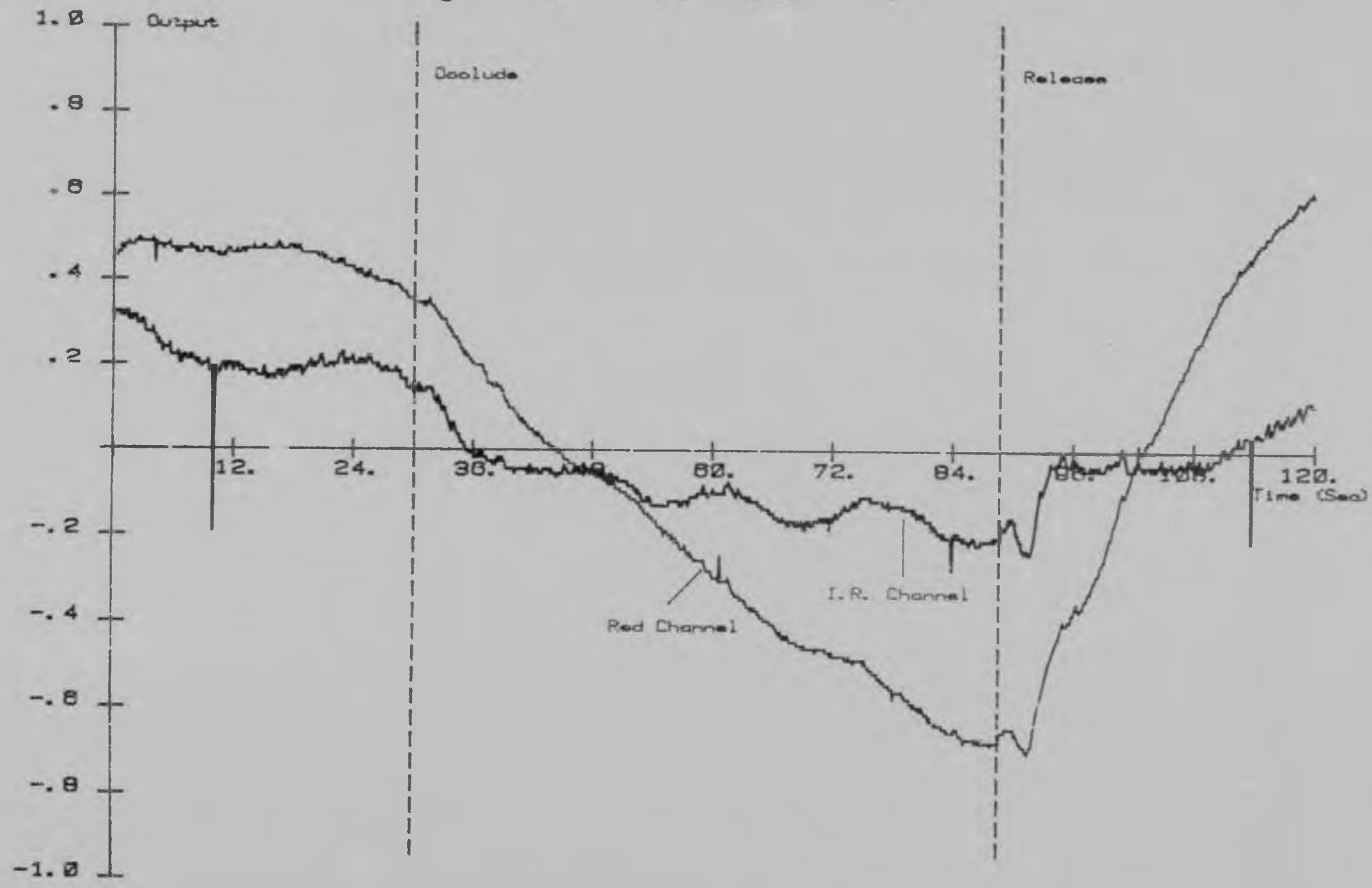


Figure A7.5 Breath Holding Test.

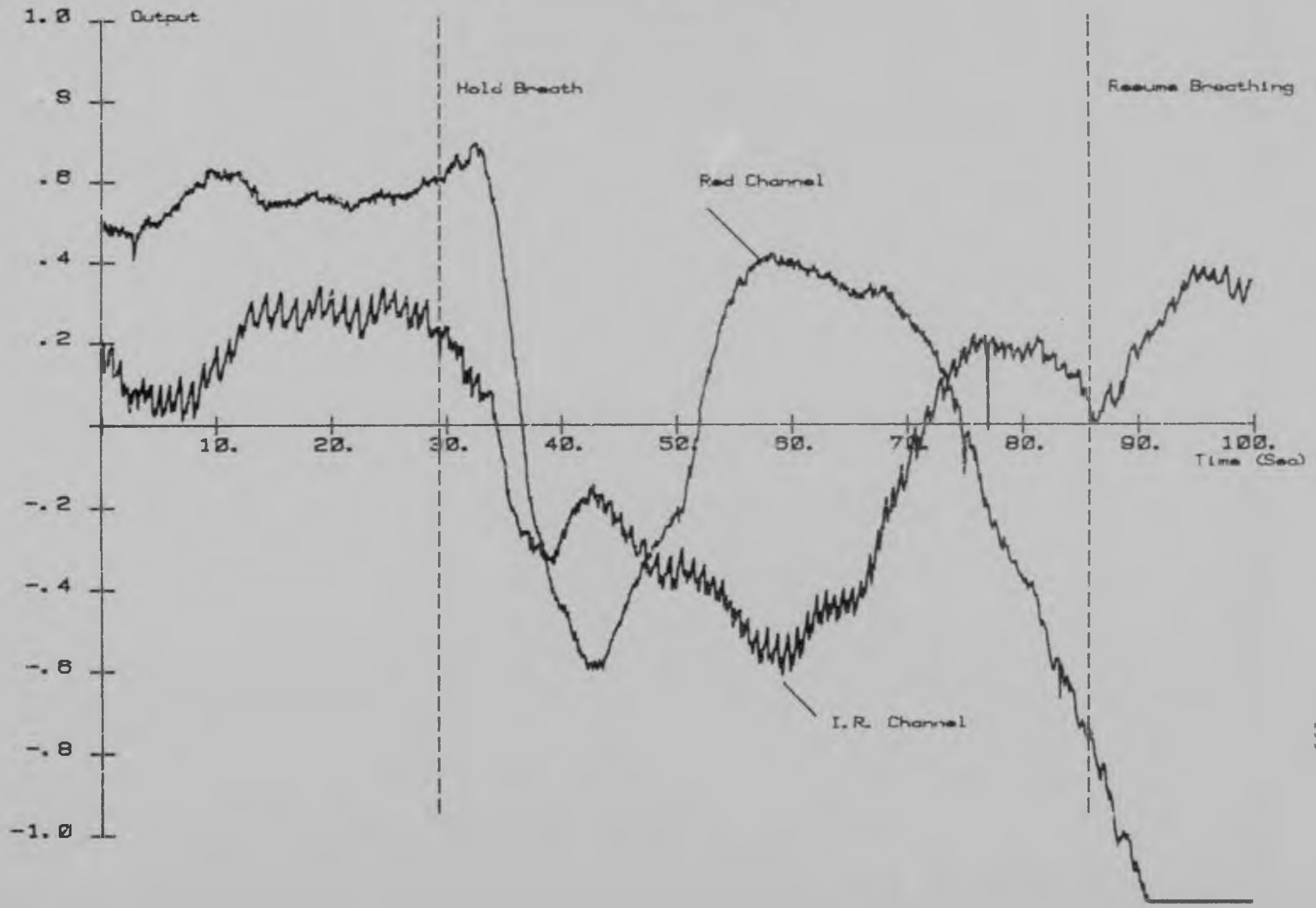


Figure A7.6 Breath Holding Test.

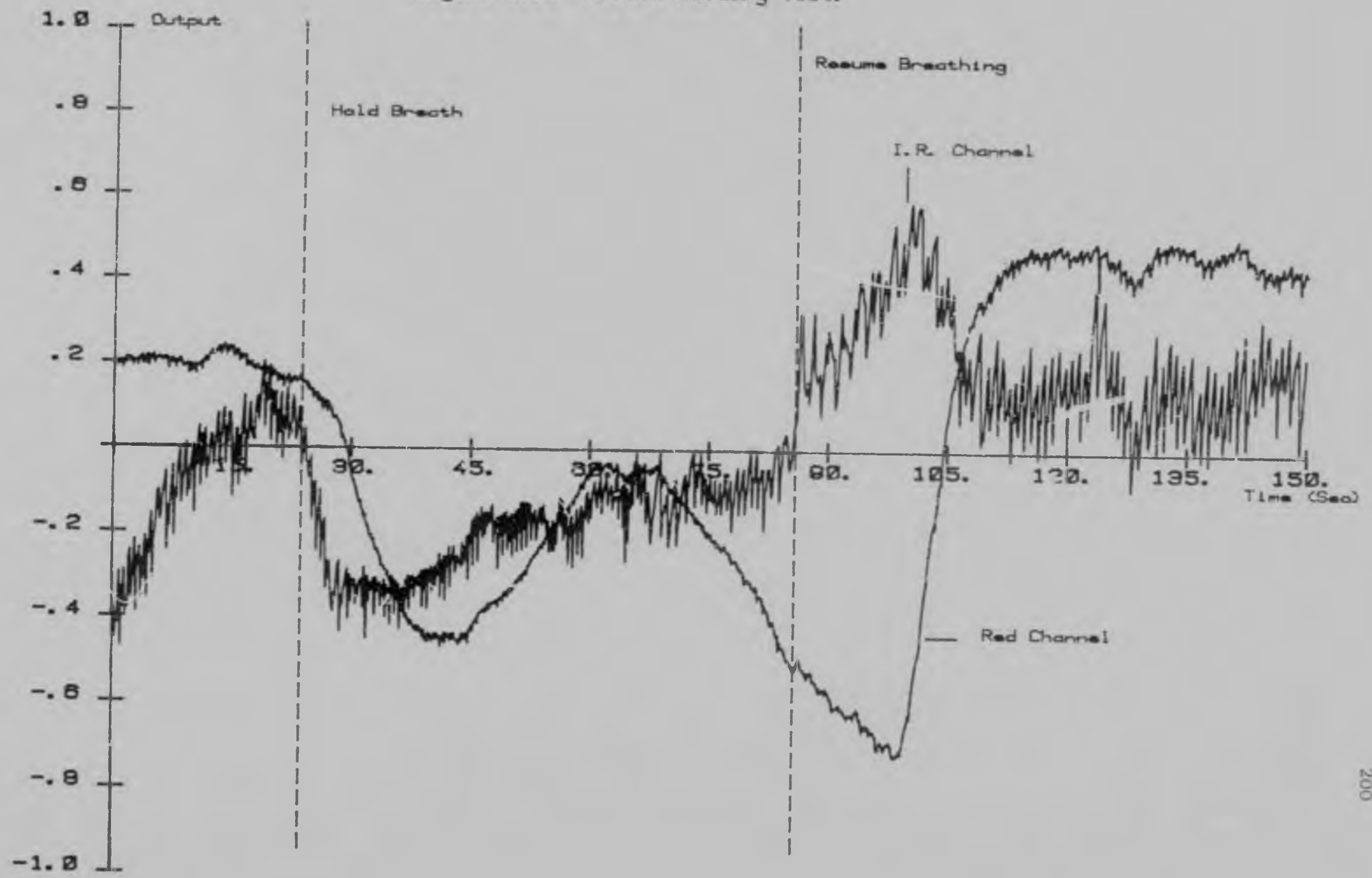


Figure A7.7 Breath Holding Test.

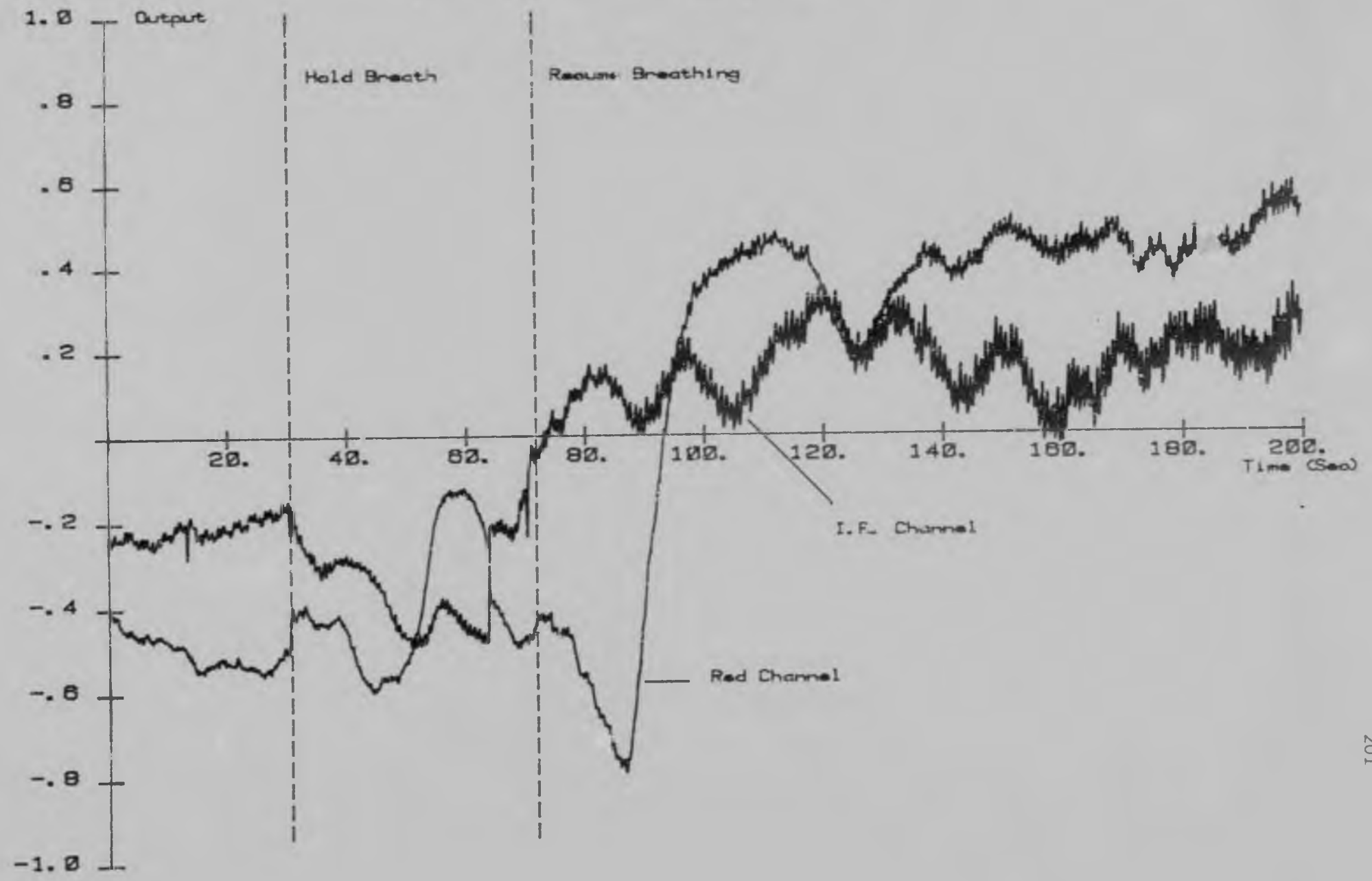


Figure A7.8 Effects of Local Heating.

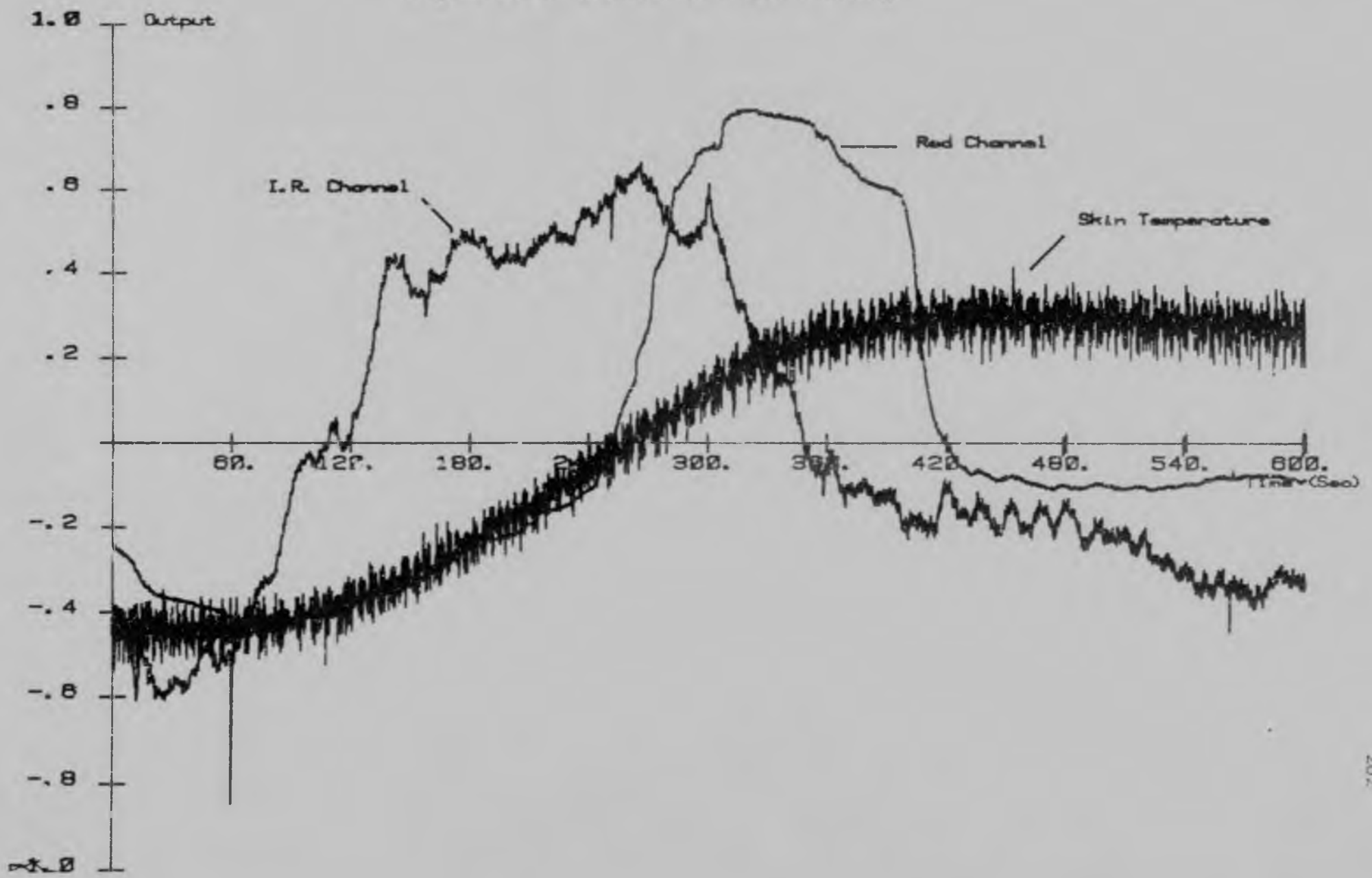


Figure A7.9 Effects of Local Heating.

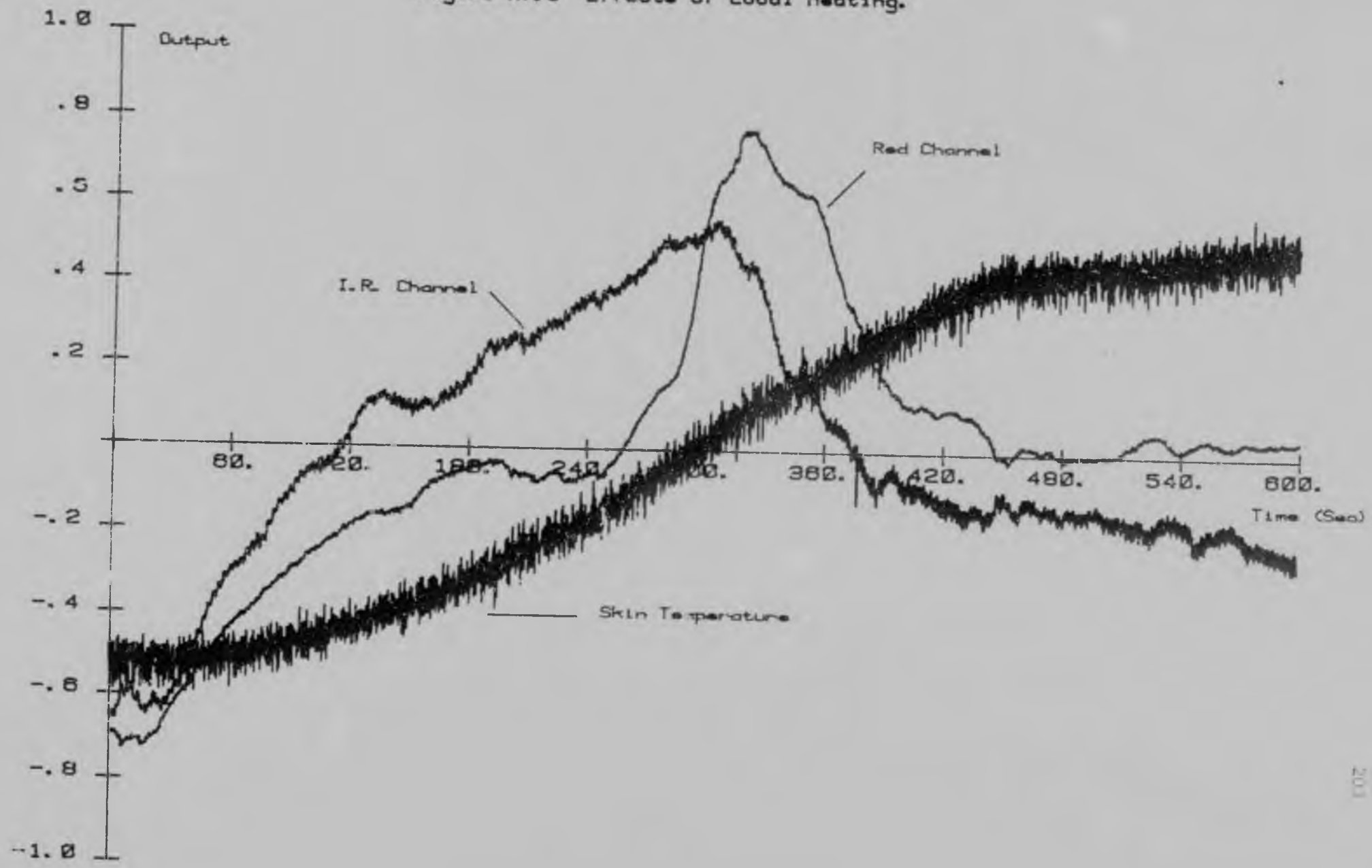


Figure A7.10 Effects of Local Heating.

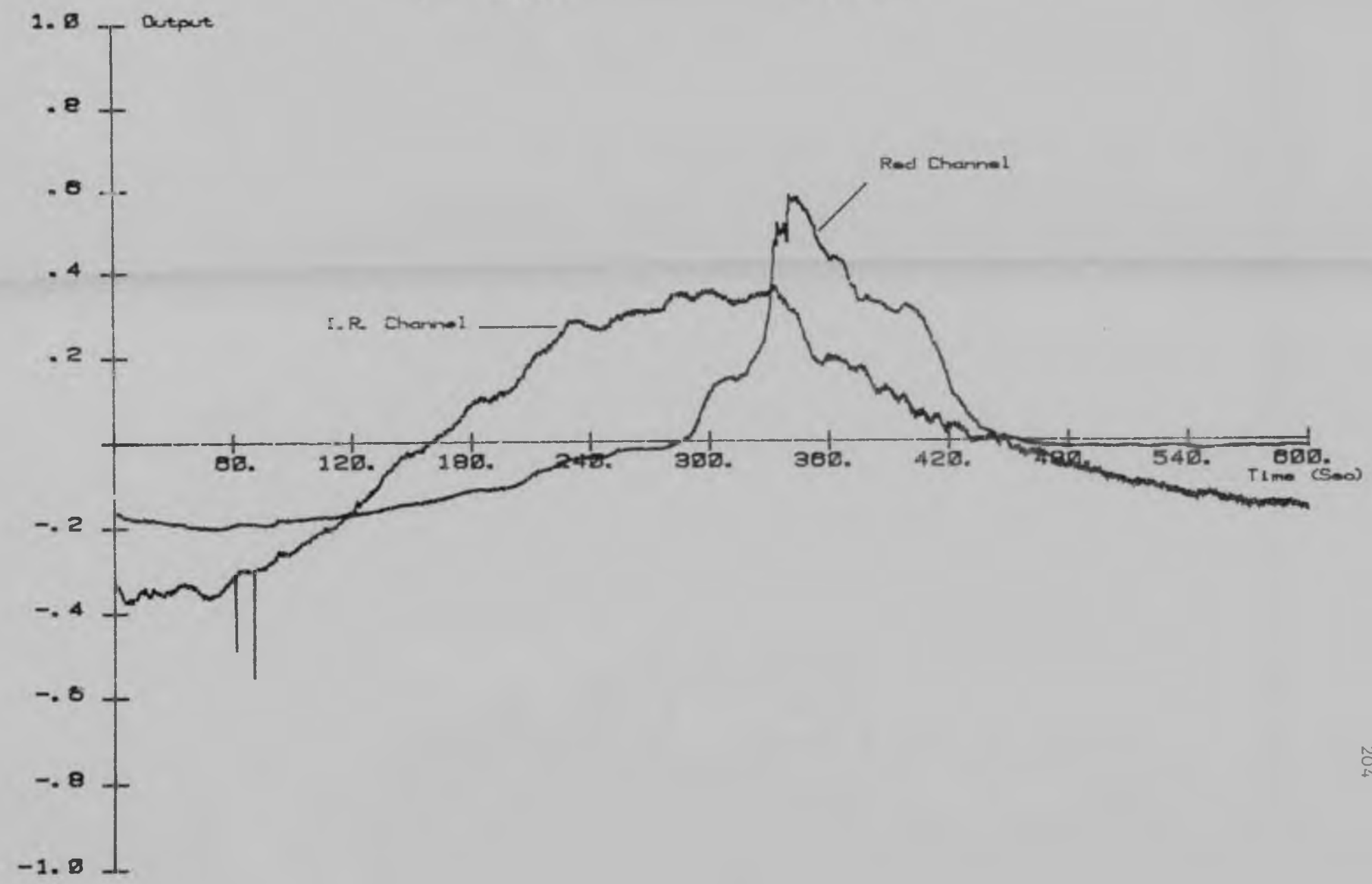


Figure A7.11 Effects of Local Heating.

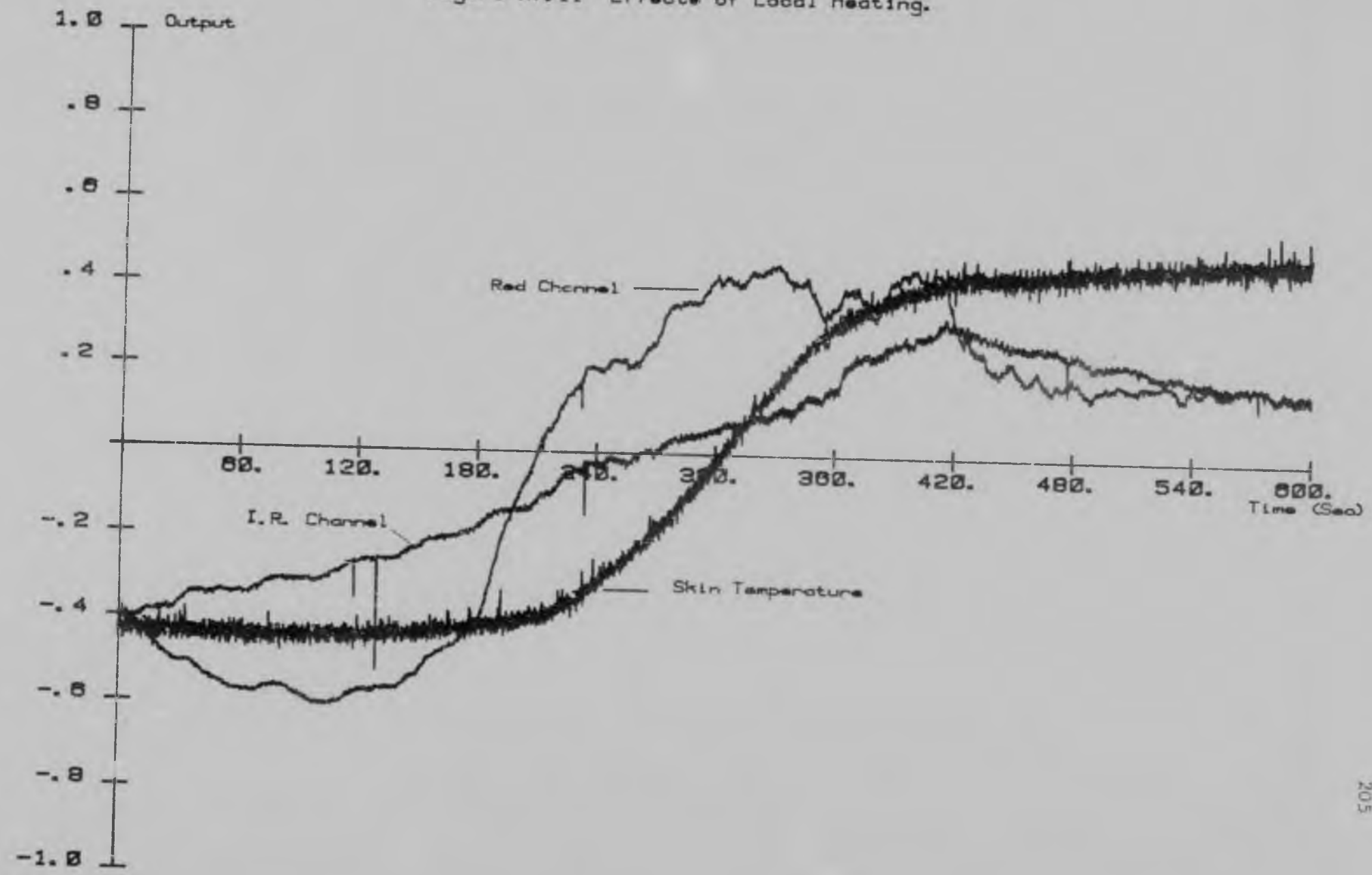


Figure A7.12 Spectrum When Sitting Still.
(Infra Red Channel)

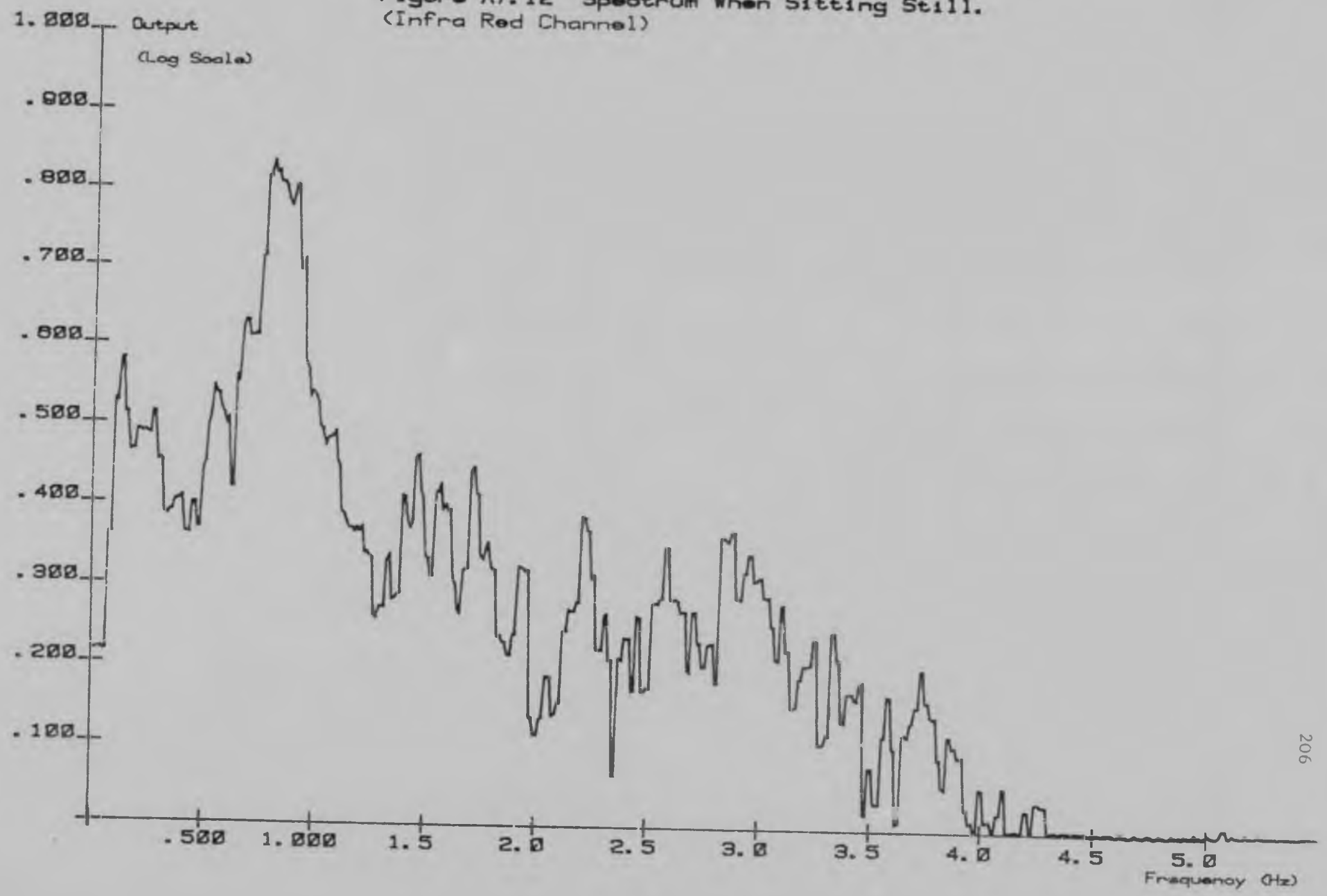


Figure A7.13 Spectrum When Breathing at 0.2Hz.
(Infra Red Channel)

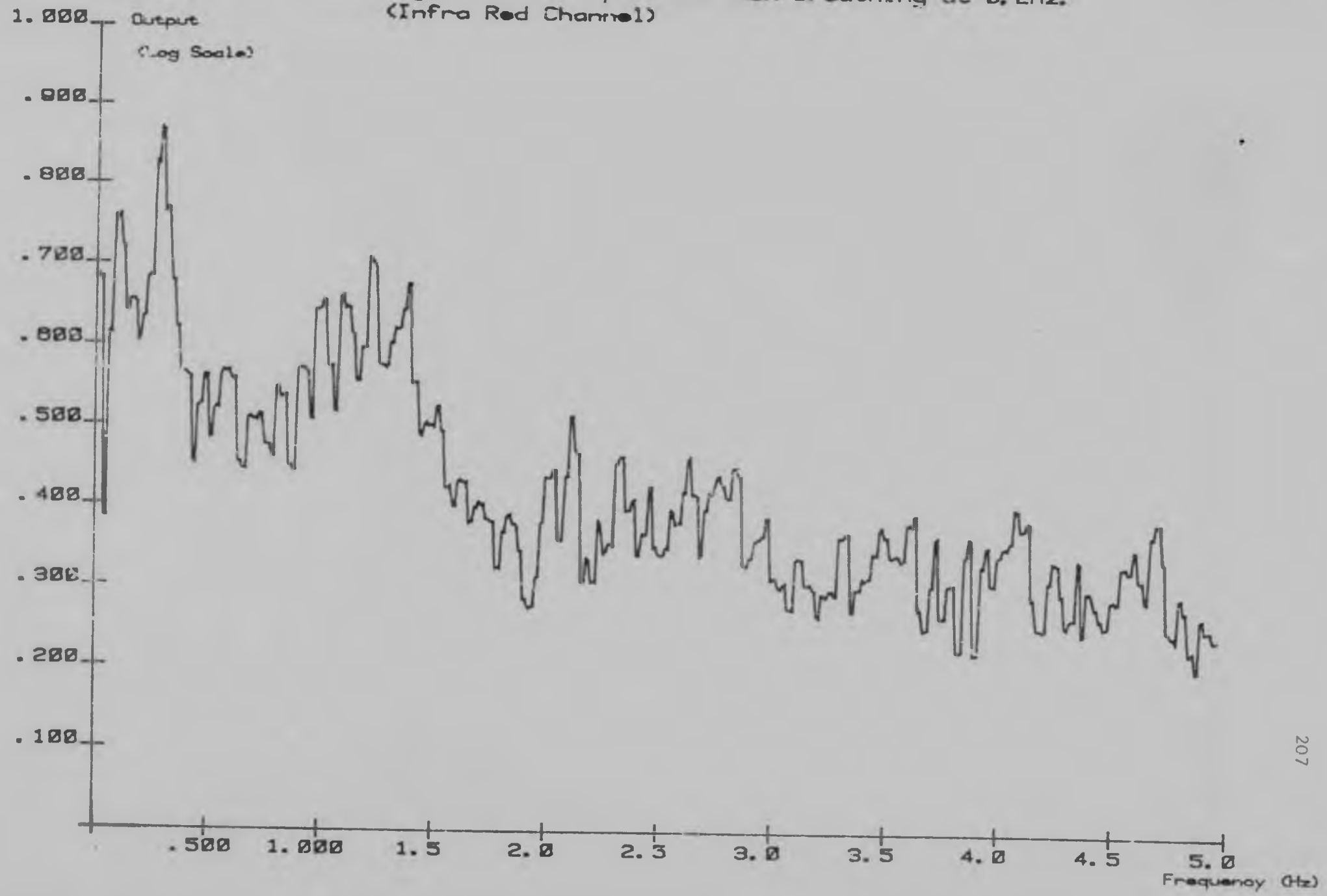


Figure A7.14 Spectrum When Breathing at 0.1Hz.
(Infra Red Channel)

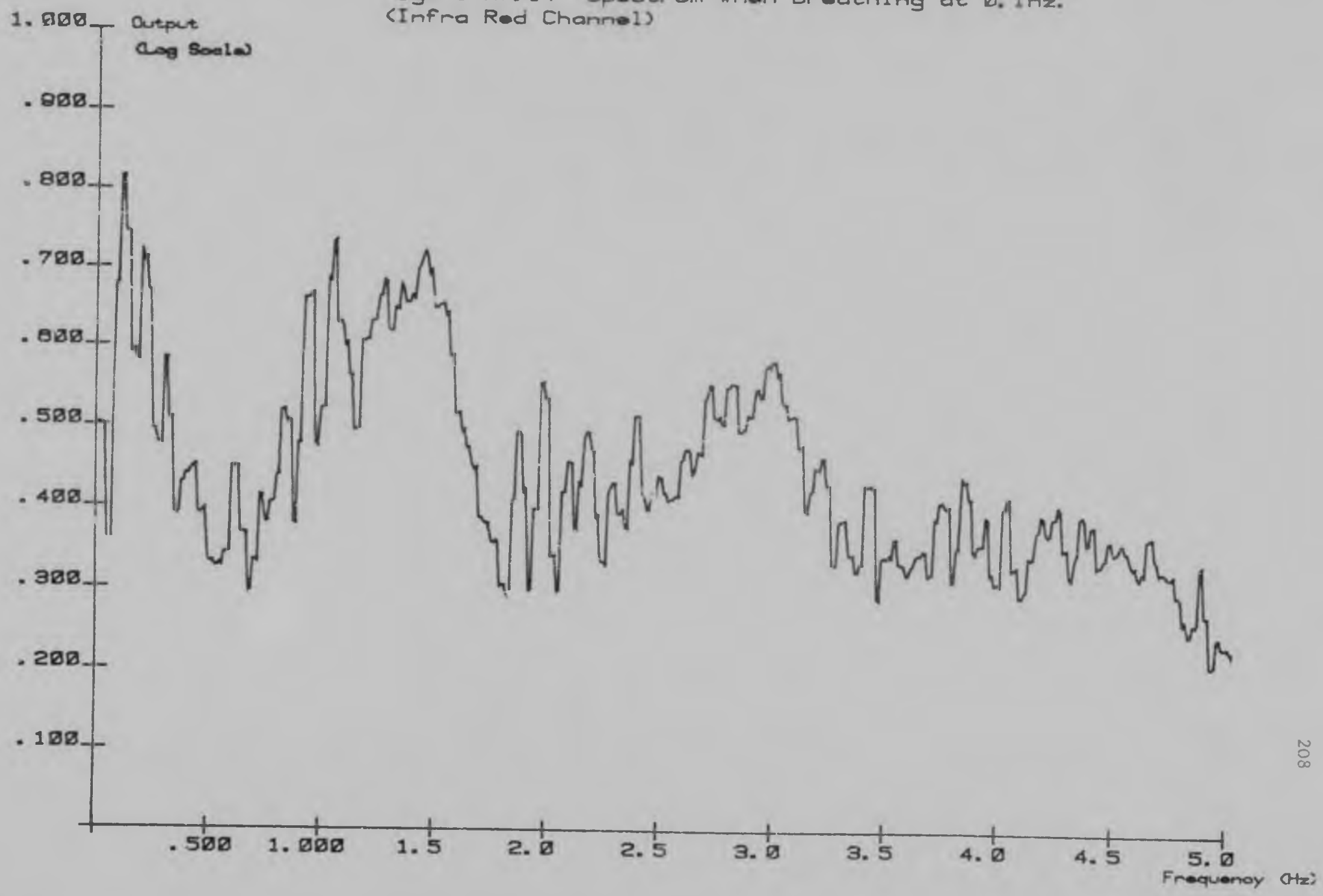


Figure A7.15 Spectrum After Vigourous Exercise

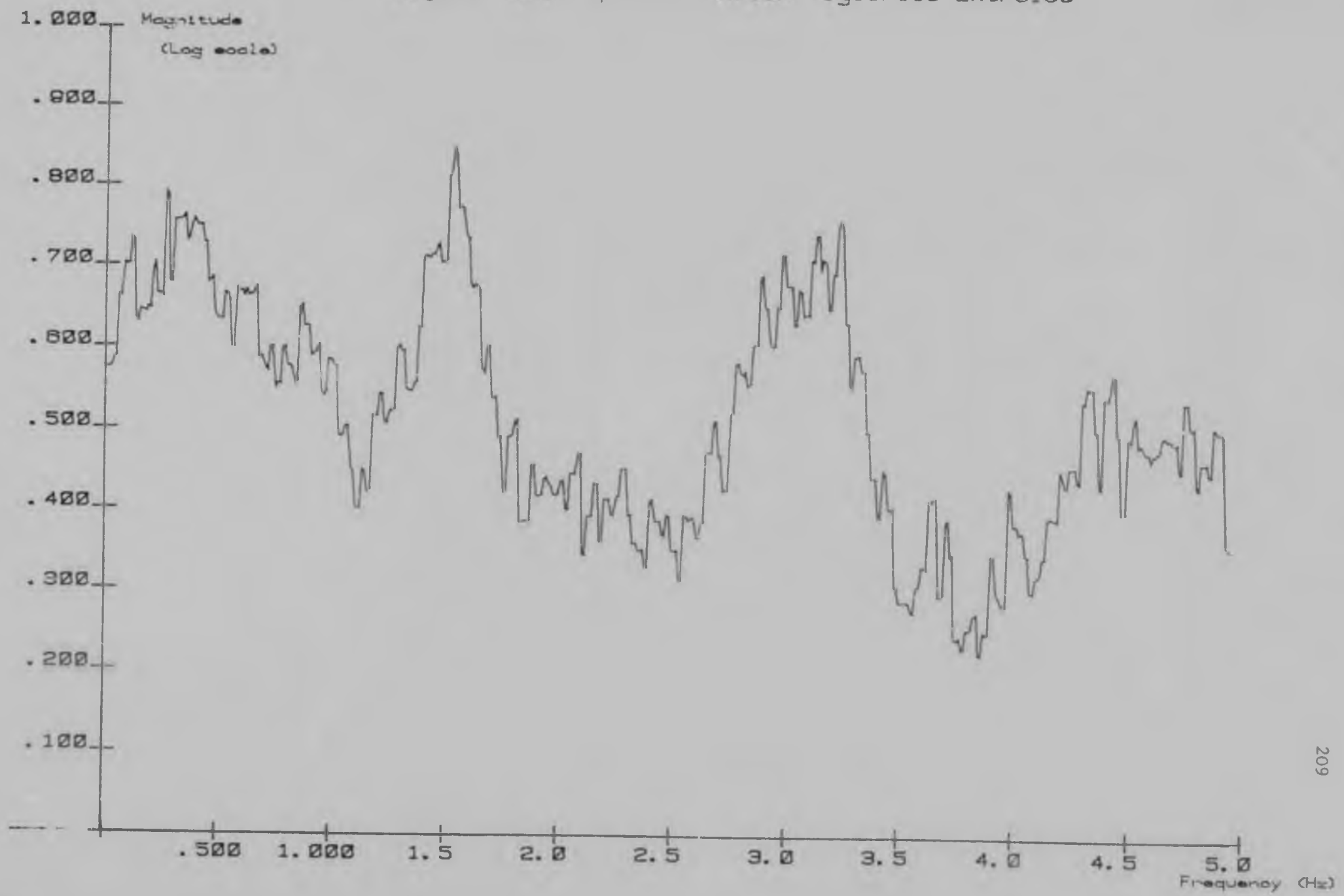


Figure A7.18 Spectrum Half an Hour After Exercising

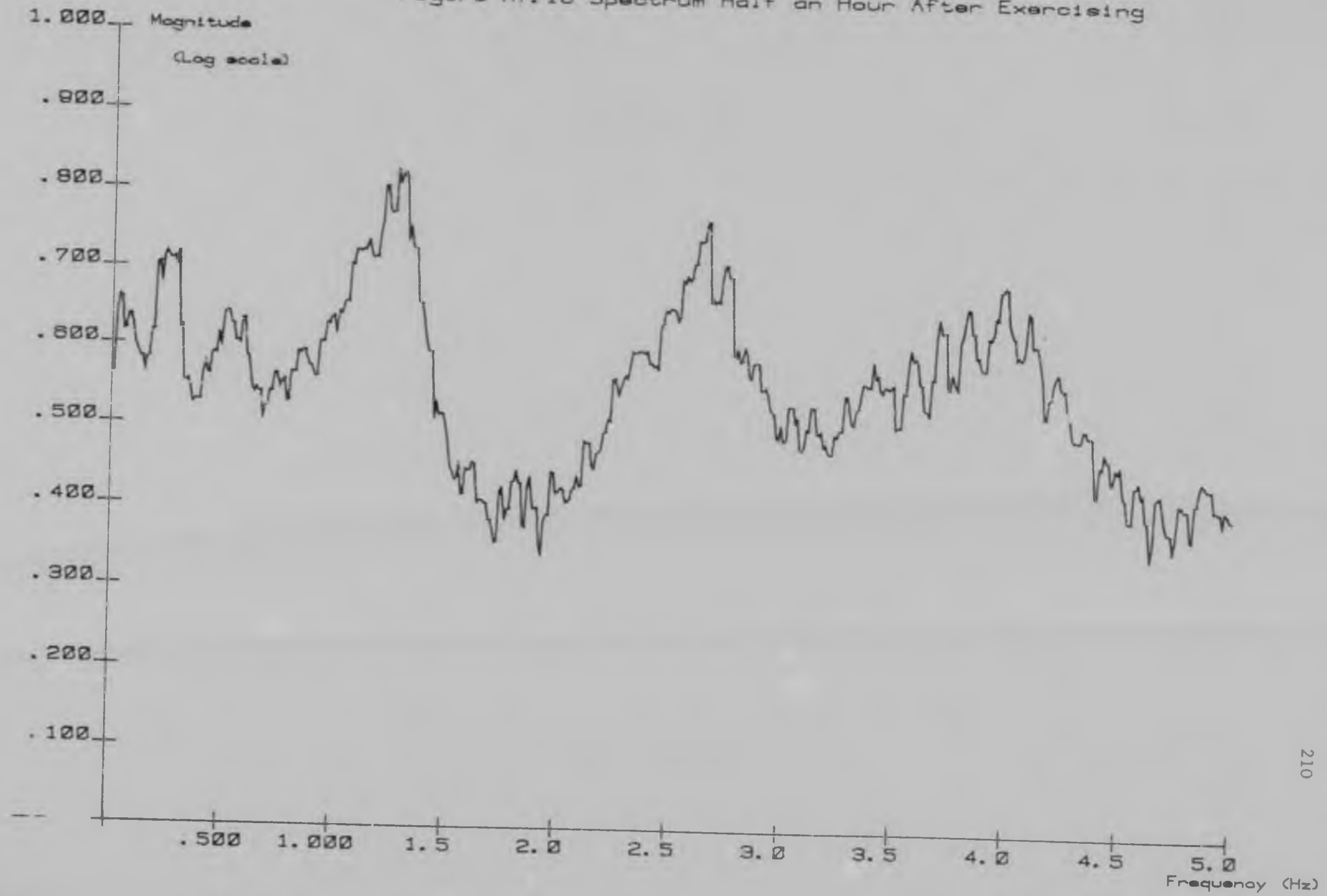


Figure A7.17 Output From I.R. Channel and Pulse Monitor, Showing Phase Relationships.

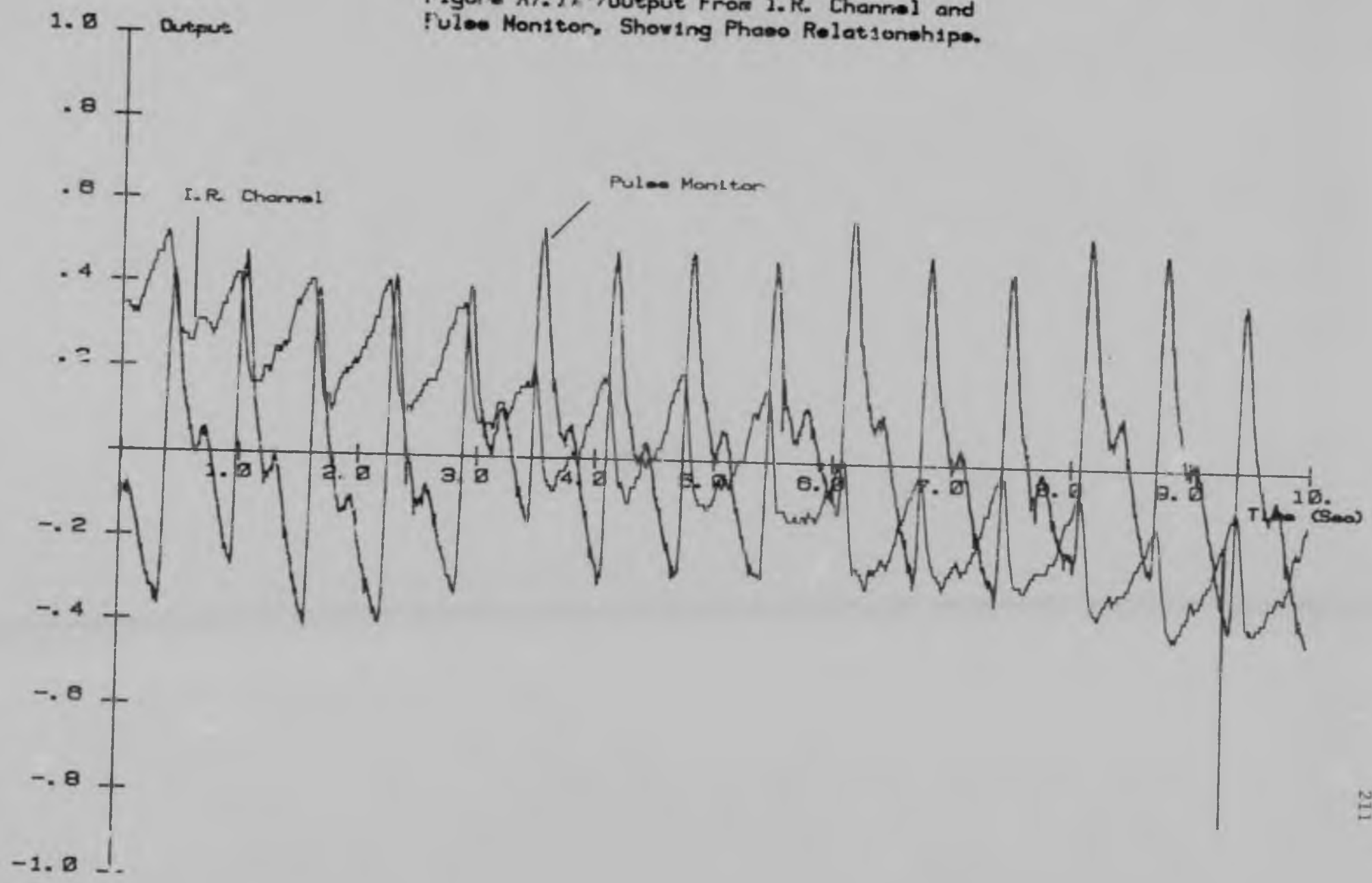
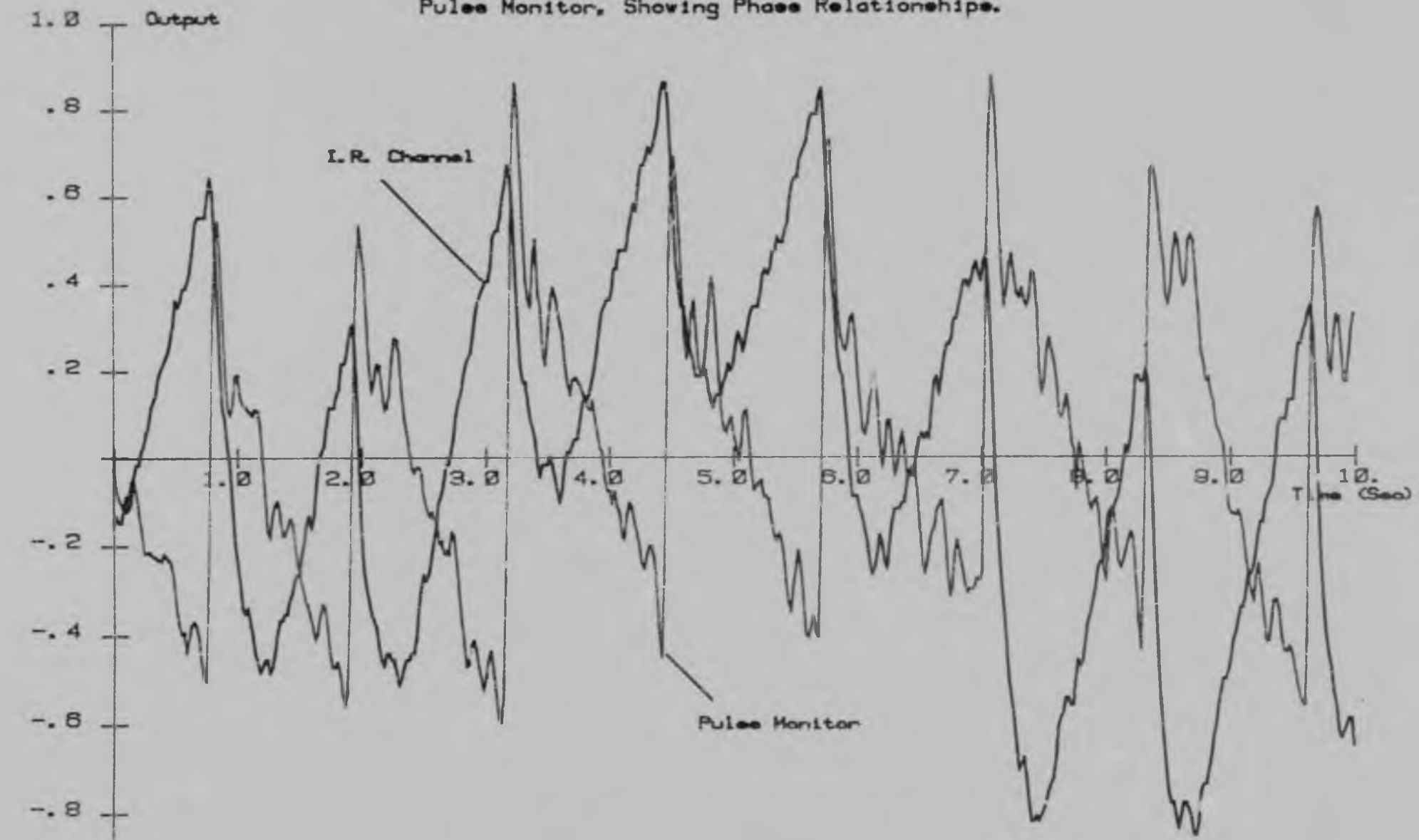


Figure A7.18 Output From I.R. Channel and Pulse Monitor, Showing Phase Relationships.



APPENDIX 8 PROGRAM LISTINGS

This appendix presents the program listings that were used for the microNova, H.P. terminal and the IBM as discussed in appendix 4. The listings appear in the following order:

MicroNova	pages 214-217
H.P. Terminal	pages 218-224
Central IBM 370	pages 225-228

```
0001   .MAIN
       000002           .LOC 2
00002  000100 RTCI:     100          ;ADDRESS OF RTC INTERUPT ROUTINE
       000020           .LOC 20
00020  000000 DPTA:     0
00021  000000 ESTA1:    0
       000030           .LOC 30
00030  000000 NPTS:     0
00031  000000 STIM:     0
       000040           .LOC 40
00040  000000 NPTS1:    0          ;NUMBER OF SAMPLES
00041  000000 STIM1:    0         ;NUMBER OF CLOCK TICKS
00042  000355 DPTA1:    355        ;STARTING ADDRESS IN MEMORY
00043  000000 NOINP:    0          ;NUMBER OF CHANNELS
00044  000000 NINP1:    0
00045  000335 ESTA:     335          ;ADDRESS OF ESC SEQUENCE FOR EDITTING
       000060           .LOC 60
00060  062677 STRT:     IORST     ;INITIALISE PROGRAM
00061  024041           LDA       1,STIM1
00062  044031           STA       1,STIM
00063  024040           LDA       1,NPTS1
00064  044030           STA       1,NPTS
00065  024042           LDA       1,DPTA1
00066  044020           STA       1,DPTA
00067  071177           DOAS      2,CPU
00070  000132           JMP       IDEL      ;WAITE FOR INT. FROM RT CLOCK
       000100           .LOC 100
00100  060177           INTEN     ;RE-ENABLE RT CLOCK
00101  014031           DSZ       STIM
00102  002000           JMP @0    ;NOT TIME FOR SAMPLE
00103  102000           ADC       0,0       ;GET SAMPLES FROM RTP
00104  024041           LDA       1,STIM1
00105  044031           STA       1,STIM
00106  030043           LDA       2,NOINP
00107  150000           COM       2,2
00110  151423 SAMPL:    INCZ      2,2,SNC
00111  000115           JMP       INPUT
00112  014030           DSZ       NPTS
00113  000132           JMP       IDEL
00114  000135           JMP       OUT
00115  024134 INPUT:    LDA       1,COMM
00116  066032           DOB       1,32
00117  101420           INCZ      0,0
00120  125100           MOVL      0,1
00121  125100           MOVL      1,1
00122  125100           MOVL      1,1
00123  125100           MOVL      1,1
00124  065032           DOA       1,32
00125  063532           SKPBZ     32
00126  000125           JMP       .-1
00127  064432           DIA       1,32
00130  046020           STA       1,@DPTA
00131  000110           JMP       SAMPL
00132  000133 IDEL:     JMP       .+1
00133  000132           JMP       .-1
00134  002403 COMM:     2403
00135  065277 OUT:      DOAC      1,CPU       ;DISABLE REAL TIME CLOCK
00136  024042           LDA       1,DPTA1
00137  044020           STA       1,DPTA
0002   .MAIN
00140  024040           LDA       1,NPTS1
00141  044030           STA       1,NPTS

00142  004211           JSR       SOUT
00143  024043 SLOOP:    LDA       1,NOINP         ;BEGINING OF SAMPLE OUTP LOOP
```

```
00144 044044          STA     1,NINP1
00145 014334 CHLOP:   DSZ     NVAL1
00146 000150          JMP     .+2
00147 004230          JSR     ELNE      ;OUTPUT END OF RECORD MARK
00150 032020          LDA     2,@DATA   ;LOOP TO OUTP ALL CHANNELS
00151 050313          STA      2,OUTP
00152 030320          LDA     2,DIV1     ;LOOK AT
00153 050321          STA     2,DIV2       ;FIRST HEX DIGIT
00154 102440          SUBO    0,0
00155 024313          LDA     1,OUTP
00156 073101          DIV
00157 030314          LDA     2,HEX7
00160 133400          AND     1,2
00161 020316          LDA     0,COUNT
00162 040317          STA     0,CONT1
00163 004240 HEX:     JSR     SHEX   ;OUTP A HEX DIGIT
00164 014317          DSZ     CONT1      ;HAVE ALL DIGITS BEEN OUTPTED
00165 000175          JMP     .+10
00166 030326          LDA     2,HHEX    ;OUTP A H
00167 004272          JSR     STTO
00170 014044          DSZ     NINP1     ;HAVE ALL CHANNELS BEEN OUTPTED
00171 000145          JMP     CHLOP
00172 014030          DSZ     NPTS  ;HAVE ALL SAMPLES BEEN OUTPTED
00173 000143          JMP     SLOOP
00174 000300          JMP      FINIS
00175 102440          SUBO    0,0        ;DIVIDE DIV
00176 024321          LDA     1,DIV2     ;BY 10H
00177 030322          LDA     2,HEXT
00200 073101          DIV
00201 044321          STA     1,DIV2
00202 102440          SUBO    0,0        ;GETTING HOLD
00203 024313          LDA     1,OUTP    ;OF THE NEXT HEX DIGIT
00204 030321          LDA     2,DIV2
00205 073101          DIV
00206 152440          SUBO    2,2       ;PLACE RESULT
00207 133000          ADD     1,2       ;IN AC2
00210 000163          JMP     HEX
00211 054330 SOUT:    STA     3,PC       ;SUBROUTINE THAT
00212 030336          LDA     2,ESC      ;STARTS THE OUTPUTTING
00213 004272          JSR     STTO       ;OF DATA TO TERMINAL
00214 030350          LDA     2,HME      ;BY CLEARING
00215 004272          JSR     STTO       ;THE SCREEN
00216 030336          LDA     2,ESC
00217 004272          JSR     STTO
00220 030351          LDA     2,CLR
00221 004272          JSR     STTO
00222 024344          LDA     1,E           ;AND ENABLING EDIT MODE
00223 044342          STA     1,LET
00224 004260          JSR     EDIT
00225 024335          LDA     1,NVAL2         ;AT START MUST LOAD  9
00226 044334          STA     1,NVAL1         ;INTO NO. OF CHAR BEFORE E.O.R.M
00227 002330          JMP     @PC
00230 054330 ELNE:    STA     3,PC              ;SUBROUTINE THAT
00231 030345          LDA     2,CR       ;OUPUTS AN
0003   .MAIN
00232 004272          JSR     STTO       ;END OF
00233 030327          LDA     2,LF       ;RECORD MARK
00234 004272          JSR     STTO
00235 024333          LDA     1,NVAL
00236 044334          STA     1,NVAL1
00237 002330          JMP     @PC

00240 024331 SHEX:    LDA     1,SEVT      ;MAKE SURE ONLY
00241 133400          AND     1,2         ;GOT 1 HEX DIGIT
```

```
00242 024323          LDA     1,ELEV
00243 146433          SUBZ# 2,1,SNC
00244 000252          JMP     ALPH    ;HEX DIGIT IS AN ALPHA
00245 024324          LDA     1,SIXTY
00246 133000          ADD     1,2
00247 054330          STA       3,PC
00250 004272          JSR     STTO
00251 002330          JMP     @PC
00252 132440 ALPH:    SUBO    1,2
00253 024325          LDA     1,HUND
00254 133000          ADD     1,2
00255 054330          STA       3,PC
00256 004272          JSR     STTO
00257 002330          JMP     @PC
00260 054352 EDIT:    STA     3,PC1         ;SUBROUTNE THAT
00261 024315          LDA     1,HEX8        ;PREPARES TERMINAL
00262 044317          STA     1,CONT1       ;FOR EDIT MODE
00263 024045          LDA     1,ESTA
00264 044021          STA     1,ESTA1
00265 032021          LDA     2,@ESTA1
00266 004272          JSR     STTO
00267 014317          DSZ     CONT1
00270 000265          JMP     .-3
00271 002352          JMP     @PC1
00272 063511 STTO:    SKPBZ   TTO     ;OUTP ROUTINE TO TERMINAL
00273 000272          JMP     .-1
00274 071111          DOAS    2,TTO
00275 063511          SKPBZ   TTO
00276 000275          JMP     .-1
00277 001400          JMP     0,3
00300 004230 FINIS:   JSR     ELNE        ;TELL TERMINAL
00301 024347          LDA     1,D
00302 044342          STA     1,LFT
00303 004260          JSR     EDIT
00304 030344          LDA     2,E         ;THAT SAMPLING
00305 004272          JSR     STTO        ;IS FINISHED
00306 030346          LDA     2,N
00307 004272          JSR     STTO
00310 030347          LDA     2,D
00311 004272          JSR     STTO
00312 063077          HALT
00313 000000 OUTP:    0         ;DUMMY ADDR. FOR DATA CURRENTLY BEING OUTPUTTED
00314 000007 HEX7:    7           ;USED AS MASK TO GET FIRST 3 BITS
00315 000010 HEX8:    10            ;COUNT FOR EDIT MODE LOOP
00316 000003 COUNT:   3
00317 000000 CONT1:   0
00320 000400 DIV1:    400
00321 000000 DIV2:    0
00322 000020 HEXT:    20
00323 000011 ELEV:    11
0004   .MAIN
00324 000060 SIXTY:   60
00325 000100 HUND:    100
00326 000110 HHEX:    110
00327 000012 LF:      12
00330 000000 PC:      0
00331 000017 SEVT:    17
00332 000001 ONE:     1
00333 000022 NVAL:    22
00334 000000 NVAL1:   0
00335 000023 NVAL2:   23
00336 000033 ESC:     33
```

```
00337 000054 COMMA:   54
00340 000143 C:       143
00341 000040 SP:      40
00342 000105 LET:     105
00343 000040 SP1:     40
00344 000105 E:       105
00345 000015 CR:      15
00346 000116 N:       116
00347 000104 D:       104
00350 000150 HME:     150
00351 000112 CLR:     112
00352 000000 PC1:     0          ;USED AS SECOND LEVEL OF SUBROUTINE RETURN ADD
                      .END
```

```
00337 000054 COMMA:   54
00340 000143 C:       143
00341 000040 SP:      40
00342 000105 LET:     105
00343 000040 SP1:     40
00344 000105 E:       105
00345 000015 CR:      15
00346 000116 N:       116
00347 000104 D:       104
00350 000150 HME:     150
00351 000112 CLR:     112
00352 000000 PC1:     0          ;USED AS SECOND LEVEL OF SUBROUTINE RETURN ADD
                      .END
```

```
D
10 DIM S$[79],Sload$[79]
20 DIM C$[20],Aver(4)
30 INTEGER Nc ticks
40 DATA "0123456789:;<=>?"
50 READ Ntabl$[1,16]
60 Lf$=CHR$(10)
70 Cr$=CHR$(13)
80 INPUT "GIVE ADDRESS OF ONE UNUSED PAGE ZERO MEMORY LOCATION ? ",D$
90 L=1
100 C$=Cr$
110 Pflag=0
120 GETDCM ON
130 GOSUB 870
140 C$="10A"
150 L=3
160 Pflag=1
170 GOSUB 870
180 C$=TRIM$(D$)
190 L=LEN(C$)
200 GOSUB 870
210 C$=Cr$
220 L=1
230 Pflag=0
240 GOSUB 870
250 REM ON ERROR GOTO 282
260 C$=RPT$(" ",200)
270 D=0
280 X=GETDCM(T$)
290 IF X=0 THEN GOTO 340
300 GOTO 280
310 PRINT "ERROR OCCURRED IN LAST COMMAND "
320 ON ERROR GOTO 310
330 GOTO 350
340 PRINT " "
350 LINPUT "COMMAND ? ",C$
360 Oy=-2
370 Pflag=1
380 C$=TRIM$(C$)
390 Err=1
400 IF POS(C$,"LOAD")<>0 THEN GOTO 480
410 IF POS(C$,"END")<>0 THEN GOTO 1180
420 IF POS(C$,"SAMP")<>0 THEN GOTO 1220
430 IF POS(C$,"PLOT")<>0 THEN CALL Splot(Err,C$,-1,Aver(),"DNO",.1," ")
440 IF POS(C$,"AVER")<>0 THEN CALL Sav(Err,C$)
450 IF POS(C$,"GRAP")<>0 THEN CALL Graph(Err)
460 IF Err=0 THEN GOTO 340
470 GOTO 310
480 ASSIGN "RIGHT TAPE " TO #10
490 L=LEN(C$)
500 S$[1,10]="FIND FILE "
510 S$[11,13]=C$[5,L]
520 S$[14,28]=" ON RIGHT TAPE"
530 S$[29,29]=CHR$(13)
540 COMMAND S$[1,29]
550 Pflag=0
560 LINPUT #10;Sload$
570 REM PRINT Sload$;"*"
580 IF POS(Sload$,".END")<>0 THEN GOTO 820
590 IF Sload$[4,8]="      " THEN GOTO 560
600 IF LEN(Sload$)<7 THEN GOTO 560
610 IF Sload$[3,3]<>" " THEN GOTO 560
620 Y=0
630 FOR I=4 TO 8
640 Yt=VAL(Sload$[I,I])
650 Y=Y+Yt*8^(8-I)
660 NEXT I
670 IF Y=Oy+1 THEN GOTO 750
680 C$=CHR$(13)
```

```
700 GOSUB 870
710 C$=Sload$[4,8]
720 L=LEN(C$)+1
730 C$[L,L]="/"
740 GOSUB 870
750 C$[1]=Sload$[10,15]
760 L=LEN(C$)+1
770 C$[L]=Lf$
780 GOSUB 870
790 Os=Y
800 PRINT "LOC= ";Sload$[4,8];"  CONTENTS= ";Sload$[10,15]
810 GOTO 560
820 C$[1,1]=CHR$(13)
830 L=1
840 GOSUB 870
850 ASSIGN * TO #10
860 GOTO 280
870 REM SUB PUT AND GET
880 REM PRINT "OUTPUT";C$[1,L]
890 GOSUB 1110
900 GOSUB 980
910 IF POS(S$,"?")=0 THEN GOTO 940
920 PRINT S$
930 GOTO 310
940 IF Pflag=0 THEN RETURN
950 IF POS(S$,"!")<>0 THEN PRINT Cr$;Lf$;
960 PRINT S$;
970 RETURN
980 REM Novaget(S$)
990 J=1
1000 S$=" "
1010 Ys=GETDCM(T$)
1020 IF Ys=0 THEN GOTO 1080
1030 S$[J;1]=T$[1,1]
1040 IF T$[1,1]=Lf$ THEN GOTO 1010
1050 IF T$[1,1]=Cr$ THEN GOTO 1010
1060 J=J+1
1070 GOTO 1010
1080 J=J-1
1090 IF J=0 THEN PRINT "NO RESPONSE FROM MICRO"
1100 RETURN
1110 REM Novaput(C$)
1120 FOR I=1 TO L
1130 T$=C$[I,I]
1140 Xx=PUTDCM(T$)
1150 IF Xx<>1 THEN GOTO 1140
1160 NEXT I
1170 RETURN
1180 C$=CHR$(13)
1190 L=1
1200 GOSUB 870
1210 END
1220 PRINT "TYPE IN THE NUMBER OF SAMPLES REQUIRED"
1230 INPUT Nsamp
1240 PRINT "TYPE IN THE SAMPLING INTERVAL"
1250 INPUT "NUMBER OF HOURS?",Nhours
1260 INPUT "NUMBER OF MINUTES?",Nmin
1270 INPUT "NUMBER OF SECONDS?",Nsec
1280 PRINT "TYPE IN THE NUMBER OF CHANNELS BEING USED"
1290 INPUT Nchan
1300 PRINT "WHAT FILE NUMBER DO YOU WANT TO USE ON THE RIGHT DRIVE?"
1310 INPUT Fnum$
1320 S$[1,10]="FIND FILE "
1330 S$[11,13]=Fnum$
1340 S$[14,28]=" ON RIGHT TAPE"
1350 COMMAND S$
```

```
1360 ASSIGN "RIGHT TAPE" TO #10
1370 Stime=Nhours*3600+Nmin*60+Nsec
1380 REM CALCULATE NO. OF CLOCK TICKS PER SAMPLE
1390 Nctlcks=Stime/(Nsamp*1.8E-03)
1400 REM CALCULATE TOTAL NO. OF SAMPLES TAKEN
1410 Ntot=Nsamp*Nchan
1420 CALL Octalc((Nsamp),Octal)
1430 C$="40/"
1440 GOSUB 1530
1450 C$="41/"
1460 CALL Octalc((Nctlcks),Octal)
1470 GOSUB 1530
1480 C$="43/"
1490 CALL Octalc((Nchan),Octal)
1500 GOSUB 1530
1510 GOTO 1610
1520 REM PUT PARAMETRS OUT TO NOVA
1530 L=3
1540 GOSUB 870
1550 C$=VAL$(Octal)
1560 L=LEN(C$)
1570 C$[L+1,L+1]=Cr$
1580 L=L+1
1590 GOSUB 870
1600 RETURN
1610 GETKBD ON
1620 PRINT #10;Nsamp;Stime;Nchan;0;0;0;0;0
1630 ON KEY #83 GOTO 1690
1640 COMMAND "ASSIGN SOURCE TO DISPLAY"
1650 PRINT " "
1660 PRINT "**START THE SAMPLING BY PUTTING TERMINAL INTO REMOTE**"
1670 PRINT "                **AND HITTING KEY 'S'**"
1680 SLEEP
1690 ON KEY #83 GOTO 1760
1700 L=3
1710 C$="50R"
1720 GOSUB 870
1730 PRINT LIN(3)
1740 PRINT "**WHEN NOVA HAS FINISHED,TAKE IT OUT OF REMOTE AND HIT KEY 'S'**"
1750 SLEEP
1760 GETKBD OFF
1770 WAKEUP
1780 COMMAND "ASSIGN SOURCE TO LEFT TAPE"
1790 PRINT "ADJh";
1800 COMMAND "COPY FILE FROM DISPLAY TO RIGHT TAPE"
1810 PRINT LIN(3),TAB(9),"*****TYPE IN A HEADING FOR THE PAST TEST*****"
1820 LINPUT S$
1830 PRINT #10;S$
1840 COMMAND "MARK FILE HEADER ON RIGHT TAPE"
1850 GOTO 340
1860 SUB Octalc(Decimal,Octal)
1870 Octal=0
1880 Counter=-1
1890 Counter=Counter+1
1900 Mult=INT(Decimal DIV 8)
1910 Over=Decimal-Mult*8
1920 Octal=Octal+Over*(10^Counter)
1930 Decimal=Mult
1940 IF Decimal><0 THEN GOTO 1890
1950 REM ************************************************
1960 SUBEND
1970 SUB Sread1(C$,Nsa,Nti,Nchan,Aver())
1980 DIM S$[79],Pstn(7)
1990 REM PRIMER ROUTINE FOR READING DATA FROM TAPE
2000 ASSIGN "RIGHT TAPE" TO #10
2010 L=LEN(C$)
2020 S$[1,10]="FIND FILE "
2030 S$[11,13]=C$[5,L]
```

```
2040 S$[14,28]=" ON RIGHT TAPE"
2050 COMMAND S$
2060 LINPUT #1C S$
2070 Pstn(0)=POS(S$,"  ")
2080 FOR I=1 TO 6
2090 Pstn(I)=POS(S$[Pstn(I-1)+2,72],"  ")+Pstn(I-1)+1
2100 NEXT I
2110 Pstn(7)=72
2120 Nsa=VAL(S$[1,Pstn(0)])
2130 Nti=VAL(S$[Pstn(0),Pstn(1)])
2140 Nchan=VAL(S$[Pstn(1),Pstn(2)])
2150 FOR I=2 TO 6
2160 Aver(I-2)=VAL(S$[Pstn(I),Pstn(I+1)])
2170 NEXT I
2180 SUBEND
2190 SUB Splot(Err,C$,Chan,Aver(),Ans$,Scle,Srtn$)
2200 REM ******INITIALISES PLOTTER, GETS HEADER & INITIALISES LEFT********
2210 REM ******TAPE IF NECESSARY TO COPY DATA TO ********************
2220 DIM Dat(35),S$[72],Dum(4),Y(4)
2230 INTEGER I,I1,I2,Entry,M,N
2240 PLOTR
2250 IF POS(Ans$[1,1],"D")><0 THEN GOSUB 2630
2260 IF POS(Ans$[1,1],"Y")><0 THEN GCLR
2270 LOCATE (20,200,25,95)
2280 IF POS(Ans$[2,2],"Y")=0 THEN CALL Sread1(C$,Nsa,Nti,Nchan,Aver())
2290 IF POS(Ans$[2,2],"Y")><0 THEN GOSUB 2710
2300 SCALE (0,Nti,-1,1)
2310 Err=0
2320 FXD (1,2)
2330 LGRID (Nti/10,.2,0,0,2,1)
2340 FRAME
2350 Srtn$=TRIM$(Srtn$)
2360 PRINT "hJ"
2380 Entry=0
2390 Nlnes=INT(Nsa*Nchan/18)
2400 IF Nlnes-(Nsa*Nchan/18)><0 THEN Nlnes=Nlnes+1
2410 M=0
2420 M=M+1
2430 IF M*18-INT(M*18/Nchan)*Nchan><0 THEN GOTO 2420
2440 FOR I=1 TO Nlnes STEP M
2450 CALL Sread2(Dat(),N,M)
2460 IF POS(Ans$[2,2],"Y")><0 THEN GOSUB 2880
2470 FOR I1=1 TO N-1 STEP Nchan
2480 Entry=Entry+1
2490 FOR I2=1 TO Nchan
2500 Y(I2-1)=Dat(I1-2+I2)
2510 NEXT I
2520 Xp=((I-1)*18+I1)*Nti/(Nsa*Nchan)
2530 IF POS(Srtn$,"AVER")><0 THEN CALL Paver(Y(Chan),Aver(Chan),Yp)
2540 IF POS(Srtn$,"MARK")><0 THEN CALL Smark(Y(Chan),Yp)
2550 IF POS(Srtn$,"DIV")><0 THEN CALL Sdiv(Y(),Yp,Aver())
2560 Yp=Yp*Scle
2570 PLOT (Xp,Yp)
2580 NEXT I1
2590 NEXT I
2600 IF POS(Ans$[2,2],"Y")><0 THEN GOTO 3040
2610 GOTO 3090
2620 REM ********* FIND PLOTTER DETAILS & WHETHER TO COPY TO LEFT TAPE ******
2630 INPUT "GRAPHICS TO BE CLEARED ?",Ans$[1,1]
2640 INPUT "SCALE FACTOR ?",Scle
2650 INPUT "CHANNEL NO.?",Chan
2660 INPUT "COPY DATA TO LEFT TAPE?",Ans$[2,2]
2670 IF POS(Ans$[2,2],"Y")><0 THEN INPUT "FILE NO. ?",Ans$[3,3]
2680 INPUT "FUNCTION TO BE PERFORMED ?",Srtn$
2690 RETURN
2700 REM **********READ AND WRITE HEADER TO THE LEFT TAPE **********
```

```
2710 Ans$=TRIM$(Ans$)
2720 L=LEN(Ans$)
2730 S$[1,10]="FIND FILE "
2740 S$[11,13]=Ans$[3,L]
2750 S$[14,28]=" ON LEFT TAPE"
2760 COMMAND S$
2770 ASSIGN "LEFT TAPE" TO #9
2780 FOR Ii=0 TO 4
2790 Dum(Ii)=Aver(Ii)
2800 NEXT Ii
2810 CALL Sread1(C$,Nsa,Nti,Nchan,Aver())
2820 FOR Ii=0 TO 4
2830 Aver(Ii)=Dum(Ii)
2840 NEXT Ii
2850 PRINT #9;Nsa;Nti;Nchan;Aver(0);Aver(1);Aver(2);Aver(3);Aver(4)
2860 RETURN
2870 REM ********** WRITE DATA TO LEFT TAPE ********************
2880 FOR I5=0 TO M-1
2890 N1=N-I5*18
2900 IF N1>18 THEN N1=18
2910 FOR I4=1 TO N1
2920 Dat$=TRIM$(VAL$(Dat(I5*18+I4-1)*2048))
2930 L=LEN(Dat$)
2940 IF L=4 THEN GOTO 2970
2950 Dat1$[1,4-L]="
2960 Dat1$[5-L,4]=Dat$
2970 Dat1$[5-L,4]=Dat$
2980 S$[(I4-1)*4+1,I4*4]=Dat1$
2990 NEXT I4
3000 PRINT #9;S$[1,N1*4]
3010 NEXT I5
3020 RETURN
3030 REM *******WRITE FILE MARKER ON LEFT TAPE ***********
3040 ASSIGN "RIGHT TAPE" TO #10
3050 LINPUT #10;S$
3060 PRINT #9;S$
3070 COMMAND "MARK FILE HEADER ON LEFT TAPE"
3080 GOTO 3110
3090 ASSIGN "RIGHT TAPE" TO #10
3100 LINPUT #10;S$
3110 CSIZE (5,.5)
3120 MOVE (0,1)
3130 PRINT #0;S$;
3140 SUBEND
3150 SUB Sread2(Dat(),N,M)
3160 REM ************************************************
3170 DIM S$[72]
3180 N=0
3190 ASSIGN "RIGHT TAPE" TO #10
3200 FOR I=0 TO M-1
3210 LINPUT #10;S$
3220 L=LEN(TRIM$(S$[4,72]))
3230 IF L/4=INT(L/4) THEN N1=INT(L/4) ELSE N1=INT(L/4)+1
3240 N=N+N1
3250 FOR I1=1 TO N1
3260 Dat(I*18+I1-1)=VAL(S$[(I1-1)*4+1,I1*4])/2048
3270 NEXT I1
3280 IF N1>=18 THEN GOTO 3310
3290 M=I
3300 GOTO 3320
3310 NEXT I
3320 SUBEND
3330 SUB Sav(Err,C$)
3340 REM ************************************************************
3350 DIM Dat(35),Aver(4)
3360 INTEGER N,M
3370 INPUT "SHOULD THE GRAPHICS BE CLEARED?",Ans$
```

```
3380 INPUT "SCALE FACTOR?",Scle
3390 INPUT "COPY DATA TO LEFT TAPE?",Ans$[2,2]
3400 IF POS(Ans$[2,2],"Y")<>0 THEN INPUT "FILE NO. ?",Ans$[3,3]
3410 Err=0
3420 CALL Sread1(C$,Nsa,Nt1,Nchan,Aver())
3430 FOR Chan=0 TO Nchan-1
3440 Aver(Chan)=0
3450 NEXT Chan
3460 Nlnes=INT(Nsa*Nchan/18)
3470 IF Nlnes-(Nsa*Nchan/18)<>0 THEN Nlnes=Nlnes+1
3480 M=0
3490 M=M+1
3500 IF M*18-INT(M*18/Nchan)*Nchan<>0 THEN GOTO 3490
3510 FOR I=1 TO Nlnes STEP M
3520 CALL Sread2(Dat(),N,M)
3530 FOR Chan=0 TO Nchan
3540 Ttle(Chan)=0
3550 FOR I1=1 TO N STEP Nchan
3560 IF Chan<Nchan THEN Ttle(Chan)=Ttle(Chan)+Dat(I1-1+Chan)
3570 IF Dat(I1-1)=0 THEN GOTO 3590
3580 IF Chan=Nchan THEN Ttle(Chan)=Ttle(Chan)+Dat(I1)/Dat(I1-1)
3590 NEXT I1
3600 Aver(Chan)=Aver(Chan)+Ttle(Chan)
3610 NEXT Chan
3620 NEXT I
3630 FOR Chan=0 TO Nchan
3640 Aver(Chan)=Aver(Chan)/Nsa
3650 PRINT "AVERAGE=",Aver(Chan)
3660 NEXT Chan
3670 CALL Splot(Err,C$,1,Aver(),Ans$,Scle,"AVER")
3680 SUBEND
3690 SUB Faver(Y,Aver,Yp)
3700 Yp=Y-Aver
3710 SUBEND
3720 SUB Smark(Y,Yp)
3730 REM ********** ROUTNE FOR MARKING PERTINANT EVENTS *********
3740 Yp=-1
3750 IF Y>.4 AND Y<.6 THEN Yp=1
3760 SUBEND
3770 SUB Sdiv(Y(),Yp,Aver())
3780 Yp=(Y(1)/Y(0))-Aver(4)
3790 SUBEND
3800 SUB Graph(Err)
3810 REM ***********Routine FOR PLOT TimsGraphs*********************
3820 Err=0
3830 PLOTR
3840 INPUT "CLEAR GRAPHICS?",Ans$
3850 IF POS(Ans$,"Y")=1 THEN GCLR
3860 LOCATE (15,200,15,95)
3870 INPUT "RANGE OF X-VALS?",Xmin,Xmax
3880 INPUT "RANGE OF Y-VALS?",Ymin,Ymax
3890 INPUT "RANGE OF THETA VALS.",Tmin,Tmax
3900 INPUT "FUNCTION TO BE PERFORMED?",Ans$
3910 SCALE (Xmin,Xmax,Ymin,Ymax)
3920 FXD (1,2)
3930 PRINT "hJ"
3940 LGRID ((Xmax-Xmin)/10,(Ymax-Ymin)/10,0,0,2,2)
3950 FRAME
3960 H=(Tmax-Tmin)/100
3970 Entry=0
3980 Eof=0
3990 FOR Xc=Tmin TO Tmax STEP H
4000 Entry=Entry+1
4010 X=Xc
4020 IF POS(Ans$,"FUNC")=1 THEN CALL Funct(X,Y)
4030 IF POS(Ans$,"DATA")=1 THEN CALL Sdata(X,Y,Entry,Eof)
```

```
4040 IF Eof-1 THEN GOTO 4070
4050 PLOT (X,Y)
4060 NEXT Xc
4070 SUBEND
4080 SUB Funct(X,Y)
4090 REM ****************Routine TO PLOT A FUNCTION ************
4100 Th=X
4110 R=1+1/Th
4120 X=R*COS(Th)
4130 Y=R*SIN(Th)
4140 SUBEND
4150 SUB Sdata(X,Y,Entry,Eof)
4160 REM ****************Routine TO PLOT DATA POOINTS ***************
4170 DIM S$[72]
4180 ON ERROR GOTO 4310
4190 IF Entry><1 THEN GOTO 4260
4200 INPUT "FILE NUMBER?",Ans$[1,1]
4210 S$[1,10]="FIND FILE "
4220 S$[11,13]=Ans$[1,1]
4230 S$[14,28]=" ON RIGHT TAPE"
4240 COMMAND S$
4250 PRINT "hJ"
4260 ASSIGN "RIGHT TAPE" TO #10
4270 LINPUT #10;S$
4280 X=VAL(S$[4,9])
4290 Y=VAL(S$[11,20])-.2*(-.045*X+1)
4300 GOTO 4340
4310 Eof=1
4320 RESUME NEXT
4330 ON ERROR GOTO 0
4340 SUBEND
```

```
C                          FILE PROC
C    This program reads the data files generated by the data capture
C    system and processes them for use by the IBM 370/158
       DIMENSION IX(20),IY(20)
       DIMENSION X(20),Y(20),AVER(5),HEAD(15),SCLE(5)
       INTEGER COMM(5),ICHAN(5) ENTRY
       INTEGER CHOS,PICK,NCALL
       PICK=-674642990
       CHOS=-1010247966
1      WRITE(6,113)
113    FORMAT(/3X,'DO YOU WANT AXES? (TYPE 0 = AXES; 1 = NO AXES 2 =NOT RELEVANT)
       READ(9,104)NOAXS
       IF(NOAXS.LT.2)WRITE(5,104)NOAXS
104    FORMAT(Y)
       READ(5,103)RNUM,XMAX,ACHAN,(AVER(I),I=1,5)
       WRITE(6,110)
110    FORMAT(/4X,'HOW MANY CHANNELS DO YOU WANT TO PROCESS?')
103    FORMAT(8Y)
       XMIN=0
       READ(9,100)NGRAP
100    FORMAT(Y)
       WRITE(5,111)RNUM,NGRAP,XMAX
111    FORMAT(E13.7,I3,E13.7)
       DO 5 I=1,NGRAP
       WRITE(6,102)
102    FORMAT(/3X,'COMMAND;CHANNEL NO. AND SCALE FACTOR')
       READ(9,115)COMM(I),ICHAN(I),SCLE(I)
115    FORMAT(A4,2Y)
5      CONTINUE
       XINC=(XMAX-XMIN)/RNUM
       DO 4 IC=1,NGRAP
       NCALL=IC
       CALL INF(RNUM,XMAX,ACHAN,AVER,SCLE(IC),ICHAN(IC),NGRAP,COMM(IC),NCALL)
4      CONTINUE
       READ(5,101)(HEAD(I),I=1,15)
101    FORMAT(15A4)
       WRITE(5,101)(HEAD(  ,I=1,15)
       IF(COMM(1).EQ.PICK)STOP
       IF(COMM(1).EQ.CHOS)STOP
       CALL SCALE(XMAX,XMIN,-415219648)
       YMAX=1.
       YMIN=-1.
       IF(YMIN.LT.0.0)GO TO 6
       YDIFF=(YMAX-YMIN)/4.0
       IF(YDIFF.GE.YMIN)YMIN=0.0
7      CALL SCALE(YMAX,YMIN,-398442432)
9      WRITE(6,112)
112    FORMAT(/4X,'WHEN YOU RECEIVE THE PROMPT (?) TYPE /XEQ PLOT1(MDR)')
       STOP
6      IF(YMAX.GE.0.0)GO TO 7
       YDIFF=(YMAX-YMIN)/4.0
       IF(YDIFF.GE.ABS(YMAX))YMAX=0.0
       GO TO 7
       END
C
C
       SUBROUTINE SCALE(MAX,MIN,AXIS)
       DIMENSION SCAL(11)
       REAL MAX,MIN
       INTEGER EXP,AXIS
       RMAX=MAX
       RMIN=MIN
       EXP=0
       BLANK=.2510
8      FAC=(RMAX-RMIN)/10.0
```

```
      SCAL(1)=RMIN
      DO 3 I=2,11
      SCAL(I)=SCAL(I-1)+FAC
3     CONTINUE
      FAC=1000./((RMAX-RMIN)*10.0**(EXP*3))
      WRITE(5,100)RMAX,RMIN,FAC
100   FORMAT(3(E13.7))
      DO 6 I=1,11
      IF(ABS(SCAL(I)).LE.1.E-04)GO TO 5
      IF(ABS(SCAL(I)).LT.10.0)WRITE(5,105)SCAL(I)
105   FORMAT(F4.1)
      IF(ABS(SCAL(I)).GE.10.0.AND.SCAL(I).GT.(-100.0))WRITE(5,101)SCAL(I)
      IF(SCAL(I).LE.(-100.0))WRITE(5,106)SCAL(I)
106   FORMAT(F5)
      GO TO 6
5     WRITE(5,102)(BLANK,IC=1,3)
102   FORMAT(3(A1))
6     CONTINUE
101   FORMAT(F5)
      IF(EXP.EQ.0)GO TO 4
      EXP=EXP*3
      WRITE(5,103)EXP
103   FORMAT('x10',/I2)
      RETURN
4     DO 7 I=1,2
7     WRITE(5,104)
104   FORMAT('    ')
      RETURN
      END
C
      SUBROUTINE INP(ANSA,ANTI,ACHAN,AVER,SCLE,CHAN,NGRA,COMM,NCALL)
      REAL AVER(5),X(11),Y(10),Y1(4),YMAX(5),YMIN(5)
      INTEGER DATA(36),CHAN,ENTRY,NCALL
      INTEGER OFSET DIVS,MARK,CHOS,COMM,PICK
      MARK=-725493294
      CHOS=-1010247966
      DIVS=-993401374
      PICK=-674642990
      PLOT=-673982749
C NCHA is a dummy variable used to deter .ne if MARK should be called
      NCHA=0
      NSA=ANSA
      NTI=ANTI
      NCHAN=ACHAN
      IF(NGRA.GT.2)NCHA=NCHAN
      K=1
      NLNES=(ANSA*ACHAN/18)
      ALNES=NLNES
      NLAST =ANSA*ACHAN/18.-ALNES)*18.001-1
      IF(ALN=.NE.(ANSA*ACHAN/18))NLNES=NLNES+1
      M=0
1     M=M+1
      IF(M*18.NE.(M*18/NCHAN)*NCHAN)GO TO 1
      OFSET=17
      ENTRY=0
      DO 2 LNES=1,NLNES,M
      N=0
      DO 3 I=1,M
      IF((LNES).NE.NLNES)GO TO 6
      LMTL=(I-1)*18+1
      OFSET=NLAST
      I=M
      GO TO 7
6     LMTL=(I-1)*18+1
7     LMTU=LMTL+OFSET
```

```
      READ(5,100)(DATA(J),J=LMTL,LMTU)
100   FORMAT(18I4)
3     N=N+18
      DO 2 I1=1,N,NCHAN
      DO 5 I2=1,NCHAN
      Y1(I2)=DATA(I1+I2-1)
5     Y1(I2)=Y1(I2)/2048.
      ALN=LNES
      X(K)=((ALN-1)*18.+I1)*ANTI/(ANSA*ACHAN)
      ENTRY=ENTRY+1
C     In prog. DIVS CHAN must be set equal to the number of chans used
      IF(COMM.EQ.DIVS)CALL DIV(Y1,AVER,SCLE,Y(K),CHAN+1)
      IF(COMM.EQ.PLOT)CALL SPLOT(Y1(CHAN),AVER(CHAN),Y(K),SCLE,YMAX(CHAN))
      IF(COMM.EQ.MARK)CALL SMARK(Y1(CHAN),YOLD,X(K),NSA,ENTRY,K)
      IF(COMM.EQ.PICK)CALL SDAT(Y1,YOLD,CHAN,ENTRY,NSA,K,X(K))
      IF(COMM.EQ.CHOS)CALL CHOSE(Y1(CHAN),AVER(CHAN),SCLE,K,NCALL,NSA,ENTRY)
      NCALL=NCALL+1
      YOLD=Y1(CHAN)
      IF(K.EQ.10)CALL OUTP(X,Y,K)
      K=K+1
2     CONTINUE
      RETURN
      END
C
C
      SUBROUTINE OUTP(X,Y,K)
      REAL X(11),Y(10)
      WRITE(5,100)(X(I),I=1,10)
      WRITE(5,100)(Y(I),I=1,10)
100   FORMAT(10(E12.6))
      K=0
      RETURN
C
C
      SUBROUTINE SPLOT(Y,AVE,YP,SCLE,YMAX)
      YP=(Y-AVE)*SCLE
      RETURN
1     WRITE(6,100)
100   FORMAT(/3X,'**** DIVISION BY ZERO IN SPLOT ***')
      YP=1.
      RETURN
      END
C
C
      SUBROUTINE SMARK(Y,YOLD,X,NSA,ENTRY,K)
      INTEGER ENTRY
      Y1=Y
      Y=0.0
      IF(Y1.GE.0.4.AND.Y1.LE.0.6)Y=0.5
      IF(ENTRY.EQ.NSA)GO TO 2
      IF(ENTRY.EQ.1)YOLD=Y
      IF(ABS(Y-YOLD).LT.0.1)GO TO 1
3     WRITE(5,100)X
100   FORMAT(E12.6)
1     K=1
      ICALL=1
      RETURN
2     X=0
      GO TO 3
      END
C
C
      SUBROUTINE DIV(Y1,AVER,SCLE,Y,CHAN)
      INTEGER CHAN
      REAL Y1(4),AVER(5)
```

```
      ICALL=1
      Y=(Y1(2)/Y1(1)-AVER(CHAN))*SCLE                                  228
      RETURN
      END
C
C
      SUBROUTINE SDAT(Y,YOLD,CHAN,ENTRY,NSA,K,X)
      REAL Y(4),YMAX(2),YMIN(2)
      INTEGER ENTRY,CHAN,COUNT,COUNT2,K
C     Count counts the number of markers encountered
C     Count2 counts the number of data points written out.
      Y1=Y(CHAN)
      Y(CHAN)=0
      IF(ENTRY.NE.1)GO TO 1
C     Initialise on first pass
      COUNT2=0
      COUNT=0
      YOLD=Y(CHAN)
      DO 4 I=1,2
      YMAX(I)=0.0
4     YMIN(I)=1.0
1     IF(Y1.GE.0.4.AND.Y1.LE.0.6)Y(CHAN)=0.5
      IF(ABS(Y(CHAN)-YOLD).LT.0.1)GO TO 2
C     GO TO 2
C     ENCOUNTERED A MARKER.
      COUNT=COUNT+1.
2     IF(COUNT.NE.1)GO TO 3
      WRITE(5,100)X,Y(1),Y(2)
100   FORMAT(3Y)
      DO 5 I=1,2
      IF(Y(I).GT.YMAX(I))YMAX(I)=Y(I)
5     IF(Y(I).LT.YMIN(I))YMIN(I)=Y(I)
      COUNT2=COUNT2+1.
3     IF(ENTRY.EQ.NSA)WRITE(5,101)COUNT2,(YMAX(I),YMIN(I),I=1,2)
      IF(ENTRY.EQ.NSA)WRITE(6,102)COUNT2
102   FORMAT(/5X,'NUMBER OF POINTS CHOSEN=',Y)
101   FORMAT(5Y)
      K=1
      RETURN
      END
C
C
      SUBROUTINE CHOSE(Y,AVER,SCALE,K,NCALL,NSA,ENTRY)
      REAL Y,AVER,SCALE
      INTEGER K,NCALL,NSA,ENTRY
      K=1
      IF(NCALL.GT.1)GO TO 1
      WRITE(6,100)NSA
100   FORMAT(/3X,'NUMBER OF DATA POINTS=',I5,/3X,'ENTER THE NO. OF POINTS TO BE)
      READ(9,101)NFFT
101   FORMAT(Y)
C     WRITE(5,102)NFFT
102   FORMAT(I5)
      SUM=0.0
1     IF(NCALL.LT.NFFT)RETURN
      SUM=SUM+Y
      IF(NCALL.EQ.NSA)WRITE(6,20)SUM
20    FORMAT(/3X,'SUM=',Y)
      IF(ENTRY.LE.NSA)WRITE(5,103)Y
103   FORMAT(E13.7)
      RETURN
      END
C
C
/DATA
 500  10   3   .400444   .598783   .29655   1.49646   0
/INC DAT
/INC DAT
/INC DAT
```

Author Revow M D
Name of thesis An Investigation into the dynamic performance of a two wavelength skin reflectance oximeter 1980

PUBLISHER:
University of the Witwatersrand, Johannesburg
©2013

LEGAL NOTICES:

Copyright Notice: All materials on the University of the Witwatersrand, Johannesburg Library website are protected by South African copyright law and may not be distributed, transmitted, displayed, or otherwise published in any format, without the prior written permission of the copyright owner.

Disclaimer and Terms of Use: Provided that you maintain all copyright and other notices contained therein, you may download material (one machine readable copy and one print copy per page) for your personal and/or educational non-commercial use only.

The University of the Witwatersrand, Johannesburg, is not responsible for any errors or omissions and excludes any and all liability for any errors in or omissions from the information on the Library website.